DISSERTATION

MATHEMATICAL MODELING OF RESPONSE FROM SMALL WATERSHED

Submitted by

Ruh-Ming Li

In partial fulfullment of the requirements

for the Degree of Doctor of Philosophy

Colorado State University

Fort Collins, Colorado

August, 1974

CED74-75RML1

COLORADO STATE UNIVERSITY

August 19 74

WE HEREBY RECOMMEND THAT THE THESIS PREPARED UNDER OUR SUPERVISION

BY RUH-MING LI

ENTITLED MATHEMATICAL MODELING OF RESPONSE FROM SMALL WATERSHED

BE ACCEPTED AS FULFILLING IN PART REQUIREMENTS FOR THE DEGREE OF

DOCTOR OF PHILOSOPHY

Committee on Graduate Work

Adviser

Head of Department

ABSTRACT OF DISSERTATION

MATHEMATICAL MODELING OF RESPONSE FROM SMALL WATERSHED

The physical quantities which describe the major watershed response to the precipitation are the water yield, the sediment yield, and the resultant stream morphology. This study provides the theoretical background and numerical methods for modeling physical processes governing the watershed response.

A method of nonlinear kinematic wave approximation for flow routing has been developed to route water and sediment over land and in channels. The numerical scheme developed in this study is unconditionally stable and may be used with a wide range of time increment to space increment ratio without loss of significant accuracy. From theoretical considerations, it has been found that the flow discharge is the better selection for the unknown in numerical computations than the depth or area. The applicability of the numerical method has been tested in various cases - overland flow, natural channel, and small drainage system and has been found satisfactory for modeling of watershed response. As the applications of this flow routing procedure, a rainfall-runoff model for simulating hydrographs from small watersheds and a rainfall-erosion model for calculating time-dependent erosion rates from overland flow areas have been developed.

The rainfall-runoff model simulates hydrographs on the single storm basis. The model includes the water balance simulation for land surface hydrologic cycle and the water routing features for both overland flow

and channel systems. Unlike the conventional approach to parametric modeling of watershed response, this model contains much more information on the physics of flow and requires much less assistance from optimization schemes than any existing water models known to the writer. For the tested basin the simulated hydrographs agree reasonably well with the measured hydrographs. The sensitivity analysis indicates that soil data are very sensitive to the computed hydrograph. Flow resistance parameters and vegetation data are less sensitive to the simulated results. In addition, this physically oriented model has the capability to predict watershed treatment effects on water yields.

The rainfall-erosion model simulates both water flow and sediment flow routing in overland flow areas and produces time-dependent erosion rates comparable with the available experimental data from a soil plot. The model can generate time-dependent land forms, and the generated land form tends to be concave in shape which frequently appears in nature. It was also found that the soil erosion rate was very sensitive to the bed slope and shape. The general practice of assuming a uniform shape may result in serious errors.

The mathematical models in this study may provide the short-term and the long-term responses. Theoretical interpretation of the long-term response was also made. The equations describing the basic physical processes in small watershed channels sculptured in noncohesive

alluvial materials have been employed to derive the hydraulic geometry equations. Both downstream and at-a-station relations were developed. This work provides information on stream morphology response to the modified amount of precipitation or to watershed treatment effects.

Ruh-Ming Li
Department of Civil Engineering
Colorado State University
Fort Collins, Colorado 80523
August 1974

ACKNOWLEDGMENTS

No words can adequately describe the writer's profound gratitude to his major professor, Dr. Daryl B. Simons, for his continued guidance and encouragement. Two years close association has been very stimulating and enlightening.

Profound thanks are extended to Dr. Michael A. Stevens for his constant counsel and encouragement throughout the period of this investigation. The writer also wishes to acknowledge the direction given to this research by Dr. Hsieh W. Shen, the writer's major professor in the early stage of his Ph.D. program.

The writer also expresses his grateful appreciation to all the members of his graduate committee, Drs. S. Karaki, J. W. Labadie, J. R. Meiman, H. W. Shen, and M. A. Stevens for their critical review of the manuscript. Also, appreciation is extended to Mr. Carlos Rodriquez, graduate student, for his proofreading the manuscript.

Sarah Edlund spent a great deal of time in typing the first draft and the final copy; for this, the writer wishes to express his great appreciation.

The financial support for this study was provided by the Colorado State University Experiment Station, Fort Collins, Colorado and the U.S. Rocky Mountain Forest and Range Experiment Station, Flagstaff, Arizona.

TABLE OF CONTENTS

Chapter		Page
	LIST OF TABLES	x
	LIST OF FIGURES	xi
	LIST OF SYMBOLS	xv
I	INTRODUCTION	1
	1.1. General	1
	1.2. Review of Related Literature	2
	1.2.1. Water yield and flow routing	2
	1.2.2. Soil erosion	6
	1.2.3. Stream morphology	7
	1.3. Scope of Present Study	8
II	NONLINEAR KINEMATIC-WAVE APPROXIMATION FOR FLOW ROUTING	10
	2.1. Governing Equations	10
	2.1.1. Continuity equation	10
	2.1.2. Momentum equation	10
	2.1.3. Resistance equations	11
	2.1.4. Discharge and flow area relation	13
	2.2. Numerical Scheme	15
	2.2.1. Nonlinear scheme	15
	2.2.2. Linear scheme	19
	2.2.3. Stability	20
	2.2.4. Convergence	23
	2.3. Applications	28
	2.3.1. Overland flow plots	28
	2.3.2. Natural channel	32
	2.3.3. Confined catchment	34
	2.4. Summary	34
III	RAINFALL-RUNOFF MODEL FOR NATURAL WATERSHEDS	37
	3.1. Model Structure	37
	3.2. Segmentation of a Watershed	37
	3.3. Water Balance	39
	3.3.1. Net rainfall	41
	3.3.2. Ground response to net rainfall	46
	3.3.2.1. Infiltration	49
	3.3.2.2. Soil moiture adjustment	56
	3.3.3. Mean rainfall excess rate	57
	3.4. Flow Routing in Natural Watersheds	58
	3.4.1. Relation between wetted perimeter and flow area for natural channel	59

Chapter		Page
	3.4.2. Resistance equations for natural watersheds	59
	3.4.3. Flow discharge and flow area relations	66
	3.5. Applications	66
	3.5.1. Input data	67
	3.5.1.1. Basin characteristics data	67
	3.5.1.2. Storm characteristics data	73
	3.5.2. Model calibration	74
	3.5.3. Test results	79
	3.5.4. Sensitivity analysis	86
	3.5.5. Applications to predict watershed treatment effects	86
	3.6. Summary	91
IV	MECHANICS OF OVERLAND FLOW SOIL EROSION	94
	4.1. Need for the Study	94
	4.2. Sediment Routing Procedure	94
	4.2.1. Sediment transport equation	95
	4.2.2. Degradation and aggradation	99
	4.3. Applications	101
	4.3.1. Experimental data by Kilinc and Richardson	102
	4.3.2. Estimation of coefficient	102
	4.3.3. Mean erosion rate and sediment hydrographs	106
	4.3.4. Land form evolution and effect of slope shape on erosion rate	112
	4.4. Summary	116
V	STREAM MORPHOLOGY OF SMALL WATERSHEDS	118
	5.1. Governing Physical Process	118
	5.2. Theoretical Development	120
	5.2.1. Threshold conditions in the watershed	120
	5.2.2. The "threshold" channel section	122
	5.2.3. Geometry of the threshold channel	126
	5.2.3.1. Top width	126
	5.2.3.2. Cross-sectional area	126
	5.2.3.3. Wetted perimeter	127
	5.2.3.4. Hydraulic depth	128
	5.2.3.5. Hydraulic radius	128
	5.2.4. Hydraulic geometry of the threshold section	129
	5.2.4.1. Downstream relations	131
	5.2.4.2. At-a-station relations	133
	5.3. Field Observations	138
	5.3.1. Validity of assumptions	138
	5.3.2. Hydraulic geometry equations	141
	5.4. Summary	144

Chapter		Page
VI	CONCLUSIONS	146
	REFERENCES	151
	Appendix A: INTEGRATION OF SUSPENDED SEDIMENT LOAD	156
	A.1. Need for the Method	156
	A.2. Power Series Expansion	157
	A.2.1. Derivation	157
	A.2.2. Comparison between power series and Simpson's formula	161
	A.2.3. Criterion for convergence of new method	166
	A.3. Summary	168
	Appendix B: CALIBRATION TECHNIQUE FOR SYSTEM MODELING	170
	B.1. Need for the Technique	170
	B.2. Minimization Problem	171
	B.3. One-Dimensional Calibration Technique	172
	B.4. Multi-Dimensional Calibration Technique	177
	B.5. Summary	181
	Appendix C: LISTINGS OF COMPUTER PROGRAMS	183
	C.1. PROGRAM WATER: Rainfall-Runoff Model	183
	C.2. PROGRAM SEDIM: Rainfall-Erosion Model	193
	C.3. PROGRAM UNIMO: One-Dimensional Calibration Technique	200
	C.4. PROGRAM BROSEN: Multi-Dimensional Calibration Technique	205

LIST OF TABLES

Table		Page
3.1	Rain Reaching the Ground	43
3.2	Geometry of Carrizal Basin, Venezuela	69
3.3	Computational Sequence	70
3.4	Rainfall Records for Storms used in Analysis	75
3.5	Estimated Values of ψ_g, I_s and $m_o(o)$	77
3.6	Summary of Estimated Errors in Water Hydrograph Simulation	85
3.7	Sensitivity Analysis of the Rainfall-Runoff Model.	87
4.1	Summary of Experimental Data by Kilinc and Richardson (1973)	103
4.2	Summary of Regression Results for Sediment Transport Equation	106
4.3	Summary of Estimated Errors in Soil Erosion Simulation	111
5.1	Values of the Q Exponent in the Hydraulic Geometry Equations	144
B.1	Summary of Search Path for Each Stage	181

LIST OF FIGURES

Figure		Page
2.1	Rectangular network in x - t plans	16
2.2	Comparison of numerical results with analytical solutions	24
2.3	Relation between error in continuity and time to space increment ratio	26
2.4	Relation between mean absolute error and time to space increment ratio	27
2.5	Example of overland flow modeling for small Reynolds number.	29
2.6	Example of overland flow modeling for large Reynolds number	31
2.7	Flood routing in the Río Amana in Venezuela	33
2.8	Runoff from SPL 1 parking area, Johns Hopkins University	35
3.1	Rainfall-runoff model flow chart	38
3.2	Example of geometric segmentation	40
3.3	Rain reaching ground	42
3.4	Control volume on the ground	47
3.5	Control volume below the ground	47
3.6	Schematic diagram of moisture distribution	51
3.7	Typical representation of soil-moisture depletion curve	53

Figure		Page
3.8	Cumulative distribution function of infiltration rate	55
3.9	Typical wetted perimeter-flow area relation for channels in Carrizal Basin, Venezuela	60
3.10	Schematic diagram of resistance to flow in natural watersheds	61
3.11	Geometric segmentation of the Carrizal Basin, Venezuela	68
3.12	Ground cover resistance for tested storms	78
3.13	Computed maximum infiltration rates for July 9 storm	80
3.14	Hydrograph of Carrizal Basin, Venezuela	81
3.15	Effects of canopy cover density on outflow hydrographs	89
3.16	Effects of ground cover density on outflow hydrographs	90
4.1	Comparison between computed and measured mean erosion rate	107
4.2	Time-dependent erosion rate for different slopes (rainfall intensity 3.65 in/hr)	109
4.3	Time-dependent erosion rate for different rainfall intensity (bed slope 30 percent)	110
4.4	Example of land form evolution	113

Figure		Page
4.5	Definition sketch of slope shape	114
4.6	Effect of slope shape on erosion rate	115
5.1	Cross-sectional geometry for the threshold channel	123
5.2	Dimensionless geometric-coefficients for the threshold channel	130
5.3	Geometry for a partially-full threshold channel	134
5.4	Power functions for the hydraulic geometry of the partially-full threshold channel . . .	137
5.5	The variation of exponents in the at-a-station hydraulic geometry equations with angle of repose	139
5.6	The variation of exponents in the at-a-station hydraulic geometry equations with the lift-to-drag ratio	140
5.7	Downstream variation of the width-to-depth ratio for threshold channel	142
5.8	Downstream variation of the product of hydraulic depth and bed slope for threshold channel	143
A.1	Variation of percentage deviation with exponent ω (G = 0.5)	163
A.2	Variation of percentage deviation for first and tenth order approximation	164

Figure		Page
A.3	Relation between percentage deviation for J_1 and order of approximation (G = 0.9)	165
A.4	Relation between computer time and order of approximation	167
A.5	Variation of order of approximation and percentage deviation for convergence limit 10^{-3}	169
B.1	Quadratic approximation for unidimensional search	174
B.2	Search path for the sample problem	178

LIST OF SYMBOLS

Symbol	Description
A or $A(x,t)$	cross-sectional area of flow
A^* or $A^*(x,t)$	true value of A in the numerical computation
A_o	flow area of bankful flows or the threshold discharge
A_1	total projected area perpendicular to flow to describe bed form resistance for an area
A_2	total projected area perpendicular to flow to describe ground cover resistance for an area
A_g^c	area with ground cover within area A_t^c
A_t^c	total area covered by trees in an overland flow unit
A_j^n	quantity of A at grid point $x = j\Delta x$, $t = n\Delta t$
A_g^o	area with ground cover within area A_t^o
A_t^o	total area without trees in an overland flow unit
$A_i^{(k)}$	a function
$a(m,t)$	error-component amplitude in the numerical computation
$\overline{a}$	thickness of bed layer
a^*	optimal coefficient for quadratic approximation
a_1, a_1'	constants describing P - A relation
a_2, a_3	constants describing flow resistance
B	constant describing velocity profile which depends on boundary roughness
$B_1(k), B_2(k)$	some functions of k
b^*	optimal coefficient for quadratic approximation
b_1, b_1'	exponents describing P-A relation

Symbol	Description
b_2, b_3	exponents describing flow resistance
C	Chezy resistance coefficient
$C(k)$	a function of k
C_a	area coefficient, $\frac{A_o}{y_o T_o}$
C_d	drag coefficient
C_o	known sediment concentration at a distance $\bar{a}$ above the bed
C_p	wetted perimeter coefficient, $\frac{P_o}{y_o}$
C_s	sediment concentration in volume, $\frac{q_s}{q}$
C_t	width-to depth coefficient, $\frac{T_o}{y_o}$
C_ξ	sediment concentration at the distance ξ from the bed
C_1, C_2, C_3	some constants of integration
$(C_s y)_j^n$	quantity of $C_s y$ at grid point $x = j\Delta x$, $t = n\Delta t$
D	hydraulic depth for the partially-full threshold channel, $\frac{A}{T}$
$D(k)$	a function of k
D_c	canopy cover density, ratio of the area covered by trees to the total area
D_g	ground cover density, ratio of the area covered by ground cover to the total area
D_o	hydraulic depth at threshold discharge, $\frac{A_o}{T_o}$
d_s	particle size
d_{50}	size of the sediment on the bed of which 50 percent is finer by weight

Symbol	Description
E	mean evaporation rate from the interception storages
$E(k)$	a function of k
E_a	relative mean absolute error (percent)
E_p	percentage error in the peak flow (percent)
E_t	percentage error in the time to peak flow (percent)
E_v	percentage error in the total volume (percent)
$\overline{E}_a$	mean absolute error
$F(\cdot)$	optimization function
F_d	drag force on the particle
F_ℓ	lift force on the particle
f	Darcy-Weisbach fraction factor for grain resistance
f'	overall Darcy-Weisbach friction factor
$f(\cdot)$	a function
f_b	added friction factor due to bed form resistance
f_g	added friction factor due to ground cover drag resistance
f_i	infiltration rate
$f_m(t)$	maximum infiltration rate at time t
$f_m^c(t)$	maximum infiltration rate at time t for areas under canopy
$f_m^o(t)$	maximum infiltration rate at time t for areas without trees
$\overline{f}_i^c(t)$	average infiltration rate at time t for areas under canopy

Symbol	Description
$\bar{f}_i^o(t)$	average infiltration rate at time t for areas without trees
G	depth ratio, $\frac{\bar{a}}{y}$
$\bar{G}$	$\frac{G^{\omega-1}}{(1-G)^{\omega}} [(\frac{V}{V^*} + 2.5) J_1 + 2.5 J_2]$
g	gravitational acceleration
h	maximum depth of the partially-full channel
$\bar{h}$	magnitude of the ponded water head at the surface
I_s	initial interception storage content, ratio of the initial storage capacity to the total interception storage capacity
i or i(t)	rainfall rate (rainfall intensity) at time t
i_c or $i_c(t)$	rate at which rain is being stored in the canopy at time t
i_e	rainfall excess rate
i_g or $i_g(t)$	rate at which rain is being stored in the ground cover at time t
i_n	net rainfall rate
i_o	throughfall rate
$\bar{i}_e^c(t)$	average rainfall excess rate at time t for areas under canopy
$\bar{i}_n^c$ or $\bar{i}_n^c(t)$	average net rainfall rate at time t for areas under canopy
$\bar{i}_e^o(t)$	average rainfall excess rate at time t for areas without trees

Symbol	Description
$\bar{i}_n^o$ or $\bar{i}_n^o(t)$	average net rainfall rate at time t for areas without trees
$\bar{i}_e(t)$	overall mean rainfall excess rate at time t
$\bar{i}$	effective rainfall intensity for raindrop impact effects
J_1	$\int_G^1 (\frac{1-r}{r})^\omega \, dr$
J_2	$\int_G^1 (\frac{1-r}{r})^\omega \ell nr \, dr$
$J_1(k+1)$	partial sum of the first k+1 terms of the series solution for J_1 integral
$J_2(k+1)$	partial sum of the first k+1 terms of the series solution for J_2 integral
K_1, K_2, K_3, K_4, K_5	constants describing relations in the stream morphology
k	order of approximation or iteration
$\bar{k}$	$\frac{\tan \Phi}{\sqrt{1 + \tan^2 \phi - \bar{r}^2}}$
k_o	constant representing Darcy-Weisbach friction factor due to grain resistance without rainfall for $N_r \leq 900$
k_r	constant describing the added Darcy-Weisbach friction factor due to raindrop impact
k_s	saturated hydraulic conductivity, coefficient of permeability
k_1	constant representing Darcy-Weisbach friction factor due to grain resistance with rainfall for $N_r \leq 900$
k_2	constant representing Darcy-Weisbach friction factor due to grain resistance for $2,000 \leq N_r \leq 25,000$

Symbol	Description
k_3	constant representing Darcy-Weisbach friction factor due to grain resistance for $N_r \geq 100{,}000$
k_1'	constant describing overall Darcy-Weisbach friction factor for $N_r \leq 900$
k_2'	constant describing overall Darcy-Weisbach friction factor for $2{,}000 \leq N_r \leq 25{,}000$
k_3'	constant describing overall Darcy-Weisbach friction factor for $N_r \geq 100{,}000$
L	length of overland flow plot or channel reach
ℓ_g	average length of ground covers in the direction of flow
M	total number of segments in an overland flow plot
m_s	moisture content of the upper soil profile at saturation
m_w	moisture content of the upper soil profile at wilting point
$m_o(t)$	soil moisture content at time t
$m_o(0)$	antecedent moisture content
$m_o^c(t)$	current moisture content for areas under canopy
$m_o^o(t)$	current moisture content for areas without trees
N	number of time increments extending from the beginning to the end of the runoff event
N_f	number of function evaluation in the search by an optimization scheme
N_p	number of unknown parameters needed to be identified
N_r	flow Reynolds number, $\frac{QR}{\nu A}$

Symbol	Description
n	Manning's roughness coefficient
P	wetted perimeter
P_c	magnitude of the capillary potential head of the soil
P_d	percentage deviation
P_o	wetted perimeter of bankful flows or the threshold discharge
P_w	capillary potential head at wilting point
$\overline{P}_c(t)$	magnitude of the capillary potential head of the wetting front at time t
Q or $Q(x,t)$	flow discharge
Q^* or $Q^*(x,t)$	ture value of Q in the numerical computation
Q_o	threshold discharge or water discharge of bankful flows
Q_s	sediment discharge in the channel
$Q_a(t)$	analytical solution of outflow water discharge at time t
$Q_i(t)$	inflow water discharge at time t
$Q_m(t)$	measured runoff at time t
$Q_o(t)$	simulated runoff at time t
Q_{ap}	analytical solution of flow peak
Q_{mp}	measured flow peak
Q_{op}	simulated flow peak
Q_j^n	quantity of Q at grid point $x = j\Delta x$, $T = n\Delta t$
q	unit-width discharge
q_b	unit-width bed-load transport rate
q_ℓ	lateral inflow rate per unit length of channel
q_p	unit-width discharge at the end of soil plot
q_s	unit-width sediment transport rate

Symbol	Description
$q_{sm}(j)$	measured unit-width sediment discharge at the time j^{th} sample was taken
$q_{so}(j)$	simulated unit-width sediment discharge at the time j^{th} sample was taken
$q_{\ell\ j}^{n}$	quantity of q_ℓ at grid point $x = j\Delta x$, $t = n\Delta t$
$q_{s\ j}^{n}$	quantity of q_s at grid point $x = j\Delta x$, $t = n\Delta t$
$\bar{q}_s$	mean erosion rate
$\bar{q}_{so}$	simulated mean sediment discharge
R	hydraulic radius, $\frac{A}{P}$
R_o	hydraulic radius at the threshold discharge
r	$\frac{\xi}{y}$
$\bar{r}$	$\bar{\beta} \tan \phi$
r'	Q_{j+1}^{n+1}
r^k	value of r' at the k^{th} iteration
r^o	initial guess of r'
r^*	solution of r'
r_v	ratio of V_c to V_g
S_c	ratio of evaporating surface to the projected area for a tree canopy
S_f	friction slope
S_g	ratio of evaporating surface to the projected area for a typical ground cover
S_o	bed slope
S_q	amount of the integration of suspended load
$S_{o_j}^{n}$	quantity of S_o at grid point $x = j\Delta x$, $t = n\Delta t$

Symbol	Description
$\hat{S}_i(k)$	orthonormal directions for multi-dimensional search
s_s	specific gravity of sediment
T	top width
T_o	top width of the threshold channel
t	time
t_{mp}	measured time to peak flow
t_{op}	simulated time to peak flow
U_*	shear velocity, $\sqrt{\frac{\tau}{\rho}}$
u_ξ	point mean velocity at the distance ξ from the bed
V	mean velocity of flow
V_c	interception storage capacity of a tree canopy per unit area
V_g	interception storage capacity of the ground cover per unit area
V_o	mean velocity at the threshold discharge
V_p	mean flow velocity at the end of plot
V_s	settling velocity of the sediment particle
v_η	hypothetical infiltration velocity, local flow rate average over a finite area of the porous medium
$\overline{v}_\eta$	average value of v_η
W	width of a rectangular area
X	independent variable or parameter
$\overline{X}$	value of J_1 or J_2 computed by method of power series expansion

Symbol	Description
X^*	optimal value for F(X)
X_i	unknown parameters
X_ℓ	lower limit of X
X_u	upper limit of X
X_i^ℓ	lower limit of X_i
X_i^u	upper limit of X_i
x	downslope distance
Y	dependent variable
$\overline{Y}$	value of J_1 or J_2 computed by Simpson's Formula
y	depth of flow
y_o	maximum depth of flow
y_p	depth of flow at the end of soil plot
Z	independent variable
z	bed elevation
z_d	elevation at the downstream boundary
z_u	elevation at the upstream boundary
$z_{j+\frac{1}{2}}^n$	quantity of z at grid point $x = (j+\frac{1}{2})\Delta x$, $t = n\Delta t$
α	coefficient in A - Q relation
$\alpha_1, \alpha_2, \alpha_3$	regression coefficient
β	exponent in A - Q relation
$\overline{\beta}$	ratio of the lift and the drag forces
$\beta_1, \beta_2, \beta_3, \beta_1', \beta_2'$	coefficients in sediment transport equations
γ	specific weight of water
ΔX	step size in one-dimensional search
Δx	space increment

Symbol	Description
Δt	time increment
Δz	change in elevation
ΔG_s	change in ground water storage
ΔM_s	change in soil moisture storage
Δz_j^n	quantity of Δz at grid point, $x = j\Delta x$, $t = n\Delta t$
δ	error-free factor, $\alpha\beta[Q^*(x,t)]^{\beta-1}$
ε	convergence limit or tolerance
$\bar{\varepsilon}$	porosity of the sediment
η	ratio of h to y_o
$\bar{\eta}$ or $\bar{\eta}(t)$	magnitude of the gravitational potential head of the wetted front at time t
η'	magnitude of the gravitational potential head
$\eta^*(x,t)$	value of the error in $Q(x,t)$
η_a	depth of the zone of aeration
η_s	height of roughness
η_j^n	quantity of $\eta^*(x,t)$ at grid point $x = j\Delta x$, $t = n\Delta t$
θ	local side slope angle
θ'	angle between the channel bed and the horizontal direction
λ	time increment to space increment ratio, $\frac{\Delta t}{\Delta x}$
λ_1^*	optimal step size along direction i in the multi-dimensional search
ν	kinematic viscosity of water
ξ	distance from a reference point
$\xi^*(x,t)$	value of the error in $A(x,t)$

Symbol	Description
ξ_j^n	quantity of $\xi^*(x,t)$ at grid point $x = j\Delta x$, $t = n\Delta t$
ρ	density of water
σ	ratio of F_d to τ
τ	boundary shear stress or tractive force
τ_c	critical shear stress
τ_o	maximum tractive force
ϕ	angle of repose
Ψ	$2\pi m\Delta x/L$
ψ	constant representing the ratio of added friction factor to the grain resistance factor without rainfall
ψ_b	bed form resistance description, a constant representing the ratio for added friction due to bed forms
ψ_g	ground cover resistance description, a constant representing the ratio for added friction due to ground cover when the ground cover density is equal to unity
Ω	$\frac{\Delta t}{\Delta x} Q_j^{n+1} + \alpha(Q_{j+1}^n)^\beta + \Delta t\left(\frac{q_{\ell_{j+1}}^{n+1} + q_{\ell_{j+1}}^n}{2}\right)$
$\overline{\Omega}$	$1 - \eta + \overline{r}\eta$
ω	exponent for sediment concentration, $\frac{V_s}{0.4\ U^*}$

Chapter I

INTRODUCTION

1.1. General

The increasing interest in land and water resource plannings has stimulated the development of particular and general watershed response models. The models, whether physical or conceptual, are used to estimate physical quantities which describe the major watershed response to precipitation such as water yield, sediment yield, and resultant stream morphology. Methods to estimate water and sediment yield and changes in the watershed geometry are urgently needed for analyzing the economic feasibility of any proposed water resources or land use development and for predicting possible adverse environmental effects associated with the proposed development.

The physical processes governing watershed response are very complicated. Many past studies have utilized a statistical interpretation of observed response data. The unit hydrograph method for water routing, the universal soil loss equation for soil erosion, and the hydraulic geometry equations for stream morphology are examples of these types of studies. It is difficult to predict the response of a watershed to various watershed developments or treatments using these methods. Because they are based on the assumption of homogeneity in time and space. Numerical modeling using the governing physical process is a viable way to estimate the time-dependent response of watersheds to precipitation with varying vegetative covers and land use.

The purpose of this study is to provide the theoretical background and numerical methods for modeling physical processes governing

watershed behavior. The objectives are: (1) To establish a simple flow routing procedure which can be applied to both overland flows and channel flows; (2) to develop a rainfall-runoff simulation model using the physical processes involved; (3) to present a mathematical simulation model for soil erosion using the physical processes which govern the mechanics of soil erosion by overland flow; and (4) to theoretically derive both downstream and at-a-station hydraulic geometry equations which describe the stream morphology response to precipitation.

1.2. Review of Related Literature

1.2.1. Water yield and flow routing

There are two approaches to water yield modeling. One is the lumped parameter approach, also called the "black box" model. Examples are those which have been developed by Sherman (1932), Wu (1963), Singh (1964), Prasad (1967), and others. The second is the distributed parameter approach or the physical process simulation model. Examples of this approach are Crawford and Linsley (1966), Schaake, Jr. (1971), and Dawdy et al. (1972).

In a lumped parameter model, the watershed is conceptually considered as a "black box" system. The input is the rainfall function; the output is the runoff. The "black box" represents the aggregation of the parameters chosen to give the correct output for a given input. The parameters may or may not be physically significant. Lumped models can be further subdivided into two types: (1) the transfer function model, (for example, Sherman, 1932, Wu, 1963, and Singh, 1964) and (2) the analytical conceptual model (for example, Prasad, 1967).

The most familiar transfer function model is the unit hydrograph, first developed by Sherman (1932). Its popularity lies mainly in its

simplicity of application. The unit hydrograph is assumed to be representative of the particular watershed. The disadvantage of this approach is that a particular unit hydrograph is dependent on the duration of the storm used to synthesize it. This weakness has led to the development of the instantaneous unit hydrograph which is based on effective rainfall of an infinitesimally small duration. A direct runoff hydrograph can be synthesized from the instantaneous unit hydrograph and rainfall excess through the use of the linear convolution integral (see Chow, 1964). In attempts to improve the unit hydrograph approach, some investigators (for example, Singh, 1964) have explored the possibilities of developing nonlinear models within the transfer function framework.

The basis of the analytical conceptual models is the assumption of a single mathematical relation between rainfall and runoff. The unknown parameters are determined by calibration using an optimization scheme (for example, Labadie and Dracup, 1969). As the model is conceptual, the form of the mathematical frame work is subjective.

Use of digital computers makes it possible to employ many mathematical approximations of the complicated physical processes describing the precipitation-runoff relation. Crawford and Linsley (1966) were the first investigators to develop a simulation water-yield model, and their efforts led to the well-known Stanford Watershed Model. Many similar models have been developed, and the more popular models are the Stanford Watershed Model IV (Crawford and Linsley, 1966), the USGS Rainfall-Runoff Simulation Model (Dawdy et al., 1972), and the Schaake Model (1971). These models are based on bulk-parameter

approximation to the physical laws governing surface runoff and are calibrated with optimization schemes.

The Stanford Watershed Model IV can be used to predict stream flow resulting from rainstorm or snowmelt. The required data are: (1) hourly rainfall data and 15-minute rainstorm data; (2) daily potential evapotranspiration data; (3) topography and watershed geometry data; (4) data required to describe initial conditions; and (5) mean daily stream flow data for model calibration. If snowfall is significant, two additional data are needed: (1) observed incoming daily short-wave radiation; and (2) daily maximum and minimum temperature. This model is both a water yield and water routing model. In the model, precipitation is stored in snowpack or in three soil moisture storage areas. These areas are the upper and lower zone storage areas, and the groundwater storage area. The three storage zones represent variable soil moisture profiles and groundwater conditions. The upper and lower storage zones control overland flow, infiltration, and interflow to the groundwater storage. The upper zone simulates the initial watershed response to rainfall and is of major importance for smaller storms, and for the first few hours of larger storms. The lower zone controls watershed response to major storms by controlling longer-term infiltration rates. Groundwater storage supplies base flow to stream channels. Evaporation and transpiration processes may be supplied with water from all of these three storage areas. The total channel inflow from overland flow, interflow, and groundwater enters the channel system and emerges as synthesized stream flow. The routing component in this model is divided into the overland flow part and channel flow part. The kinematic-wave approximation is used for

overland flow routing and a modified form of Clark's (1945) instantaneous unit hydrograph method is used for channel flow routing. The Stanford Watershed Model has been used for many watershed conditions.

The USGS Rainfall-Runoff Simulation Model can be used to predict stream flow from rainstorms. The number of parameters involved in this model are fewer than those needed for the Stanford Watershed Model. The required data in the USGS Model are: (1) daily rainfall data and 15-minute rainstorm data; (2) daily pan evaporation data; (3) topography and watershed geometry data; (4) data describing the initial conditions, and (5) daily stream flow data for model adjustment. This model deals with three components; antecedent moisture, infiltration, and surface runoff of the hydrologic cycle. The antecedent moisture accounting component is a more sophisticated version of the antecedent precipitation index, which is designed to determine the initial infiltration rate for a storm. The infiltration component uses the Philip equation. The surface runoff routing is based on Clark's (1945) instantaneous unit hydrograph method. Dawdy et al. (1972) reported that the accuracy of their model was within ±20 percent.

The Schaake Model is the simplest of the three and can be used to predict runoff from small drainage areas only. This model is more suitable for analyzing urban drainage areas than natural watersheds. The required data are: (1) minute rainfall data; (2) constants to describe the infiltration equation; (3) topography and drainage area geometry data; and (4) runoff data for model adjustment. This model computes the rainfall excess and then routes the surface runoff using the linear kinematic-wave approximation.

The flow routing component is essentially the weak link of the existing physical process simulation models. This weakness prevents

the coupling of existing water routing models with a sediment routing model. Although a number of numerical methods are available for solving unsteady gradually varied flow problems, (Morgali and Linsley, 1965, Brakensiek et al., 1966, Schaake, Jr., 1965, Liggett and Woolhiser, 1967, and Chen, 1973), there is difficulty of applying these available techniques in modeling watershed response because of one or a combination of the following reasons.

(1) The linearized numerical scheme is sometimes unstable, especially for the case of supercritical flow which frequently occurs in overland flows or steep channel flows.

(2) There are insufficient boundary conditions for the numerical scheme. Many schemes require downstream boundary conditions which are usually not available.

(3) Many numerical schemes are too complicated to apply for large-scale modeling.

A simple but practical numerical method which can be applied in a wide variety of both overland flows and channel flows is needed to cope with these difficulties.

1.2.2. Soil erosion

For a complex problem such as the estimation of soil erosion from uplands, the regression technique is a quick and effective way to analyze data. Thus many soil-loss regression equations have been developed (for example, Zingg, 1940, Musgrave, 1947, Wischmeier and Smith, 1965, Meyer and Kramer, 1968, Young and Mutchler, 1969, and Kilinc and Richardson, 1973). However, regression equations are

restricted to the conditons of the experimental data. Therefore, it is difficult to transfer the knowledge to other areas. The general form of regression equations is a power function, which assumes that the soil erosion is the result of multiplicative contributions of the governing factors. The important governing factors have been identified as the rainfall characteristics, the soil erodibility, the slope length, the percent slope, the cropping-management factor, and the conservation practice factor.

The exponents in the soil loss equations were originally determined by regression analysis. More recently, Li, Shen, and Simons (1973) demonstrated that these exponents can be derived from the equations governing the physical process of overland flow.

1.2.3. Stream morphology

Stream morphology has been studied by many investigators (Leopold and Maddock, 1953, Wolman, 1955, Brush, 1961, Leopold and Langbein, 1962, Simons and Albertson, 1960, and Henderson, 1963).

Leopold and Maddock (1953) defined the power functions relating the width, depth, slope and velocity to water discharge as the hydraulic geometry equations of the channel. Most of the other studies have involved the statistical interpretation of these power relations. Very limited theoretical work has been done to explain the mechanistic development processes of stream forms. In 1962, Leopold and Langbein offered the concept of entropy in landscape evolution but the analogy between entropy in thermodynamic systems and processes in stream channels is not apparent. In 1963, Henderson applied the theory of the "threshold" stable channel to natural channels in coarse alluvium and concluded that some remarkable similarities existed between "threshold"

theory and the Lacey "regime" theory which was developed from canal data in India. A further theoretical interpretation of river channel shapes is needed as a step toward better understanding of stream morphology.

1.3. Scope of Present Study

The first part of this dissertation is devoted to the development of a nonlinear kinematic-wave routing procedure. This simple procedure is used to compute both overland and channel flows. The routing is accomplished by a combination of a second order nonlinear and a linear scheme. A linear numerical scheme is employed to obtain a first approximation of flow conditions which are then refined by the nonlinear scheme. The nonlinear portion of the method ensures convergence and the linear portion guarantees a rapid convergence to the correct numerical answer. Instead of admitting computational errors in linear approximations to the full flow equation, this method minimizes numerical computation errors, but admits errors resulting from the limitations of the kinematic-wave approximation.

In the second part of the dissertation, a rainfall-runoff model is presented. This model simulates the land surface hydrologic cycle and consists of two parts. The first is the water balance component, the second part is the water routing componenet. The water balance component of the model determines the rainfall excess from considerations of processes which govern interception, evaporation and infiltration. The water routing component routes the water as overland flows and then as channel flow. Emphasis is on the mechanics of water routing and the model is set up for single storm hydrograph computations.

No attempt has been made to simulate the long-term water balance in the watershed.

The third part of the dissertation deals with the estimation of soil erosion by overland flow. A mathematical model is proposed. This model couples sediment routing with the water routing procedure and is able to simulate the sediment hydrograph and the changing land forms. The soil-erosion model presented in this study is the first step toward sediment yield simulation.

The last part of the dissertation is an extension of the work on stable channel design by Lane, Lin and Liu (1959). The basic equations describing threshold channel shape are employed to derive the hydraulic geometry equations of a stream channel in coarse alluvium. Both downstream and at-a-station relations are developed. This work provides useful information on stream morphology response to modified amounts of precipitation or to watershed treatment effects.

Chapter II

NONLINEAR KINEMATIC-WAVE APPROXIMATION FOR FLOW ROUTING

2.1. Governing Equations

Runoff from a catchment may be described by the equation of continuity, the equation of motion, and equations describing the law of resistance. The governing equations employed in the nonlinear routing scheme are described below.

2.1.1. Continuity equation

The equation of continuity for water flow can be expressed as

$$\frac{\partial Q}{\partial x} + \frac{\partial A}{\partial t} = q_\ell \qquad (2.1)$$

in which Q is the discharge, x is the downslope distance, A is the cross-sectional area of flow, t is the time and q_ℓ is lateral inflow rate per unit length of channel.

2.1.2. Momentum equation

If the gradients due to local and convective accelerations are assumed to be negligible, and if the water surface slope is assumed equal to the bed slope the momentum equation is

$$S_o \approx S_f = f \frac{Q^2}{8gRA^2} \qquad (2.2)$$

in which S_o is the bed slope, S_f is the friction slope, f is the Darcy-Weisbach friction factor, g is the gravitational acceleration, and R is the hydraulic radius. Equation 2.2 is called the kinematic wave representation of runoff movement. By definition

$$R = \frac{A}{P} \qquad (2.3)$$

in which P is the wetted perimeter. Usually the wetted perimeter can be expressed as a power function of flow area; i.e.,

$$P = a_1 A^{b_1} \tag{2.4}$$

where a_1 and b_1 are constants.

If Manning's equation is used, the momentum equation is

$$S_o \approx S_f = n^2 \frac{Q^2}{2.21 R^{4/3} A^2} \tag{2.5}$$

in which n is Manning's roughness coefficient.

2.1.3. Resistance equations

The Darcy-Weisbach friction factor f for open channel or overland flow on rigid boundaries is a function of the roughness of the boundary, the depth of flow, the rainfall intensity and the flow Reynolds numbers. By definition, the flow Reynolds number, N_r, is

$$N_r = \frac{QR}{\nu A} \tag{2.6}$$

in which ν is the kinematic viscosity of the fluid.

The friction factor--Reynolds number--relative roughness relation is presented in many fluid mechanics textbooks (for example, Daily and Harleman, 1966, p. 274). The Darcy-Weisbach friction factor is expressed in equation form only for certain ranges of Reynolds number.

The effect of rainfall on flow resistance is a major factor in shallow water routing. For shallow flows, the impact of raindrops in the flow causes energy losses in addition to those caused by the rigid boundary. Shen and Li (1973) have experimentally determined equations for Darcy-Weisbach friction factors for flow with rainfall impact. The general form of the equations is

$$f = \frac{a_2}{N_r^{b_2}} \tag{2.7}$$

in which a_2 and b_2 are functions of the rainfall intensity, the boundary roughness, and the flow Reynolds number.

For $N_r \leq 900$,

$$f = \frac{k_1}{N_r} = \frac{k_o + k_r i^{0.41}}{N_r} \tag{2.8}$$

in which k_1 is a parameter which varies with rainfall intensity, k_o is a constant representing the Darcy-Weisbach friction factor without rainfall, i is the rainfall intensity in inches per hour, and k_r is a number dependent on the raindrop velocity. Shen and Li (1973) have determined that k_r is equal to 27 for a raindrop fall of 8 ft.

For $N_r \geq 2000$ Shen and Li (1973) found that the friction factor was not affected by rainfall. The friction factor then may be approximated by the Blasius form of the resistance equation which is

$$f = \frac{k_2}{N_r^{0.25}} \tag{2.9}$$

in which k_2 is a constant.

In the transition range, $900 < N_r < 2000$, an estimation of friction factor is made by a linear interpolation. Interpolating from the end points of Eq. 2.8 and Eq. 2.9 one obtains the expression,

$$f = \frac{k_1 \, 900^{(1.25 \, \ell n \frac{k_1}{k_2} - 7.14)}}{N_r^{(1.25 \, \ell n \frac{k_1}{k_2} - 6.14)}} \tag{2.10}$$

The effect of flow Reynolds number on the friction factor decreases as the flow Reynolds number increases. For moderate-sized boundary roughness, the exponent, b_2 in Eq. 2.7 approaches zero for Reynolds number about 10^5, and the friction factor is independent of flow Reynolds number.

Additional resistance equations to describe the resistance to flow in natural watersheds in the form of Darcy-Weisbach friction equation are given in Chapter III. Those resistance equations for natural watersheds cover a much wider range of flow Reynolds number and include form resistance due to bed deformation and ground cover.

Manning's equation is frequently used by hydraulic engineers to describe flow in open channels. The Manning's roughness coefficient is usually determined by measurement. It can be expressed as a power function of flow discharge; i.e.,

$$n = a_3 Q^{b_3} \tag{2.11}$$

in which a_3 and b_3 are constants.

2.1.4. Discharge and flow area relation

In general, the flow cross-sectional area can be expressed as a power function of discharge or

$$A = \alpha Q^{\beta} \tag{2.12}$$

in which α and β are coefficients whose values depend on the shape and roughness of the channel.

If the Darcy-Weisbach friction factor is used, the values of α and β can be determined by first substituting Eqs. 2.3, 2.4, 2.6, and

2.7 into Eq. 2.2 and then comparing with Eq. 2.12. The solutions are

$$\alpha = \left[\frac{a_2 \nu^{b_2} a_1^{(1+b_2)}}{8gS_o} \right]^{\left(\frac{1}{3-b_1-b_1b_2}\right)} \tag{2.13}$$

and

$$\beta = \frac{2-b_2}{3-b_1-b_1b_2} \tag{2.14}$$

For overland flows or for very wide channel flow, the wetted perimeter is constant so that $b_1=0$ and $\beta = \frac{2-b_2}{3}$. As b_2 is generally greater than zero, the value of β is less than 2/3. For $N_r < 900$, the value of β is 1/3.

If Manning's equation is applied, the corresponding α and β are determined by using Eqs. 2.4, 2.5 and 2.11. The values are

$$\alpha = \left(\frac{a_1^{4/3} a_3^{2}}{2.21\ S_o} \right)^{\left(\frac{3}{10-4b_1}\right)} \tag{2.15}$$

and

$$\beta = \frac{3-3b_3}{5-2b_1} \tag{2.16}$$

The value of β for rivers is usually less than 1.0, and the average value of β for stable channels as deduced by Simons and Albertson (1960) is 0.87.

2.2. Numerical Scheme

The analytical solutions of Eq. 2.1 and Eq. 2.12 are available for the case of constant rainfall and constant channel roughness factor. At the present time, numerical solutions are necessary for the case of time-variant inflows. Herein, a nonlinear scheme with an iterative procedure is used to obtain solutions to the more complex cases of time-variant inflows and varying roughness. A linear scheme is also used to obtain the initial estimate for the nonlinear scheme.

2.2.1. Nonlinear scheme

The finite-difference forms of Eq. 2.1 can be represented as (see Fig. 2.1)

$$\frac{Q_{j+1}^{n+1} - Q_j^{n+1}}{\Delta x} + \frac{A_{j+1}^{n+1} - A_{j+1}^{n}}{\Delta t} = \frac{q_{\ell}{}_{j+1}^{n+1} + q_{\ell}{}_{j+1}^{n}}{2} \qquad (2.17)$$

in which Q_j^n is the quantity Q at grid point $x = j\Delta x$, $t = n\Delta t$ and Δx is the space increment and Δt is the time increment.

The unknowns in Eq. 2.17 are Q_{j+1}^{n+1} and A_{j+1}^{n+1}, but the discharge bears definite relation with flow area as indicated in Eq. 2.12. With two equations, the two unknowns can be obtained.

Either Q or A can be selected as the independent variable in the numerical procedure. According to the custom in backwater computations, the depth of flow (equivalent to A above) is chosen as the independent variable (see Henderson, 1966 for example); but Q is a better choice for the following reason. By taking the logarithm of

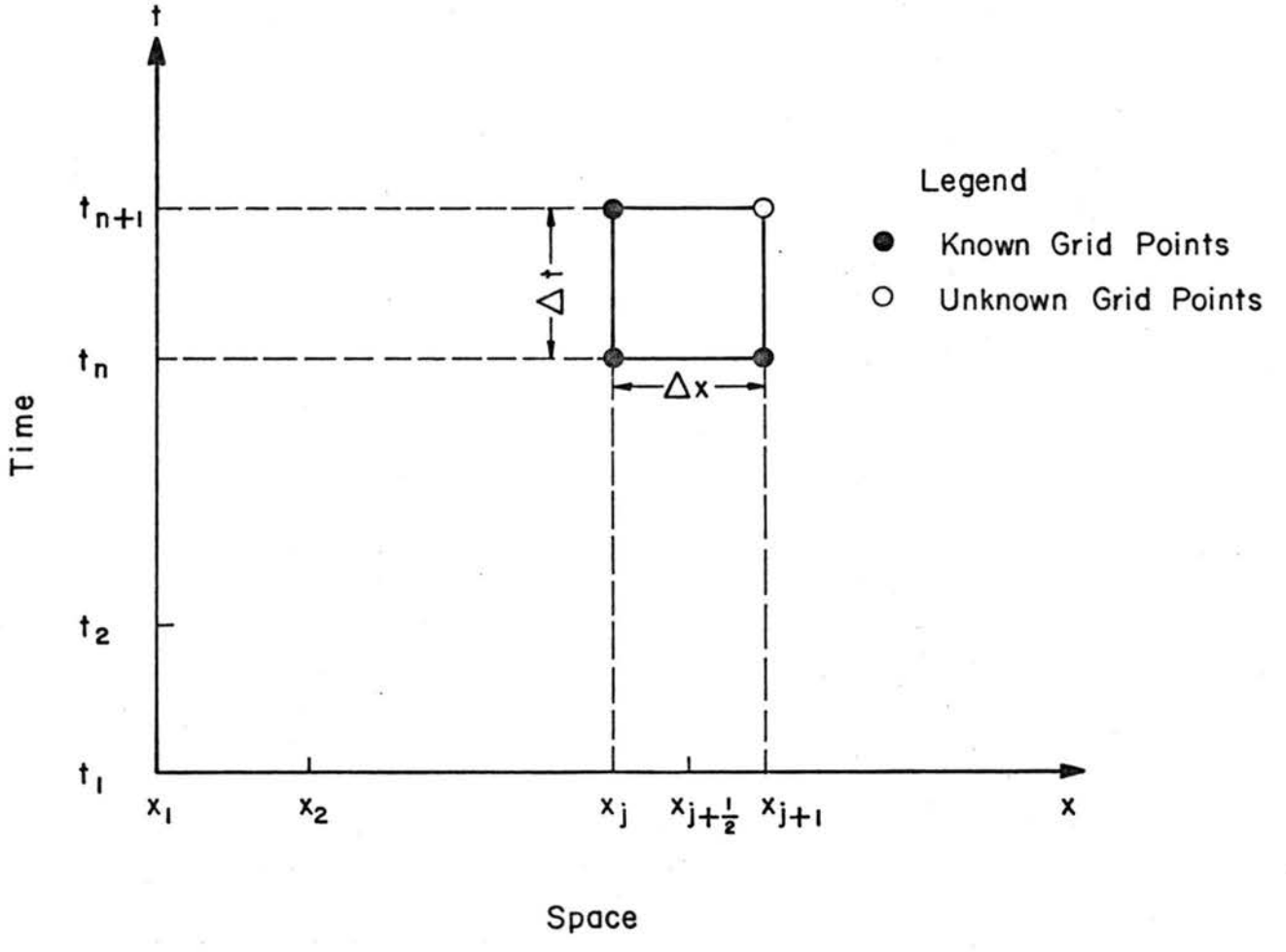

Fig. 2.1 Rectangular network in x-t plans

both sides of Eq. 2.12, one obtains

$$\ell nA = \ell n\alpha + \beta\, \ell n\, Q \tag{2.18}$$

The corresponding differential equation is

$$\frac{dA}{A} = \beta \frac{dQ}{Q} \tag{2.19}$$

As mentioned previously, β is generally less than 1.0 and has a value of one-third for Reynolds number less than 900. Consequently, if one computes discharge incorrectly, the relative error in the flow area is smaller than the relative error in the discharge. On the other hand, the error in the discharge estimation is magnified if the numerical computations were performed on the flow area. Therefore, the discharge is the better selection for the unknown in numerical computations. From the physical viewpoint, it is more appropriate to consider routing unit volumes of water rather than areas of flow.

From Eq. 2.12

$$A_{j+1}^{n+1} = \alpha (Q_{j+1}^{n+1})^{\beta} \tag{2.20}$$

and

$$A_{j+1}^{n} = \alpha (Q_{j+1}^{n})^{\beta} \tag{2.21}$$

Equations 2.20 and 2.21 are substituted in Eq. 2.17 and rearranged to yield

$$\frac{\Delta t}{\Delta x} Q_{j+1}^{n+1} + \alpha (Q_{j+1}^{n+1})^{\beta} = \frac{\Delta t}{\Delta x} Q_{j}^{n+1} + \alpha (Q_{j+1}^{n})^{\beta} + \Delta t \left(\frac{q_{\ell j+1}^{n+1} + q_{\ell j+1}^{n}}{2} \right) \tag{2.22}$$

The right side of Eq. 2.22 contains known quantities and is denoted by Ω, i.e.,

$$\Omega = \frac{\Delta t}{\Delta x} Q_j^{n+1} + \alpha (Q_{j+1}^n)^\beta + \Delta t \left(\frac{q_{\ell j+1}^{n+1} + q_{\ell j+1}^n}{2} \right) \tag{2.23}$$

Let $r' = Q_{j+1}^{n+1}$ and $\lambda = \frac{\Delta t}{\Delta x}$ so that the left side of Eq. 2.22 can be expressed as

$$f(r') = \lambda r' + \alpha r'^{\beta} \tag{2.24}$$

The solution to Eq. 2.22 is therefore the solution, r*, which satisfies the condition

$$f(r^*) = \lambda r^* + \alpha r^{*\beta} = \Omega \tag{2.25}$$

Equation 2.25 is nonlinear in r*. An approximate solution to this nonlinear equation is easily obtained by the following iterative scheme.

Let r^k be the value of r' at k-th iteration. The Taylor Series expansion of the function f(r) around r^k is

$$f(r') = f(r^k) + (r'-r^k) f'(r^k) + \frac{1}{2} (r'-r^k)^2 f''(r^k) + \frac{1}{6} (r'-r^k)^3 f'''(r^k) + \ldots \tag{2.26}$$

in which $f'(r^k)$ and $f''(r^k)$ are values of the first and second derivatives of the function at r^k.

Dropping the terms higher than third order, one obtains

$$f(r') \simeq f(r^k) + (r'-r^k) f'(r^k) + \frac{1}{2} (r'-r^k)^2 f''(r^k) \tag{2.27}$$

The purpose of iteration is to force $f(r^{k+1})$ to approach the value of Ω, or

$$\Omega \simeq f(r^k) + (r^{k+1} - r^k) f'(r^k) + \frac{1}{2} (r^{k+1}-r^k)^2 f''(r^k) \tag{2.28}$$

The solution of Eq. 2.28 is

$$r^{k+1} = r^k - \frac{f'(r^k)}{f''(r^k)} \pm \sqrt{\left(\frac{f'(r^k)}{f''(r^k)}\right)^2 - \frac{2(f(r^k)-\Omega)}{f''(r^k)}} \qquad (2.29)$$

in which

$$f(r^k) = \lambda r^k + \alpha(r^k)^\beta \qquad (2.30)$$

$$f'(r^k) = \lambda + \alpha\beta(r^k)^{\beta-1} \qquad (2.31)$$

and

$$f''(r^k) = \alpha\beta(\beta-1)(r^k)^{\beta-2} \qquad (2.32)$$

There are two solutions to Eq. 2.29. It is advisable to choose the solution which gives the smaller value of $|f(r^{k+1}) - \Omega|$. The above iteration is continued until the absolute error $|f(r^{k+1}) - \Omega|$ is less than a preassigned tolerance ε; i.e., the termination criterion is

$$|f(r^{k+1}) - \Omega| \leq \varepsilon \qquad (2.33)$$

An appropriate value for ε is 0.01Ω. However, it may be changed according to the purpose of individual problems.

The initial guess, r^o, is the key to the speed of convergence to the correct numerical solution. The best way of determing r^o is to use a linear scheme.

2.2.2. Linear scheme

The term $\frac{\partial A}{\partial t}$ in Eq. 2.1 can be expressed as

$$\frac{\partial A}{\partial t} = \frac{\partial A}{\partial Q}\frac{\partial Q}{\partial t} \qquad (2.34)$$

Also, from Eq. 2.12

$$\frac{\partial A}{\partial Q} = \alpha\beta Q^{\beta-1} \tag{2.35}$$

The substitution of Eqs. 2.35 and 2.34 into Eq. 2.1 yields

$$\frac{\partial Q}{\partial x} + \alpha\beta Q^{\beta-1}\frac{\partial Q}{\partial t} = q_\ell \tag{2.36}$$

The finite-difference forms of Eq. 2.36 is given by the expression

$$\frac{Q_{j+1}^{n+1} - Q_j^{n+1}}{\Delta x} + \alpha\beta\left(\frac{Q_{j+1}^{n} + Q_j^{n+1}}{2}\right)^{\beta-1}\frac{Q_{j+1}^{n+1}-Q_{j+1}^{n}}{\Delta t} = \frac{1}{2}\left(q_{\ell j+1}^{n+1} + q_{\ell j+1}^{n}\right) \tag{2.37}$$

$$r^o = Q_{j+1}^{n+1} = \frac{\lambda Q_j^{n+1} + \alpha\beta Q_{j+1}^{n}\left(\frac{Q_{j+1}^{n} + Q_j^{n+1}}{2}\right)^{\beta-1} + \Delta t\left(\frac{q_{\ell j+1}^{n+1} + q_{\ell j+1}^{n}}{2}\right)}{\lambda + \alpha\beta\left(\frac{Q_{j+1}^{n} + Q_j^{n+1}}{2}\right)^{\beta-1}} \tag{2.38}$$

Equation 2.38 provides the best initial estimate, r^o, for the nonlinear scheme. However, Eq. 2.38 is not applicable if both Q_{j+1}^{n} and Q_j^{n+1} are zero. When both Q_{j+1}^{n} and Q_j^{n+1} are zero, use $\beta = 1$ in Eq. 2.25 and then

$$r^o = \frac{\Omega}{\lambda+\alpha} \tag{2.39}$$

2.2.3. Stability

Suppose $\eta^*(x,t)$ and $\xi^*(x,t)$ are the values of the error in $Q(x,t)$ and $A(x,t)$ which occur at some time t in the computation. Then

$$\eta^*(x,t) = Q^*(x,t) - Q(x,t) \tag{2.40}$$

and

$$\xi^*(x,t) = A^*(x,t) - A(x,t) \tag{2.41}$$

in which Q^* and A^* represent the true values of the discharge and flow area, respectively.

From Eq. 2.12

$$A^*(x,t) = \alpha[Q^*(x,t)]^{\beta} \tag{2.42}$$

If A and Q are in error by the values of the error functions $\eta^*(x,t)$ and $\xi^*(x,t)$, then

$$\begin{aligned} A^*(x,t) - \xi^*(x,t) &= \alpha[Q^*(x,t) - \eta^*(x,t)]^{\beta} \\ &= \alpha[Q^*(x,t)]^{\beta}\left[1 - \frac{\eta^*(x,t)}{Q^*(x,t)}\right]^{\beta} \end{aligned} \tag{2.43}$$

Assuming that $\frac{\eta^*(x,t)}{Q^*(x,t)} << 1$, the power series expansion of $\left[1 - \frac{\eta^*(x,t)}{Q^*(x,t)}\right]^{\beta}$ is approximately $1 - \beta \frac{\eta^*(x,t)}{Q^*(x,t)}$. This substitution into Eq. 2.43 results in the expression

$$A^*(x,t) - \xi^*(x,t) = \alpha[Q^*(x,t)]^{\beta} - \alpha\beta[Q^*(x,t)]^{\beta-1}\eta^*(x,t) \tag{2.44}$$

When Eq. 2.44 is subtracted from Eq. 2.42, the result is

$$\xi^*(x,t) = \alpha\beta[Q^*(x,t)]^{\beta-1}\,\eta^*(x,t) = \delta\eta^*(x,t) \tag{2.45}$$

in which δ is the error-free factor $\alpha\beta[Q^*(x,t)]^{\beta-1}$. If at a given time, t_n, in the calculations, A_j^n and Q_j^n are in error by the value of error functions ξ_j^n and η_j^n, respectively, then A_j^{n+1} and Q_j^{n+1} will be in error by amounts ξ_j^{n+1} and η_j^{n+1}, respectively. When written for this case Eq. 2.17 becomes

$$\frac{Q_{j+1}^{n+1} + \eta_{j+1}^{n+1} - Q_j^{n+1} - \eta_j^{n+1}}{\Delta x} + \frac{A_{j+1}^{n+1} + \xi_{J+1}^{n+1} - A_{j+1}^{n} - \xi_{j+1}^{n}}{\Delta t}$$

$$= \frac{q_{\ell}{}_{j+1}^{n+1} + q_{\ell}{}_{j+1}^{n}}{2} \qquad (2.46)$$

When Eq. 2.17 is subtracted from Eq. 2.46, the result is

$$\lambda(\eta_{j+1}^{n+1} - \eta_j^{n+1}) + \xi_{j+1}^{n+1} - \xi_{j+1}^{n} = 0 \qquad (2.47)$$

By substituting Eq. 2.45 into Eq. 2.47, then

$$\lambda(\eta_{j+1}^{n+1} - \eta_j^{n+1}) + \delta(\eta_{j+1}^{n+1} - \eta_{j+1}^{n}) = 0 \qquad (2.48)$$

When decomposed x-wise into the Fourier series, the function $\eta^*(x,t)$ takes the form

$$\eta^*(x,t) = \sum_m a(m,t)\, e^{i2\pi mx/L} \qquad (2.49)$$

in which $a(m,t)$ is the error-component amplitude, L is the length of the reach being computed, and i is $\sqrt{-1}$. Substitution of Eq. 2.49 into Eq. 2.48 and examination of each Fourier component separately shows that

$$\lambda a(m,t_{n+1})e^{i2\pi m(x_j+\Delta x)/L} - \lambda a(m,t_{n+1})e^{i2\pi mx_j/L}$$

$$+ \delta a(m,t_{n+1})e^{i2\pi m(x_j+\Delta x)/L} - \delta a(m,t_n)e^{i2\pi m(x_j+\Delta x)/L} = 0 \qquad (2.50)$$

Following division by $\exp(i2\pi mx_j/L)$ and denoting $\Psi = 2\pi m\Delta x/L$, Eq. 2.50 reduces to

$$\lambda a(m,t_{n+1})e^{i\Psi} - \lambda a(m,t_{n+1}) + \delta a(m,t_{n+1})e^{i\Psi}$$

$$- \delta a(m,t_n)e^{i\Psi} = 0 \qquad (2.51)$$

Then

$$\left|\frac{a(m,t_{n+1})}{a(m,t_n)}\right| = \left|\frac{1}{1 + \frac{\lambda}{\delta}(1 - e^{-i\Psi})}\right| = \left|\frac{1}{1 + \frac{\lambda}{\delta} - \frac{\lambda}{\delta}\cos\Psi + i\frac{\lambda}{\delta}\sin\Psi}\right| \leq 1 \tag{2.52}$$

That is, the amplitude of the error decreases with succeeding time increment. Therefore the scheme represented by Eq. 2.17 is unconditionally stable.

2.2.4. Convergence

In order to test the convergence of this numerical scheme comparisons of numerical results with analytical solutions for a hypothetical case are made. In the hypothetical case, the bed slope is 0.005, the rainfall intensity is 3 in./hr, the rainfall duration is 5 min, and the Darcy-Weisbach friction factor is 0.07 and constant. The numerical results (Δt = 0.1 min and $\frac{\Delta t}{\Delta x}$ = 60 sec/ft) are compared with the analytical solution in Fig. 2.2. The agreement is excellent. The analytical solution is given by Streeter, 1966, p. 643.

In assessing the agreement, it is important to note three types of errors. These are the error in total volume, the error in shape of the hydrograph, and the error in the peak of hydrograph. The effect of the ratio of time increment to space increment, ($\Delta t/\Delta x$), on these errors is described as follows.

The error in total volume is defined as

$$E_v = 100\left[1 - \frac{\sum_{t=1}^{N} Q_o(t)\Delta t}{\sum_{t=1}^{N} Q_i(t)\Delta t}\right] \tag{2.53}$$

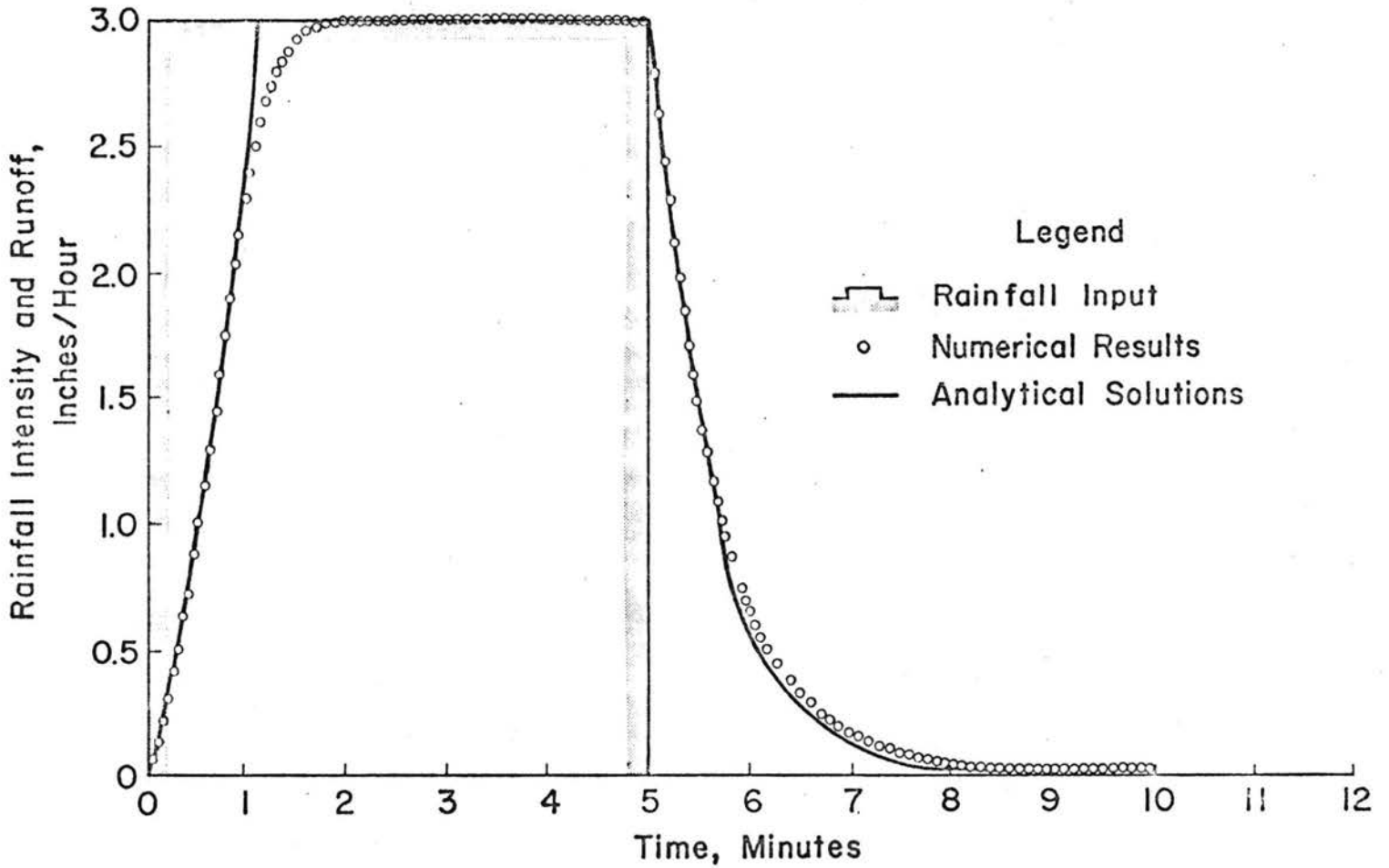

Fig. 2.2 Comparison of numerical results with analytical solutions

in which $\sum_{t=1}^{N} Q_o(t)\Delta t$ is the volume of the outflow hydrograph and $\sum_{t=1}^{N} Q_i(t)\Delta t$ is the volume of the inflow hydrograph being routed. The value $Q_i(t)$ is replaced by the rainfall input for overland flows. N is the number of time increments extending from the beginning to the end of the runoff event. The errors were computed for various values of $\frac{\Delta t}{\Delta x}$ for the hypothetical case described above. As shown in Fig. 2.3, the errors in total volume are generally less than 1.0 percent for a wide range of $\frac{\Delta t}{\Delta x}$.

The error in the shape of hydrograph may be represented by the mean absolute error; i.e.,

$$\overline{E}_a = \frac{1}{N} \sum_{t=1}^{N} |Q_a(t) - Q_o(t)| \qquad (2.54)$$

in which $Q_a(t)$ and $Q_o(t)$ are the analytical and numerical solution of the outflow discharge respectively. The variations of $\overline{E}_a$ with $\Delta t/\Delta x$ for the hypothetical case are given in Fig. 2.4. For a fixed Δt, $\overline{E}_a$ decreases as Δx decreases, and for a fixed Δx, $\overline{E}_a$ decreases as Δt decreases. Thus, in general, $\overline{E}_a$ decreases as Δt and Δx decrease. This is the desired nature of convergence. The mean absolute error in shape for the tested range of Δt and Δx is less than 0.3 in./hr or one-tenth of the maximum flow rate of 3 in./hr. Therefore, a wide range of $\Delta t/\Delta x$ may be used without introducing large errors in the shape of the outflow hydrograph.

The error in the peak flow is defined as

$$E_p = 100\left(1 - \frac{Q_{ap}}{Q_{op}}\right) \qquad (2.55)$$

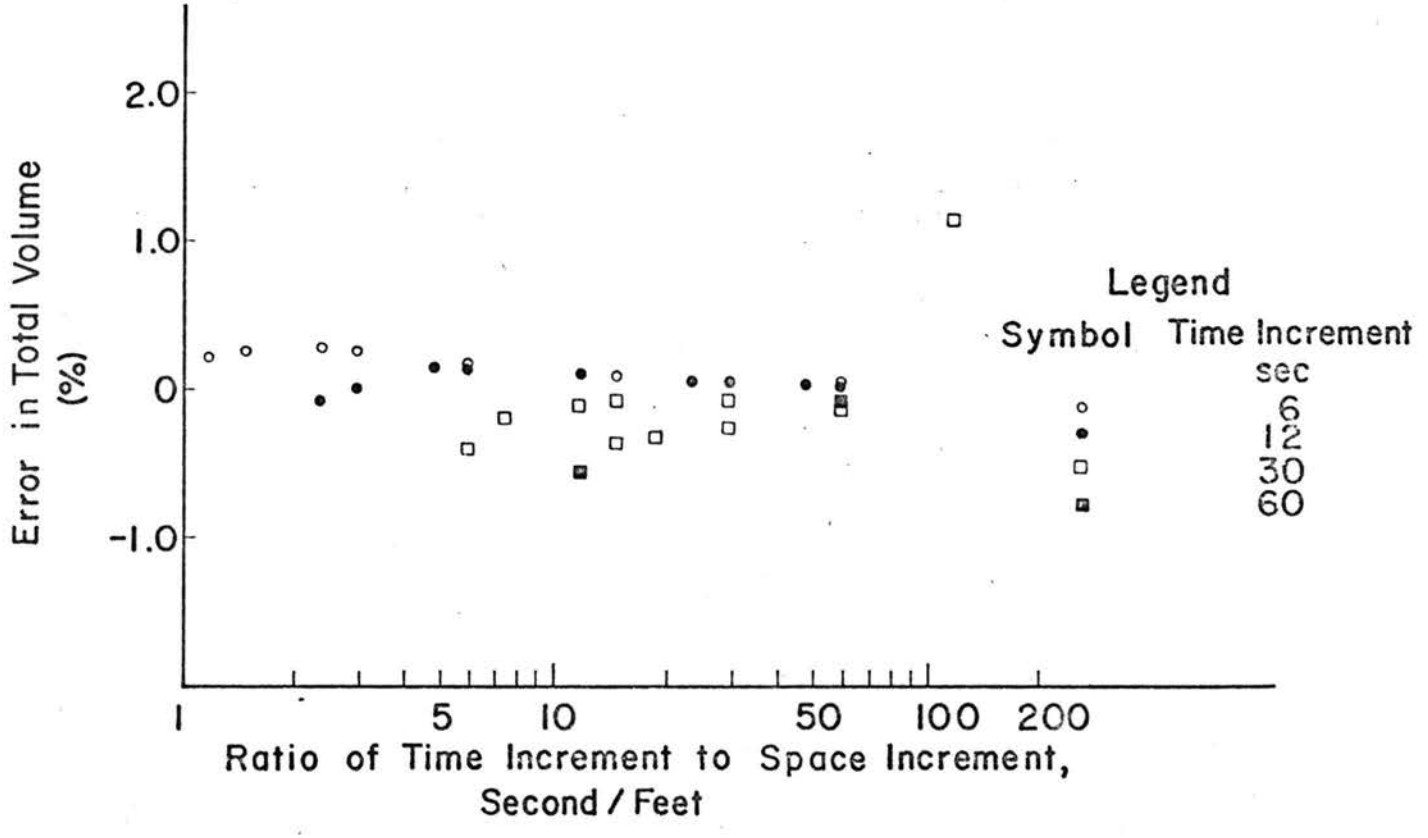

Fig. 2.3 Relation between error in continuity and time to space increment ratio

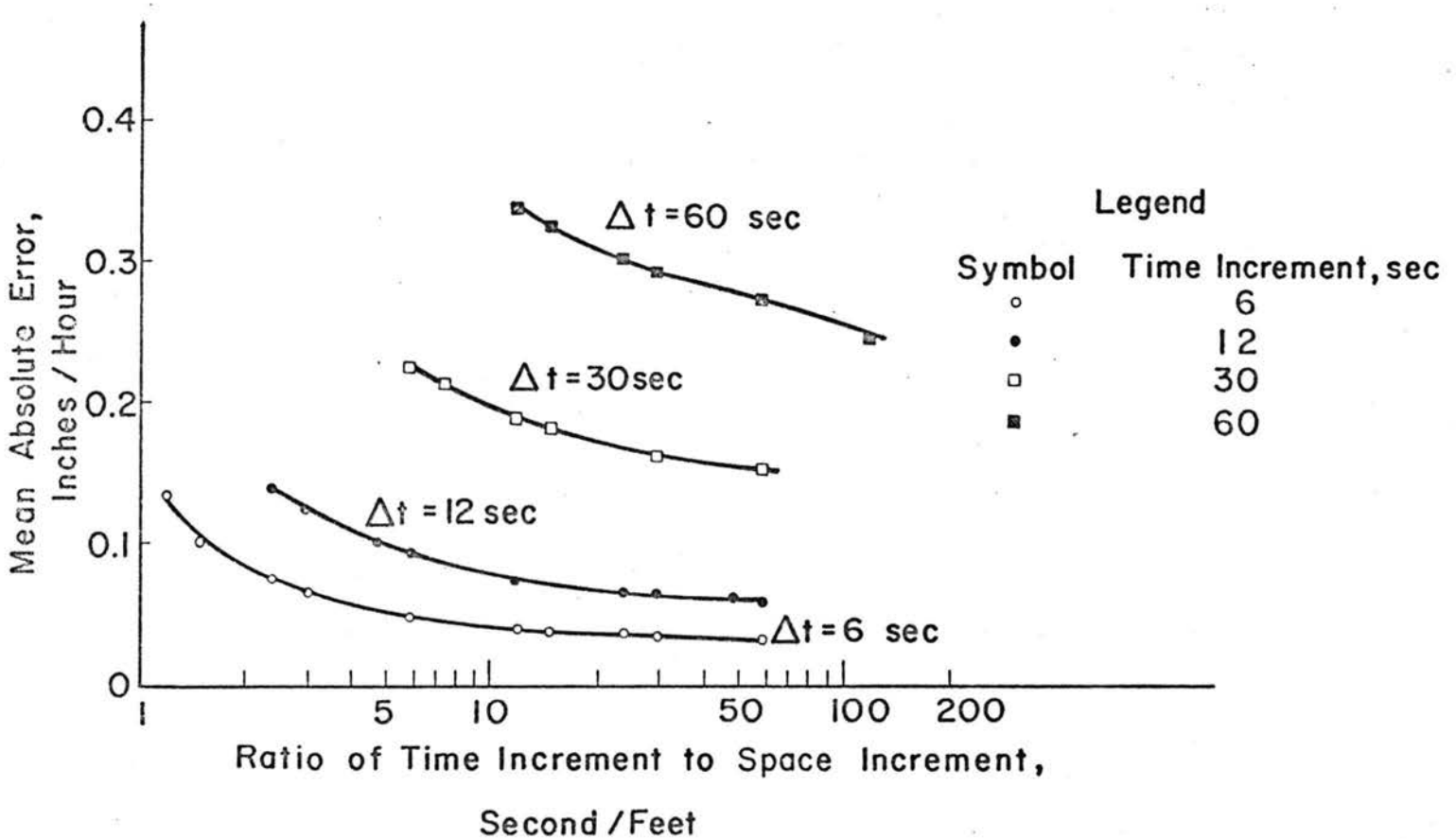

Fig. 2.4 Relation between mean absolute error and time to space increment ratio

Here Q_{ap} is the peak discharge determined by the analytical solution to the hypothetical case and Q_{op} is the peak discharge computed by the numerical scheme. It is found that the errors in the peak flow are very small (generally less than ±0.5 percent) for the tested range of $\frac{\Delta t}{\Delta x}$.

The foregoing examinations show that the convergence of the numerical scheme is ensured. This ensurance is due to the fact that the convergence criterion is always satisfied by the nonlinear scheme for each computation grid-point.

2.3. Applications

The applicability of the proposed model is examined by the comparison of computed hydrographs with measured hydrographs. These measured data include experimental data from test plots for overland flow, a measured hydrograph from a parking lot and a flood event in a natural river.

2.3.1. Overland flow plots

An overland flow hydrograph with small flow Reynolds number is shown in Fig. 2.5. This hydrograph was obtained by Izzard (1946) in his experimental work. In his experiment, the bed slope was 0.005, the slope length, L, was 72 ft, the rainfall intensities were 1.89 to 3.78 in./hr, and the maximum flow Reynolds number was approximately 630. The flow resistance parameters are estimated as $k_o = 24$ (smooth boundary) and $k_r = 10$ (raindrop fall of 3 ft). The friction factor is considered a function of time and space.

The comparison of the numerical solution and the measured hydrograph is shown in Fig. 2.5. In the numerical solution $\Delta t = 0.2$ min and $\frac{\Delta t}{\Delta x} = 12$ sec/ft. The numerical solution agrees very well with the

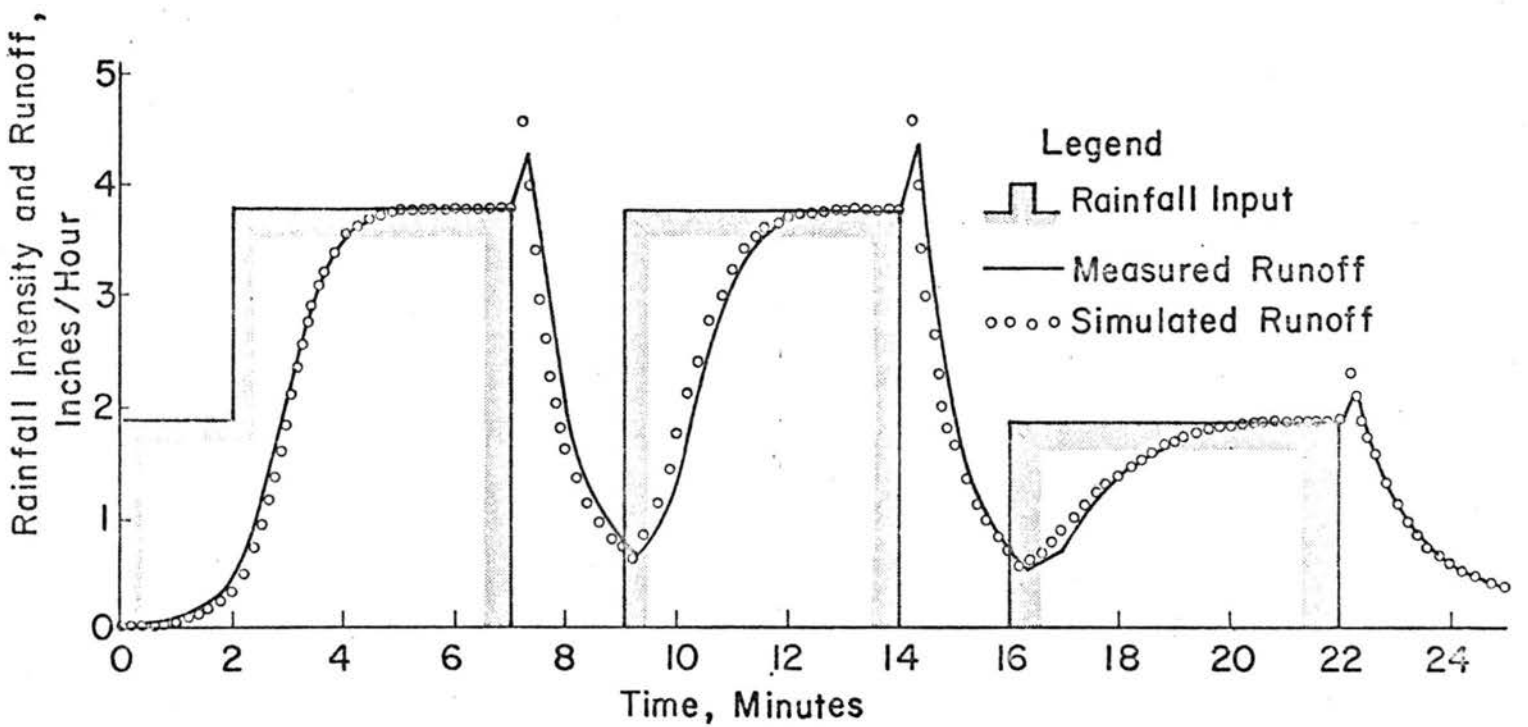

Fig. 2.5 Example of overland flow modeling for small Reynolds number

measured results. The interesting phenomena of "pip" and "dip" which occur at the ceasing or starting of high rainfall intensity on shallow flows are also successfully reproduced by the numerical method. These phenomena are due to the sudden changes of flow resistance and are explained herein. Equation 2.8 shows that the friction factor f suddenly decreases as rainfall ceases or if the rainfall intensity decreases abruptly. A sudden decrease in friction factor results in an instantaneous increase in flow rate. On the other hand, the friction factor f suddenly increases if the rainfall intensity increases abruptly which causes the sudden retardation of flow rate. The results in abrupt changes in flow are the "pip" and "dip" in the hydrograph.

Yu and McNown (1964) reported the measured hydrographs shown in Fig. 2.6. In their overland flow experiment, the flow Reynolds number was much greater than in Izzard's experiment. The bed slope was 0.02, the slope length was 500 ft, the rainfall intensity was 7.44 in./hr, and the maximum flow Reynolds number was approximately 8600. The estimated flow resistance parameters are $k_o = 30$ (concrete paved surface), $k_r = 10$ (raindrop fall of 3 ft assumed), and $k_2 = 0.4$ (concrete paved surface). In this case the friction factor, f, changes from the low Reynolds number zone through the transition zone and to the higher Reynolds number zone. As shown in Fig. 2.6, there is excellent agreement between the hydrograph produced by the numerical model ($\Delta t = 0.2$ min, and $\frac{\Delta t}{\Delta x} = 12$ sec/ft) and measured results for both the flow discharge at the outlet and the flow depth at 33 ft upstream from the outlet. Also, the "pip" phenomenon is not detectable. This

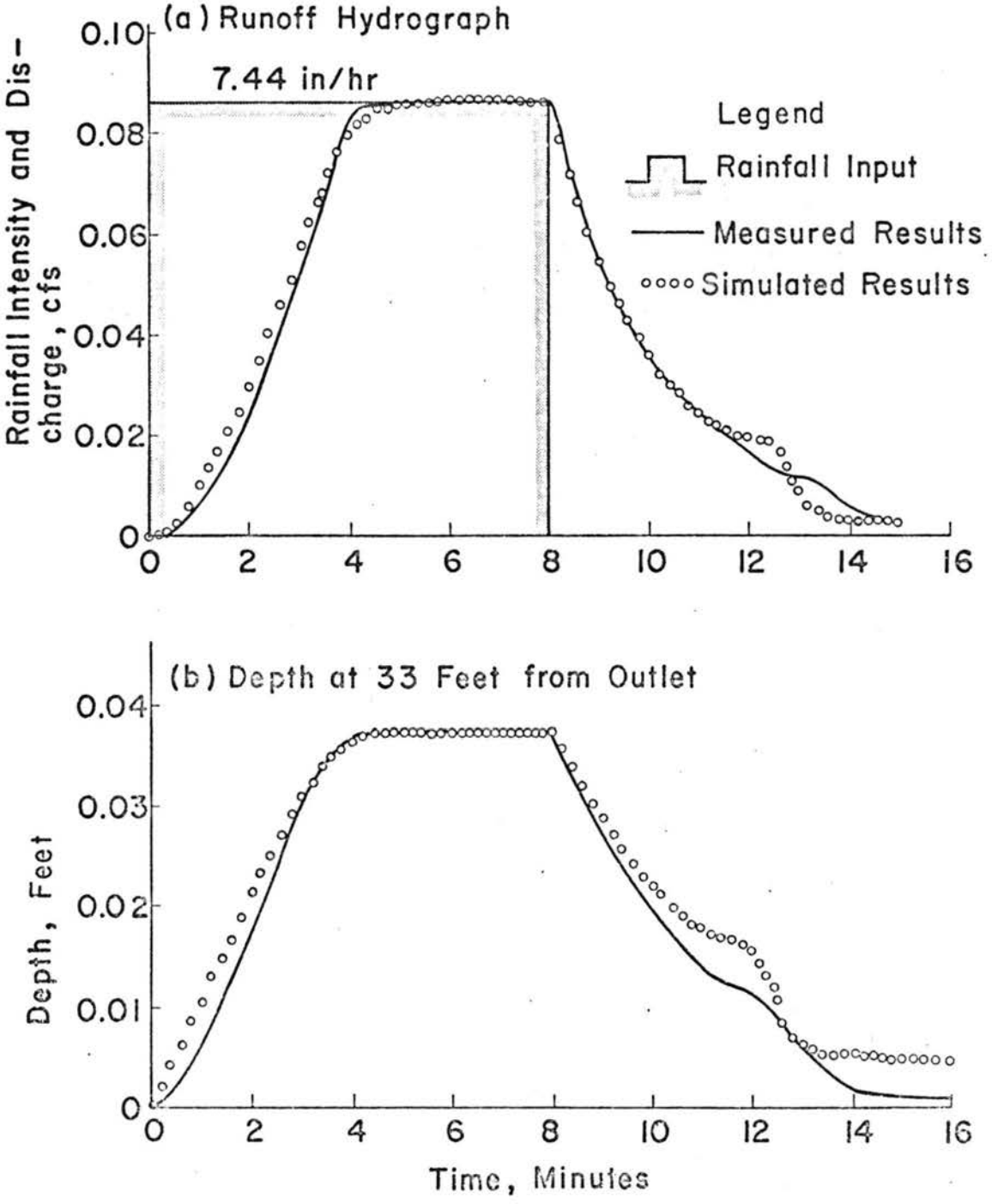

Fig. 2.6 Example of overland flow modeling for large Reynolds number

can be explained by the aid of Eq. 2.9 which shows the flow resistance is not affected by the changing of rainfall intensity if the flow Reynolds number is large.

2.3.2. Natural channel

A flood hydrograph in the Rio Amana in Venezuela was used to test the applicability of the numerical method of flood routing in a natural channel. Both inflow and outflow hydrographs were measured in 1969 in the reach of river between El Tejero and the crossing of the Maturin-Tembledor Road (See Simons et al., 1971a). As described by Simons et al. (1971b), the reach is 47.1 mile long and has an average slope of 0.00146. The bankfull top width at the downstream station is approximately 70 ft. The measured α and β values in A versus Q relation are available at the downstream station. The values are $\alpha = 1.1$ and $\beta=0.9$. For the reach, it has been assumed that β remains constant and α changes linearly with distance. The estimated value of α at the upstream station is 2.5, and the lateral outflow rate was approximately 0.26 cfs/mile. The estimated upstream α-value is much larger than the downstream value because of larger flow resistance and larger wetted perimeters for the same flow area in the upstream reach than in the downstream reach. The estimation of the upstream α-value and the lateral outflow rate was made by the multi-dimensional calibration technique described in Appendix B.

In Fig. 2.7, the numerical solutions (Δt = 2 hr, and $\frac{\Delta t}{\Delta x}$ = 0.58 sec/ft) agree reasonably with the measured results. The proposed numerical method is applicable in natural channels with steep gradients because the kinematic-wave approximation is applicable for such channels.

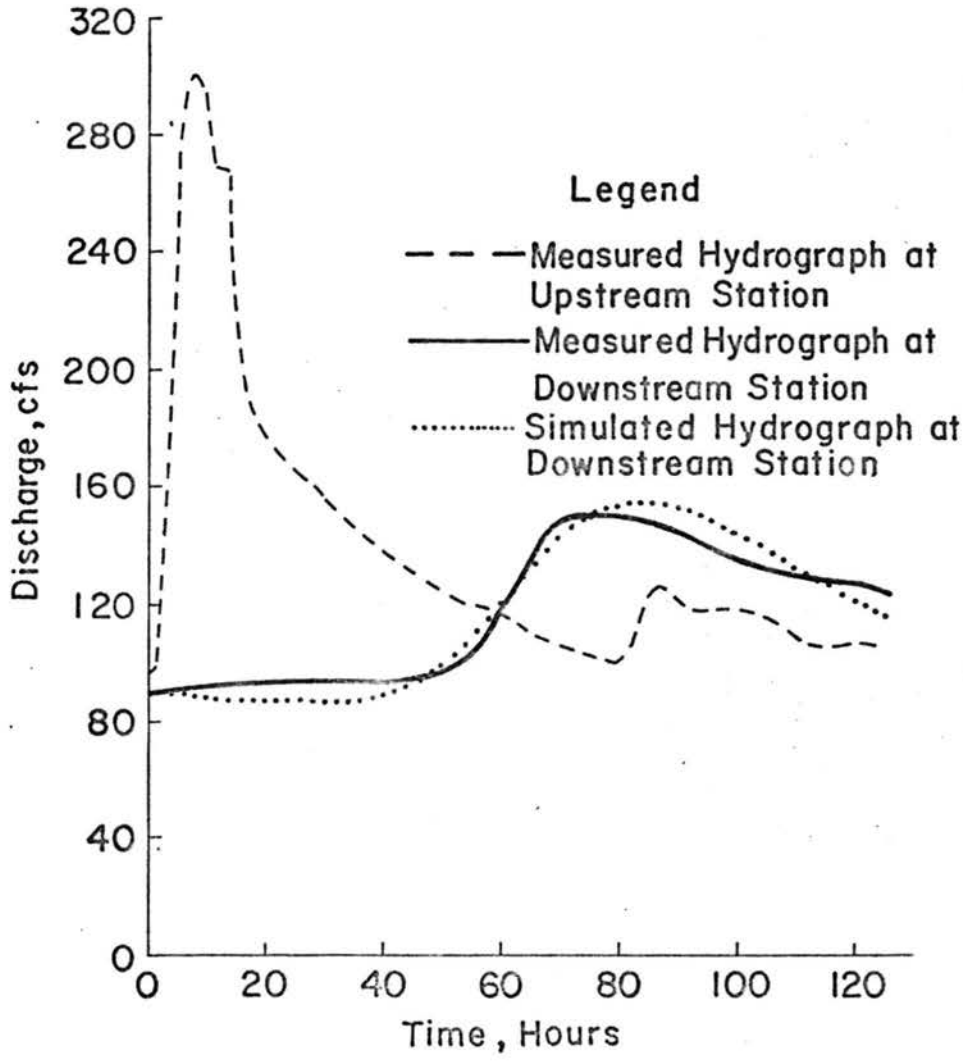

Fig. 2.7 Flood routing in the Río Amana in Venezuela

2.3.3. Confined catchment

The numerical model presented herein is valid for channel flows as well as overland flows. A catchment system is formulated by routing the overland flows to channels, and then routing the flows through the channels. The numerical solutions for hydrographs from small catchments agree very well with the measured runoff. A comparison of computed and measured hydrographs at the outlet of SPL1 parking lot at Johns Hopkins University is shown in Fig. 2.8. The storm used in this analysis is 13SPL1, which was reported by Schaake (1965). The area of the parking lot was 0.39 acres. The catchment area consisted of the overland flow area and V-shaped channels. The lengths of overland flow paths varied from 20 ft to 36 ft and the overland slopes varied from 0.0167 to 0.019. The side slopes of V-shaped channels were 1:113. The lengths of these channels varied from 50 ft to 165 ft and the channel slopes ranged from 0.0148 to 0.0213. The resistance parameters are estimated as follows: k_o = 35 (asphalt surface); k_r = 27 (assuming an 8 ft fall to give the terminal velocity for raindrops); and k_2 = 0.4 (asphalt surface). In the numerical computations Δt = 1 min and $7.3 \leq \frac{\Delta t}{\Delta x} \leq 30$ sec/ft.

The agreement between computed and observed hydrographs shown in Fig. 2.8 indicates the applicability of the proposed numerical model for time-variant inflows and watershed modeling.

2.4 Summary

A numerical model consisting of a second order nonlinear scheme combined with a linear scheme has been developed to route water overland and in channels. This numerical scheme has the advantages of both nonlinear and linear schemes. The nonlinear scheme ensures

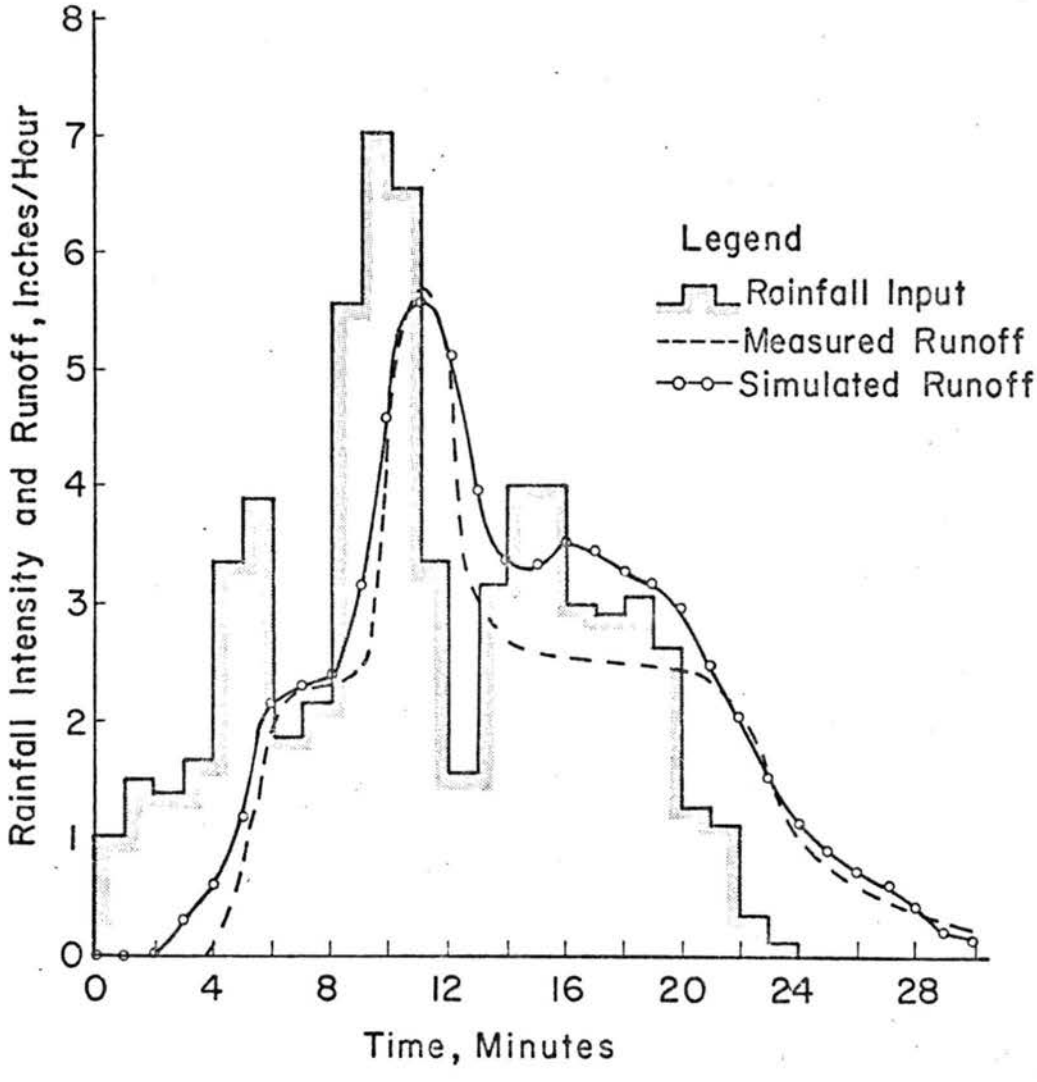

Fig. 2.8 Runoff from SPL1 parking area, Johns Hopkins University

convergence and the linear portion of the scheme provides rapid computations. The numerical scheme is unconditionally stable and may be used with wide range of $\frac{\Delta t}{\Delta x}$ without loss of accuracy. The limitation of this method is inherited from the restriction on the kinematic-wave approximation.

It has been found that the discharge Q is the better selection for the unknown in numerical computations than the depth or area. The term β in the relation $A = \alpha Q^{\beta}$ is generally less than 1.0. If the flow discharge is computed incorrectly, the flow depth estimation is influenced only to a small degree.

The model employs resistance equations which include the effect of raindrop impact on resistance. Consequently, the area versus discharge relations are time and space dependent. The interesting phenomena of "pip" and "dip" in overland flow hydrographs are successfully simulated. These phenomena are the results of sudden changes of flow resistance due to ceasing or starting of rainfall over shallow, low Reynolds number flows.

The applicability of the numerical model has been tested in various cases. The tests illustrate that this simple routing procedure simulates hydrographs which agree very well with measured overland flow hydrographs, natural channel hydrographs, and hydrographs from drainage systems. It is concluded that this model is a promising model for a large-scale modeling of watershed response.

Chapter III

RAINFALL-RUNOFF MODEL FOR NATURAL WATERSHEDS

3.1. Model Structure

The rainfall-runoff model developed herein is a physical process simulation model, which is divided into an overland flow part and a channel system part. The overland flow part simulates the processes of interception, evaporation, infiltration, and overland flow routing to the nearest channel. The channel system part routes water contributed by overland flow through the channel system.

The main components of the rainfall-runoff model are shown in Fig. 3.1.

3.2. Segmentation of a Watershed

Because most watersheds are very nonhomogeneous in topography, it is necessary to segment the watershed into smaller units for mathematical analysis. In this study, the watershed is decomposed into overland flow units and channel flow units. The sequence in segmenting the watershed into units is as follows:

(1) A rectangular grid system is superimposed on the topographic map of the watershed. The size of the grid is chosen so that the watershed boundaries and channels can be approximated by grid segments. The overland flow units are the grid units inside the watershed boundary and the channel units are segments between grid intersection points.

(2) The principal flow direction is determined for each overland flow unit. The principal flow direction is

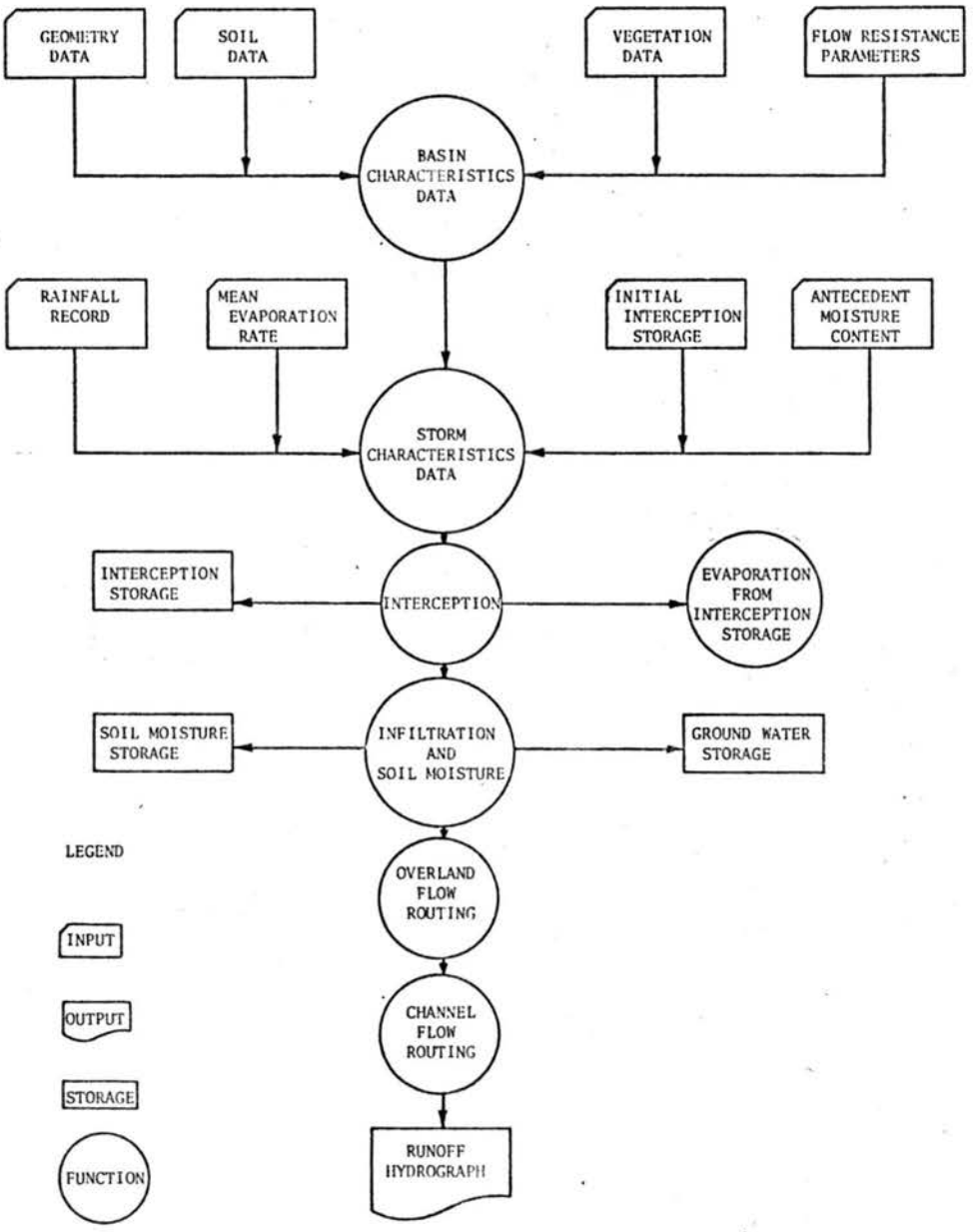

Fig. 3.1 Rainfall-runoff model flow chart

identified by the magnitude and azimuth of the bed slope (or land slope). The azimuth is normal to the elevation contours and is in the direction of decreasing elevation. The bed slope is estimated along the azimuth.

(3) It is assumed that the water flows in the direction of the bed slope azimuth to the next overland flow unit or to the adjacent channel. Thus water cascades from overland flow unit to overland flow unit and then into the channel system.

If the bed slopes of the overland flow units in cascade are nearly the same, these overland flow units are combined into a larger overland flow unit. The representative slope length for the larger unit is the ratio of total area of the cascade to the width of the overland flow unit where it joins the channel. The bed slope is an average value of the bed slopes of all the small units.

(4) The computational sequence for the flow network is established. The method employed is simply to follow the logics of the gravity flow and the flow continuity.

A plan view of a typical segmented watershed is shown in Fig. 3.2. In this watershed there are overland flow units and channel segment units.

3.3. Water Balance

In this study, the water budget for an overland flow unit is simulated to determine the rainfall excess resulting from an individual storm. Due to the different nature of water balance under a canopy as

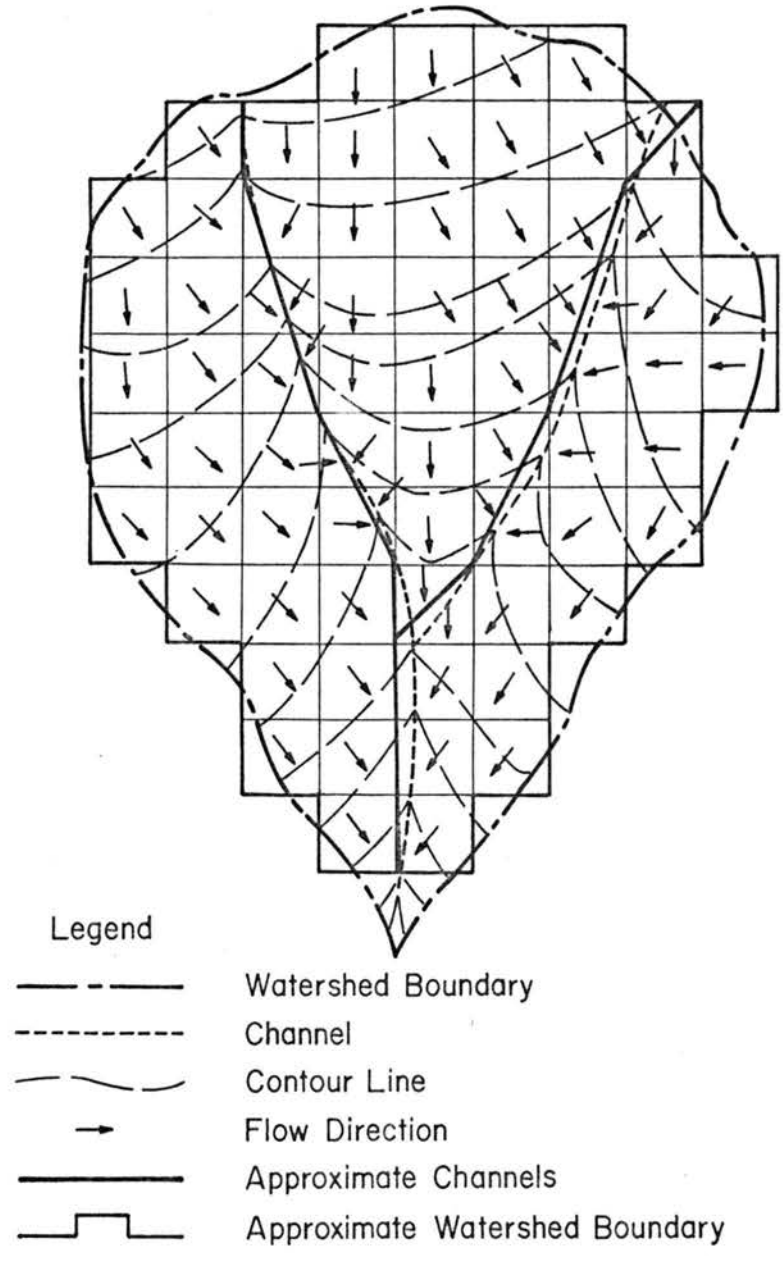

Fig. 3.2 Example of geometric segmentation

compared to an area without trees, the rainfall excess determination is carried out for a point under the canopy and for another point in the area without trees. A weighting procedure based on canopy cover density is used to obtain a mean rainfall excess rate. (See Section 3.3.3.). The canopy cover density is defined as the ratio of the area covered by trees to the total area. Either under a canopy or in an area without trees, the water balance computation may be subdivided into the net rainfall determination and the ground response to the net rainfall.

3.3.1. Net rainfall

Net rainfall is defined as the quantity of rainfall which actually reaches the ground, the sum of the throughfall and stemflow. (Zinke, 1965). The rate of net rainfall for different interception conditions is as follows.

Let i or $i(t)$ be the rainfall rate (or intensity) at time t and refer to Fig. 3.3.a, the control volume for a tree canopy. If the rain falls onto trees a portion is stored in the canopy and the remainder i_o passes through the trees. Let i_c or $i_c(t)$ be the rate at which rain is being stored in the canopy at time t. Then, under trees, the rainfall rate is reduced to the throughfall rate (stemflow rate is neglected).

$$i_o = i - i_c \tag{3.1}$$

The area under the trees can consist of a bare portion and a portion with ground cover (litter, tree mulch, rocks, shrubs, grass, etc.)

Refer to Fig. 3.3.b and let i_g or $i_g(t)$ be the rate at which rain is being stored in the ground cover at time t. Then under the tree, the rate at which rain reaches the ground (net rainfall rate) is

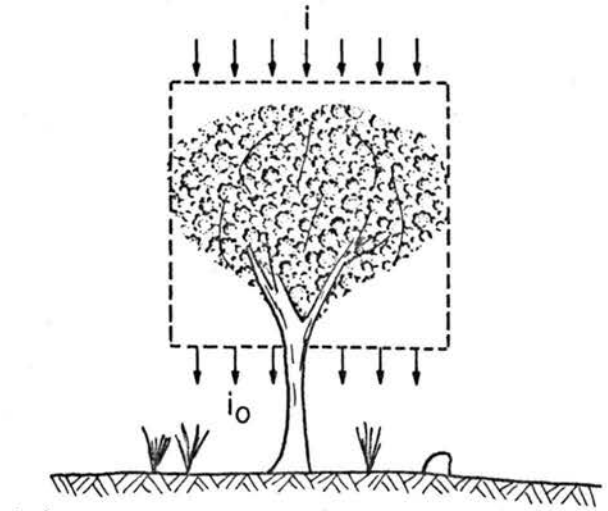

(a) Control Volume for a Tree Canopy

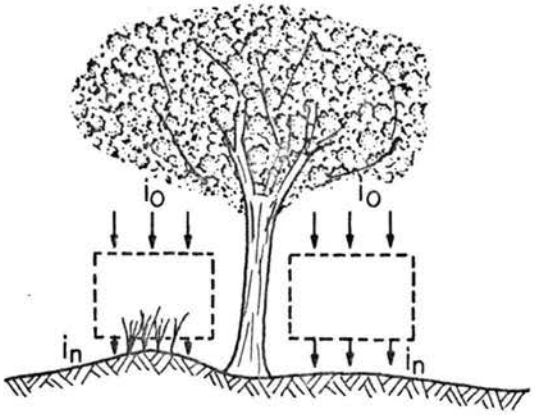

(b) Control Volumes Under Canopy

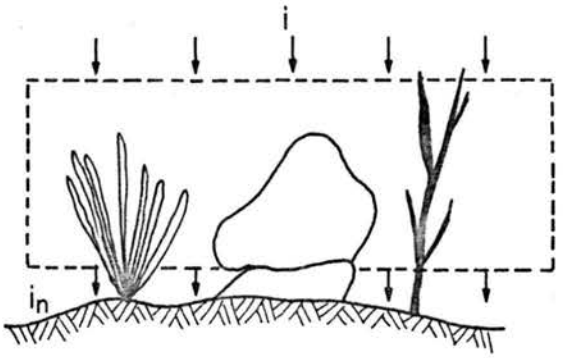

(c) Control Volume for Ground Cover Only

Fig. 3.3 Rain reaching ground

$$i_n = i_o - i_g = i - i_c - i_g \tag{3.2}$$

where there is ground cover, and

$$i_n = i_o = i - i_c \tag{3.3}$$

where there is no ground cover.

The area without trees (see Fig. 3.3c) can also consist of a bare portion and a portion with ground cover. Where there are no trees, but there is ground cover, the net rainfall rate is

$$i_n = i - i_g \tag{3.4}$$

where there are no trees and no ground cover.

$$i_n = i \tag{3.5}$$

A summary of rainfall rate reaching the ground for different interception conditions is given in Table 3.1.

Table 3.1. Rain Reaching the Ground

Area	Condition	Net Rainfall Rate i_n
Under canopy	trees, ground cover	$i - i_c - i_g$
	trees, no ground cover	$i - i_c$
Without trees	no trees, ground cover	$i - i_g$
	no trees, no ground cover	i

Let A_t^c be the total area covered by trees in an overland flow unit. Also let A_g^c be the area with ground cover within area A_t^o. Then the average net rainfall rate under a canopy is

$$\bar{i}_n^c = \frac{1}{A_t^c}\left\{(i - i_c - i_g)\, A_g^c + (i - i_c)\,(A_t^c - A_g^c)\right\}$$

$$= i - i_c - \frac{A_g^c}{A_t^o} i_g \qquad (3.6)$$

Similarly, the average net rainfall rate in an area without trees is

$$\bar{i}_n^o = i - \frac{A_g^o}{A_t^o} i_g \qquad (3.7)$$

in which A_t^o is the total area without trees in an overland flow unit, and A_g^o is the area with ground cover within area A_t^o.

Assume the ground cover has the same density over the entire area of an overland flow unit either under canopy or over the area without trees. One then obtains

$$\frac{A_g^c}{A_t^c} = \frac{A_g^o}{A_t^o} = D_g \qquad (3.8)$$

in which D_g is the ground cover density, which is the ratio of the area covered with ground cover to the total area in an overland flow unit.

The substitution of Eq. 3.8 into Eqs. 3.6 and 3.7 yields

$$\bar{i}_n^c = i - i_c - D_g i_g \qquad (3.9)$$

for areas under canopy and

$$\bar{i}_n^o = i - D_g i_g \qquad (3.10)$$

for areas without trees.

According to Horton (1919), total interception equals leaf storage capacity plus evaporation loss during the storm. Zinke (1965)

indicated that "usually for a storm, there is an initial period during which the vegetation cover is wetted and a so-called interception storage capacity is satisfied. This is followed by loss from this storage, and the loss is dependent upon the evaporation opportunity during the remainder of the storm." The foregoing statements suggested that

$$i_c(t) = i(t) \quad \text{if} \quad \sum_{t'=1}^{t} i(t')\,\Delta t \leq (1 - I_s)\,V_c \tag{3.11}$$

$$i_c(t) = E\,S_c \quad \text{if} \quad \sum_{t'=1}^{t} i(t')\,\Delta t > (1 - I_s)\,V_c \tag{3.12}$$

and

$$i_g(t) = i(t) \quad \text{if} \quad \sum_{t'=1}^{t} i(t')\,\Delta t \leq (1 - I_s)\,V_g \tag{3.13}$$

$$i_g(t) = E\,S_g \quad \text{if} \quad \sum_{t'=1}^{t} i(t')\,\Delta t > (1 - I_s)\,V_g \tag{3.14}$$

in which V_c is the interception storage capacity of a tree canopy per unit area, V_g is the interception storage capacity of the ground cover per unit area, E is the mean evaporation rate from the interception storages, S_c and S_g are respectively the ratios of the evaporating surface to the horizontal projected area for a tree canopy and for a typical ground cover and I_s is the initial interception storage content which is defined as the ratio of the initial storage capacity to the total interception storage capacity.

Let r_v be the ratio of V_c to V_g, or

$$V_c = r_v V_g \tag{3.15}$$

then one may assume

$$S_c = r_v S_g \tag{3.16}$$

The average net rainfall rate under canopy at time t can be determined by combining Eqs. 3.9, 3.11, 3.12, 3.13, 3.14, 3.15 and 3.16., i.e.,

$$\bar{i}_n^c(t) = 0 \quad \text{if} \quad \sum_{t'=1}^{t} i(t')\,\Delta t \leq (r_v + D_g)\,(1 - I_s)\,V_g \tag{3.17}$$

and

$$\bar{i}_n^c(t) = i(t) - E\,(r_v + D_g)\,S_g \quad \text{if} \quad \sum_{t'=1}^{t} i(t')\,\Delta t > (r_v + D_g)\,(1 - I_s)\,V_g \tag{3.18}$$

Similarly, the average net rainfall rate for the area without trees is

$$\bar{i}_n^o(t) = 0 \quad \text{if} \quad \sum_{t'=1}^{t} i(t')\,\Delta t \leq (1 - I_s)\,D_g V_g \tag{3.19}$$

and

$$\bar{i}_n^o(t) = i(t) - E\,D_g S_g \quad \text{if} \quad \sum_{t'=1}^{t} i(t')\Delta t > (1 - I_s)\,D_g V_g \tag{3.20}$$

3.3.2. Ground response to net rainfall

Because this study concerns the water yield on the single storm basis, the transpiration from soil through vegetation and evaporation from the soil are small and therefore neglected. The net rainfall which reaches the ground either infiltrates into the soil, or is stored in surface puddles as "depression storage" or becomes surface runoff (see Fig. 3.4). The infiltrated water into the soil will increase the

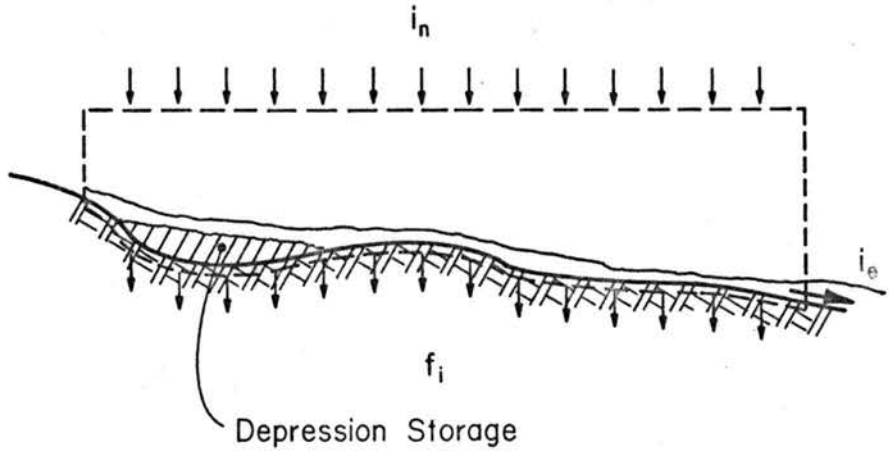

Fig. 3.4 Control volume on the ground

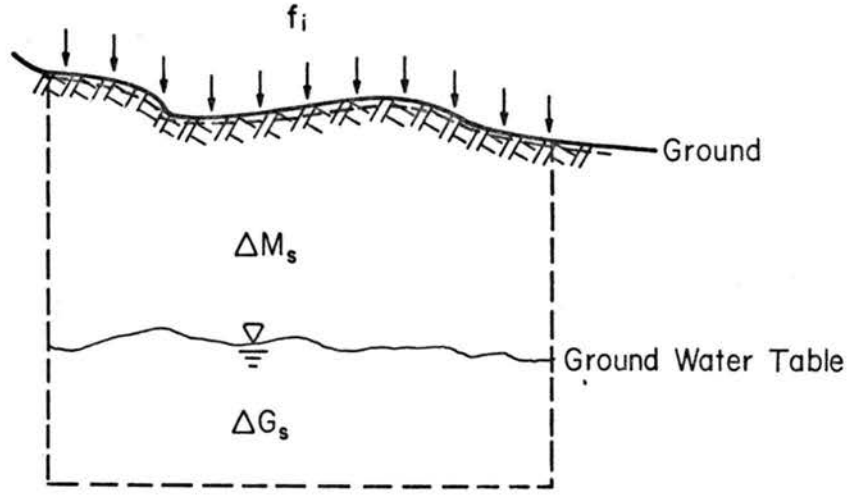

Fig. 3.5 Control volume below the ground

soil moisture storage in the upper soil profile and may change the ground water storage (see Fig. 3.5).

When rainfall intensity exceeds the infiltration capacity, the rainfall excess begins to fill surface depressions. Each depression has its own capacity and, when filled, further inflow is balanced by outflow plus infiltration. Depressions of various sizes are both superimposed and interconnected. Soon after the beginning of rainfall excess, the smallest depressions become filled and overland flow begins. Most of this water in turn fills larger depressions, but portions of the excess follow unobstructed paths to the stream channel. This chain of events continues with beginning successively larger portions of overland flow. Very little is known concerning the magnitude of depression storage. Defining depression storage in itself is difficult and meaningful observations cannot be easily obtained. Thus, the depression storage is usually combined with interception and treated as initial loss with respect to storm runoff (Linsley, et al., 1958). For simplicity, the depression storage is neglected in this study, but implicitly is included in the interception storage capacity described in section 3.3.1.

Referring to Fig. 3.4 and neglecting depression storage the water balance equation is

$$i_e = i_n - f_i \tag{3.21}$$

in which i_e is the rainfall excess rate and f_i is the infiltration rate.

The average rainfall excess rate under canopy and in the area without trees are respectively,

$$\overline{i}_e^c(t) = \overline{i}_n^c(t) - \overline{f}_i^c(t) \qquad (3.22)$$

for areas under canopy and

$$\overline{i}_e^o(t) = \overline{i}_n^o(t) - \overline{f}_i^o(t) \qquad (3.25)$$

for areas without trees in which $\overline{f}_i^c(t)$ and $\overline{f}_i^o(t)$ are respectively the average infiltration rates for areas under canopy and for areas without trees.

3.3.2.1. Infiltration

Darcy's Law for flow through porous medium (Daily and Harleman, 1966, p. 181) is

$$v_\eta = -k_s \frac{\partial(-P_c - \overline{h} - \eta')}{\partial \eta'} = k_s \frac{\partial(P_c + \overline{h} + \eta')}{\partial \eta'} \qquad (3.24)$$

in which v_η is the hypothetical infiltration velocity defined as the local flow rate averaged over a finite area of the porous medium, k_s is the saturated hydraulic conductivity (coefficient of permeability), P_c is the magnitude of the capillary potential head, $\overline{h}$ is the magnitude of the ponded water head at the surface and η' is the magnitude of the gravitational potential head of the wetted front in the soil column.

Assuming one-dimensional flow and neglecting $\overline{h}$, Eq. 3.24 becomes

$$v_\eta = k_s \frac{d(P_c + \eta')}{d\eta'}$$

or

$$v_\eta d\eta' = k_s \, d(P_c + \eta') \qquad (3.25)$$

Integration of Eq. 3.25 yields

$$\int_0^{\bar{\eta}} v_\eta d\eta' = k_s(\bar{P}_c + \bar{\eta}) \tag{3.26}$$

in which $\bar{\eta}$ and $\bar{P}_c$ are respectively the magnitudes of the gravitational potential head and the capillary potential head of the wetted front at a particular time.

Let $\bar{v}_\eta$ denote the average value of v_η, so that

$$\int_0^{\bar{\eta}} v_\eta d\eta' = \bar{v}_\eta \bar{\eta} \tag{3.27}$$

From Eqs. 3.26 and 3.27, one obtains

$$\bar{v}_\eta = k_s \left(1 + \frac{\bar{P}_c}{\bar{\eta}}\right) \tag{3.28}$$

In a natural watershed, the infiltration rate is not homogeneous in space. A reasonable assumption is that the infiltration rate is uniformly distributed between values of zero and a maximum rate $f_m(t)$ for the area under canopy and the area without trees. This maximum infiltration rate is time-dependent and is different for the area under canopy and the area without trees. For convenience in deriving the infiltration equation, let $f_m(t)$ be the maximum infiltration rate for both areas temporarily.

Assume $f_m(t)$ to be $\bar{v}_\eta$ in Eq. 3.28, i.e.,

$$f_m(t) = k_s \left(1 + \frac{\bar{P}_c(t)}{\bar{\eta}(t)}\right) \tag{3.29}$$

in which $\bar{P}_c(t)$ and $\bar{\eta}(t)$ are respectively $\bar{P}_c$ and $\bar{\eta}$ at the time t.

The soil moisture profile in the upper soil zone (zone of aeration) at time $t - \Delta t$ is represented in Fig. 3.6a (after Hewlett and Nutter, 1969, p. 57). When infiltration occurs, a wetting front moves

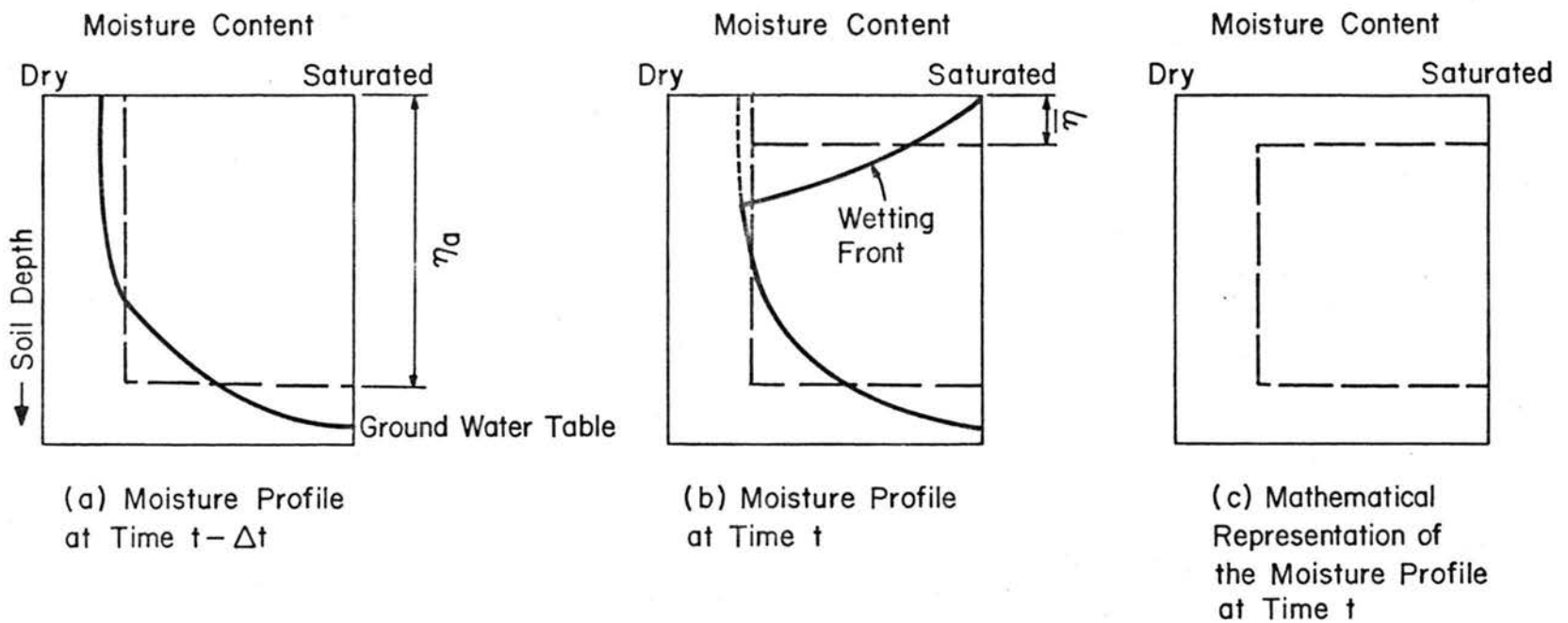

Fig. 3.6 Schematic diagram of moisture distribution

through the upper soil zone and the moisture profile at time t is shown in Fig. 3.6.b. In this study, the soil moisture profile at time t is represented by the simple mathematical functions shown in Fig. 3.6c. Then, the gravitational potential head of the wetted front at time t is

$$\bar{n}\ (t) = \frac{f_m(t)\ \Delta t}{m_s - m_o(t-\Delta t)} \tag{3.30}$$

in which m_s is the moisture content at satuation and $m_o(t)$ is the current moisture content of the zone of aeration at time t , the adjustment of moisture content is given later in section 3.3.2.2.

The magnitude of the capillary potential head or the moisture tension head of the wetted front $\bar{P}_c(t)$ is a function of soil moisture content (Zahner, 1965). A typical representation of soil moisture depletion curve is given in Fig. 3.7. From Fig. 3.7, the capillary potential head at time t can be approximated by a linear interpolation as follows

$$\bar{P}_c(t) = \left[\frac{m_s - m_o(t-\Delta t)}{m_s - m_w} \right] P_w \tag{3.31}$$

in which m_w is the soil moisture content at wilting point, or defined as the moisture content at which permanent wilting of plants occurs, and P_w is the capillary potential head at wilting point.

The substitution of Eqs. 3.30 and 3.31 into Eq. 3.29 yields

$$f_m(t) = k_s \left\{ 1 + \frac{[m_s - m_o(t-\Delta t)]^2}{(m_s - m_w) f_m(t) \Delta t} \right\} \tag{3.32}$$

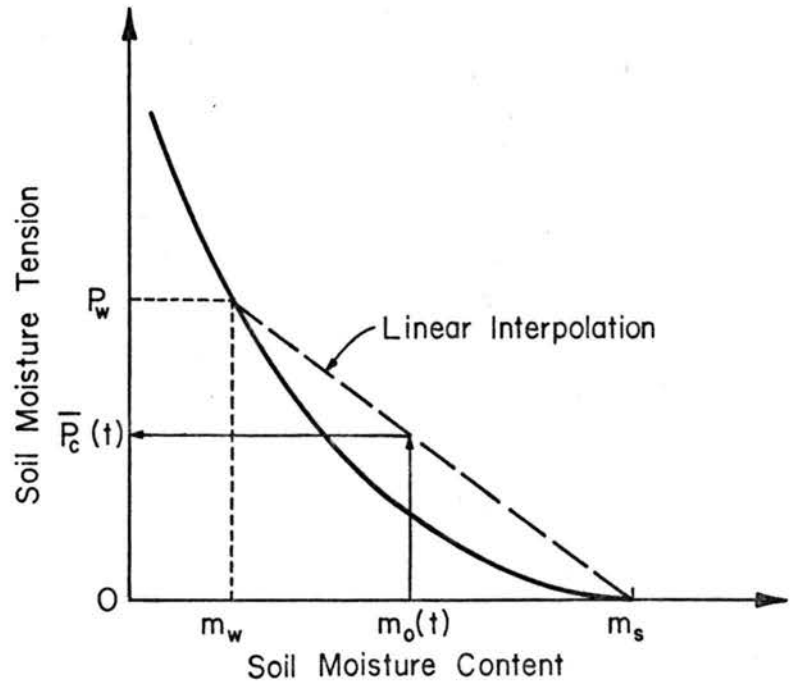

Fig. 3.7 Typical representation of soil-moisture depletion curve

$f_m(t)$ can be obtained by solving the quadratic equation of Eq. 3.32, i.e.,

$$f_m(t) = \frac{k_s}{2}\left\{1 + \sqrt{1 + \frac{4\ P_w\ [m_s - m_o(t-\Delta t)]^2}{k_s \Delta t\ (m_s - m_w)}}\right\} \qquad (3.33)$$

The current moisture contents for areas under canopy and for areas without trees are different due to different rate of water supply to the ground. Thus, the values of $f_m(t)$ are different for the area under canopy and the area without trees. They are

$$f_m^c(t) = \frac{k_s}{2}\left\{1 + \sqrt{1 + \frac{4P_w[m_s - m_o^c(t-\Delta t)]^2}{k_s \Delta t\,(m_s - m_w)}}\right\} \qquad (3.34)$$

for areas under canopy and

$$f_m^o(t) = \frac{k_s}{2}\left\{1 + \sqrt{1 + \frac{4P_w[m_s - m_o^o\ (t-\Delta t)]^2}{k_s \Delta t\,(m_s - m_w)}}\right\} \qquad (3.35)$$

for areas without trees in which $m_o^c(t)$ and $m_o^o(t)$ are respectively the moisture contents for the area under canopy and the area without trees.

As stated earlier in this study the spatial distribution of infiltration rate is assumed uniform between values of zero and $f_m(t)$ for both the area under canopy and the area without trees. The cumulative distribution function of the infiltration rate is shown in Fig. 3.8. Then the average infiltration rates for area under canopy and area without trees are as follows

$$\overline{f}_i^c\ (t) = \frac{1}{2}\ f_m^c(t) \quad \text{if } \overline{i}_n^c(t) \geq f_m^c(t) \qquad (3.36)$$

and

$$\overline{f}_i^c\ (t) = \overline{i}_n^c(t) - \frac{1}{2}\frac{[\overline{i}_n^c(t)]^2}{f_m^c(t)} \quad \text{if } \overline{i}_n^c(t) < f_m^c(t) \qquad (3.37)$$

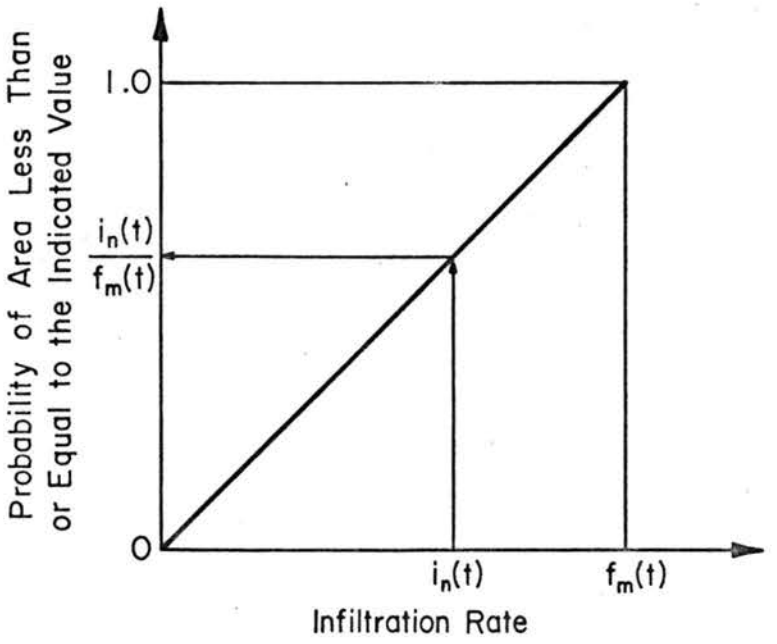

Fig. 3.8 Cumulative distribution function of infiltration rate

for areas under canopy and

$$\overline{f}_i^o(t) = \frac{1}{2} f_m^o(t) \quad \text{if} \quad \overline{i}_n^o(t) \geq f_m^o(t) \tag{3.38}$$

and

$$\overline{f}_i^o(t) = \overline{i}_n^o(t) - \frac{1}{2} \frac{[\overline{i}_n^o(t)]^2}{f_m^o(t)} \quad \text{if} \quad \overline{i}_n^o(t) < f_m^o(t) \tag{3.39}$$

for areas without trees.

3.3.2.2. Soil moisture adjustment

After certain amounts of water infiltrate into the soil, the soil moisture is adjusted. For simplicity, the soil moisture is assumed to be adjusted uniformly through the zone of aeration.

Referring to Fig. 3.5, the control volume below the ground, and neglecting movement of ground water flow and subsurface flow, the water balance can be expressed as follows.

$$f_i = \frac{\Delta M_s}{\Delta t} + \frac{\Delta G_s}{\Delta t} \tag{3.40}$$

in which ΔM_s is the change in soil moisture storage, and ΔG_s is the change in ground water storage.

It is assumed that before the upper soil profile is saturated, no water enters the ground water storage, and after the upper soil profile is saturated all infiltrated water enters the ground water storage.

The moisture content prior to the saturation of upper soil profile is determined by the following equations.

$$m_o^c\ (t + \Delta t) = m_o^c\ (t) + \frac{\overline{f}_i^c\ \Delta t}{\eta_a} \tag{3.41}$$

for areas under canopy and

$$m_o^o\ (t + \Delta t) = m_o^o\ (t) + \frac{\overline{f}_i^o\ \Delta t}{\eta_a} \tag{3.42}$$

for areas without trees in which η_a is the depth of the zone of aeration.

After the moisture content reaches the state of saturation, all content is equal to the moisture content at saturation, i.e.,

$$m_o^c\ (t + \Delta t) = m_s \quad \text{if } m_o^c\ (t + \Delta t) > m_s \tag{3.43}$$

and

$$m_o^o\ (t + \Delta t) = m_s \quad \text{if } m_o^o\ (t + \Delta t) > m_s \tag{3.44}$$

For simplicity, the starting moisture contents for areas under canopy and for areas without trees are assumed to be the same, i.e.,

$$m_o^c\ (0) = m_o^o\ (0) = m_o\ (0) \tag{3.45}$$

in which $m_o(0)$ is the antecedent moisture content.

3.3.3. Mean rainfall excess rate

From Eqs. 3.22, 3.36 and 3.37, one can determine that the average rainfall excess rate for areas under canopy is

$$\overline{i}_e^c\ (t) = \overline{i}_n^c\ (t) - \frac{1}{2} f_m^c\ (t) \quad \text{if } \overline{i}_n^c(t) \geq f_m^c(t) \tag{3.46}$$

and

$$\overline{i}_e^c\ (t) = \frac{1}{2} \frac{[\overline{i}_n^c(t)]^2}{f_m^c(t)} \quad \text{if } \overline{i}_n^c(t) < f_m^c(t) \tag{3.47}$$

Similarly, the average rainfall excess rate for areas without trees can be determined by Eqs. 3.23, 3.38 and 3.39. The equations are

$$\bar{i}_e^o(t) = \bar{i}_n^o(t) - \frac{1}{2} f_m^o(t) \quad \text{if } \bar{i}_n^o(t) \geq f_m^o(t) \tag{3.48}$$

and

$$\bar{i}_e^o(t) = \frac{1}{2} \frac{[\bar{i}_n^o(t)]^2}{f_m^o(t)} \quad \text{if } \bar{i}_n^o(t) < f_m^o(t) \tag{3.49}$$

It is not practical to route water in the area under canopy and in the area without trees separately because these two types of areas are interconnected. A weighting procedure may be used to obtain an overall mean rainfall excess as follows:

$$\bar{i}_e(t) = D_c \, \bar{i}_e^c(t) + (1 - D_c) \, \bar{i}_e^o(t) \ , \tag{3.50}$$

in which D_c is the canopy cover density. This overall mean rainfall excess $\bar{i}_e(t)$ is the quantity of lateral inflow rate q_ℓ in Eq. 2.1.

3.4. Flow Routing in Natural Watersheds

The nonlinear kinematic-wave routing procedure, which was presented in Chapter II, is applied to natural watersheds. The same numerical method is used, but a modified relation between discharge and flow area is needed to account for the complexity of a natural watershed system. The major modifications are: (1) the relation between the wetted perimeter and the flow area, and (2) the resistance equations.

3.4.1. Relation between wetted perimeter and flow area for natural channels

In a natural channel, a single relation between the wetted perimeter P and the flow area A is usually not satisfactory to describe the relation when overbank flow occurs; another set of P-A relations is needed in this case. For example, in Fig. 3.9 two sets of P-A relation are shown exist.

The P-A relation for a natural channel is

$$P = a_1 A^{b_1} \quad \text{for } A \leq A_o \tag{3.51}$$

and

$$P = a_1' A^{b_1'} \quad \text{for } A > A_o \tag{3.52}$$

in which a_1, b_1, a_1', and b_1' are constants determined from channel survey data, and A_o is the flow area of bankfull flow.

3.4.2. Resistance equations for natural watersheds

For a natural watershed, the form resistance due to bed forms (both channel and overland) and ground covers play a very important role in the resistance to flow. Similar approach as the work by Li and Shen (1973) may be used to establish the variation of flow resistance.

Assume that the factors for describing resistance to flow are independent then, referring to Fig. 3.10, the force balance for uniform flow over a rectangular area with length L and width $\overline{W}$ is

Downslope water weight component = Grain resistance

+ Form resistance due to bed forms

+ Form resistance due to ground cover.

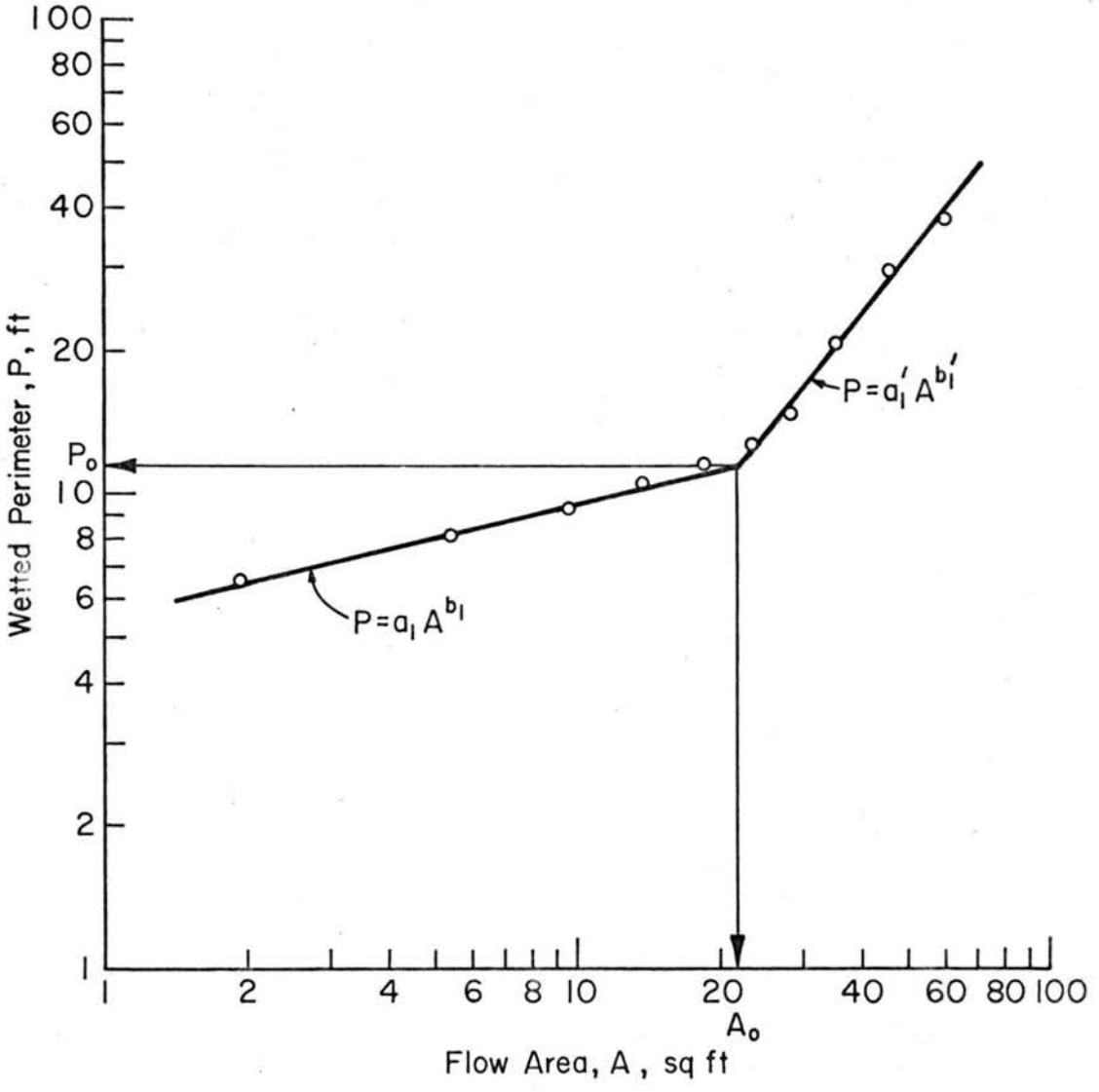

Fig. 3.9 Typical wetted perimeter-flow area relation for channels in Carrizal Basin, Venezuela

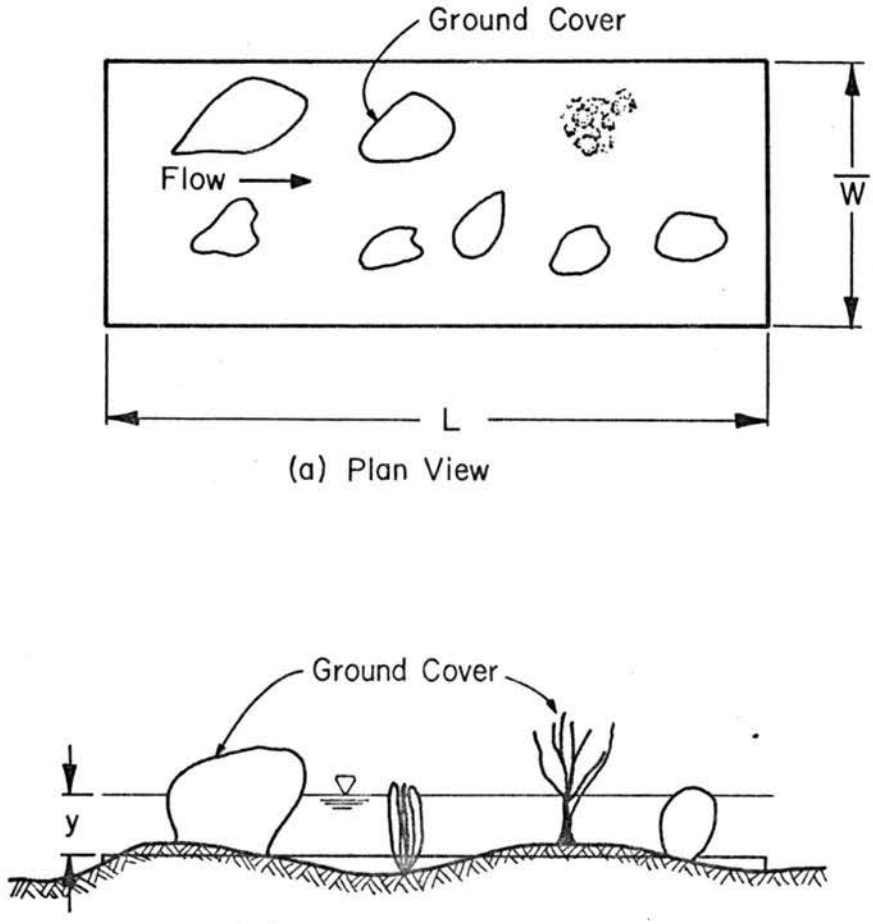

Fig. 3.10 Schematic diagram of resistance to flow in natural watersheds

That is,

$$\gamma L\bar{W}yS_o \approx \frac{1}{8} f\rho V^2 L\bar{W} + \frac{1}{2} C_d\rho V^2 A_1 + \frac{1}{2} C_d\rho V^2 A_2 \qquad (3.53)$$

in which γ is the specific weight of water, y is the flow depth, f is the Darcy-Weisbach friction factor for grain resistance, ρ is the density of water, V is the mean velocity of water flow, C_d is the drag coefficient, and A_1, A_2 are respectively the total projected area perpendicular to the flow direction to describe bed form resistance and ground cover resistance within the area $L\bar{W}$.

The total projected area for drag resistance due to ground covers A_2 is proportional to the mean flow depth and to the area of ground cover, or

$$A_2 = D_g L\bar{W} \frac{y}{\ell_g} \qquad (3.54)$$

in which ℓ_g is the average length of ground covers in the direction of flow.

According to the definition of the Darcy-Weisbach equation

$$S_o = f' \frac{V^2}{8gy} \qquad (3.55)$$

in which f' is the overall Darcy-Weisbach friction factor.

From Eqs. 3.51, 3.52 and 3.53, one obtains

$$f' \approx f + 4 C_d \frac{A_1}{L\bar{W}} + 4 C_d D_g \frac{y}{\ell_g} \qquad (3.56)$$

or by notation

$$f' \approx f + f_b + f_g \qquad (3.57)$$

in which f_b and f_g are respectively the added friction factors due to bed from resistance and ground-cover drag resistance.

As stated in Chapter II, f is a function of flow Reynolds number N_r (defined in Eq. 2.6). The drag coefficient C_d is usually a function of "obstacle" reynolds number (the cylinder Reynolds number if the "obstacle" is a cylinder, for example, see Daily and Harleman, 1966, p. 380). It is expedient to assume that C_d can also be expressed as a function of flow Reynolds number. So that similar friction equations to those in Chapter II may be developed. Because f, f_b and f_g are functions of flow Reynolds number, then f' is a function of flow Reynolds number. As shown in Eq. 3.54, f_g is also a function of flow depth.

Based on the above considerations, the Darcy-Weisbach friction factor may be described for different flow conditions.

The general form of the flow resistance factor was given by Eq. 2.7.

$$f' = \frac{a_2}{N_r^{b_2}} \tag{3.58}$$

in which a_2 and b_2 are functions of rainfall intensity, boundary roughness, bed forms, ground cover, canopy cover, and the flow Reynolds number.

For $N_r \leq 900$, it is more convenient to route water under different covers (canopy cover, ground cover and no cover) separately, and an average raindrop-impact effect is introduced. Then,

$$f' = \frac{k_1'}{N_r} = \frac{k_o(1 + \psi) + k_r i^{-0.41}}{N_r} \tag{3.59}$$

and

$$\bar{i} = (1 - D_c)\ (1 - D_g)\ i \tag{3.60}$$

in which k_1' is a constant representing overall resistance factor for $N_r < 900$, ψ is a constant representing the ratio of added friction factor (f_b and f_g) to the grain resistance factor without rainfall f, i.e., $\psi = \frac{f_b + f_g}{f}$ which will be given in detail later, and $\bar{i}$ is the effective rainfall intensity for raindrop impact effects.

For $2000 \leq N_r \leq 25{,}000$

$$f' = \frac{k_2'}{N_r^{0.25}} = \frac{k_2(1+\psi)}{N_r^{0.25}} \tag{3.61}$$

in which k_2' and k_2 are respectively constants representing the overall friction factor and grain resistance factor only for the specified flow Reynolds number range.

For $N_r \geq 100{,}000$, the friction factor is independent of N_r, or

$$f' = \frac{k_3'}{N_r^{0.0}} = k_3(1+\psi) \tag{3.62}$$

in which k_3' and k_3 are respectively constants representing the overall and grain resistance factor for $N_r > 100{,}000$.

In the transition ranges, estimation of friction factor are made by linear interpolations.

For $900 < N_r < 2000$

$$f' = \frac{k_1'\ 900^{\left(1.25\ \ln \frac{k_1'}{k_2'} - 7.14\right)}}{N_r^{\left(1.25\ \ln \frac{k_1'}{k_2'} - 6.14\right)}} \tag{3.63}$$

and for $25,000 < N_r < 100,000$

$$f' = \frac{k_3' \; 100,000^{(0.72 \ln \frac{k_2'}{k_3'} - 1.83)}}{N_r^{(0.72 \ln \frac{k_2'}{k_3'} - 1.83)}} \tag{3.64}$$

The constant, ψ, representing the ratio $(f_b+f_g)/f$ is determined in the following manner.

For overland flow and overbank portion of channel flow, both f_b and f_g are important, then

$$\psi = \psi_b + \psi_g D_g \tag{3.65}$$

in which ψ_b is the bed form resistance descriptor, a constant representing the ratio for added friction due to bed forms (f_b/f), and ψ_g is the ground cover resistance descriptor, a constant representing the ratio for the added friction factor due to ground cover when the ground cover density is equal to unity (f_g/f).

For channel flow less than bankfull flow, f_g is negligible, and

$$\psi = \psi_b \tag{3.66}$$

For overbank flow, both f_b and f_g are important. A linear weighting function is assumed, to determine an average resistance descriptor

$$\psi = \frac{P_o}{P} \psi_b + (1 - \frac{P_o}{P}) (\psi_b + \psi_g D_g) \tag{3.67}$$

in which P_o is the wetted perimeter of bankfull flow, and P is the total wetted perimeter.

3.4.3. Flow discharge and flow area relations

The values of α and β in Eq. 2.12 can be determined by substituting Eqs. 2.6, 3.51, 3.52, and 3.58 into Eq. 2.2. The solutions are

$$\alpha = \left[\frac{a_2^{\nu} \, a_1^{b_2(1+b_2)}}{8gS_o}\right] \frac{1}{(3-b_1-b_1b_2)} \tag{3.68}$$

and

$$\beta = \frac{2-b_2}{3-b_1-b_1b_2} \tag{3.69}$$

for $A \leq A_o$ and

$$\alpha = \left[\frac{a_2^{\nu} \, a_1'^{b_2(1+b_2)}}{8gS_o}\right] \frac{1}{(3-b_1'-b_1'b_2)} \tag{3.70}$$

and

$$\beta = \frac{2-b_2}{3-b_1'-b_1'b_2} \tag{3.71}$$

for $A > A_o$.

3.5. Applications

A computer program based on the mathematical formulations presented above was developed to simulate water outflow hydrographs of small watersheds. The listing of the computer program is given in Appendix C. (PROGRAM WATER).

Four rainfall-runoff events in Carrizal Basin, Venezuela for the summer of 1972 were used to test the applicability of the proposed mathematical model. Carrizal Basin is a small drainage catchment with

an area of 2.8 square kilometers. The four rainfall-runoff events used in this study are respectively the storms which occurred on July 9, September 2, September 3, and September 4, 1972.

The required data for model input and for parameter calibration were obtained from information presented by Berryman (1974). The required data were rainfall records, streamflow records, soil infiltration tests, evaporation studies, and channel surveys.

The details of input data, tested results, and possible applications to predict watershed treatment effects are given below.

3.5.1. Input data

The two groups of data required are the basin characteristics data and the storm characteristics data. The basin characteristics data include geometry, soil data, vegetation data, and flow resistance parameters. They are assumed to be time-invariant, i.e., they are independent of storms. The storm characteristics data are mean evaporation rate, antecedent moisture content, interception storage volume at the start of storm and rainfall records. These characteristics change from storm to storm.

3.5.1.1. Basin characteristics data

(a) Geometry

The geometric segmentation of the Carrizal Basin is shown in Fig. 3.11, and a typical P-A relation is given in Fig. 3.9. Table 3.2 provides a summary of the geometry for each segment of the basin.

The computation sequence, which was established by the logics of gravity flow and flow continuity requirement, is shown in Table 3.3 The computational order (Column 2) is the order for the computation of flow routing in the segment of Column 1. The numbers in Column 3

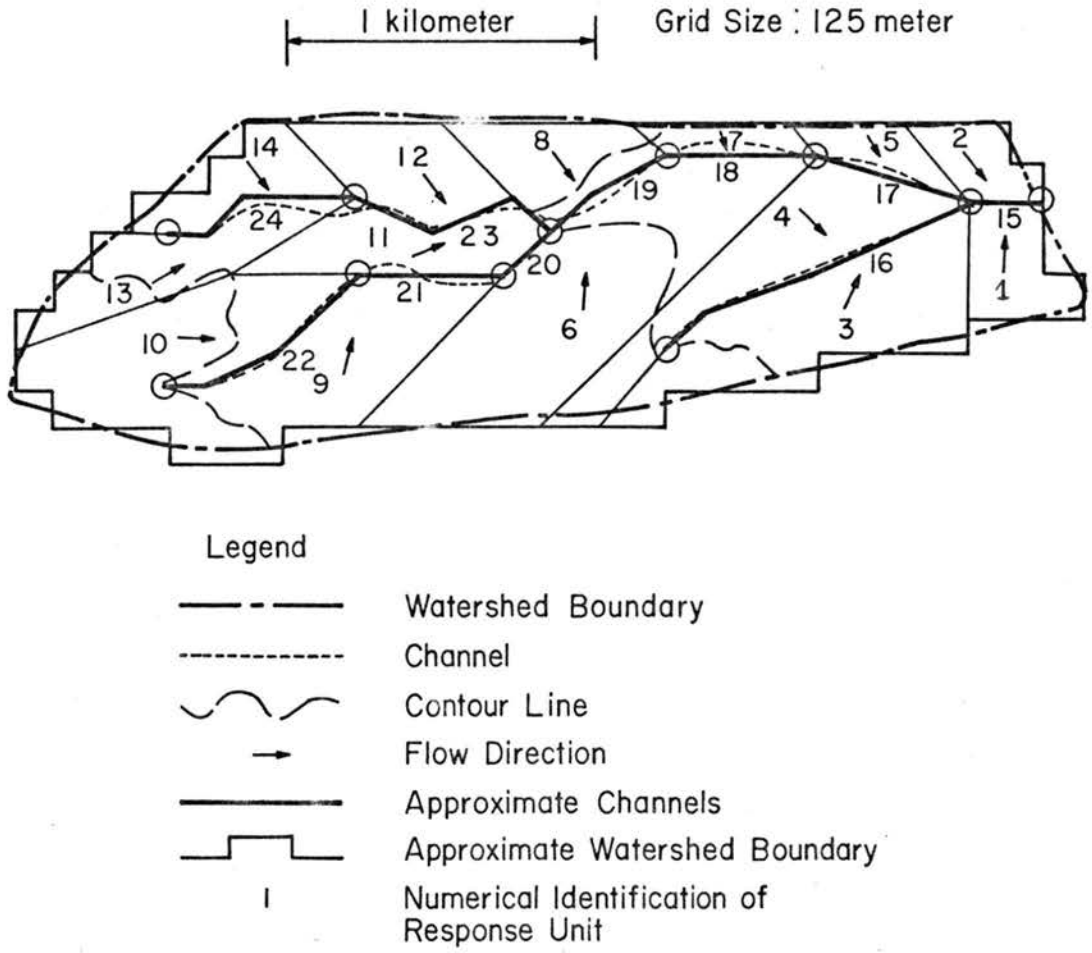

Fig. 3.11 Geometric segmentation of the Carrizal Basin, Venezuela

Table 3.2. Geometry of Carrizal Basin, Venezuela

Index	Length	Slope	Wetted Perimeter-Flow Area Relations					Type
	L (ft)	S_o	a_1	b_1	a_1'	b_1'	A_o (sq.ft)	
1	1436	0.002	0	0	1	0	0	O.F.
2	1026	0.002	0	0	1	0	0	O.F.
3	1044	0.0025	0	0	1	0	0	O.F.
4	703	0.0025	0	0	1	0	0	O.F.
5	448	0.0025	0	0	1	0	0	O.F.
6	1562	0.003	0	0	1	0	0	O.F.
7	410	0.003	0	0	1	0	0	O.F.
8	1068	0.0035	0	0	1	0	0	O.F.
9	951	0.005	0	0	1	0	0	O.F.
10	1540	0.005	0	0	1	0	0	O.F.
11	628	0.004	0	0	1	0	0	O.F.
12	698	0.004	0	0	1	0	0	O.F.
13	1256	0.005	0	0	1	0	0	O.F.
14	698	0.005	0	0	1	0	0	O.F.
15	820	0.002	5.297	0.25	0.177	1.25	30	C.F.
16	3706	0.005	2.655	0.55	0.757	1.25	6	C.F.
17	1689	0.002	4.208	0.35	0.232	1.25	25	C.F.
18	1640	0.002	3.750	0.40	0.294	1.25	20	C.F.
19	1496	0.0025	3.342	0.45	0.383	1.25	15	C.F.
20	578	0.003	2.979	0.5	0.530	1.25	10	C.F.
21	1640	0.004	2.979	0.5	0.626	1.25	8	C.F.
22	2075	0.005	2.655	0.55	1.006	1.25	4	C.F.
23	2411	0.004	2.979	0.5	0.530	1.25	10	C.F.
24	1808	0.005	2.655	0.55	1.006	1.25	4	C.F.

NOTE: O.F. is overland flow; C.F. is channel flow.

Table 3.3. Computational Sequence

Index (1)	Computational Order (2)	Upstream Inflow Segments (3)			Lateral Inflow Segments (4)	
1	1	0	0	0	0	0
2	2	0	0	0	0	0
3	3	0	0	0	0	0
4	4	0	0	0	0	0
5	5	0	0	0	0	0
6	6	0	0	0	0	0
7	7	0	0	0	0	0
8	8	0	0	0	0	0
9	9	0	0	0	0	0
10	10	0	0	0	0	0
11	11	0	0	0	0	0
12	12	0	0	0	0	0
13	13	0	0	0	0	0
14	14	0	0	0	0	0
15	24	16	17	0	1	2
16	23	0	0	0	3	4
17	22	18	0	0	5	0
18	21	19	0	0	6	7
19	20	20	23	0	6	8
20	19	21	0	0	6	0
21	18	22	0	0	9	0
22	17	0	0	0	9	10
23	16	24	0	0	11	12
24	15	0	0	0	13	14

indicate the upstream inflow segments to the segment in Column 1 and the numbers in Column 4 are the lateral inflow segments. When no upstream inflow segments or lateral inflow segments are involved, a "0" is indicated.

(b) Soil Data

The saturated hydraulic conductivity k_s was estimated from the saturated infiltration rate determined from the soil infiltration tests (Berrymen, 1974). The value of k_s was 0.3 in./hr.

For a typical soil, the moisture contents at the wilting point m_w and at the saturation m_s are approximately 0.1 and 0.5 respectively (Linsley, et al., 1958, p. 125). These values were used in this study.

The magnitude of the capillary potential at the wilting point P_w is usually about 15 atmosphere (Linsley, et al., 1958, p. 126), which is approximately 6100 inches of waterhead. This value was adopted in the analysis.

It is known that the depth of zone of aeration η_a was at least 3 feet (36 inches). This value of 3 feet was employed in the analysis.

(c) Vegetation

From aerial photos and ground survey data, the canopy cover density D_c was determined to be 0.4 and the ground cover density D_g was approximately 0.5.

The mean interception storage capacity of ground cover $D_g V_g$ was assumed to be 0.05 inch, the value given by Zinke (1965) for shrub or grass lands. Equivalently, V_g was assumed to be 0.1 inch. According to Penman (1965), the ratio of evaporating surface to the horizontal projected area for ground cover S_g was of the order of 10, 11 or 12 for grasses and had a value on the order of 5, 6 or 7 for agricultural

crops. In this study, S_g was assumed to be 7.0. The vegetation in tropical areas usually has larger leaves than that in other areas. Thus, a high value of r_v may be expected. According to Zinke (1965) the maximum measured interception storage for forest lands was around 0.36 inch and according to Linsley, et al., (1958) the interception storage for a four feet high cotton was 0.33 inch. In this study r_v was assumed to be 2.5 which implied that the interception storage volume under canopy was assumed to be 0.3 inch.

(d) Flow Resistance Parameters

The flow resistance parameters include k_o, k_r, k_2, k_3, ψ_b and ψ_g. These parameters are independent of storms. As mentioned in Section 3.4.2., ψ_g is a function of flow depth, which is a function of the size of storm. A large value of ψ_g may be expected for large storms.

For a natural and plain surface, the resistance can be estimated by assuming $k_r = 27$ (assuming an 8 ft fall to give the terminal velocity for raindrops), $K_o = 40$, $k_2 = 0.5$ (for asphalt surface $k_o = 35$, $k_2 = 0.4$), and $k_3 = 0.04$. Recall that k_3 is the Darcy-Weisbach friction factor for large Reynolds number flows ($N_r > 100{,}000$). The discharge coefficient $C/\sqrt{g}$ can be determined from the value of k_3 by,

$$\frac{C}{\sqrt{g}} = \sqrt{\frac{8}{k_3}} \qquad (3.72)$$

in which C is the Chezy resistance coefficient.

For k_3 of 0.04, the Chezy discharge coefficient as determined by Eq. 3.72 is 14.1, which is a common value of grain resistance in rivers (Simons and Richardson, 1966).

The added resistance due to bed forms and ground cover can be determined by the measured flow area-discharge (A-Q) relation at large Reynolds number flows ($N_r > 100,000$).

From Eqs. 2.2, 2.3, 3.51, 3.62 and 3.66, one obtains that

$$\psi_b = \frac{8gS_o A^{(3-b_1)}}{Q^2 a_1 k_3} - 1 \qquad (3.73)$$

The discharge measurements taken near the outlet of the watershed (Berryman, 1974) indicated that ψ_b varied from 5.8 to 11.0. Because ψ_b is a measure of added roughness due to bed deformations only and a larger value of ψ_b may be due to the inclusion of ground cover resistance. Thus, ψ_b was assumed to be 6.0 in the subsequent analysis.

Velocity measurements in the channel and floodplain were also reported by Berryman. With the measured data in the overbank portion, the values ψ_g were estimated using the equation

$$\psi_g = \frac{1}{D_g}\left(\frac{8gS_o y}{V^2 k_3} - 1 - \psi_b\right) \qquad (3.74)$$

in which V is the mean velocity across the entire depth at a specific location. Equation 3.74 is obtained from Eqs. 3.55, 3.62 and 3.65.

The values of ψ_g varied from 17 to 29. Therefore the range of ψ_g was assumed to be $16 \leq \psi_g \leq 30$. The proper value of ψ_g for each storm should be estimated by a calibration procedure which will be presented in Section 3.5.2.

3.5.1.2. Storm characteristics

The storm characteristics data include the rainfall records i(t), the mean evaporation rate E, the initial interception storage content I_s and the antecedent moisture content $m_o(0)$.

The rainfall records for the storms used in this study are given in Table 3.4. The intensities were derived from the accumulation of precipitation over a five-minute interval.

The evaporation studies in Carrizal Basin (Berryman, 1974) indicated that the average pan evaporation rate was 0.03 in/hr for a six-day measurement and was 0.01 in/hr during the storm of June 19, 1972. It was assumed that the average evaporation rate was 0.01 in/hr for all storms in this study.

From the rainfall records for the rainy season (Berryman, 1974) the amount of rainfall needed to recharge the Basin to produce runoff was determined, thus the ranges of initial interception storage content $m_o(0)$ could be estimated. Assuming that the initial rainfall for the storm being considered (the cumulative amount of rainfall before runoff) all entered the interception storage, it was determined that the values of I_s were between 0.5 and 1.0. Because the storms used in this analysis all started with very wet ground condition, it is estimated that the value of $m_o(0)$ was greater than the field capacity of the soil (9.4 for clay). The value of $m_o(0)$ was assumed to be $0.4 \leq m_o(0) \leq 0.5$.

The proper values of I_s and $m_o(0)$ for different storms were estimated by a calibration procedure given in the following section.

3.5.2. Model calibration

The values of the three unknowns (ψ_g, I_s, and $m_o(0)$) must be estimated. The ranges of these three unknowns as discussed in the previous sections are:

$$16 \leq \psi_g \leq 30 \qquad (3.74)$$

Table 3.4. Rainfall Records for Storms Used in Analysis

Local Time(hr)	Rainfall Intensity(in/hr)
July 9	
1625	0.14
1630	3.07
1635	3.17
1640	2.60
1645	1.32
1650	0.99
1655	1.56
1700	1.89
1705	1.32
1710	0.85
1715	0.14
1720	0.09
1725	0.14
1730	0.03
1735	0.03
1740	0.03
September 2	
0510	0.05
0515	0.05
0520	0.05
0525	0.80
0530	0.99
0535	0.57
0540	0.24
0545	0.61
0550	0.99
0555	1.79
0600	0.71
0605	1.09
0610	0.24
0615	0.33
0620	0.05
0625	0.05
0630	0.05
0635	0.00
0640	0.24
0645	0.09
0650	0.14
0655	0.47
0700	0.14
0705	0.09
0710	0.14
0715	0.94
0720	0.14
0725	0.09
0730	0.09
0735	0.05
0740	0.09
0745	0.14
0750	0.47
0755	1.32
0800	2.03
0805	3.35
0810	0.61
0815	0.09
0820	0.09
0825	0.09
0830	0.14
0835	0.24
0840	0.33
0845	0.28
0850	0.33
0855	0.38
0900	0.24
0905	0.47
0910	0.09
0915	0.28
0920	0.24
0925	0.09
0930	0.14
0935	0.33
0940	0.24
0945	0.09
0950	0.05
0955	0.14
1000	0.05
1005	0.05
1010	0.05
1015	0.09
1020	0.05
1025	0.05
1030	0.14
1035	0.33
1040	0.24
1045	0.09
1050	0.05
1055	0.05
1100	0.00
1105	0.05
1110	0.05
September 3	
0635	0.38
0640	0.09
0645	0.14
0650	0.05
0655	0.05
0700	0.05
0705	0.07
0710	0.07
0715	0.05
0720	0.05
0725	0.24
0730	0.14
0735	0.05
0740	0.05
0745	0.07
0750	0.07
0755	0.07
0800	0.07
0805	0.09
0810	0.14
0815	0.33
0820	1.32
0825	1.23
0830	0.80
0835	1.09
0840	1.70
0845	1.56
0850	0.33
0855	0.14
0900	0.38
0905	0.09
0910	0.14
0915	0.09
0920	0.14
0925	0.09
0930	0.14
September 4	
1540	1.94
1545	1.65
1550	0.24
1555	0.14
1600	0.00
1605	0.00
1610	0.00
1615	0.00
1620	0.00
1625	1.80
1630	0.85
1635	1.18
1640	0.85
1645	0.38

$$0.5 \leq I_s \leq 1.0 \tag{3.75}$$

$$0.4 \leq m_o(0) \leq 0.5 \tag{3.76}$$

Estimations for these unknowns can be made by using the multi-dimensional calibration technique described in Appendix B, but that technique is very time consuming in computer operations. Herein, based on the physical significance, an easy and practical way to estimate these values is presented.

From a physical point of view, the values of I_s and $m_o(0)$ control the water balance between the rainfall input and the streamflow output. The parameter ψ_g determines the time to peak flow and the shape of the hydrograph. In order to simplify the calibration procedure, separate calibrations for water balance and flow routing should be made. The steps of calibration are as follows:

(1) Assume a value of I_s based on the initial rainfall and the moisture condition of the basin. Then, the value of $m_o(0)$ can be estimated by adjusting the estimated volume of rainfall excess to be nearly equal to the total volume of the measured runoff. This adjustment can be made by trial and error or by the one-dimensional calibration technique presented in Appendix B.

(2) With the values of I_s and $m_o(0)$ estimated in step 1, adjust the value of ψ_g to obtain the correct time to peak flow. Again, this adjustment can be achieved by either trial and error or by the one-dimensional calibration technique.

(3) If the magnitude of the peak flow or the shape of the hydrograph is not correct, select another value of I_s and repeat steps 1 and 2 until a satisfactory answer is found.

The estimated values of ψ_g, I_s, and $m_o(0)$ are given in Table 3.5. The estimated ground cover resistance for different magnitudes of storms is also given in Fig. 3.12. The value of ψ_g increases as the magnitude of storm increases.

Table 3.5. Estimated Values of ψ_g , I_s , and $m_o(0)$

Storm	ψ_g	I_s	$m_o(0)$
July 9	20	0.6	0.475
September 2	30	1.0	0.488
September 3	21	1.0	0.500
September 4	18	0.6	0.486

The estimated values of I_s are respectively 1.0 for September 2 and September 3 storms and 0.6 for July 19 and September 4 storms. This is because the September 2 and September 3 storms occurred at daybreak, while, July 9 and September 4 storms occurred in the late afternoon. Less water escapes from interception storage for a storm occurring at daybreak.

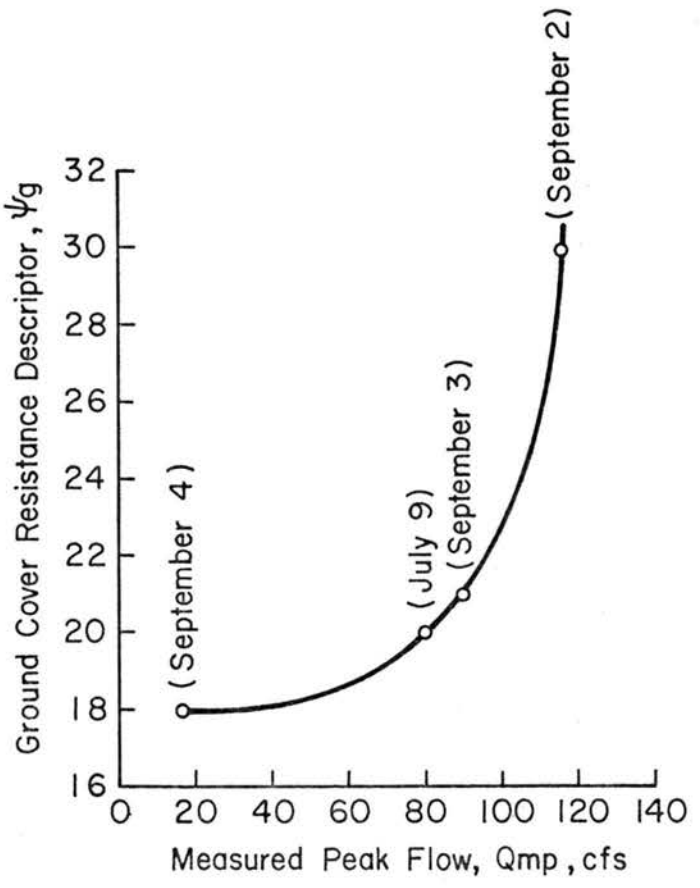

Fig. 3.12 Ground cover resistance for tested storms

The antecedent moisture content of the July 9 storm is comparatively lower than for the storms occurring on September 2, 3 and 4. This coincides with the overall rainfall records. Due to the long recession of the big storm on September 2, the September 3 storm started with a completely wet condition. The estimated value of $m_o(0)$ was 0.5.

3.5.3. Test results

In the numerical computation for runoff from the Carrizal Basin, the time increment Δt was chosen as 5.0 min. and the ratio of time increment to space increment was in the range of $0.62 \leq \frac{\Delta t}{\Delta x} \leq 3.66$ sec/ft.

The computed maximum infiltration rates $f_m(t)$ for the July 9 storm are given in Fig. 3.13. The rates are different for areas under canopy and areas without trees. The value of $f_m(t)$ under the canopy is uniformly larger than that in areas without trees.

The comparisons of the simulated and the measured hydrographs for July 9, September 2, September 3, and September 4 storms are given in Fig. 3.14. The agreement between the measured hydrographs and the computed hydrographs is satisfactory. The accuracy of simulation is expressed in terms of the percentage error in total volume of runoff E_v, the relative mean absolute error E_a, the percentage error in the peak flow E_p, and the percentage error in the time to peak flow E_t. The terms are defined as follows:

$$E_v = 100 \left[1 - \frac{\sum_{t=1}^{N} Q_o(t)\ \Delta t}{\sum_{t=1}^{N} Q_m(t)\ \Delta t} \right] \tag{3.77}$$

$$E_a = \frac{100}{N} \sum_{t=1}^{N} \frac{|Q_o(t) - Q_m(t)|}{Q_{mp}} \tag{3.78}$$

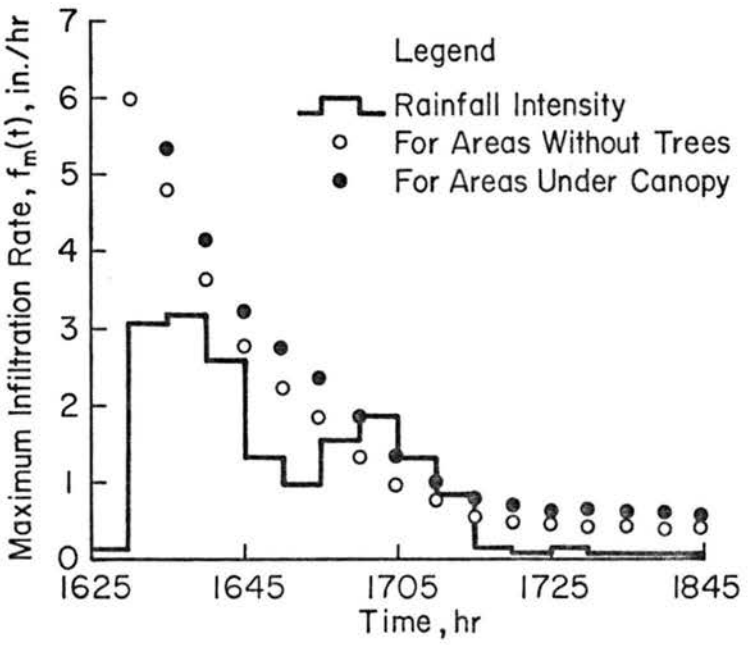

Fig. 3.13 Computed maximum infiltration rates for July 9 storm

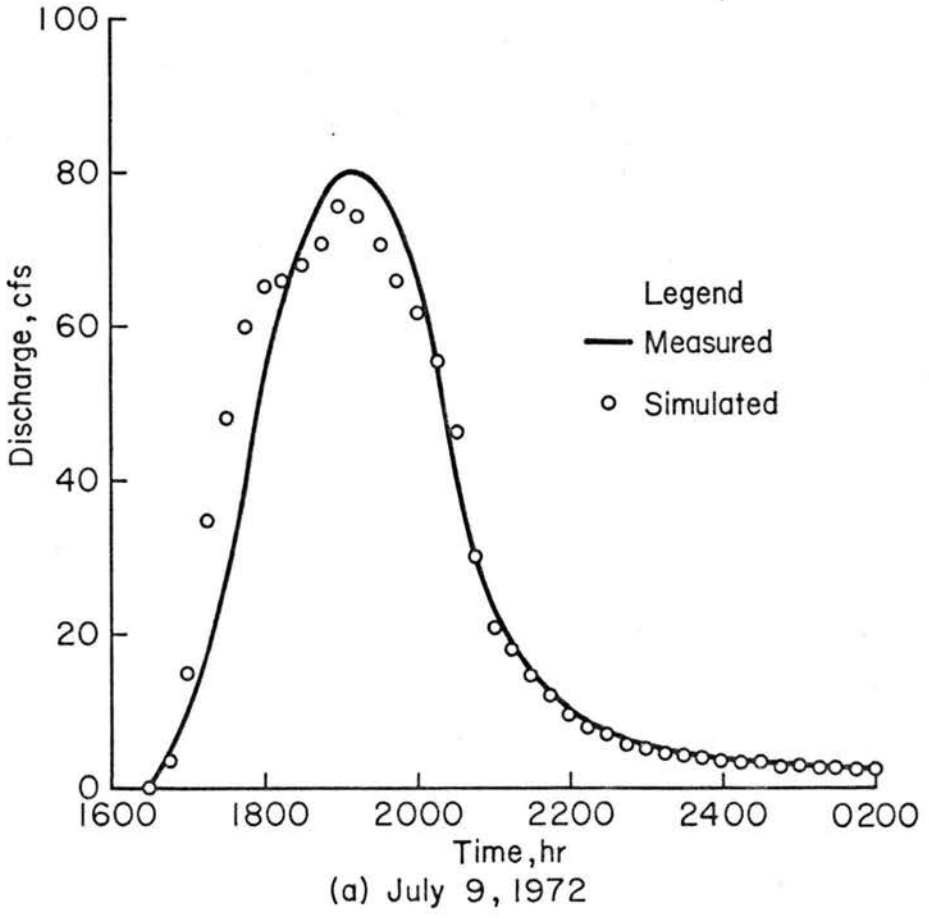

Fig. 3.14 Hydrographs of Carrizal Basin, Venezuela

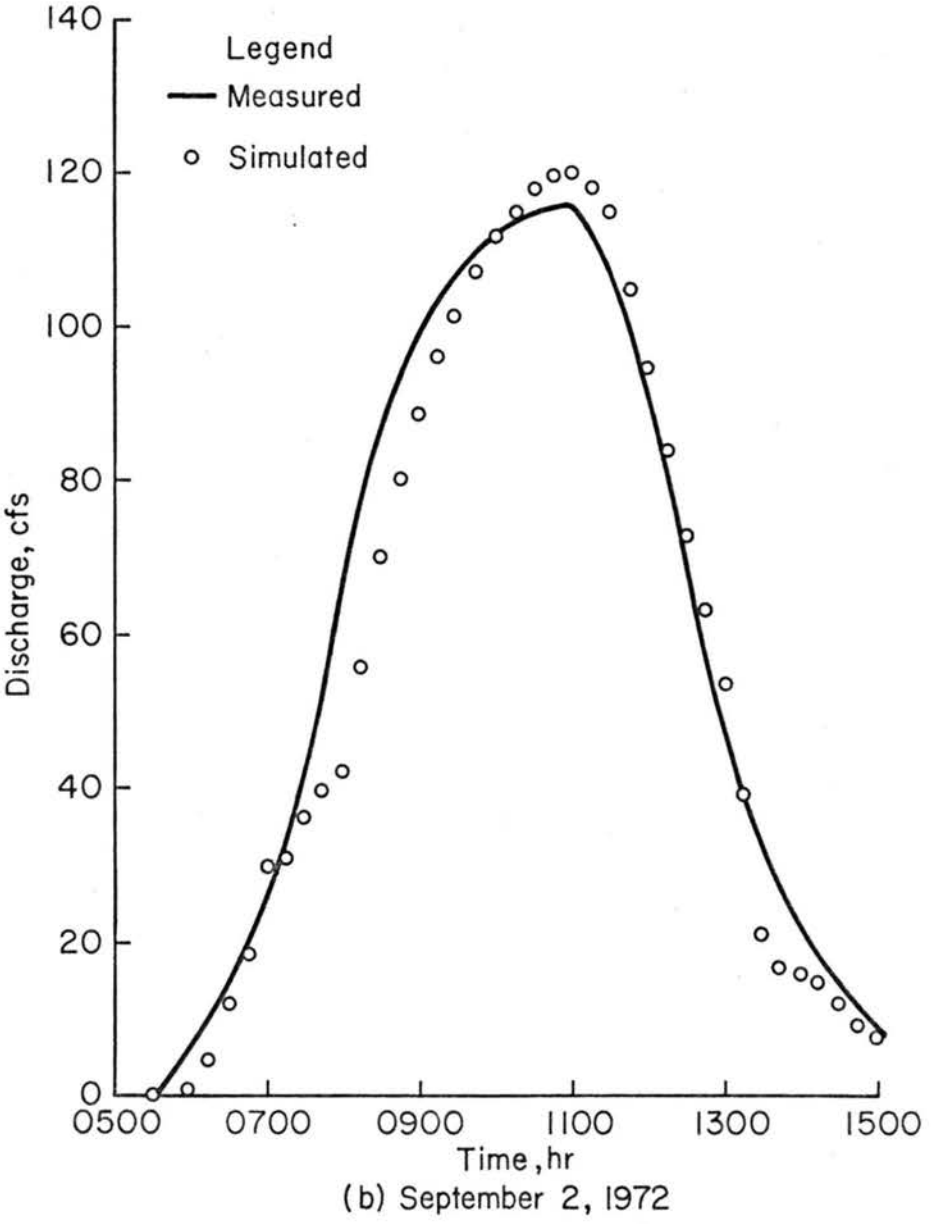

Fig. 3.14 Hydrographs of Carrizal Basin, Venezuela (continued)

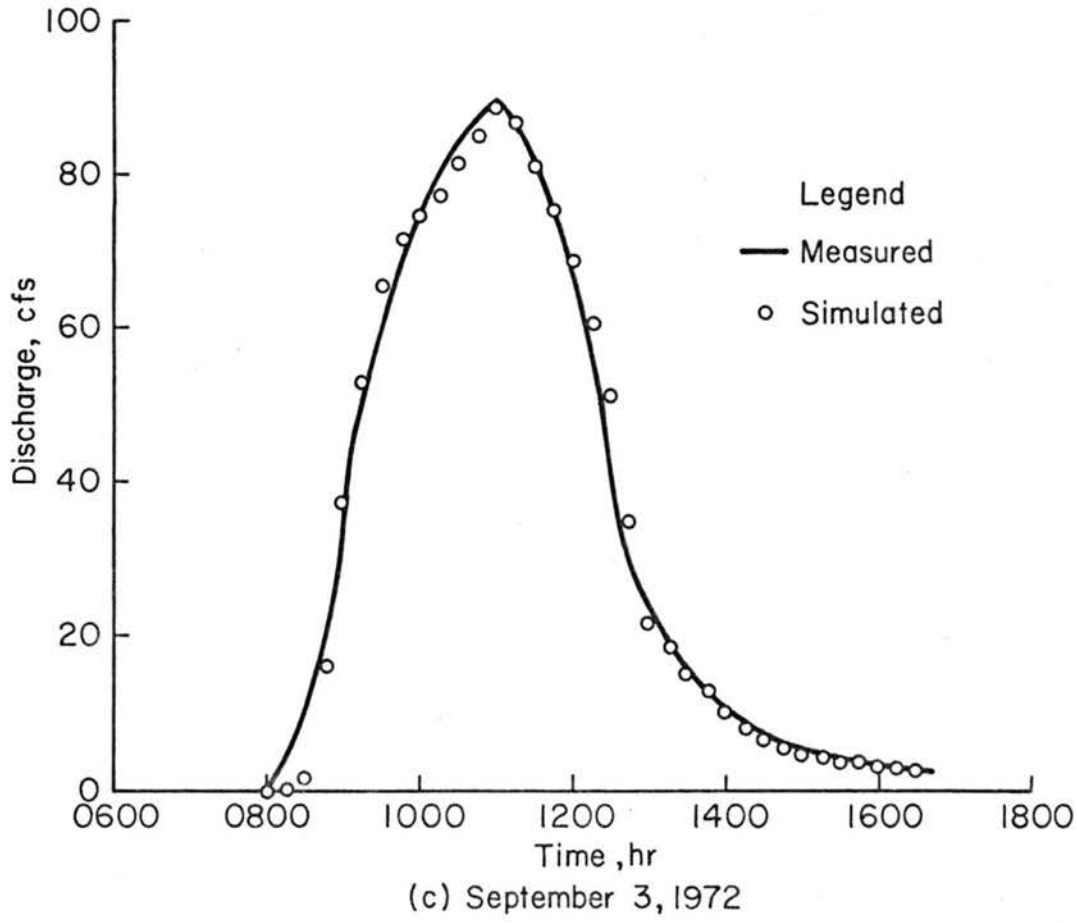

Fig. 3.14 Hydrographs of Carrizal Basin, Venezuela (continued)

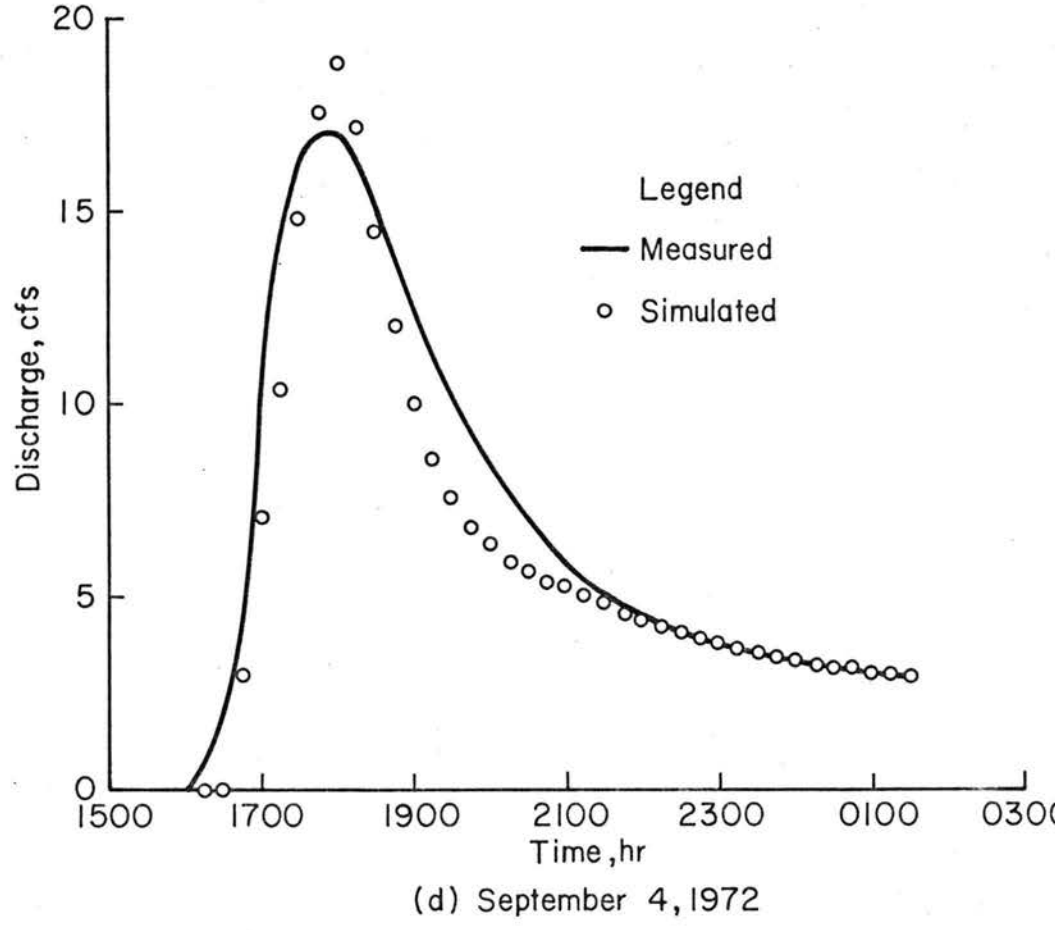

Fig. 3.14 Hydrographs of Carrizal Basin, Venezuela (continued)

$$E_p = 100 \left(1 - \frac{Q_{op}}{Q_{mp}}\right) \tag{3.79}$$

and

$$E_t = 100 \left(1 - \frac{t_{op}}{t_{mp}}\right) \tag{3.80}$$

Here N is the number of time increments extending from the beginning to the end of the runoff event, $Q_o(t)$ and $Q_m(t)$ are respectively the simulated and the measured runoff at time t , Q_{op} and Q_{mp} are respectively the simulated and the measured peak flow, and t_{op} and t_{mp} are respectively the simulated and the measured time to peak flow.

The values of E_v , E_a , E_p and E_t for the four runoff events are given in Table 3.6. These estimated errors indicate that the

Table 3.6. Summary of Estimated Errors in Water Hydrograph Simulation

Storm	Error (%)			
	E_v	E_a	E_p	E_t
July 9	3.2	4.5	-5.5	3.2
September 2	-5.2	6.0	3.7	-1.4
September 3	0.5	2.0	-1.3	1.9
September 4	-10.7	5.4	11.2	0

proposed model can simulate the size, shape and peak of the hydrographs produced by the study basin generally within $\pm$ 12 percent.

3.5.4. Sensitivity analysis

Based on the July 9 storm, partial sensitivities of selected parameters or data were examined. This sensitivity analysis was expressed in terms of percentage changes in the total volume, the peak flow, and the time to peak flow of the computed hydrograph. These changes were estimated by assigning errors of -30, -20, -10, +10, +20 and +30 percent to the calibrated value of the parameter being examined, values of the other parameter or data were kept the same as those identified in the calibration.

Results of the analysis are given in Table 3.7. This analysis indicates that soil data are very sensitive to the total volume, the peak flow rate and the time to peak flow. Flow resistance parameters and vegetation data are less sensitive to the computed results. The total volume of the computed hydrograph is nearly independent of flow resistance parameters. However, the results of this analysis are limited to the physical conditions of the tested basin, different results may be obtained for a different watershed.

3.5.5. Applications to predict watershed treatment effects

Watershed treatment includes the vegetation treatment and the mechanical treatment. Some types of vegetation treatment are variations in planting patterns in the amount and patterns of logging, in the amount and type of litter or mulch, and in the amount of burning in forest watersheds. Mechanical treatments include dam building, road construction and other erosion or flood control measures.

The vegetation treatment effects can be estimated by changing the canopy cover density and the ground cover density. The prediction

Table 3.7. Sensitivity Analysis of the Rainfall-Runoff Model

(a) Sensitivity in total volume

Percentage Error in Estimated Data or Parameters	Percentage Change in Computed Total Volume (%)																	
	Soil Data						Vegetation Data						Flow Resistance Parameters					
(%)	k_s	m_w	m_s	P_w	η_a	$m_o(0)$	D_c	D_g	V_g	S_g	r_v	I_s	k_o	k_r	k_2	k_3	ψ_b	ψ_g
-30	11.1	1.4	--[a]	9.3	53.8	--	7.0	5.0	3.3	5.9	6.3	-6.0	3.1	0.1	-0.9	0.3	1.2	1.4
-20	6.9	0.9	--	5.8	34.2	-99.6	4.6	3.2	2.3	3.9	4.2	-4.4	2.3	0.1	-0.5	0.2	0.7	1.1
-10	2.9	0.6	--	2.4	15.2	-96.8	2.1	1.6	-2.7	1.9	1.9	-2.4	0.9	0.1	-0.4	0.1	0.2	0.5
10	- 2.9	-0.5	-96.6	-2.3	-12.0	--	-3.1	-1.8	1.6	-2.0	-2.2	1.8	-0.9	0.0	0.4	-0.1	-0.3	-0.5
20	- 5.4	-1.1	-99.4	-4.4	-21.3	--	-5.5	-3.8	-3.2	-4.0	-4.5	3.3	-1.7	-0.1	0.7	-0.2	-0.7	-1.0
30	- 7.2	-1.9	--	-6.0	-27.8	--	-7.8	-5.5	-4.4	-5.8	-6.3	5.5	-2.5	-0.1	1.1	-0.3	-1.1	-1.3

(b) Sensitivity in Peak Flow

Percentage Error in Estimated Data or Parameters	Percentage Change in Computed Peak Flow (%)																	
	Soil Data						Vegetation Data						Flow Resistance Parameters					
(%)	k_s	m_w	m_s	P_w	η_a	$m_o(0)$	D_c	D_g	V_g	S_g	r_v	I_s	k_o	k_r	k_2	k_3	ψ_b	ψ_g
-30	11.6	1.3	--	9.2	49.1	--	7.0	13.4	4.0	5.5	6.3	-5.4	2.7	0.3	1.5	12.1	5.4	9.4
-20	7.2	1.1	--	6.2	32.4	-99.5	4.7	8.8	2.5	3.8	4.4	-4.5	3.1	0.3	0.9	7.9	3.4	6.3
-10	2.9	0.6	--	2.4	14.5	-97.4	2.1	4.1	1.4	2.0	1.8	-1.6	1.1	0.3	1.0	3.7	1.5	2.9
10	- 2.4	0.1	-97.3	-2.0	-11.9	--	-2.8	- 3.1	-1.1	-1.3	-1.4	1.7	-0.3	0.3	0.2	- 4.0	-0.8	-2.3
20	- 5.3	-0.6	-99.4	-3.9	-20.6	--	-5.4	- 7.9	-2.7	-4.0	-4.6	4.0	-1.4	0.0	-0.7	- 6.8	-2.6	-4.9
30	- 7.1	-1.4	--	-5.9	-24.7	--	-7.2	-11.1	-4.5	-5.8	-6.1	6.1	-2.2	-0.3	-0.9	-10.0	-3.8	-6.9

(c) Sensitivity in Time to Peak Flow

Percentage Error in Estimated Data or Parameters	Percentage Change in Computed Time to Peak Flow (%)																	
	Soil Data						Vegetation Data						Flow Resistance Parameters					
(%)	k_s	m_w	m_s	P_w	η_a	$m_o(0)$	D_c	D_g	V_g	S_g	r_v	I_s	k_o	k_r	k_2	k_3	ψ_b	ψ_g
-30	3.0	0.0	--	3.0	12.1	--	3.0	-6.1	3.0	3.0	3.0	-3.0	-6.1	0	-3.0	-6.1	-6.1	-9.1
-20	3.0	0.0	--	3.0	9.1	136.4	3.0	-3.0	0	3.0	3.0	-3.0	0.0	0	0.0	-3.0	-3.0	-3.0
-10	0.0	0.0	--	0	6.1	57.6	0.0	-3.0	0	0.0	0.0	0.0	0.0	0	0.0	-3.0	-3.0	-3.0
10	0.0	0.0	54.5	0	- 6.1	--	-3.0	3.0	0	0.0	0.0	0.0	3.0	0	3.0	3.0	3.0	3.0
20	-3.0	0.0	124.2	+3.0	-15.2	--	-3.0	3.0	-3.0	-3.0	-3.0	3.0	3.0	0	3.0	3.0	3.0	6.1
30	-3.0	0.0	--	-3.0	-27.3	--	-3.0	6.1	-3.0	-3.0	-3.0	3.0	3.0	0	3.0	3.0	6.1	6.1

[a] Neglected due to improper physical conditions

of mechanical treatment effects can be accomplished by redividing the response units.

Based on the July 9 storm, examples of vegetation treatment effects on the Carrizal Basin have been estimated as follows.

Fig. 3.15 shows that for a constant ground cover density (D_g=0.5) the total runoff volume and the peak flow are increased as the canopy cover density is decreased. The increase results because the interception is reduced when vegetation is removed. However, Fig. 3.13 also indicates that the time to peak flow is lengthened as the canopy cover is decreased. This flow retardation is due to the augmenting of raindrop impact resistance by increasing areas of exposure and the attenuation by overbank flows. In this hypothetical case the watershed is subjected to different amounts of cutting treatment but the forest floor remains undisturbed.

If the watershed is under clear cutting treatment and the forest litter, tree mulch, etc. are also removed in different degrees, or if the ground cover is completely destroyed by a burning treatment, the associated response can be estimated by changing the ground cover density in the model. An example is shown in Fig. 3.16. The total runoff volume and the peak flow rate are increased as the ground cover density is decreased. The time to peak flow is shortened as the ground cover density is decreased. The short time to peak flow is due to the decrease of flow resistance when the ground cover density is decreased.

In the above examples, it was assumed that the initial conditions and the physical parameters were unchanged for different treatment conditions. Actually, the initial interception storage content I_s, the antecedent moisture content, $m_o(0)$, and the saturated hydraulic

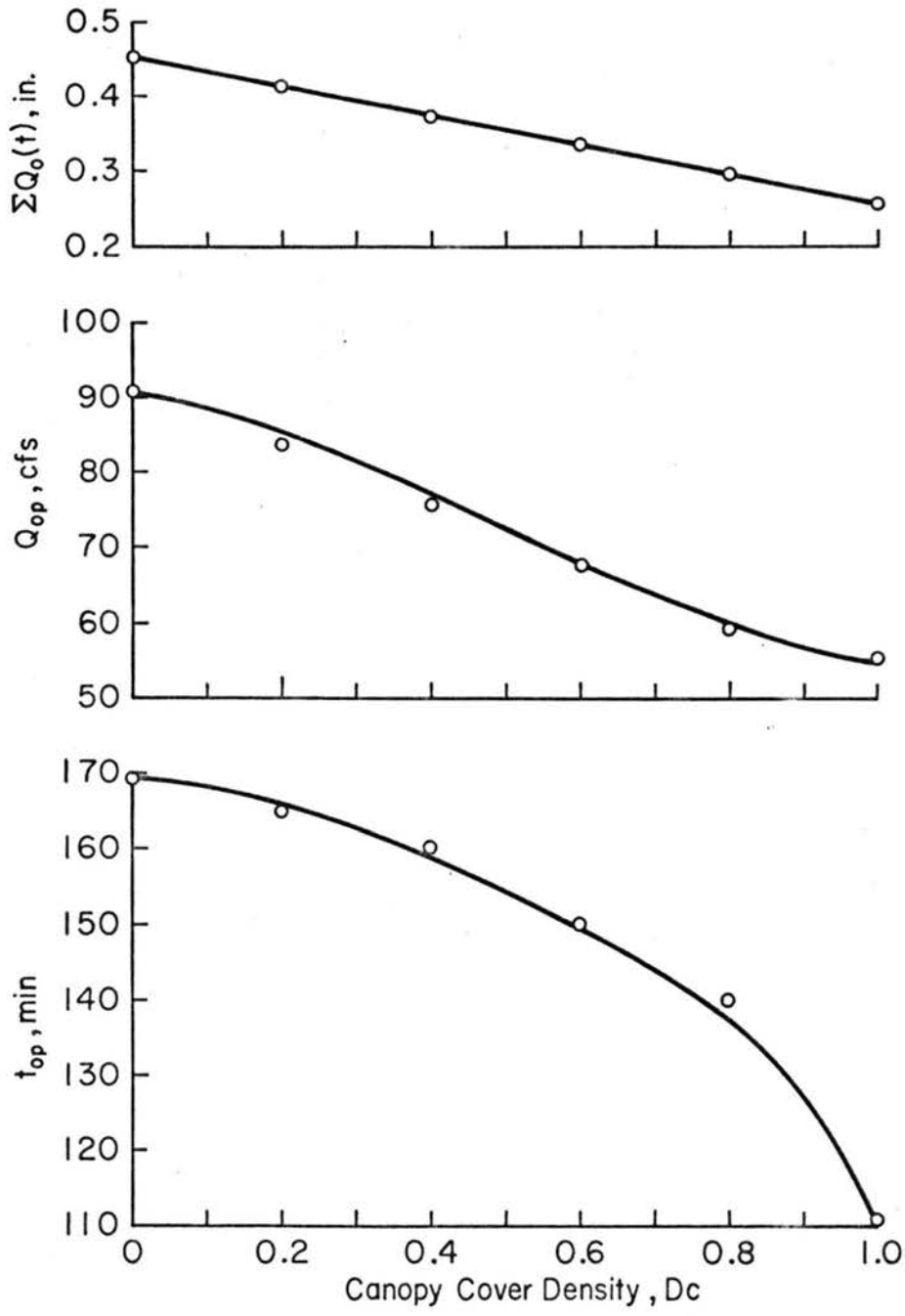

Fig. 3.15 Effects of canopy cover density on outflow hydrographs

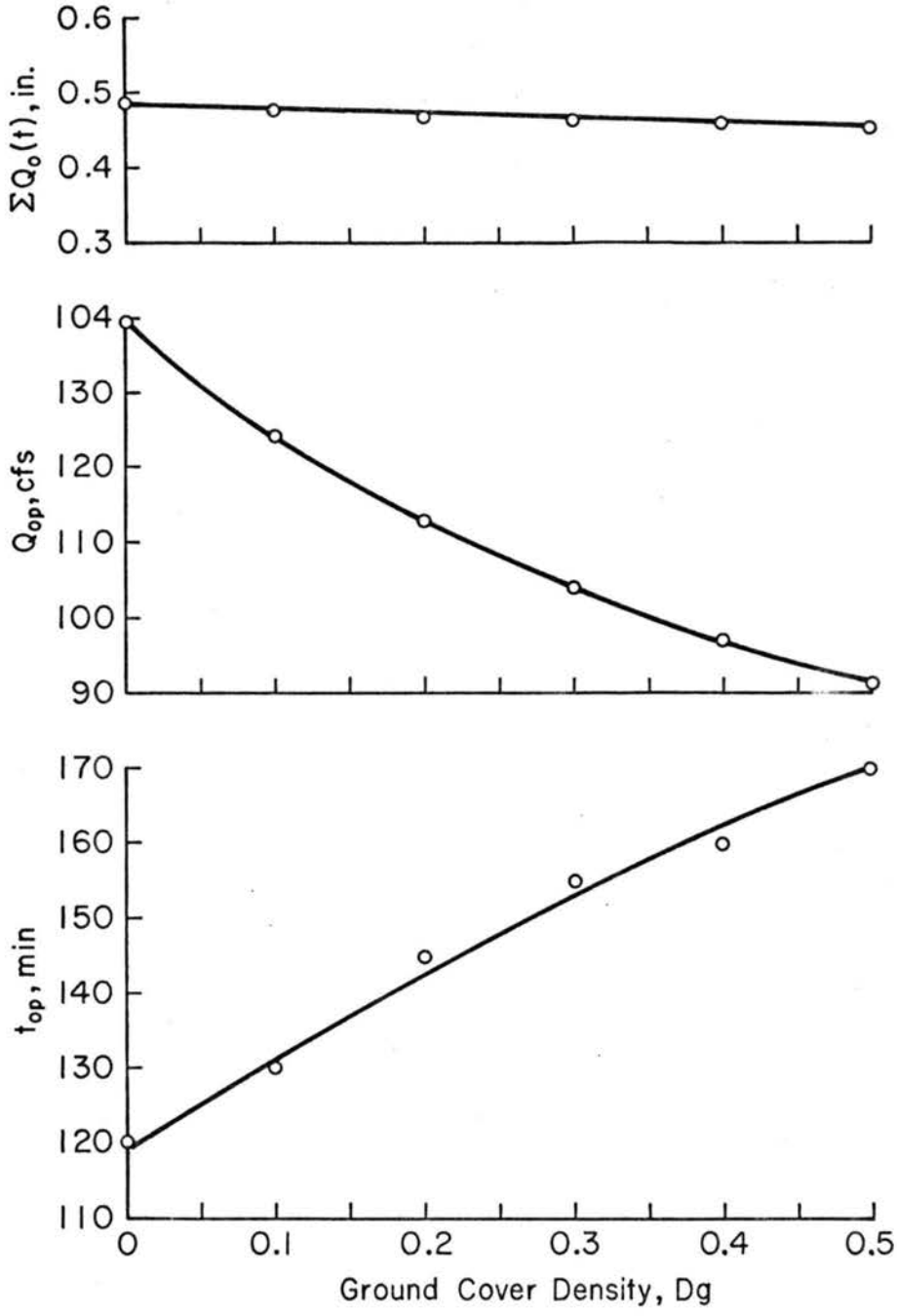

Fig. 3.16 Effects of ground cover density on outflow hydrographs

conductivity of soil, k_s may be altered by different treatments. For example, the hydraulic conductivity may be significantly reduced by a burning treatment which seals the ground surface. If the proper changes in these values can be estimated, the proposed model will provide values for the anticipated responses.

3.6. Summary

A mathematical model for simulating hydrographs from small watersheds has been developed. This model is designed to simulate the response of the basin to rainfall. The model includes the water balance simulation for land surface hydrologic cycle on the single storm basis and the water routing features for both overland flow and channel systems. Unlike the conventional approach to parametric modeling of watershed response, this model is based on the physical process governing the mechanics of water flow and requires less assistance from optimization schemes than any existing water models known to the writer.

For the Carrizal Basin in Venezuela the simulated hydrographs agree well with the measured hydrographs. The differences between the simulated and measured hydrographs indicate that the proposed model is able to simulate the total volume, the hydrograph shape, the peak flow and the time to peak flow generally within 12 percent. The sensitivity analysis shows that soil data are very sensitive to the total volume, the peak flow and the time to peak flow of the computed hydrograph. Flow resistance parameters and vegetation data are less sensitive to the simulated results. In addition, this physically oriented model has the capability to predict watershed treatment effects on water yields under the assumed conditions.

The applicability of the proposed model is limited to the following conditions: (1) the streams within the watershed are ephemeral, and the movement of subsurface flow and ground water flow are negligible; (2) the kinematic-wave approximation for flow routing is valid, i.e., the gradients due to local and convective accelerations are negligible, and the water surface slope is nearly equal to the bed slope; and (3) the water yield simulation is on the single storm basis. Incorporating with a water balance model for simulating the water budget during interstorm periods; this model may estimate the long-term response of the water yield.

The input required for this simulation model can be summarized as follows.

(1) Geometry data--slope length, bed slope, wetted perimeter —flow area relation, and computational order for each segment.

(2) Soil data--saturated hydraulic conductivity, moisture contents at the wilting point and at the saturation, magnitude of the capillary potential at the wilting point, and depth of aeration.

(3) Vegetation data--canopy cover density, ground cover density, interception storage capacity of ground cover, ratio of evaporating surface to the horizontal projected area for ground cover, and ratio of the interception storage capacity of a tree canopy to the interception storage capacity of ground cover.

(4) Flow resistance parameters--constants describing grain resistance for different Reynolds numbers, constant

representing added roughness due to raindrop impact, bed form resistance descriptor and ground cover resistance descriptor.

(5) Storm characteristics data--rainfall records, mean evaporation rate, initial interception storage content and antecedent moisture content.

Chapter IV

MECHANICS OF OVERLAND FLOW SOIL EROSION

4.1. Need for the Study

The estimation of soil erosion by overland flow is an important factor in the prediction of sediment yield from watersheds. An improved understanding of the physical process which governs overland flow erosion is apparently needed. As reviewed in Chapter I, the existing soil loss equations are mainly dependent on statistical analyses of observed data in experimental plots or natural watersheds. Li, Shen and Simons (1973) indicated the possibilities of introducing the physics of overland flow into soil erosion studies. A model with physical significance appears to be more useful than those by regression analysis in estimating time-dependent erosion rate. In this Chapter, an unsteady overland flow soil erosion model is presented. This model was developed to simulate sediment outflow hydrographs and land form evolution process in a plain overland flow surface with sandy soil. Because of the sandy soil used, the soil detaching and transporting capacity of raindrop impact was ignored. However, the effect of raindrop impact on flow resistance was included.

Although this study concerns a rather simplified case, it provides a good understanding of the mechanics of overland flow soil erosion.

4.2. Sediment Routing Procedure

The water and sediment routing can be accomplished by using the continuity equations for water and sediment and the momentum equation for sediment-laden flow (Chang and Richards, 1971 or Chen, 1973).

These three equations can be solved simutaneously (Chang and Richards, 1971) or they can be solved sequentially (Chen, 1973). For simplicity, it is assumed that the changes in bed slope and bed elevation within a short time interval are small in comparison with changes in other variables involved in water and sediment routing. Then, the water and sediment routing can be accomplished by solving water routing and sediment routing sequentially (Chen, 1973).

In this study, the solutions of water and sediment routing are obtained by using a simplified procedure. This procedure includes solving water routing first and adjusting bed slopes later based on the sediment continuity equation and a sediment transport equation.

The detail of overland flow water routing on a plain surface was given in Chapter II. The coupled sediment routing procedure is presented herein.

4.2.1. Sediment transport equation

Sediment bed material load consists of bed load and suspended load. According to Shen (1971), for a constant bed material, the bed-load discharge may fit either of the following two functions

$$q_b = \beta_1 \tau^{\beta_2} \tag{4.1}$$

or

$$q_b = \beta_1' (\tau-\tau_c)^{\beta_2'} \tag{4.2}$$

Here q_b is the bed-load transport rate, τ is the boundary shear stress, τ_c is the critical shear stress, and β_2, β_1, β_1' and β_2' are constants.

The boundary shear stress as determined by the kinematic-wave approximation (see Chapter II) is,

$$\tau = \gamma y S_o \tag{4.3}$$

in which y is determined by the water routing procedure described in Chapter II. In overland flow, the flow area A per unit width of overland flow is y.

The critical shear stress τ_c as reported by Gessler (1965) is

$$\tau_c = 0.047\ \gamma(s_s - 1)\ d_{50} \tag{4.4}$$

in which s_s is the specific gravity of sediment, and d_{50} is the size of the sediment on the bed of which 50 percent is finer by weight.

The sediment concentration profile as reported by Einstein (1950) is

$$\frac{C_\xi}{C_o} = \left(\frac{y-\xi}{\xi}\ \frac{\bar{a}}{y-\bar{a}}\right)^{\omega} \tag{4.5}$$

in which C_ξ is the sediment concentration at the distance ξ from the bed, C_o is the known concentration at a distance $\bar{a}$ above the bed, y is the total depth of flow, and ω is a parameter, which is defined as

$$\omega = \frac{V_s}{0.4U_*} \tag{4.6}$$

Here V_s is the settling velocity of the sediment particle and U_* is the shear velocity of flow defined as

$$U_* = \sqrt{\frac{\tau}{\rho}} \tag{4.7}$$

Yoon (1970) measured velocity profiles in sheet flow under simulated rainfall and found that two separate velocity defect laws could be used to fit the upper and the lower velocity profiles (divided by the position of maximum velocity which was at approximately two-third of the depth). Unfortunately, Yoon's results did not provide enough information for predicting the velocity profile. This is because the maximum velocity must be measured. A logarithmic velocity profile is commonly adopted to describe the velocity distribution in turbulent flows. For simplicity, a logarithmic velocity profile is assumed in this study. The equation is

$$\frac{u_\xi}{U_*} = B + 2.5 \ln\left(\frac{\xi}{\eta_s}\right) \tag{4.8}$$

in which u_ξ is the point mean velocity at the distance ξ from the bed, B is a constant dependent on roughness, and η_s is the roughness height.

The integral of suspended load above a distance a can be obtained by combining Eqs. 4.5 and 4.8 or

$$S_q = \int_{\bar{a}}^{y} u_\xi C_\xi \, d\xi$$

$$= \int_{\bar{a}}^{y} \left[B + 2.5 \ln\left(\frac{\xi}{\eta_s}\right)\right] U_* C_o \left(\frac{y-\xi}{\xi}\,\frac{\bar{a}}{y-\bar{a}}\right)^{\omega} d\xi \tag{4.9}$$

Let $r = \frac{\xi}{y}$ and $G = \frac{\bar{a}}{y}$. Then one obtains

$$S_q = C_o U_* \bar{a} \frac{G^{\omega-1}}{(1-G)^{\omega}} \left\{\left[B + 2.5 \ln\left(\frac{y}{\eta_s}\right)\right] \int_G^1 \left(\frac{1-r}{r}\right)^{\omega} dr \right.$$

$$\left. + 2.5 \int_G^1 \ln r \left(\frac{1-r}{r}\right)^{\omega} dr\right\} \tag{4.10}$$

in which G is defined as depth ratio in this study.

According to Einstein (1950), the concentration near the "bed layer" C_o may be related to the bed-load transport rate q_b, by the expression

$$q_b = \beta_3 C_o U_* a \tag{4.11}$$

in which "a" is now defined as the thickness of the bed layer and β_3 is some constant. Einstein (1950) assumed that "a" was equal to two diameters of the sediment particle. Because the flow depth is very small in overland flow and because a large turbulent intensity is induced by raindrop impact (Yoon, 1970), the thickness of the bed layer is defined herein to be one diameter of the median size of particle (d_{50}).

The average flow velocity V is defined by the equation

$$\frac{V}{U_*} = \frac{\int_o^y u_\xi \, d\xi}{\int_o^y d\xi} \tag{4.12}$$

Using Eq. 4.8

$$\frac{V}{U_*} = B + 2.5 \ln \left(\frac{y}{\eta_s}\right) - 2.5 \tag{4.13}$$

Einstein (1950) defined the two integrals in Eq. 4.10 by

$$J_1 = \int_G^1 \left(\frac{1-r}{r}\right)^\omega dr \tag{4.14}$$

and

$$J_2 = \int_G^1 \left(\frac{1-r}{r}\right)^\omega \ln r \, dr \tag{4.15}$$

The integrals J_1 and J_2 cannot be integrated in closed form for most values of ω, a numerical integration is necessary. A method based on power series expansion is developed in this study and is presented in Appendix A.

The substitution of Eqs. 4.11, 4.13, 4.14 and 4.15 into Eq. 4.10 yields

$$S_q = \frac{q_b}{\beta_3} \frac{G^{\omega-1}}{(1-G)^{\omega}} \left[\left(\frac{V}{U_*} + 2.5 \right) J_1 + 2.5 J_2 \right] \tag{4.16}$$

in which G, V, U_* are determined in the water routing procedure, J_1 and J_2 are determined by the method presented in Appendix A, and q_b is computed by either Eq. 4.1 or Eq. 4.2.

Let

$$\overline{G} = \frac{G^{\omega-1}}{(1-G)^{\omega}} \left[\left(\frac{V}{U_*} + 2.5 \right) J_1 + 2.5 J_2 \right] \tag{4.17}$$

then, the total sediment transport rate is

$$q_s = q_b + S_q = q_b \left(1 + \frac{\overline{G}}{b_3}\right) \tag{4.18}$$

The selection of a suitable bed load function and the estimation of parameters are given in Section 4.3.2.

4.2.2. Degradation and aggradation

The estimation of degradation and aggradation is one facet of sediment routing. The governing equation for this process is the continuity equation for sediment. The sediment continuity equation for overland flow is

$$\frac{\partial q_s}{\partial x} + \frac{\partial C_s y}{\partial t} + (1 - \overline{\varepsilon}) \frac{\partial z}{\partial t} = 0 \tag{4.19}$$

in which C_s is sediment concentration in volume, $\bar{\varepsilon}$ is the porosity of the sediment on the bed of the overland flow area, and z is the bed elevation.

The sediment concentration in volume is defined as

$$C_s = \frac{q_s}{q} \tag{4.20}$$

in which q is the unit width discharge. For overland flow, q is equal to Q in Chapter II.

According to Fig. 2.1, the finite difference formulation for Eq. 4.19 is

$$\frac{q_{s_{j+1}}^{n+1} - q_{s_j}^{n+1}}{\Delta x} + \frac{(C_s y)_{j+1}^{n+1} - (C_s y)_{j+1}^{n}}{\Delta t} + (1 - \bar{\varepsilon}) \frac{\Delta z_{j+1}^{n+1}}{\Delta t} = 0 \tag{4.21}$$

or

$$\Delta z_{j+1}^{n+1} = \frac{1}{(1-\bar{\varepsilon})} [\lambda (q_{s_j}^{n+1} - q_{s_{j+1}}^{n+1}) + (C_s y)_{j+1}^{n} - (C_s y)_{j+1}^{n+1}] \tag{4.22}$$

and $\lambda = \frac{\Delta t}{\Delta x}$.

If Δz_{j+1}^{n+1} is positive the bed is aggrading, and if negative the bed is under degradation.

In an overland flow plot, there are two base points; one at the upstream boundary and the other at the downstream boundary. The elevations of these two base points are assumed to be unaltered during degradation or aggradation processes.

The elevations of the interior points in an overland flow plot can be estimated by the equation

$$z^{n+1}_{j+\frac{1}{2}} = z^{n+1}_{j+\frac{1}{2}} + \frac{1}{2}\left(\Delta z^{n+1}_{j} + \Delta z^{n+1}_{j+1}\right) \tag{4.23}$$

With the adjusted bed elevations, the adjustment of bed slope can be made as follows:

(a) for the segment in the upstream boundary

$$S_{o_1}^{n+1} = \frac{z_u - z^{n+1}_{1+\frac{1}{2}}}{\Delta x} \tag{4.24}$$

(b) for the interior segments

$$S_{o_j}^{n+1} = \frac{z^{n+1}_{j-\frac{1}{2}} - z^{n+1}_{j+\frac{1}{2}}}{\Delta x} \tag{4.25}$$

and (c) for the segment in the downstream boundary

$$S_{o_M}^{n+1} = \frac{z^{n+1}_{M-\frac{1}{2}} - z_d}{\Delta x} \tag{4.26}$$

Here z_u is the elevation at the upstream boundary, M is the total number of segments, and z_d is the elevation at the downstream boundary.

4.3. Applications

A computer program has been developed to incorporate the sediment routing procedure described in the previous section with the water routing procedure presented in Chapter II. A listing of the computer program is given in Appendix C. (PROGRAM SEDIM).

The experimental data by Kilinc and Richardson (1973) were used to test the applicability of this soil erosion model. A brief

description of Kilinc and Richardson's data, the method of parameter estimation, tested results and discussions are given below.

4.3.1. Experimental data by Kilinc and Richardson

Kilinc and Richardson (1973) made 24 experimental runs of soil erosion under simulated rainfall. Their test flume was 4 feet high by 5 feet wide by 15 feet long, with an adjustable slope. The flume was filled with sandy soil having median diameter of 0.35 mm and porosity of 43 percent. The rainfall intensities tested were 1.25, 2.25, 3.65 and 4.60 inches per hour, and bed slopes were 5.7 percent, 10 percent, 15 percent, 20 percent, 30 percent and 40 percent. The infiltration rate of each run was constant and measured, and the sediment load was sampled every five to ten minutes during each hour-long run. A summary of the experimental data is given in Table 4.1.

4.3.2. Estimation of coefficient

Sediment transport equation is an important component of the sediment routing model. Unfortunately, there is no universally accepted sediment transport equation, especially for overland flows. As mentioned in Section 4.2.1., either Eq. 4.1 or Eq. 4.2 may be used as the equation form for bed-load function. However, the coefficients in Eqs. 4.1 or 4.2 must be estimated. The coefficients are either β_1, β_2, and β_3 or β_1', β_2', and β_3.

It is assumed that the bed slope is practically unchanged when the flow just reaches the equilibrium (around 5 minutes after starting of rainfall). Then, based on the measurements made at or near 5 minutes after starting of rainfall, the estimation of coefficients can be made by the following method.

Table 4.1. Summary of Experimental Data by Kilinc and Richardson (1973)

Run No.	Rainfall Intensity (in./hr)	Infiltration Rate (in./hr)	Bed Slope (%)	Average Measured Sediment Discharge (lb/sec/ft)
1	1.25	0.496	5.7	0.00010
2	2.25	0.314	5.7	0.00030
3	3.65	0.210	5.7	0.00065
4	4.60	0.200	5.7	0.00148
5	1.25	0.397	10.0	0.00029
6	2.25	0.287	10.0	0.00151
7	3.65	0.170	10.0	0.00372
8	4.60	0.130	10.0	0.00588
9	1.25	0.353	15.0	0.00055
10	2.25	0.253	15.0	0.00297
11	3.65	0.134	15.0	0.00714
12	4.60	0.056	15.0	0.01288
13	1.25	0.308	20.0	0.00064
14	2.25	0.249	20.0	0.00569
15	3.65	0.124	20.0	0.01490
16	4.60	0.033	20.0	0.02606
17	1.25	0.281	30.0	0.00092
18	2.25	0.239	30.0	0.01015
19	3.65	0.062	30.0	0.02265
20	4.60	0.010	30.0	0.03752
21	1.25	0.262	40.0	0.00113
22	2.25	0.230	40.0	0.01310
23	3.65	0.045	40.0	0.03700
24	4.60	0.005	40.0	0.06508

From Eqs. 4.1, 4.2 and 4.17, the total sediment load can be expressed as

$$q_s = \beta_1 \tau^{\beta_2} (1 + \frac{\overline{G}}{\beta_3}) \tag{4.27}$$

or

$$q_s = \beta_1' (\tau - \tau_c)^{\beta_2'} (1 + \frac{\overline{G}}{\beta_3}) \tag{4.28}$$

in which q_s was measured at or near 5 minutes after starting of rainfall. The values of τ and $\overline{G}$ at the end of soil plot were determined as follows.

The approximate momentum equation (Eq. 2.2) for overland flow can be rewritten as

$$S_o = f \frac{q^2}{8gy^3} \tag{4.29}$$

When the flow reaches equilibrium, the unit-width discharge at the end of soil plot q_p is

$$q_p = q_\ell L \tag{4.30}$$

Then, the depth of flow at the end of soil plot y_p can be determined by,

$$y_p = (f \frac{q_p^2}{8gS_o})^{\frac{1}{3}} \tag{4.31}$$

and the mean flow velocity at the end of soil plot V_p is

$$V_p = \frac{q_p}{y_p} \tag{4.32}$$

With the values of y_p and V_p, the magnitudes of τ and $\overline{G}$ can be determined by Eqs. 4.3, 4.7 and 4.17.

The general form of either Eq. 4.27 or Eq. 4.28 can be written as the following nonlinear regression equation

$$Y = \alpha_1 X^{\alpha_2} (1 + \alpha_3 Z) \tag{4.33}$$

in which Y is the dependent variable, X and Z are the independent variables, and α_1, α_2, and α_3 are regression coefficients.

The regression coefficients can be estimated by a trial and error procedure. The steps are as follows:

(1) Assume a value of α_3. Then Eq. 4.33 can be regarded as a simple power function.

(2) Estimate α_1 and α_2 based on the simple power function regression technique and determine the correlation coefficient.

(3) Try another α_3 value and repeat steps 1 and 2 until the maximum correlation coefficient is found.

The above trial and error procedure was made by using the one dimensional calibration technique (see Appendix B) coupled with the least square regression method.

The data at the lowest rainfall intensity (1.25 in./hr) were not used in developing the sediment transport equation due to possible errors in measurement. The regression results using both Eq. 4.1 and Eq. 4.2 are given in Table 4.2. The results indicated that Eq. 4.2 was the better equation form for bed-load function in this case, and was adopted in the subsequent analyses.

Table 4.2. Summary of Regression Results for Sediment Transport Equation

Type of Bed-Load Function	Correlation Coefficient	Standard Error of Estimate	Estimate Coefficients		
			$\beta_1(\beta_1')$	$\beta_2(\beta_2')$	β_3
Eq. 4.1	0.978	0.306	334.0	3.10	12.08
Eq. 4.2	0.983	0.271	65.2	2.47	11.96

The coefficient β_2 is very close to 3.0 in the Einstein-Brown bed-load function and the coefficient β_2' is also comparable to 2.5 in the Brown-Kalinske bed-load equation. The most interesting result is that the coefficients β_3 for both cases are very close to 11.6 as proposed by Einstein (1950).

4.3.3. Mean erosion rate and sediment hydrographs

In the numerical computations Δt was 1 minute and $\frac{\Delta t}{\Delta x}$ was equal to 60 sec/ft.

The comparisons between computed and measured results were made in both the mean erosion rate and the time-dependent erosion rate.

The mean erosion rate $\bar{q}_s$ is defined as

$$\bar{q}_s = \frac{1}{N} \sum_{t=1}^{N} q_s(t) \tag{4.34}$$

in which N is the number of time increments, and $q_s(t)$ is the sediment discharge at the end of soil plot and at time t.

The comparison of mean erosion rate is given in Fig. 4.1. The agreement between the measured and computed sediment transport rates is generally good except for those runs with the lowest rainfall

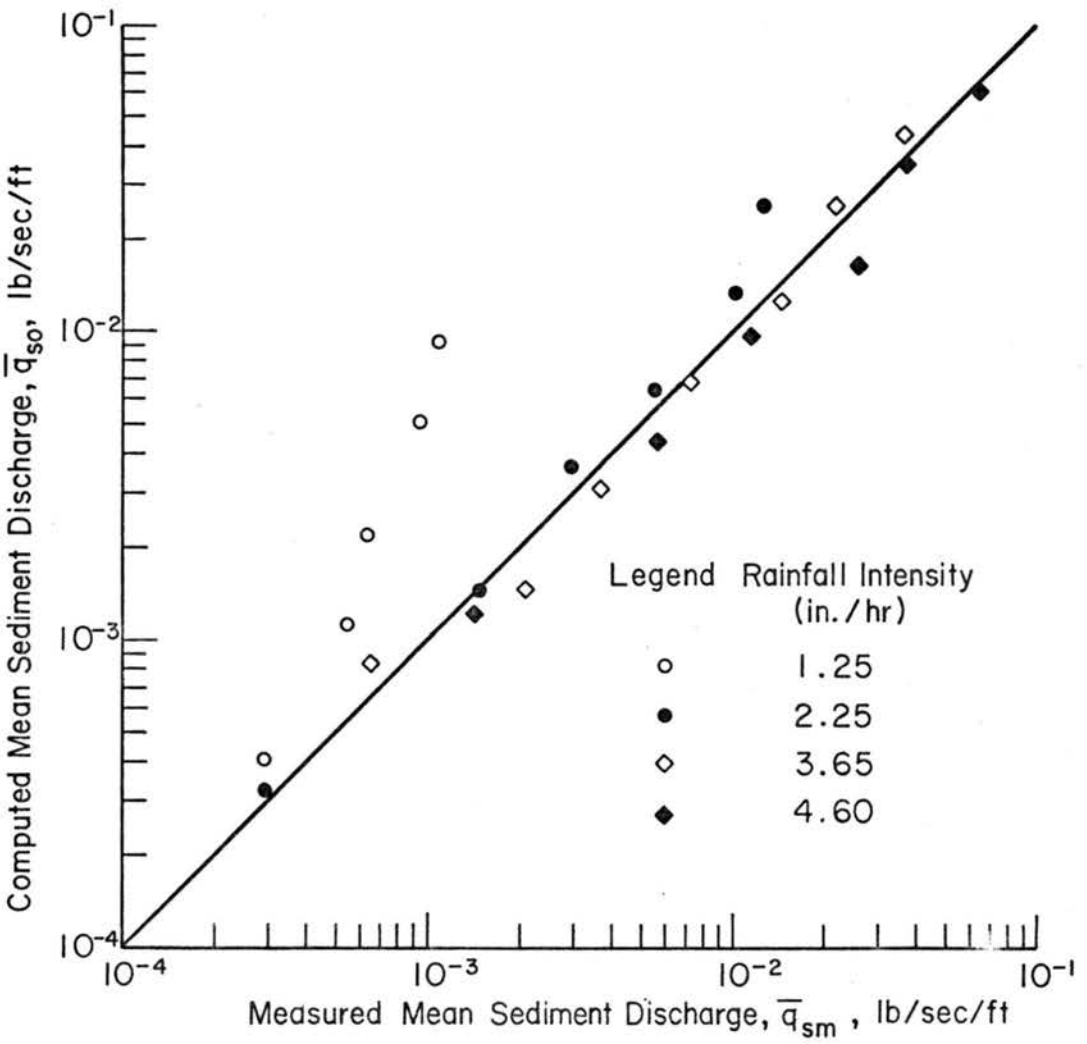

Fig. 4.1 Comparison between computed and measured mean erosion rate

intensity (1.25 in./hr). The error at the lowest rainfall intensity may be due to consistently high infiltration rates (21 percent to 40 percent of rainfall) in these runs. Although the excess rainfall was used in the analysis, there was still the possibility of errors in infiltration rates or rainfall intensity measurements. Another source of error may be due to uneven slope profiles; this source of error is discussed later.

The time-dependent erosion rates are shown in Figs. 4.2 and 4.3. In Fig. 4.2, erosion rates for different slopes with constant rainfall intensity (3.65 in./hr) are presented. The erosion rate decreases as time increases and increases as bed slope increases. Figure 4.3 gives examples of erosion rates for different rainfall intensity with the same bed slope (30 percent). The erosion rate increases as rainfall intensity increases. A survey of the accuracy of simulation was made in terms of the percentage error in total volume E_v, and the relative mean absolute error E_a. These errors are defined as follows.

$$E_v = 100 \left[1 - \frac{\sum_{j=1}^{N} q_{so}(j)}{\sum_{j=1}^{N} q_{sm}(j)} \right] \tag{4.35}$$

and

$$E_a = \frac{100}{N} \sum_{j=1}^{N} \frac{|q_{so}(j) - q_{sm}(j)|}{q_{sm}} \tag{4.36}$$

in which N is the number of sampling points, $q_{so}(j)$ and $q_{sm}(j)$ are respectively the simulated and the measured sediment discharge at the time the jth sample was taken, and $\bar{q}_{sm}$ is the average value of the measured sediment discharges.

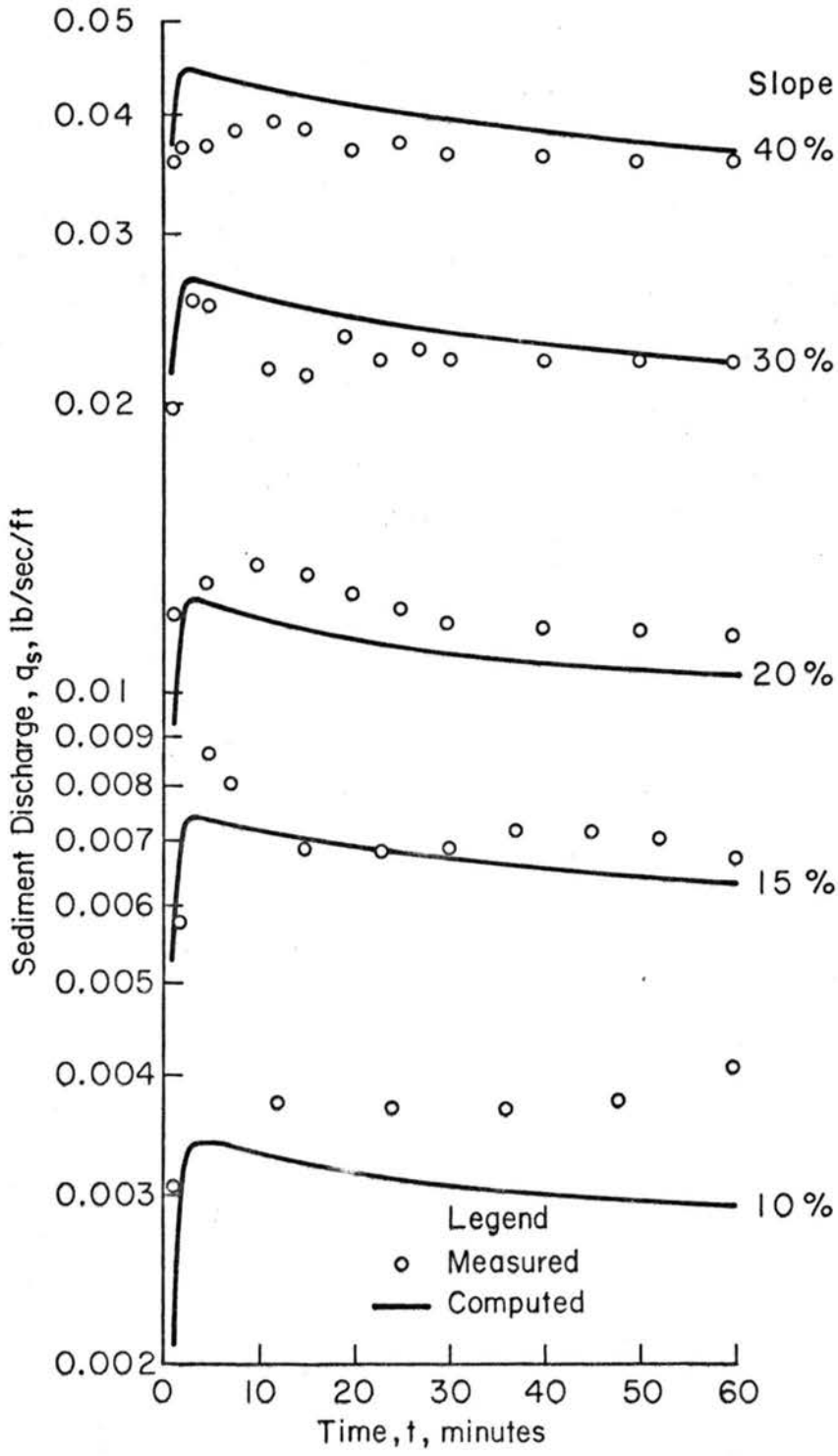

Fig. 4.2 Time-dependent erosion rate for different slopes (rainfall intensity 3.65 in./hr)

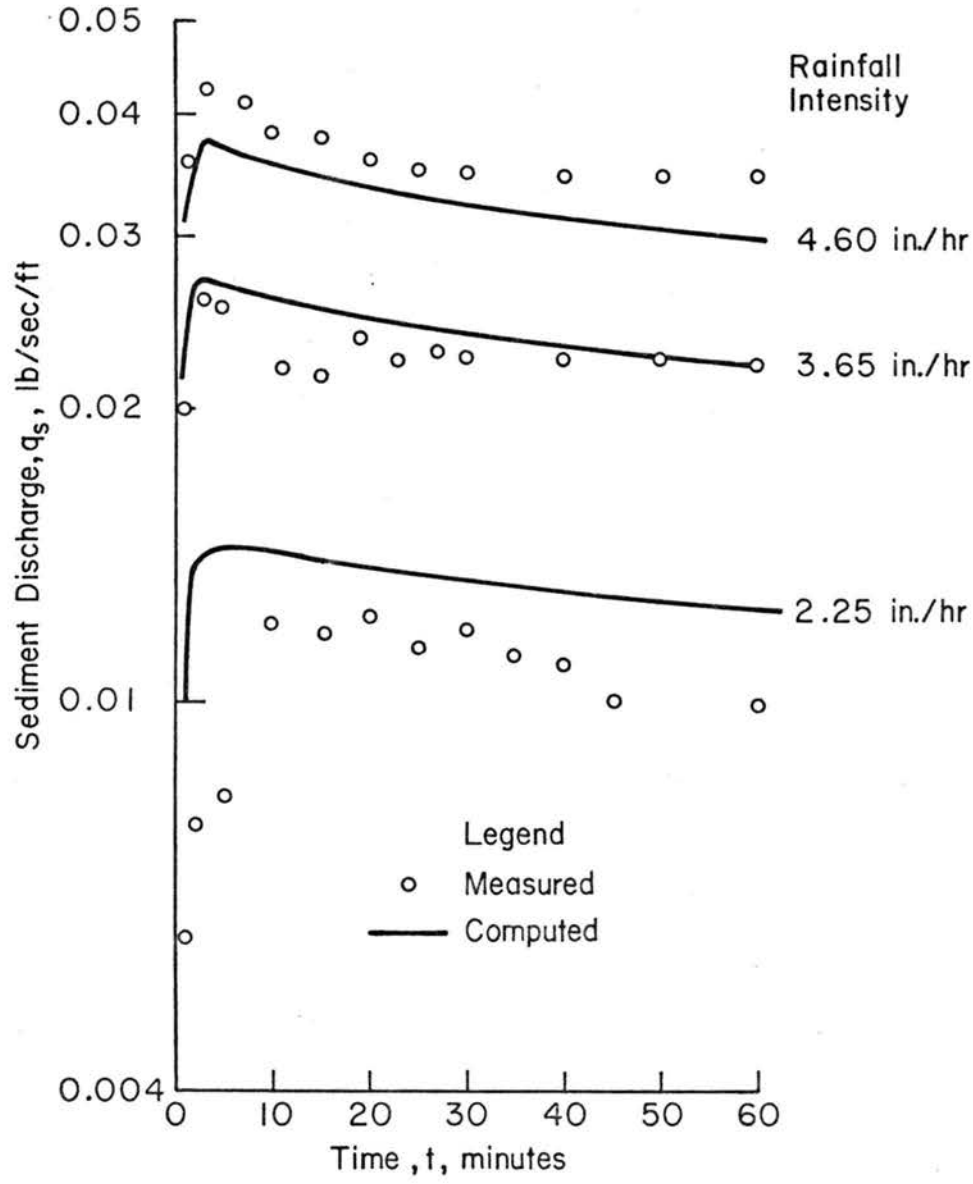

Fig. 4.3 Time-dependent erosion rate for different rainfall intensities (bed slope 30 percent)

Table 4.3 gives the computed errors for the runs in Figs. 4.2 and 4.3. These estimated errors indicate that the proposed model is able to simulate the time-dependent erosion rates to the order of ±30 percent for the tested cases.

Table 4.3. Summary of Estimated Errors in Soil Erosion Simulation

(a) For different slopes (Fig. 4.2)

Bed Slope (%)	Run No.	Estimated errors (%)	
		E_v	E_a
10	7	-22.2	22.3
15	11	- 4.5	8.8
20	15	- 7.5	7.5
30	19	6.8	6.9
40	23	11.3	11.3

(b) For different rainfall intensities (Fig. 4.3)

Rainfall Intensity (in./hr)	Run No.	Estimated errors (%)	
		E_v	E_a
2.25	18	30.7	30.7
3.65	19	6.8	6.9
4.60	20	-11.4	10.7

4.3.4. Land form evolution and effect of slope-shape on erosion rate

The example of land form evolution as generated by the proposed model is given in Fig. 4.4. The rainfall intensity is 3.65 in./hr (infiltration rate is 0.17 in./hr). The generated land form is in a concave shape which frequently appears in nature. This example provides a physical picture about the degradation and aggradation process in overland flow.

The general practice of determining bed slope is to assume a uniform slope shape for any land form. A quantitative evaluation on the effect of slope shape on erosion rate was made in this study.

In Fig. 4.5, three different slope shapes (convex, uniform, and concave) having the same relief are shown. Under 3.65 in./hr rainfall, and 0.17 in./hr infiltration rate, the time-dependent erosion rates for different slopes are given in Fig. 4.6. The erosion rates on the convex slope are nearly five times greater than those on the uniform slope. The erosion rates on the concave slope are much less than those on the uniform slope. This example demonstrates that the erosion rate is very sensitive to the slope shape. The sensitivity of erosion rate to slope may be one of the reasons for the scatters in Fig. 4.1. The other interesting point is that the erosion rate on a concave slope increases as time increases. This behavior is different from that on a convex slope or on a uniform slope.

The erosion rate is sensitive to the bed slope. The common assumption that $S_o = \tan \theta' \approx \sin \theta'$ (θ' is the angle between the channel bed and the horizontal direction) in open channel flow results in an error in the computed erosion rate for larger θ'.

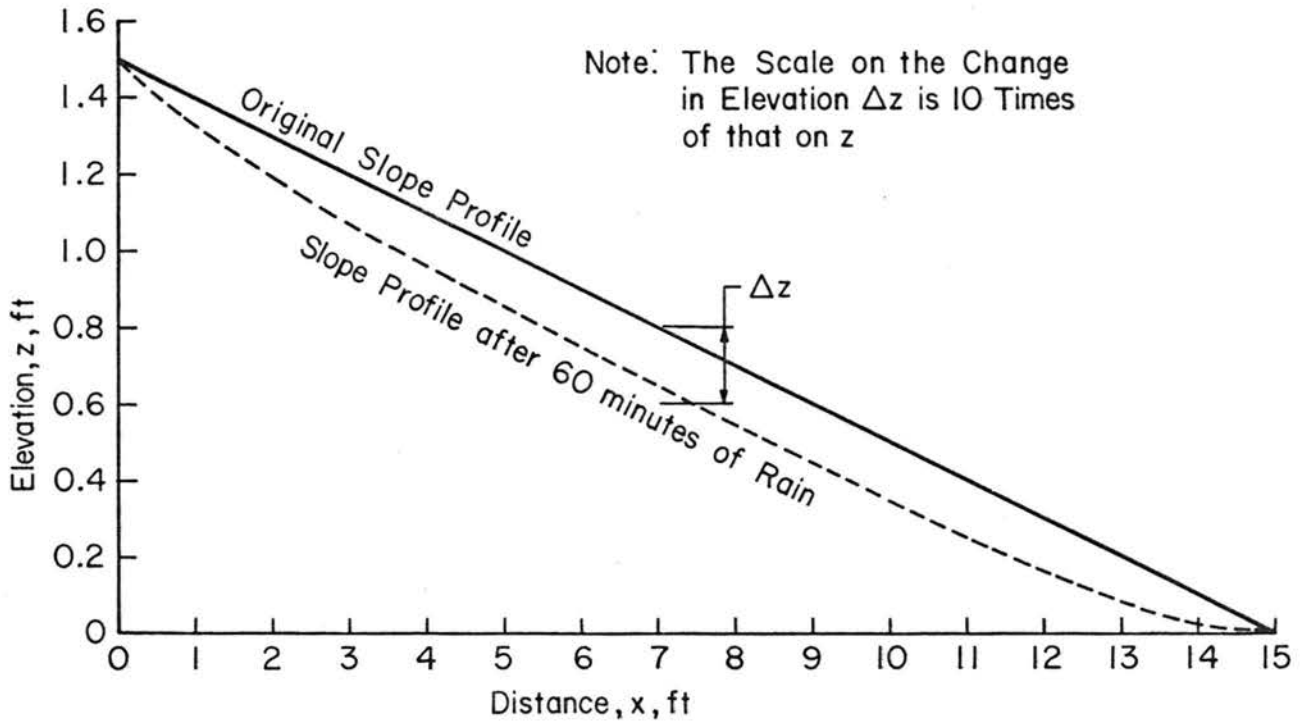

Fig. 4.4 Example of land form evolution

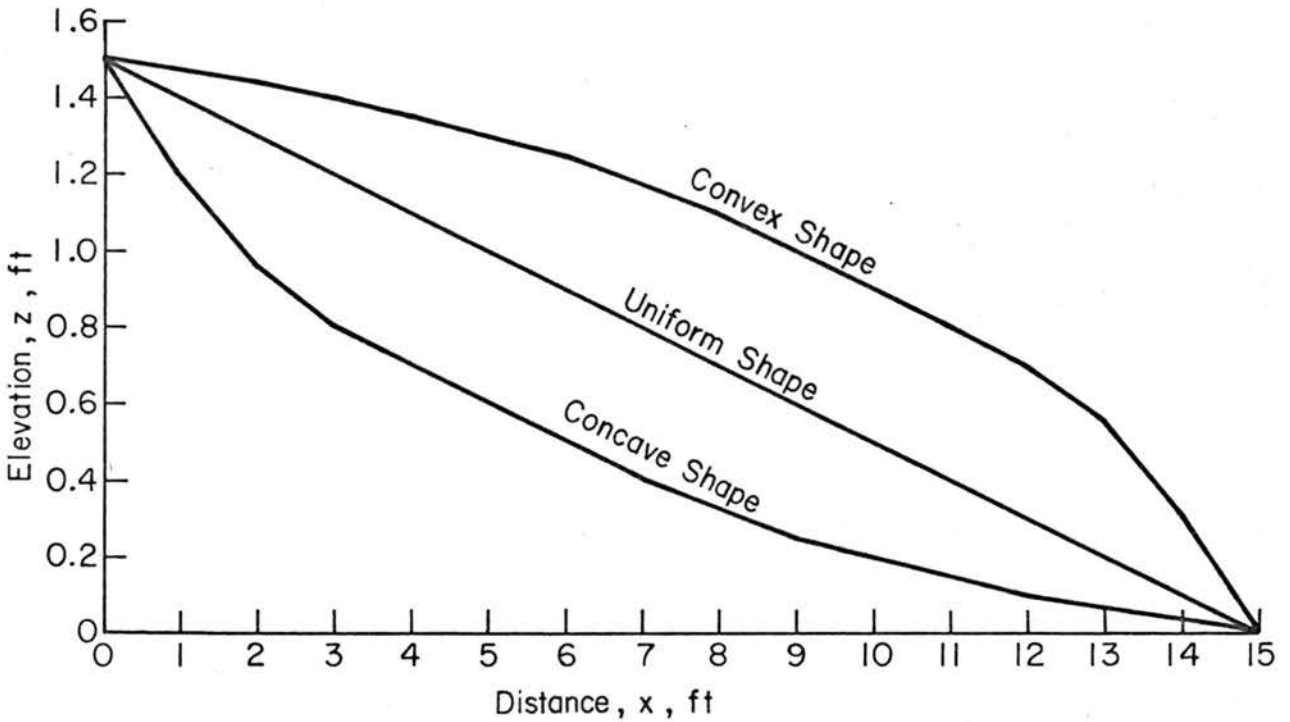

Fig. 4.5 Definition sketch of slope shape

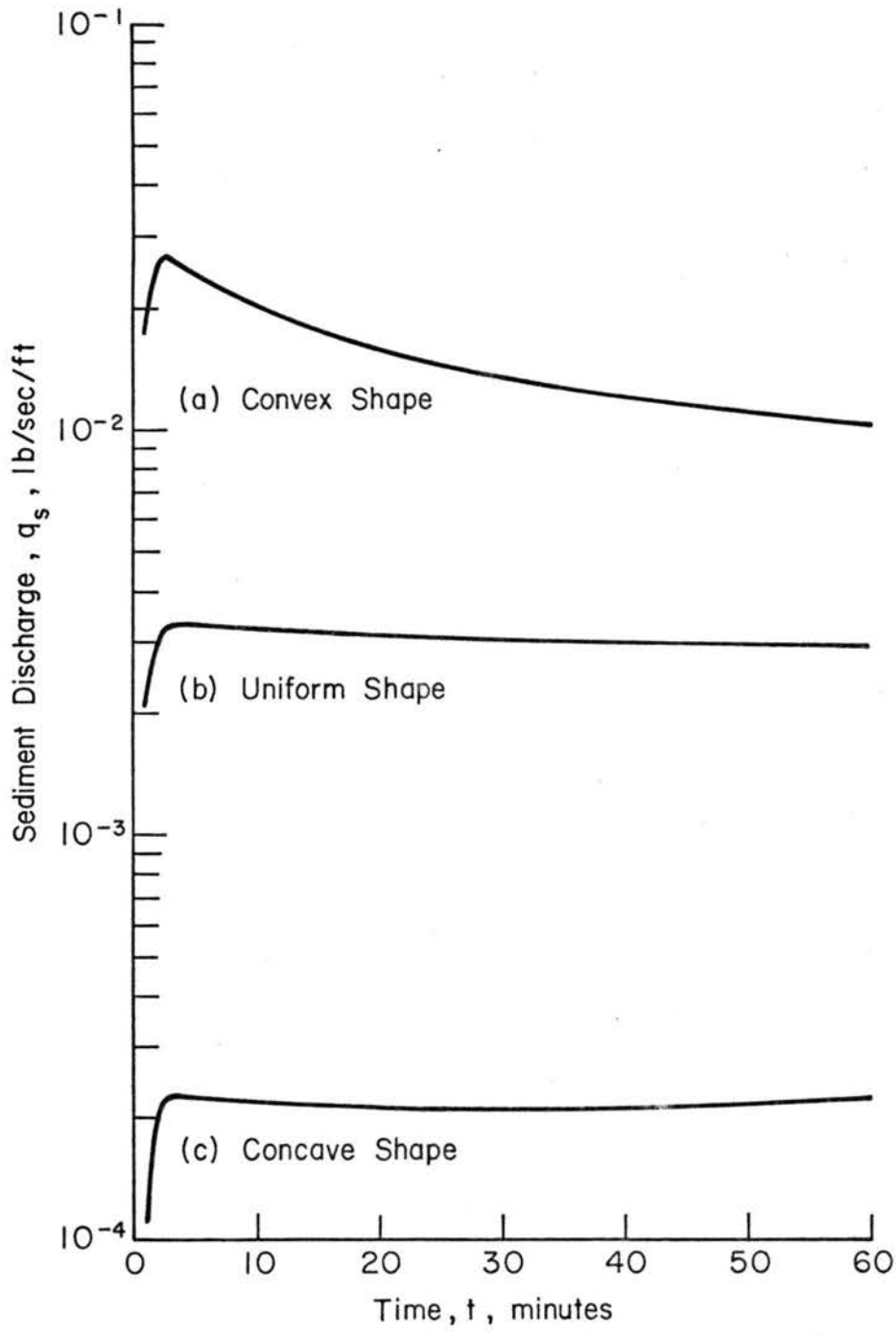

Fig. 4.6 Effect of slope shape on erosion rate

From Eqs. 4.3 and 4.31, one obtains

$$\tau \propto S_o^{2/3} \tag{4.37}$$

and from the estimated results (Section 4.3.2.),

$$q_s \propto \tau^{2.47} \tag{4.38}$$

The substitution of Relation 4.37 into Relation 4.38 yields

$$q_s \propto S_o^{1.65} \tag{4.39}$$

or by differentiation

$$\frac{dq_s}{q_s} = 1.65 \frac{dS_o}{S_o} \tag{4.40}$$

As implied by Relation 4.40 the percentage error in the erosion rate is approximately 1.65 times of the percentage error in bed slope.

Now, if S_o is 40 percent (or $\tan \theta = 0.4$), $\sin \theta'$ is 0.37. The error involved in using S_o instead of $\sin \theta'$ is 7 percent, hence the percentage error in erosion rate estimation is 12 percent. It is found that if S_o is less than 25 percent, the assumption that $\tan \theta' \approx \sin \theta'$ will yield a percentage error of less than 5 percent in soil erosion estimation, which may be acceptable for practical purposes.

4.4. Summary

A water and sediment routing model has been developed to simulate the process of soil erosion by overland flow. The proposed model is able to simulate the soil erosion process and produces time-dependent erosion rates comparable with those measured by Kilinc and Richardson (1973). Other experimental data have not been available for comparison.

The model also generates a concave land form which frequently appears in nature.

It was found that the soil erosion rate was very sensitive to bed slope and shape. The general practice of assuming a uniform shape and slope may result in serious errors. However, the common assumption of sin θ being equal to bed slope S_o is not too serious when the bed slope is less than 25 percent.

The applicability of the proposed rainfall-erosion model is limited to the following conditions: (1) the overland flow erosion is mainly due to sheet erosion; (2) the kinematic-wave approximation for flow routing is valid, and the bed slope is less than 25 percent; (3) the detaching and transporting capacities of raindrop impact are negligible and the sediment discharge is largely the bed material load. The wash load is neglected in the present analysis.

The input required for this model can be cataloged as follows.

(1) geometry data--slope length, and bed elevations of the soil plot.

(2) soil data--porosity of the sediment, and medium diameter of the sediment.

(3) flow resistance parameters--constants describing grain resistance for different Reynolds numbers and constant representing the added roughness due to raindrop impact.

(4) sediment transport parameters--coefficients and exponent for describing bed material load transport rate.

(5) rainfall characteristics data--rainfall intensities, infiltration rates and water viscosity.

Chapter V

STREAM MORPHOLOGY OF SMALL WATERSHEDS

5.1. Governing Physical Process

The form that a channel cross section attains depends on the physical processes at work within the channel reach. The basic question is "What physical processes are most important in sculpturing the channel shape?" The choice of processes depends on the length of time and size of watershed being considered.

When the time frame being considered is limited to one or two centuries, the large scale geological processes can be eliminated from consideration. For example, it is possible that streams in the Upper Mississippi River Basin at the present time are still responding to the effects of continental glaciers which receded from the area some 10,000 years ago. In the present century, any response to the glaciation would be hardly detectable. In a period of one or two centuries, the geology of a region can be considered, conceptually at least, as fixed and independent of other processes. Precipitation alone is sufficient to sculpture the form of an alluvial stream channel in one or two centuries. However, care must be taken in limiting the selection of size and type of watershed if precipitation is to be considered as the only external input to the geomorphic process in the watershed.

The response of an overland flow area to precipitation is a resultant land form on the surface of the overland flow area and water and sediment delivered to nearby channels. These water and sediment discharges are inputs to the geomorphic processes within the channels. The cross-sectional shape of the stream channel is the

result of the process. The integral geomorphic process is a very complicated problem, in order to simplify the problem involved, it is assumed that all parts of the watershed have been subject to the same precipitation series. Under this assumption the watershed area would have to be less than the intense precipitation core area within a storm which produces large point rainfall amounts. It follows then that the watershed must be small. A small watershed is defined as a drainage system which is small enough to ensure a degree of both geologic and hydrologic homogeneity in space. In many regions this definition for a small watershed restricts the area to approximately 10 to 20 sq mi. In order to further simplify the problem, this study is limited to alluvial streams with noncohesive gravel or boulder banks and beds.

In a time period of 100 or 200 years, it is assumed that there have been a sufficient number of large precipitation events and duration to produce threshold conditions in the stream channels. That is, the alluvial materials remaining on the bed and banks of the stream channels in a small watershed have been subjected to flow conditions just sufficient to initiate movement of these particles. The channels are called threshold channels and the discharges which formed the threshold channel shapes are called collectively the threshold discharge. The surface of the overland flow area and the boundaries of the channel system in the small watershed will be in equilibrium until subjected to a precipitation event greater than those which produced the threshold channel.

5.2. Theoretical Development

5.2.1. Threshold conditions in the watershed

If the precipitation time series is stationary and if the small watershed is unaffected by man's influences, the alluvial gravels and boulders on the surface of the watershed and its stream channels will have been subjected to the threshold discharge. Bank full discharge is a good measure of threshold discharge. For discharges less than the threshold discharge, the particles on the surfaces and boundaries of the water courses do not move appreciably under the concepts put forth in Section 5.1. The small watershed morphology does not change in between periods of extreme precipitation.

The sediment continuity equation for bedload movement in the overland flow area is

$$\frac{\partial q_s}{\partial x} + (1-\bar{\varepsilon})\frac{\partial z}{\partial t} = 0 \qquad (5.1)$$

in which q_s is the sediment discharge per unit width of overland flow area, x is the downslope distance, $\bar{\varepsilon}$ is the porosity of the sediments in the bed, z is the bed elevation and t is the time.

Under conditions of equilibrium in the overland flow portion of the watershed, $\partial z/\partial t$ is zero by definition. From Eq. 5.1, it follows that

$$\frac{dq_s}{dx} = 0 \qquad (5.2)$$

or after integration with respect to x,

$$q_s = C_1 \qquad (5.3)$$

in which C_1 is a constant dependent on the boundary conditions.

At the watershed boundary, no flow depth develops. Thus, there is no shear stress and no sediment transport, i.e.,

$$q_s = 0 \tag{5.4}$$

for overland flow at $x = 0$. From Eqs. 5.3 and 5.4, it is found that C_1 is zero and therefore q_s is zero for all x in the overland flow area.

The sediment continuity equation for bedload in the channel system is

$$\frac{\partial Q_s}{\partial x} + (1-\bar{\varepsilon})\frac{\partial z}{\partial t} = q_s \tag{5.5}$$

in which Q_s is the sediment transport in the channel and the other terms have been defined previously. For equilibrium conditions in the channel, $\partial z/\partial t$ is zero for all x. Then

$$\frac{dQ_s}{dx} = q_s \tag{5.6}$$

or after integration

$$Q_s = q_s x + C_2 \tag{5.7}$$

in which C_2 is a constant dependent on the boundary conditions. It has been shown previously that the overland sediment transport rate is zero over the entire overland flow area. Thus q_s in Eq. (5.7) is zero for all x. Also at $x = 0$, Q_s is zero, so

$$Q_s = 0 \tag{5.8}$$

for all x.

In summary, if a small watershed is in geomorphic equilibrium, the entire system must be at the threshold of sediment motion.

5.2.2. The "threshold" channel section

Channels inside a small watershed in equilibrium form a cross section according to the maximum threshold discharge which has occurred. Particles on the periphery of the channel cross section are at the "threshold" of movement under the corresponding flow conditions.

Many investigators have formulated the shape of threshold channel in homogeneous coarse alluvium; i.e., Lane (1955), Lane, Lin, and Liu (1959) and Stebbings (1963). The theory developed at the U.S. Bureau of Reclamation by Lane (1955) for the shape of the threshold channel is employed here. In Lane's work the following assumptions were made:

(1) At and above the water surface, the side slope is at the angle of repose of the alluvial material.

(2) At all points on the periphery of the channel, the particles are at a condition of incipient motion. The lift and drag forces of the fluid on the particle and the downslope component of the gravity force on the particle are balanced by the friction force developed between particles. The lift and drag forces are directly proportional to the tractive force.

(3) Where the side slope is zero, the flow-wise tractive force alone is sufficient to cause incipient motion.

(4) The particles are held against the bed by the component of the submerged weight of the particle acting normal to the bed.

(5) The tractive force acts in the direction of flow and is equal to the component of the weight of the water above the area on which the force acts.

The equation describing the shape of the threshold channel in coarse noncohesive alluvium is derived as follows.

Under the condition of incipient motion on the periphery of the channel, the resultant of the drag force F_d and the downslope component of the submerged weight of the particle $W\sin\theta$ are balanced by the friction force developed between particles. The threshold channel shape is shown in Fig. 5.1. The angle θ is the local side

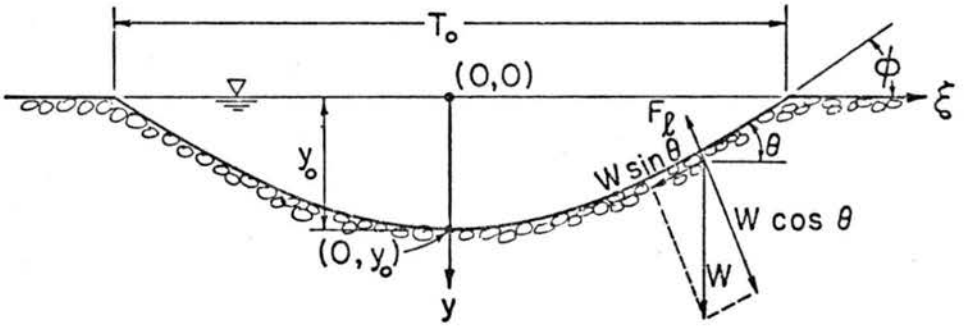

a. Definition Sketch

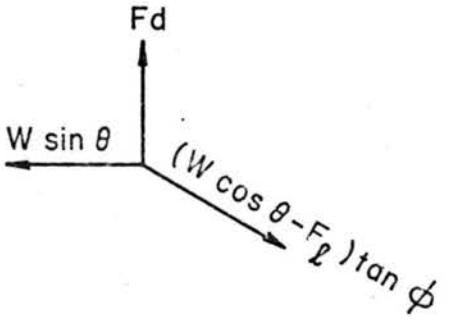

b. Force Diagram

Fig. 5.1 Cross-sectional geometry for the threshold channel

slope angle and W is the submerged weight of the particle. The friction force is the product of the normal force and the tangent of the friction angle ϕ. The normal force is $(W\cos\theta - F_\ell)$ in which $W\cos\theta$ is the normal (to the side slope) component of submerged weight and F_ℓ is the lift force on the particle. The balance of forces is expressed as

$$W^2\sin^2\theta + F_\ell^2 = (W\cos\theta - F_\ell)^2\tan\phi^2 \tag{5.9}$$

The friction angle ϕ is the angle of repose of the noncohesive material.

It is assumed that

$$F_d = \sigma\tau \tag{5.10}$$

and

$$F_\ell = \overline{\beta}F_d \tag{5.11}$$

Here τ is the local bed shear stress or tractive force and σ is a proportionality constant. The term $\overline{\beta}$ is the ratio of the lift to drag force.

By substituting Eqs. 5.10 and 5.11 in Eq. 5.9, the expression

$$\tau^2 + (\frac{W}{\sigma})^2\sin^2\theta = (\frac{W}{\sigma}\cos\theta - \overline{\beta}\tau)^2\tan^2\phi \tag{5.12}$$

is obtained.

At the center of the channel (the point 0, y_o in Fig. 5.1), $\theta = 0$ and $\tau = \tau_o$, so

$$\tau_o^2 = (\frac{W}{\sigma} - \overline{\beta}\tau)^2\tan^2\phi \tag{5.13}$$

or

$$\frac{W}{\sigma} = \frac{1 + \overline{\beta}\tan\phi}{\tan\phi}\,\tau_o \tag{5.14}$$

The tractive force τ_o is the maximum force which occurs at the centerline of the channel. Accordingly

$$\tau_o = \gamma y_o S_o \tag{5.15}$$

in which γ is the unit weight of water, y_o is the maximum depth of flow and S_o is the slope of the channel bed.

One of the assumptions is that the local tractive force varies directly as the weight of fluid above the area. At a distance ξ from the centerline of the cross section the depth of flow is y. The weight of fluid in a column of unit area and depth y is γy. This normal component of this fluid weight is $\gamma y \cos\theta$. Thus the tractive force is

$$\tau = \gamma y S_o \cos\theta \tag{5.16}$$

which reduces to Eq. 5.15 for $\xi = 0$.

If Eqs. 5.14, 5.15, and 5.16 are substituted into Eq. 5.12, and rearranged,

$$\left(\frac{y}{y_o}\right)^2 + \left(\frac{1 + \bar{\beta}\tan\phi}{\tan\phi}\right)^2 \tan^2\theta = \left(\frac{1 + \bar{\beta}\tan\phi}{\tan\phi} - \bar{\beta}\frac{y}{y_o}\right)^2 \tan\phi \tag{5.17}$$

As $\tan\theta = -dy/d\xi$

$$\left(\frac{dy}{d\xi}\right)^2 = \tan^2\phi \left[\left(1 - \frac{r}{1+r}\frac{y}{y_o}\right)^2 - \left(\frac{1}{1+r}\frac{y}{y_o}\right)^2\right] \tag{5.18}$$

Here $\bar{r}$ is defined as $\bar{\beta}\tan\phi$. Eq. 5.18 can be rewritten as

$$\frac{-d\left(\frac{y}{y_o}\right)}{\sqrt{1 - \frac{2\bar{r}}{1+\bar{r}}\frac{y}{y_o} - \frac{1-\bar{r}}{1+\bar{r}}\left(\frac{y}{y_o}\right)^2}} = \tan\phi \; d\left(\frac{\xi}{y_o}\right) \tag{5.19}$$

By integrating both sides of Eq. 5.19, one obtains

$$-\sqrt{\frac{1+\bar{r}}{1-\bar{r}}} \sin^{-1}\left\{(1-\bar{r})\frac{y}{y_o} + \bar{r}\right\} = \frac{\xi}{y_o}\tan\phi + C_3 \tag{5.20}$$

The coefficient C_3 is determined from the boundary condition $\frac{y}{y_o} = 1$ when $\frac{\xi}{y_o} = 0$, or

$$C_3 = -\frac{\pi}{2}\sqrt{\frac{1+\bar{r}}{1-\bar{r}}} \tag{5.21}$$

This value of C_3 is substituted into Eq. 5.20 so that

$$\frac{y}{y_o} = \frac{1}{1-\bar{r}}\left\{\cos\left(\tan\phi\sqrt{\frac{1-\bar{r}}{1+\bar{r}}}\frac{\xi}{y_o}\right) - \bar{r}\right\} \tag{5.22}$$

This relation for the shape of a channel formed in noncohesive material was given by Lane et al. (1959). The cosine function produces the shape shown in Fig. 5.1 ($\bar{\beta} = 0.85$, and $\phi = 35°$).

5.2.3 Geometry of the threshold channel

The geometric properties of the threshold channel at threshold discharge are derived from Eq. 5.22.

5.2.3.1. Top width

Referring to Fig. 5.1, when $y = 0$, $\xi = T_o/2$. Then, from Eq. 5.22

$$\frac{T_o}{y_o} = \frac{2}{\tan\phi}\sqrt{\frac{1+\bar{r}}{1-\bar{r}}}\cos^{-1}\bar{r} \tag{5.23}$$

or

$$\frac{T_o}{y_o} = C_t(\bar{\beta},\phi) \tag{5.24}$$

in which C_t is defined as the width-to-depth coefficient and T_o is the top width of the threshold channel. The width-to-depth ratio is a function of $\bar{\beta}$ and ϕ only.

5.2.3.2. Cross-sectional area

The cross-sectional area at threshold discharge is

$$A_o = 2\int_0^{T_o/2} y\, d\xi$$

By employing Eqs. 5.22 and 5.23,

$$\frac{A_o}{y_o T_o} = \frac{1}{1-\bar{r}} \left(\frac{\sqrt{1-\bar{r}^2}}{\cos^{-1}\bar{r}} - \bar{r} \right) \tag{5.25}$$

That is,

$$\frac{A_o}{y_o T_o} = C_a(\bar{r}) = C_a(\bar{\beta}, \phi) \tag{5.26}$$

in which C_a is the area coefficient dependent on $\bar{r}$ only. The area coefficient is the ratio of the actual cross section to the area of a rectangular section having the same top width and maximum depth as the actual cross section and is always less than 1.0.

5.2.3.3. Wetted perimeter

The wetted perimeter is

$$P_o = 2\int_0^{T_o/2} \sqrt{1 + \left(\frac{dy}{d\xi}\right)^2}\, d\xi \tag{5.27}$$

From Eq. 5.22, the derivative $dy/d\xi$ is obtained; then with Eq. 5.23, the wetted perimeter can be expressed as

$$P_o = \frac{2y_o}{(1-\bar{r})\bar{k}} \int_{\frac{\pi}{2} - \cos^{-1}\bar{r}}^{\frac{\pi}{2}} \sqrt{1 - \bar{k}^2 \sin^2\bar{\alpha}}\, d\bar{\alpha} \tag{5.28}$$

in which

$$\bar{k} = \frac{\tan\phi}{\sqrt{1 + \tan^2\phi - \bar{r}^2}} \tag{5.29}$$

The wetted perimeter is

$$\frac{P_o}{y_o} = \frac{2}{(1-\bar{r})\bar{k}} \left\{ E\left(\bar{k}, \frac{\pi}{2}\right) - E\left(\bar{k}, \frac{\pi}{2} - \cos^{-1}\bar{r}\right) \right\} \tag{5.30}$$

or

$$\frac{P_o}{y_o} = C_p(\bar{\beta}, \phi) \tag{5.31}$$

Here $E(\bar{k},\bar{\alpha})$ is the elliptic integral of the second kind with modulus $\bar{k}$. The coefficient $C_p(\bar{\beta},\phi)$ is defined as the wetted perimeter coefficient.

5.2.3.4. Hydraulic depth

The hydraulic depth D_o is the ratio of the cross-sectional area to the top width. From Eqs. 5.24 and 5.26

$$D_o = \frac{A_o}{T_o} = \frac{C_a y_o T_o}{C_t y_o} \tag{5.32}$$

or

$$\frac{D_o}{T_o} = \frac{C_a}{C_t} \tag{5.23}$$

5.2.3.5. Hydraulic radius

The hydraulic radius R_o is the ratio of the cross-sectional area to the wetted perimeter. From Eqs. 5.26 and 5.31,

$$R_o = \frac{A_o}{P_o} = \frac{C_a y_o T_o}{C_p y_o} \tag{5.34}$$

or

$$\frac{R_o}{T_o} = \frac{C_a}{C_p} \tag{5.35}$$

The coefficients C_t, C_a, and C_p are the three basic dimensionless quantities describing the geometry of the threshold channel. The equations for C_t, C_a, and C_p are complicated in form but are approximated very well by simple power-form equations. The approximate solutions depend on the value selected for the lift-to-drag ratio.

In reviewing the work of Torum (1965), Bhowmik (1968) concluded that an appropriate value for $\bar{\beta}$ is 0.85. This value is adopted in this study.

With $\bar{\beta} = 0.85$, the expression for $\bar{r}$ becomes

$$\bar{r} = 0.85 \tan\phi \ . \tag{5.36}$$

By using this value of $\bar{r}$ in Eqs. 5.23, 5.25, and 5.30 the values of C_t, C_a and C_p for various values of ϕ can be computed. These values are shown as circles in Fig. 5.2. The curves in Fig. 5.2 may be expressed by the simple power equations:

$$C_t = 210\ \phi^{-1.038} \tag{5.37}$$

$$C_a = 0.61\ \phi^{0.021} \tag{5.38}$$

$$C_p = 168\ \phi^{-0.950} \tag{5.39}$$

The deviations of these power relations from the exact solutions are very small.

If the effect of the lift force is neglected ($\bar{\beta} = 0$), $\bar{r} = 0$ and the coefficients become

$$C_t = \frac{\pi}{\tan\phi} \tag{5.40}$$

$$C_a = \frac{2}{\pi} \tag{5.41}$$

$$C_p = \frac{2}{\bar{k}}\, E(\bar{k}, \frac{\pi}{2}) \tag{5.42}$$

Equations 5.40 and 5.42 were given by Lane, Lin and Liu (1959) and Henderson (1963). The threshold channel width, area, and wetted perimeter are only slightly dependent on the lift-to-drag ratio.

5.2.4. Hydraulic geometry of the threshold cross section

Leopold and Maddock (1953) defined the power functions relating the width, depth, slope and velocity to the water discharge as the hydraulic geometry of the channel. Herein, the exponents of the hydraulic geometry equations of streams in small watersheds are derived from theoretical considerations. Both downstream and at-a-station relations are developed.

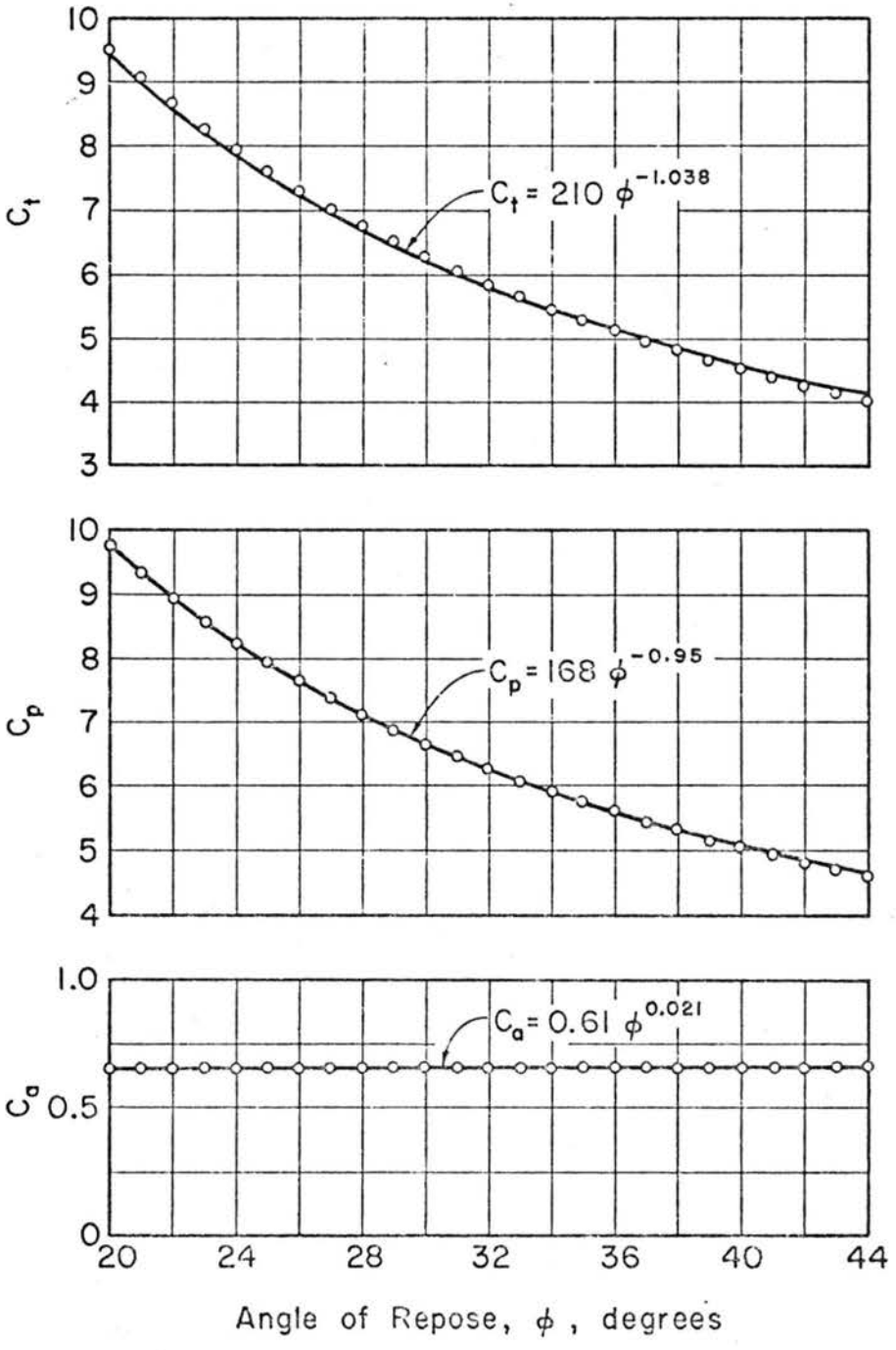

Fig. 5.2 Dimensionless geometric-coefficients for the threshold channel

5.2.4.1. Downstream relations

The channel forming discharge is that discharge which sculptures the threshold channel. If it is assumed that the bed and bank materials are uniform over the length of the small channel, then the values of ϕ and $\overline{\beta}$ are independent of space. According to Fig. 5.2, C_t, C_a and C_p are constants for a fixed ϕ. From Eqs. 5.23 and 5.33

$$\frac{D_o}{y_o} = \frac{D_o}{T_o}\frac{T_o}{y_o} = C_a = K_1 \tag{5.43}$$

from Eq. 5.33

$$\frac{T_o}{D_o} = \frac{C_t}{C_a} = K_2 \tag{5.44}$$

and from Eqs. 5.35 and 5.44

$$\frac{R_o}{D_o} = \frac{R_o}{T_o}\frac{T_o}{D_o} = \frac{C_t}{C_p} = K_3 \tag{5.45}$$

in which K_1, K_2 and K_3 are constants.

In small channels with relatively steep slopes, the friction slope is approximately equal to the bed slope. Manning's equation for the flow is then

$$Q_o = \frac{1.486}{n} A_o R_o^{2/3} S_o^{1/2} \tag{5.46}$$

or

$$Q_o = \frac{1.486}{n} T_o D_o R_o^{2/3} S_o^{1/2} \tag{5.47}$$

in which Q_o is the threshold discharge.

According to Shield's criterion (see Henderson, 1966, p. 413) for incipient motion in turbulent flow

$$d_s \propto \gamma y_o S_o \tag{5.48}$$

in which d_s is the particle size on the channel boundary and γ is the unit weight of water. If the relation of 5.48 holds, the sediment size d_s has been assumed constant over a short reach of channel, $y_o S_o$ is also constant over the same reach; i.e.,

$$y_o S_o = K_4 \tag{5.49}$$

in which K_4 is some constant. From Eqs. 5.43 and 5.49 it follows that

$$D_o S_o = K_5 \tag{5.50}$$

in which K_5 is a different constant.

Manning's roughness coefficient n is related to the particle size d_s by the Stricker formula (see Henderson, 1966, p. 98).

$$n = C\, d_s^{1/6} \tag{5.51}$$

in which C is a constant. As d_s is constant, then n is also constant.

If one substitutes Eqs. 5.44, 5.45, 5.50 and 5.51 into Eq. 5.47, then

$$Q_o \propto D_o^{13/6} \tag{5.52}$$

or

$$D_o \propto Q_o^{0.46} \tag{5.53}$$

From Eqs. 5.44 and 5.53

$$T_o \propto Q_o^{0.46} \tag{5.54}$$

and from Eqs. 5.50 and 5.53

$$S_o \propto Q_o^{-0.46} \tag{5.55}$$

Furthermore, the mean velocity for the cross section is

$$V_o = \frac{Q_o}{A_o} = \frac{Q_o}{T_o D_o} \tag{5.56}$$

Using Relation 5.53 and 5.54 with Eq. 5.56

$$V_o \propto Q_o^{0.08} \tag{5.57}$$

Relations 5.53, 5.54, 5.55 and 5.57 are the theoretically derived downstream hydraulic geometry relations for threshold channels in small wathersheds.

5.2.4.2. At-a-station relations

In the foregoing section, the threshold channel cross-sectional shape was derived assuming incipient motion conditions on the noncohesive channel boundary for the channel forming discharge. Thus, no change in stream morphology could occur unless discharges greater than the "threshold" discharge occur. In other words, when the flow is less than the threshold flow, the particles on the bed and banks are stable. The channel shape and bed slope remain unaltered for discharges less than threshold discharge. The channel shape is given by Eq. 5.22. The hydraulic geometry relations at-a-station are derived in the following manner.

The hydraulic dimensions of the threshold channel flowing partially full are defined in Fig. 5.3. The maximum depth of the partially-full channel is

$$h = y_o - y(\xi = T/2) \tag{5.58}$$

in which T is the top width of the partially-full channel. With Eq. 5.22

$$\frac{h}{y_o} = 1 - \frac{1}{1-\bar{r}} \left\{\cos\left(\tan\phi \sqrt{\frac{1-\bar{r}}{1+\bar{r}}} \frac{T}{2y_o}\right) - \bar{r}\right\} \tag{5.59}$$

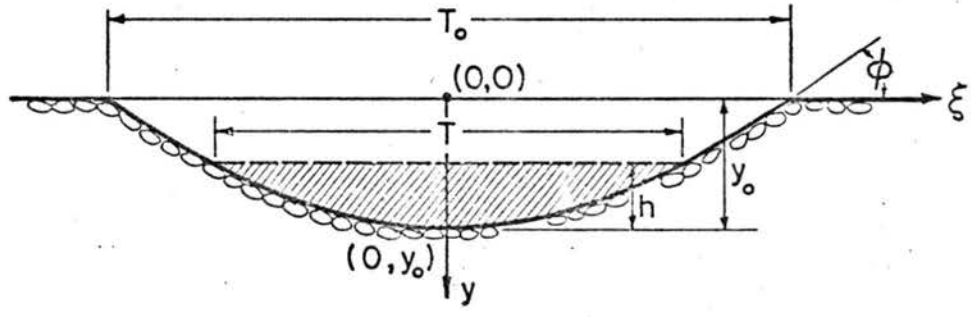

Fig. 5.3 Geometry for a partially-full threshold channel

Let

$$\eta = \frac{h}{y_o} \tag{5.60}$$

so that from Eq. 5.59, the top width becomes

$$\frac{T}{y_o} = \frac{2}{\tan\phi} \sqrt{\frac{1+\bar{r}}{1-\bar{r}}} \cos^{-1}\bar{\Omega} \tag{5.61}$$

in which

$$\bar{\Omega} = 1-\eta + \bar{r}\eta \ . \tag{5.62}$$

By using Eq. 5.23 in Eq. 5.61, the relative top width is

$$\frac{T}{T_o} = \frac{\cos^{-1}\bar{\Omega}}{\cos^{-1}\bar{r}} \tag{5.63}$$

The corresponding cross-sectional area A for the partially-full threshold channel can be derived in a similar manner. The expression is

$$\frac{A}{A_o} = \frac{\sqrt{1 - \bar{\Omega}^2} - \bar{\Omega} \cos^{-1}\bar{\Omega}}{\sqrt{1 - \bar{r}^2} - \bar{r} \cos^{-1}\bar{r}} \tag{5.64}$$

and for the wetted perimeter,

$$\frac{P}{P_o} = \frac{E(\bar{k},\frac{\pi}{2}) - E(\bar{k},\frac{\pi}{2} - \cos^{-1}\bar{\Omega})}{E(\bar{k},\frac{\pi}{2}) - E(\bar{k},\frac{\pi}{2} - \cos^{-1}\bar{r})} \ . \tag{5.65}$$

The hydraulic depth D for the partially-full threshold channel is

$$\frac{D}{D_o} = \frac{A}{A_o} \Big/ \frac{T}{T_o} \tag{5.66}$$

in which A/A_o and T/T_o are given by Eqs. 5.63 and 5.64 repectively. Similarly, the hydraulic radius R for a partially-full threshold channel is

$$\frac{R}{R_o} = \frac{A}{A_o} \Big/ \frac{P}{P_o} \tag{5.67}$$

in which A/A_o and P/P_o are given by Eqs. 5.64 and 5.65.

As the bed slope is constant at a particular section and Manning's n is assumed constant, the flow Q in the partially-full threshold is given by the equation

$$\frac{Q}{Q_o} = \left(\frac{A}{A_o}\right)^{5/3} / \left(\frac{P}{P_o}\right)^{2/3} . \tag{5.68}$$

The dimensionless ratios T/T_o, D/D_o and Q/Q_o in Eqs. 5.63, 5.66 and 5.68 have been evaluated for $\phi = 35°$ and $\overline{\beta} = 0.85$. The values are shown as the circles in Fig. 5.4. The power functions

$$\frac{T}{T_o} = \eta^{0.517} \tag{5.69}$$

$$\frac{D}{D_o} = \eta^{0.993} \tag{.570}$$

and

$$\frac{Q}{Q_o} = \eta^{2.148} \tag{5.71}$$

are approximations to the complex functions described by Eqs. 5.63, 5.66 and 5.68, and are shown as solid lines in Fig. 5.4.

From Eqs. 5.69 and 5.71, it can be shown that

$$\frac{T}{T_o} = \left(\frac{Q}{Q_o}\right)^{0.24} \tag{5.72}$$

or

$$T \alpha Q^{0.24} , \tag{5.73}$$

as Q_o and T_o are constant at a station. Similarly, from Eqs. 5.70 and 5.71, one concludes that

$$D \alpha Q^{0.46} . \tag{5.74}$$

As the bed slope is constant at a station

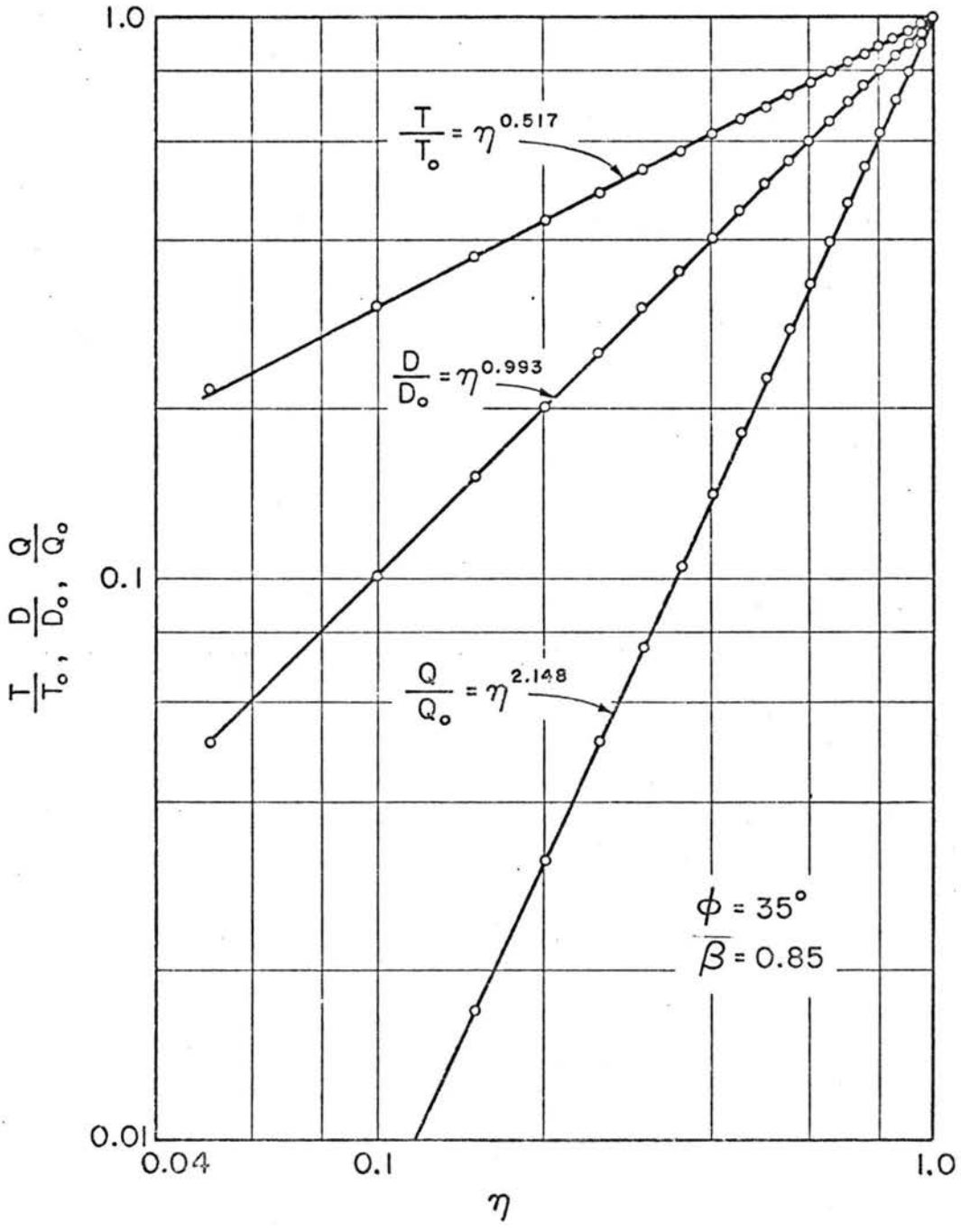

Fig. 5.4 Power functions for the hydraulic geometry of the partially-full threshold channel

$$S_o \alpha\ Q^{0.00} \tag{5.75}$$

From Eqs. 5.73 and 5.74, the mean velocity in the partially-full threshold channel varies according to the expression

$$V \alpha\ Q^{0.30} \tag{5.76}$$

Relations 5.73, 5.74, 5.75 and 5.76 are the theoretically derived at-a-station hydraulic geometry relations of the threshold channel. The variations of the exponents of Q with $\overline{\beta}$ for $\phi = 35°$ are given in Fig. 5.5. The variations of the exponents with ϕ for $\overline{\beta} = 0.0$ and $\overline{\beta} = 0.85$ are given in Fig. 5.6. The curves in Figs. 5.5 and 5.6 illustrate that the values of the exponents in Relations 5.73, 5.74 and 5.76 are not sensitive to variations in ϕ and $\overline{\beta}$. In other words, these exponents are nearly independent of the particle size.

5.3. Field Observations

5.3.1. Validity of assumptions

In the development of downstream relations for the threshold cross section, it was assumed that

$$\frac{T_o}{D_o} = K_2 \tag{5.44}$$

and

$$D_o S_o = K_5 \tag{5.50}$$

in which K_2 and K_5 were constants; that is, the ratio T_o/D_o and the product $D_o S_o$ were assumed constant in the downstream direction. It follows then that T_o/D_o and $D_o S_o$ were assumed independent of the threshold discharge. These two assumptions were tested with the field observations made by Brush (1961).

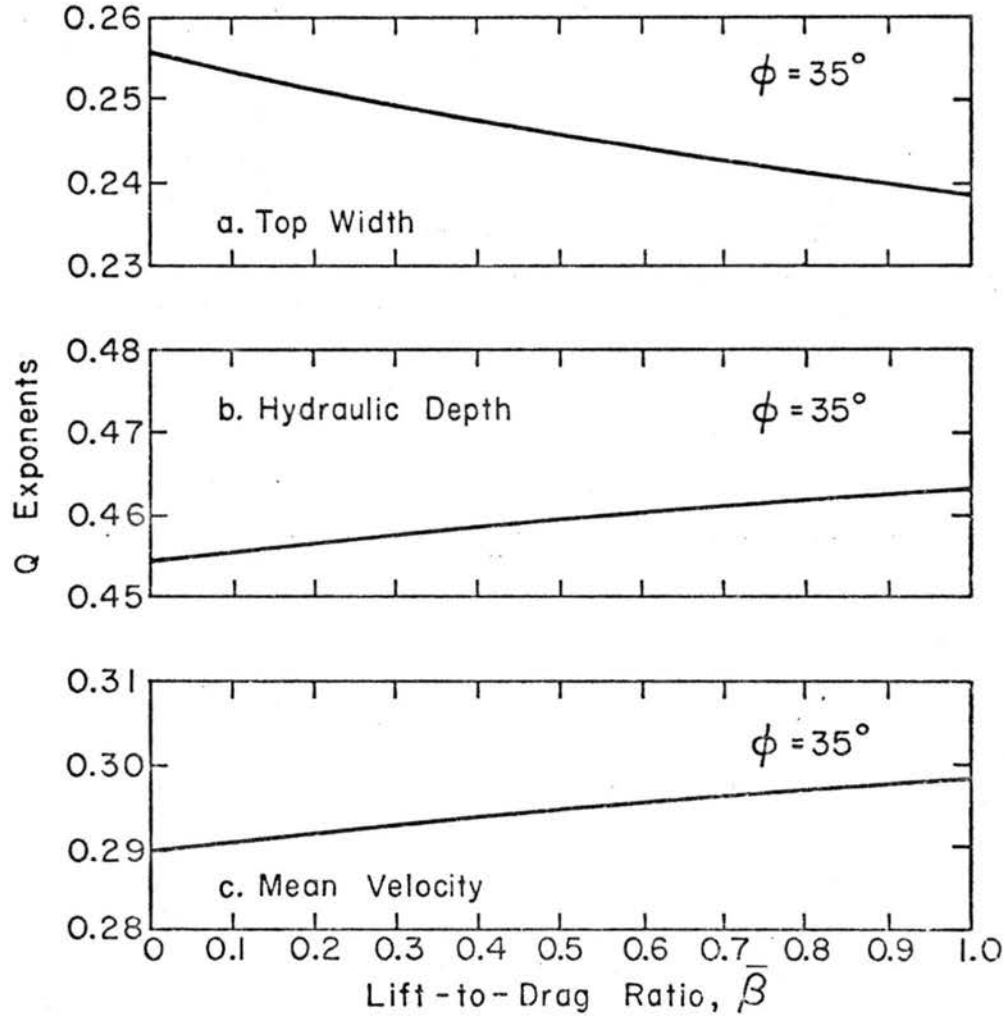

Fig. 5.5 The variation of exponents in the at-a-station hydraulic geometry equations with the lift-to-drag ratio

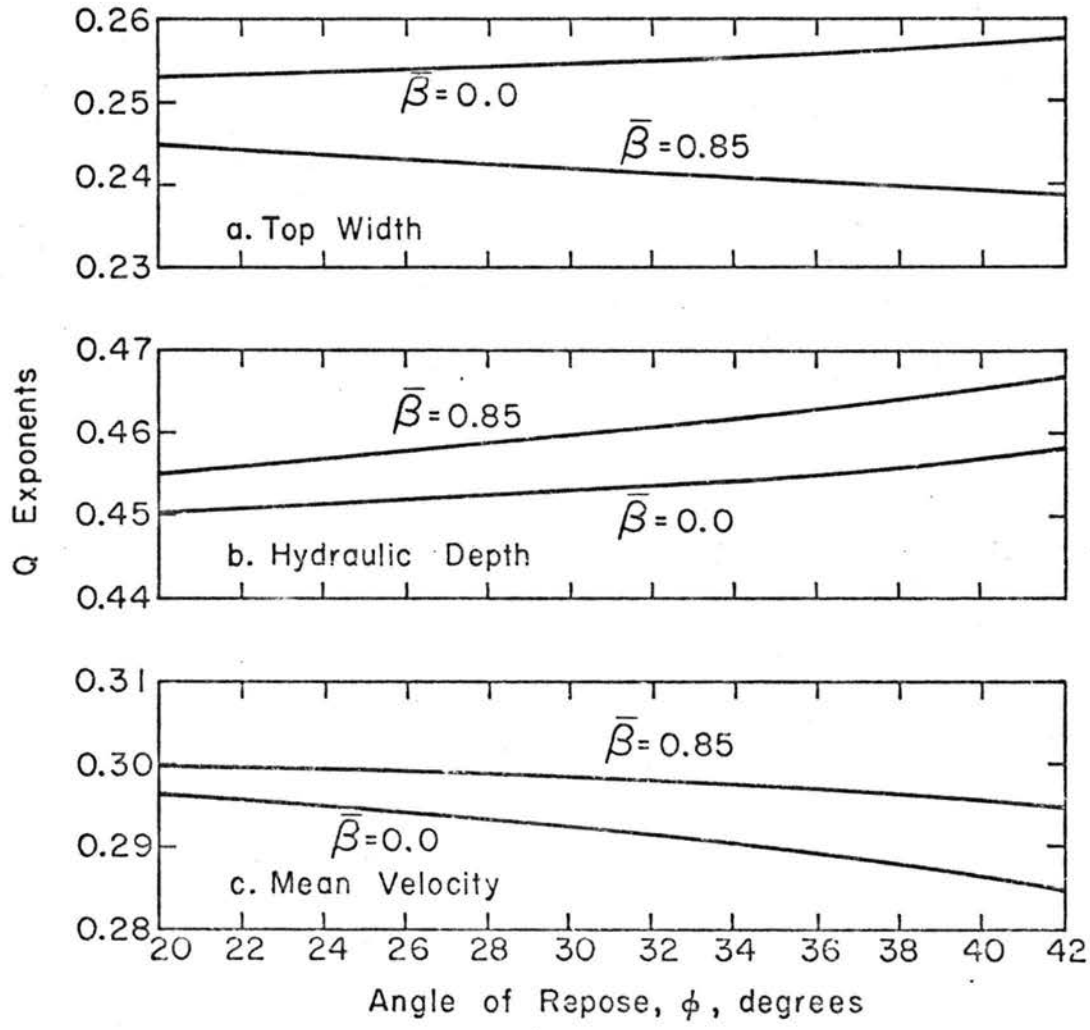

Fig. 5.6 The variation of exponents in the at-a-station hydraulic geometry equations with angle of repose

The T_o/D_o values obtained by Brush are shown in Fig. 5.7. The values are independent of drainage area. As the discharge and drainage area are directly related, it follows from Fig. 5.7 that the ratio T_o/D_o is independent of the threshold discharge in small watersheds.

Brush's data on D_oS_o are plotted in Fig. 5.8. From this information it is concluded that the ratio D_oS_o is also independent of the threshold discharge. The values of D_oS_o are practically the same for different streams except for McClain Run.

From Brush's field observations, it is concluded that the assumptions represented by Eqs. 5.44 and 5.50 are valid.

5.3.2. Hydraulic geometry equations

Brush's (1961) data were also employed to obtain field values of the hydraulic geometry exponents for the downstream relations. The channels that Brush studied have gravel banks and beds. The average values of exponents for the five streams with drainage area less than 10 sq mi (Shaver Creek, Globe Run, Weiker Run, McClain Run, and Reeds Run) are compared with the exponents derived from theory. The comparisons, given in Table 5.1, show that the theoretical results are compatible with field observations.

Judd and Peterson (1969) conducted a field survey on gravel and boulder streams and also established the at-a-station hydraulic geometry equations. The average values of the exponents for sites 70 and 71 (Boulder Creek, Colorado) are compared with the theoretical exponents in Table 5.1. Only sites 70 and 71 were selected because the measured results of these two sites satisfy the flow continuity requirement and these two sites are free of major vegetation effects. Again, the exponents from the field data compare favorably with the exponents developed from the threshold theory.

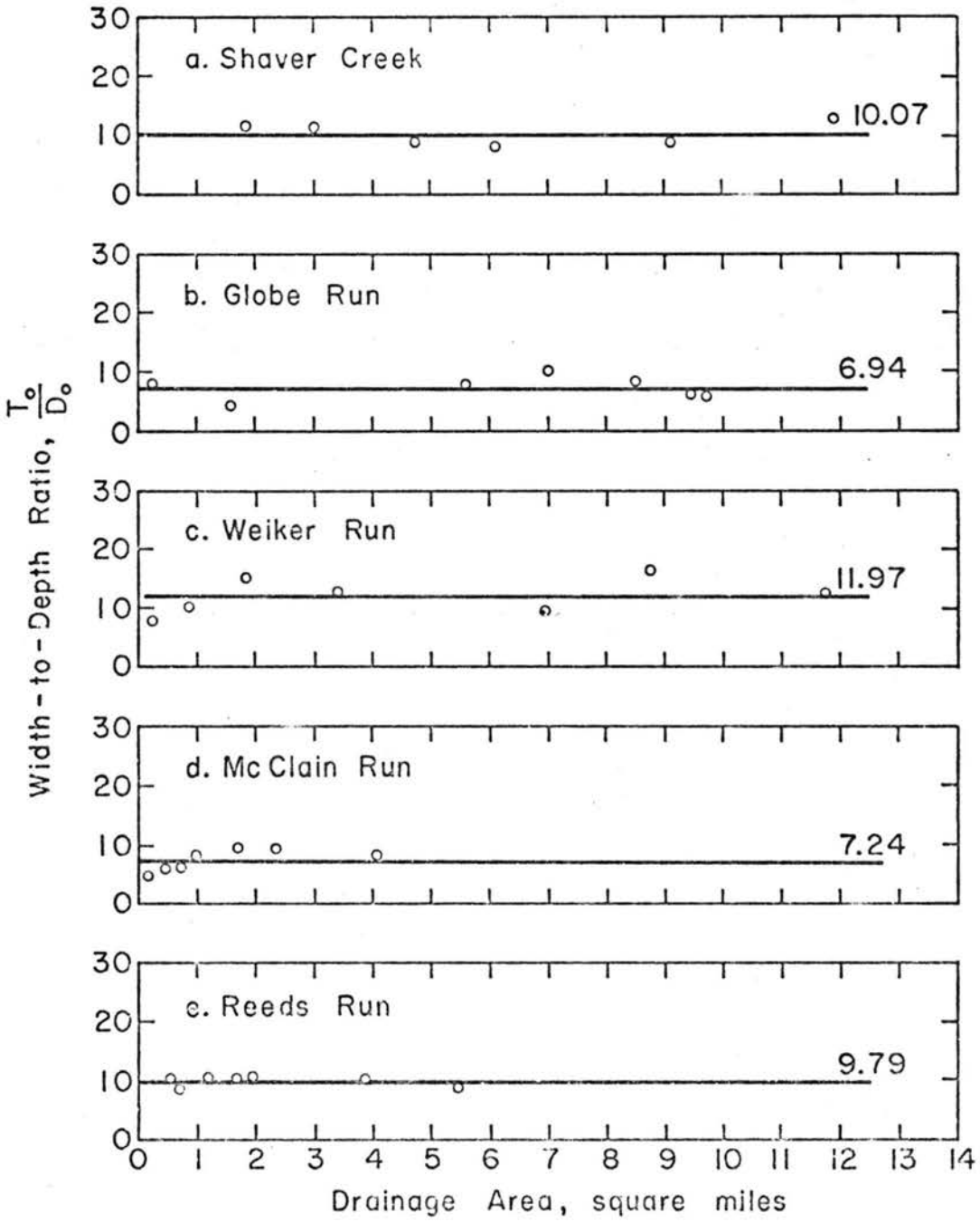

Fig. 5.7 Downstream variation of the width-to-depth ratio for threshold channel

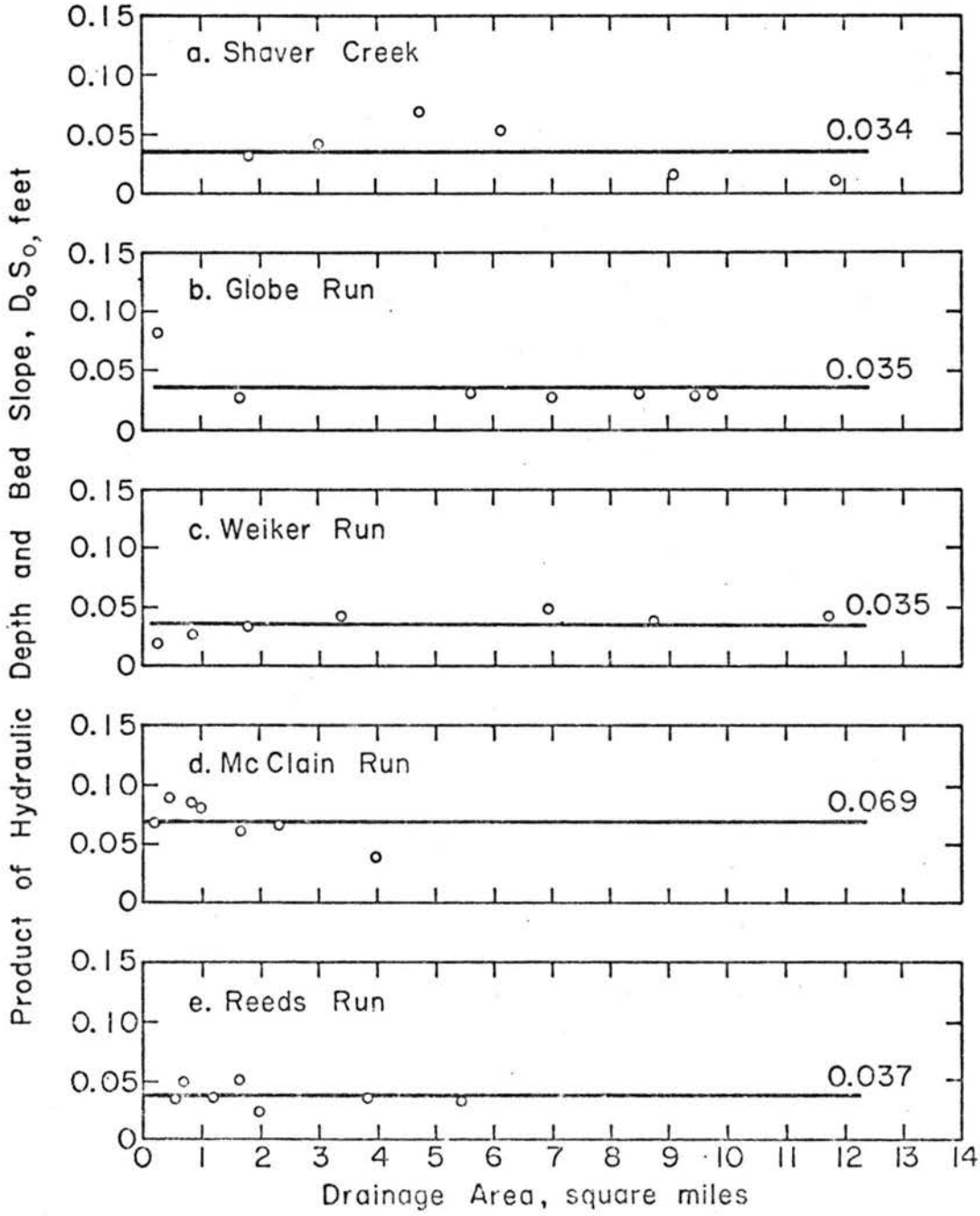

Fig. 5.8 Downstream variation of the product of hydraulic depth and bed slope for threshold channel

Table 5.1. Values of the Q Exponent in the Hydraulic Geometry Equations

Downstream Relations

Source	Value of the Q exponent for			
	T_o	D_o	S_o	V_o
Theoretical	0.46	0.46	-0.46	0.08
Brush (1961)	0.52	0.43	-0.48[a]	0.05

At-A-Station Relations

Source	Value of the Q exponent for			
	T	D	S_o	V
Theoretical	0.24	0.46	0.0	0.30
Judd and Peterson (1969)	0.18	0.51	0.0[a]	0.31

[a] estimated by the writer

5.4 Summary

A small watershed has been defined as a drainage system which is small enough to ensure both geological and hydrologic homogeneity in space and within the time span of one or two centuries. In many regions, this definition of a small watershed would restrict the small watershed area to approximately 10 to 20 sq mi.

The equations describing the basic physical processes in small watershed channels sculptured in noncohesive alluvial materials have been employed in this study to derive the hydraulic geometry

equations. Both downstream and at-a-station relations were developed. These theoretical results agree with field observations made by Brush (1961), and Judd and Peterson (1969).

The angle of repose for the noncohesive materials forming the banks and bed of the threshold channel is the dominant factor governing the shape of the threshold cross section. The width-to-depth ratio for channels in materials having a small angle of repose is larger than for channels in materials having a large angle of repose. Although ratio of the lift force on the particles to the drag force has a smaller effect on the shape than the angle of repose, the lift forces have an influence on the shaping process and are included in the theoretical analysis. The theoretical exponents of both downstream and at-a-station hydraulic geometry equations are practically independent of particle size if the particle size is constant over the reach of channel.

Chapter VI

CONCLUSIONS

The main conclusions of this study can be summarized as follows:

(1) The rainfall-runoff model developed in this study is a physical process simulation model designed to simulate the response of the basin to rainfall. The model includes the water balance simulation for land surface hydrologic cycle on the single storm basis and the water routing features for both overland flow and channel systems. Unlike the conventional approach to parametric modeling of watershed response, this model utilizes the physical process of the flow and requires less assistance from optimization schemes than any existing water models known to the writer. For the Carrizal Basin in Venezuela the simulated hydrographs agree well with the measured hydrographs. The differences between the simulated and measured hydrographs indicate that the proposed model is able to simulate the total volume, the hydrograph shape, the peak flow and the time to peak flow generally within 12 percent. The sensitivity analysis indicates that soil data are very sensitive to the computed hydrograph. Flow resistance parameters and vegetation data are less sensitive to the simulated results. In addition, this physically oriented model has the capability to predict watershed treatment effects on water yields under the assumed conditions.

This model may be used to estimate the long-term response if a water balance model is incorporated to simulate the water balance during the interstorm periods.

(2) The proposed rainfall-erosion model is able to simulate the soil erosion process and produces time-dependent erosion rates from overland flow areas. The computed results are comparable with the experimental data from a soil plot. The model also generates a concave land form which frequently appears in nature. The present model only simulates the bed material load routing. A future study is recommended to improve the model by the inclusion of wash load routing.

(3) The hydraulic geometry equations can be theoretically derived by the equations describing the basic physical processes of stream morphology in small watersheds. Both downstream and at-a-station derived relations agree with field observations. The angle of repose for the noncohesive materials forming the banks and bed of the threshold channel is the dominant factor governing the shape of the threshold cross section. The width-to-depth ratio for channels in materials having a small angle of repose is larger than for channels in materials having a large angle of repose. Although ratio of the lift force on the particles to the drag force has a smaller effect on the shape than the angle of repose, the lift forces have an influence on the shaping process and are included in the theoretical analysis. The theoretical exponents of both downstream and at-a-station hydraulic geometry equations are practically independent

of particle size if the particle size is constant over the reach of channel.

(4) The calibration of the rainfall-runoff model can be simplified by making separate calibrations for water balance and for flow routing. The calibration results indicated that the initial interception storage is larger for the storms occurred at daybreak than those occurred in the afternoon and the antecedent moisture content is highly correlated with the overall rainfall records and the recession condition of the previous storm. In addition, it was also found that the ground cover resistance descriptor ψ_g increases as the size of storm increases.

(5) The vegetation treatment effects can be estimated by changing the canopy cover density and the ground cover density for the input to the simulation model.

For a constant ground cover density, the total runoff volume and the peak flow are increased as the canopy cover density is decreased. The increase results because the interception is reduced when vegetation is removed. However, the time to peak flow is lengthened as the canopy cover is decreased. This flow retardation is due to the augmenting of raindrop impact resistance by increasing area of exposure and the attenuation by overbank flow.

For a constant canopy cover density, the total runoff volume and the peak flow rate are increased and the time to peak flow is shortened as the ground cover density is decreased. These responses are mainly due to the decrease

of flow resistance when the ground cover density is decreased.

(6) For the experimental data by Kilinc and Richardson (1973), the bed-load function which best fits the data is $q_b = \beta_1' (\tau-\tau_c)^{\beta_2'}$.

(7) It was found that the soil erosion rate was very sensitive to bed slope and shape. The general practice of assuming a uniform shape may result in serious errors. However, the common assumption of $\sin\theta'$ being equal to bed slope S_o is not too serious when the bed slope is less than 25 percent.

(8) The numerical scheme developed in this study is unconditional stable and may be used with wide range of $\frac{\Delta t}{\Delta x}$ without loss of significant accuracy. This numerical scheme has the advantages of both nonlinear and linear schemes. The nonlinear scheme ensures convergence and the linear portion of the scheme provides rapid computations. The applicability of this numerical scheme has been tested in various cases. The tests illustrate that this simple routing procedure simulates hydrographs which agree with measured overland flow hydrographs, natural channel hydrographs, and hydrographs from drainage systems. It is concluded that this scheme is promising for large-scale modeling of watershed response if the kinematic-wave approximation for flow routing is valid.

(9) It has been found that the discharge Q is the better selection for the unknown in numerical computations than the depth or area. The term β in the relation $A = \alpha Q^{\beta}$ is

generally less than 1.0. If the flow discharge is computed incorrectly, the flow depth estimation is influenced only to a small degree.

(10) In this study, the flow area versus discharge relations (A-Q) are formulated to be time and space dependent. The interesting phenomena of "pip" and "dip" in overland flow hydrographs are successfully simulated. These phenomena are the results of sudden changes of flow resistance due to ceasing or starting of rainfall over shallow, low Reynolds number flows.

REFERENCES

1. Berryman, A. D., 1974, "Hydrologic Characteristics of a Small Basin," M.S. Thesis, Department of Civil Engineering, Colorado State University, Fort Collins, Colorado.

2. Bhowmik, N. G., 1968, "The Mechanics of Flow and Stability of Alluvial Channels Formed in Coarse Materials," Ph.D. Dissertation, Colorado State University, Fort Collins, Colorado, August.

3. Brakensiek, D. L., A. L. Heath and G. H. Comer, 1966, "Numerical Techniques for Small Watershed Flood Routing," USDA, ARS 41-113, February.

4. Brush, L. M., 1961, "Drainage Basins, Channels, and Flow Characteristics of Selected Streams in Central Pennsylvania," USGS prof. paper 282-F, 180 p.

5. Chang, F. F. M. and D. L. Richards, 1971, "Deposition of Sediment in Transient Flow," Journal of the Hydraulic Division, ASCE, Vol. 97, No. HY 6, pp. 837-849, June.

6. Chen, Y. H., 1973, "Mathematical Modeling of Water and Sediment Routing in Natural Channels," Ph.D. Dissertation, Department of Civil Engineering, Colorado State University, Fort Collins, Colorado.

7. Chow, V. T., 1964, "Runoff," Section 14, Handbook of Applied Hydrology, edited by V. T. Chow, McGraw-Hill, New York.

8. Clark, C. O., 1945, "Storage and the Unit Hydrograph," Trans. ASCE, Vol. 110, pp. 1419-1488.

9. Crawford, N. H. and R. K. Linsley, 1966, "Digital Simulation in Hydrology: Stanford Watershed Model IV," Tech. Report, No. 39, Department of Civil Engineering, Stanford University, Stanford, California, July.

10. Daily, J. W. and D. R. F. Harleman, 1966, "Fluid Dynamics," Addison-Wesley, Massachusetts.

11. Dawdy, D. R., R. W. Litchy and J. M. Bergmann, 1972, "A Rainfall-Runoff Simulation Model for Estimation of Flood Peaks for Small Drainage Basin," USGS professional paper 506-B.

12. Einstein, H. A., 1950, "The Bed Load Function for Sediment Transportation in Open Channel Flows," USDA, Tech. Bulletin, No. 1026.

13. Gessler, J., 1965, "The Beginning of Bed Load Movement of Mixtures Investigated as Natural Armoring in Channels," W. M. Keck Laboratory of Hydraulics and Water Resources, California Institute of Technology, Pasadena, California.

14. Henderson, F. M., 1963, "Stability of Alluvial Channels," Trans. ASCE, Vol. 128, part I, pp. 657-686.

15. Henderson, F. M., 1966, "Open Channel Flow," Macmillan, New York.

16. Hewlett, J. D. and W. L. Nutter, 1969, "An Outline of Forest Hydrology," University of Georgia Press, Athens, Georgia.

17. Himmelblau, D. M., 1972, "Applied Nonlinear Programming," McGraw-Hill, New York.

18. Horton, R. E., 1919, "Rainfall Interception," Mon. Weather Rev. 47, 603-23.

19. Izzard, C. F., 1946, "Hydraulics of Runoff from Developed Surface," Proceedings, Highway Research Board, Twenty-sixth Annual Meeting, pp. 129-150.

20. Judd, H. E. and D. F. Peterson, 1969, "Hydraulics of Large Bed Element Channels," Report No. PRWG 17-6, Utah Water Research Laboratory, Utah State University, Logan, Utah, p. 115 August.

21. Kilinc, M. and E. V. Richardson, 1973, "Mechanics of Soil Erosion From Overland Flow Generated by Simulated Rainfall," Hydrology Paper No. 63, Colorado State University, Fort Collins, Colorado.

22. Labadie, J. W. and J. A. Dracup, 1969, "Optimal Identification of Lumped Watershed Models," Water Resources Research, Vol. 5, No. 3, June.

23. Lane, E. W., 1958, "Design of Stable Channel," Trans. ASCE, Vol. 120, pp. 1234-1279.

24. Lane, E. W., P. N. Lin and H. K. Liu, 1959, "The Most Efficient Stable Channel for Comparatively Clean Water in Non-Cohesive Material," Colorado State University Report CER59HKL5, April.

25. Leopold, L. B. and T. Maddock, Jr., 1953, "The Hydraulic Geometry of Stream Channels and Some Physiographic Implications," USGS prof. paper 252.

26. Leopold, L. B. and W. B. Langbein, 1962, "The Concept of Entropy in Landscape Evolution," USGS prof. paper 500-A.

27. Li, R. M., H. W. Shen and D. B. Simons, 1973, "Mechanics of Soil Erosion by Overland Flow," Paper presented at the 15th Congress, International Association for Hydraulic Research, Istanbul, Turkey, proc. paper A 54, pp. 437-446, September.

28. Li, R. M. and H. W. Shen, 1973, "Effect of Tall Vegetation on Flow and Sediment," Journal of the Hydraulics Division, ASCE, Vol. 99, No. HY 5, pp. 793-814, May.

29. Liggett, J. A. and D. A. Woolhiser, 1967, "Difference Solutions of the Shallow-Water Equations," Journal of the Engineering Mechanics Division, ASCE, Vol. 93, No. EM 2, pp. 39-71, February.

30. Linsley, R. K., Jr., M. A. Kohler and J. L. H. Paulhus, 1958, "Hydrology for Engineers," McGraw-Hill, New York.

31. Meyer, L. D. and L. A. Kramer, 1968, "Relation Between Land-Slope Shape and Soil Erosion," Paper presented at the 1968 Winter Meeting of ASAE, Chicago, Illinois, December 10-13.

32. Morgali, J. R. and R. K. Linsley, 1965, "Computer Analysis of Overland Flow," Journal of the Hydraulic Division, ASCE, Vol. 91, No. HY 3, pp. 81-100, March.

33. Musgrave, G. W., 1947, "The Quantitative Evaluation of Factors in Water Erosion a First Approximation," Journal of Soil and Water Conservation, Vol. 2, No. 3, pp. 133-138.

34. Palmer, J. R., 1969, "An Improved Procedure for Orthogonalizing the Search Vectors in Rosenbrock's and Swann's Direct Search Optimization Methods," Computer Journal, Vol. 12, pp. 69-71.

35. Penman, H. L., 1965, "Discussion of 'Mathematical Theory of Interception' by R. E. Leonard," International Symposium on Forest Hydrology, edited by W. E. Sopper and H. W. Lull, p. 136, September.

36. Powell, M. J. D., 1964, "Efficient Method for Finding Minimum of Function of Several Variables Without Calculating Derivatives," Computer Journal, Vol. 7, No. 2, pp. 155-162, July.

37. Prasad, R., 1967, "A Nonlinear Hydrologic System Response Model," Journal of the Hydraulic Division, ASCE, Vol. 93, No. HY 4, pp. 201-221, July.

38. Rana, S. A., 1971, "Sediment Sorting in Alluvial Channels," M.S. Thesis, Department of Civil Engineering, Colorado State University, Fort Collins, Colorado.

39. Rosenbrock, H. H., 1960, "An Automatic Method for Finding the Greatest or Least Value of a Function," Computer Journal, Vol. 4, pp. 175-184.

40. Schaake, J. C., Jr., 1965, "Synthesis of the Inlet Hydrograph," Tech. Report No. 3, Storm Drainage Project, The Johns Hopkins University, June.

41. Schaake, J. C., Jr., 1971, "Deterministic Urban Runoff Model," Chapter VIC, Treatise on Urban Water Systems, edited by M. L. Albertson, L. S. Tucker and D. C. Taylor, Colorado State University, Fort Collins, Colorado, July.

42. Shen, H. W., 1971, "Wash Load and Bed Load," Chapter 11, River Mechanics, edited by H. W. Shen, Colorado State University, Fort Collins, Colorado.

43. Shen, H. W. and R. M. Li, 1973, "Rainfall Effect on Sheet Flow Over Smooth Surface," Journal of Hydraulics Division, ASCE, Vol. 99, No. HY 5, pp. 771-792, May.

44. Sherman, L. K., 1932, "Streamflow from Rainfall by the Unit Hydrograph Method," Engineering News-Record, Vol. 108, pp. 501-505.

45. Simons, D. B. and M. L. Albertson, 1960, "Uniform Water Conveyance Channels in Alluvial Material," Journal of Hydraulics Division, ASCE, Vol. 86, No. HY 5, pp. 33-71, May.

46. Simons, D. B. and E. V. Richardson, 1966, "Resistance to Flow in Alluvial Channels," USGS, professional paper 422-J.

47. Simons, D. B., E. V. Richardson, M. A. Stevens, J. H. Duke and V. C. Duke, "Venezuelan International Meteorological and Hydrological Experiment," Vol. II, Stream, Groundwater and Ground Response Data, CER70-71DBS-EVR-MAS-JHD-VCD-50, August.

48. Simons, D. B., E. V. Richardson, M. A. Stevens, J. H. Duke and V. C. Duke, "Venezuelan International Meteorological and Hydrological Experiment," Vol. III, Geometric and Hydraulic Properties of the River, CER70-71DBS-EVR-MAS- JHD-VCD-36, October.

49. Singh, K. P., 1964, "Nonlinear Instantaneous Unit-Hydrograph Theory," Journal of the Hydraulics Division, ASCE, Vol. 90, No. HY 2, part I, pp. 313-347, March.

50. Stebbings, J., 1963, "The Shapes of Self-Formed Model Alluvial Channels," Proc. of the Institution of Civil Engineers, Vol. 25, session 1962-63, paper No. 6642, pp. 485-510, August.

51. Streeter, V. L., 1966, "Fluid Mechanics," McGraw-Hill, New York.

52. Torum, A., 1965, "Stability of Gravel Mound Exposed to Simultaneous Action of Waves and Currents," XI Congress, International Association for Hydraulics Research, Leningrad, U.S.S.R., p.9.

53. Wischmeier, W. H. and D. D. Smith, 1965, "Predicting Rainfall-Erosion Losses from Cropland East of the Rocky Mountains," Agriculture Handbook, No. 282, USDA.

54. Wolman, M. G., 1955, "The Natural Channel of Brandywine Creek, Pennsylvania," USGS, Professional paper 271.

55. Wu, I. P., 1963, "Design Hydrographs for Small Watersheds in Indiana," Journal of the Hydraulic Division, ASCE, Vol. 89, No. HY 6, part I, pp. 35-66, November.

56. Young, R. A. and C. K. Mutchter, 1969, "Soil Movement on Irregular Slopes," Water Resources Research, Vol. 5, No. 5, pp. 1084-1089.

57. Yoon, N. Y., 1970, "The Effect of Rainfall on the Mechanics of Steady Spatially Varied Sheet Flow on a Hydraulically Smooth Boundary," Ph.D. Thesis, Department of Civil Engineering, University of Illinois, Urbana, Illinois.

58. Yu, Y. S. and J. S. McNown, 1964, "Runoff from Impervious Surfaces," Journal of Hydraulic Research, IAHR, Vol. 2, No. 1, pp. 2-24.

59. Zahner, R., 1965, "Refinement in Empirical Functions for Realistic Soil-Moisture Regimes Under Forest Cover," International Symposium on Forest Hydrology, edited by W. E. Sopper and H. W. Lull, pp. 261-274, September.

60. Zingg, A. N., 1940, "Degree and Length of Land Slope as it Affects Soil Loss in Runoff," Agricultural Engineering, February, pp. 59-64.

61. Zinke, P. J., 1965, "Forest Interception Studies in the United States," International symposium on Forest Hydrology, edited by W. E. Sopper and H. W. Lull, pp. 137-161, September.

Appendix A

INTEGRATION OF SUSPENDED SEDIMENT LOAD

A.1. Need For The Method

If a logarithmic velocity profile is assumed for the vertical velocity distribution, the numerical intergration of J_1 and J_2 integrals (Eqs. 4.13 and 4.14) is required for intergrating the suspended sediment load. The two integrals are

$$J_1 = \int_G^1 \left(\frac{1-r}{r}\right)^{\omega} dr \qquad (A.1)$$

and

$$J_2 = \int_G^1 \left(\frac{1-r}{r}\right)^{\omega} \ell nr \, dr \qquad (A.2)$$

The two integrals J_1 and J_2 cannot be integrated in closed form for most values of ω. The numerical integration is necessary. Einstein (1950) employed the Simpson formula of numerical integration in his work. Rana (1971) incorporated the same formula in a computer program for the Einstein method of computing sediment transport rate (Einstein, 1950).

Past experiences reveal that the use of Simpson's formula to evaluate J_1 and J_2 occupy a major portion of computer time required in studying unsteady sediment transport problems. A more efficient method of numerical integration is needed. Chen (1973) used a method of polynomial approximations based on four reference values of J_1 or J_2 with constant values of G and integer values of ω and shortened the computer time appreciably. However, the validity of Chen's method is limited to a small range of G and ω.

Herein an efficient and flexible method to evaluate J_1 and J_2 that requires less computation time than either the Simpson's formula or Chen's method is presented. This method is based on power series expansion and has the following advantages over the Simpson's formula. First, with nearly the same degree of accuracy, the new method requires only one-tenth of the computer time needed for the Simpson's formula. Second, the desired degree of accuracy may be changed by the user to satisfy the purpose of individual problems. Third, the integration of the power series can be performed to any desired accuracy.

A.2. Power Series Expansion

A.2.1. Derivation

Equation A.1 and Eq. A.2 can be rewritten as

$$J_1 = \int_G^1 r^{-\omega}(1-r)^{\omega}dr \tag{A.3}$$

and

$$J_2 = \int_G^1 r^{-\omega}\ell nr(1-r)^{\omega}dr \tag{A.4}$$

The power series expansion of the term $(1-r)^{\omega}$ is

$$(1-r)^{\omega} = 1-\omega r + \frac{\omega(\omega-1)}{2!} r^2 - \frac{\omega(\omega-1)(\omega-2)}{3!} r^3 + \ldots$$

$$+ (-1)^k \frac{\omega(\omega-1)(\omega-2)\cdots(\omega-k+1)}{k!} r^k + \ldots \tag{A.5}$$

The ratio test shows that this series is absolutely convergent when r is less than 1.0. By employing Eq. A.5 in Eqs. A.3 and A.4 and by integrating term by term, one obtains the following series solutions for J_1 and J_2

$$J_1 = \frac{1-G^{(1-\omega)}}{1-\omega} - \omega \frac{1-G^{(2-\omega)}}{2-\omega} + \frac{\omega(\omega-1)}{2!} \frac{1-G^{(3-\omega)}}{3-\omega} + \cdots$$

$$+ (-1)^k \frac{\omega(\omega-1)(\omega-2)\cdots(\omega-k+1)}{k!} \frac{1-G^{(k+1-\omega)}}{k+1-\omega} + \cdots \tag{A.6}$$

in which

$$\frac{1-G^{(k+1-\omega)}}{k+1-\omega} = -\ell nG \quad \text{when } \omega=k+1, \text{ for } k=0,1,2\ldots \tag{A.7}$$

and

$$J_2 = \frac{G^{(1-\omega)}-1}{(1-\omega)^2} - \frac{G^{(1-\omega)}\ell nG}{1-\omega} - \omega\left[\frac{G^{(2-\omega)}-1}{(2-\omega)^2} - \frac{G^{(2-\omega)}\ell nG}{2-\omega}\right]$$

$$+ \frac{\omega(\omega-1)}{2!}\left[\frac{G^{(3-\omega)}-1}{(3-\omega)^2} - \frac{G^{(3-\omega)}\ell nG}{3-\omega}\right] + \cdots$$

$$+ (-1)^k \frac{\omega(\omega-1)(\omega-2)\cdots(\omega-k+1)}{k!}\left[\frac{G^{(k+1-\omega)}-1}{(k+1-\omega)^2} - \right.$$

$$\left.\frac{G^{(k+1-\omega)}\ell nG}{k+1-\omega}\right] + \cdots \tag{A.8}$$

in which

$$\frac{G^{(k+1-\omega)}-1}{(k+1-\omega)^2} - \frac{G^{(k+1-\omega)}\ell nG}{k+1-\omega} = -\frac{1}{2}(\ell nG)^2$$

$$\text{when } \omega = k+1 \text{ for } k = 0,1,2,\ldots \tag{A.9}$$

Theoretically, as k approaches infinity, the above series solutions for J_1 and J_2 converge to the exact solutions. However, the numerical values obtained by the partial sum of the first $k+1$ terms of the series (defined as k-th order approximations) are

satisfactory answers for practical purposes. Therefore, the various orders of approximation are examined herein.

The sum of the first $k+1$ terms of the series solutions for J_1 and J_2 are respectively

$$J_1(k+1) = \frac{1-G^{(1-\omega)}}{1-\omega} - \omega\,\frac{1-G^{(2-\omega)}}{2-\omega} + \frac{\omega(\omega-1)}{2!}\,\frac{1-G^{(3-\omega)}}{3-\omega} + \cdots + (-1)^k\,\frac{\omega(\omega-1)(\omega-2)\cdots(\omega-k+1)}{k!}\,\frac{1-G^{(k+1-\omega)}}{k+1-\omega} \tag{A.10}$$

and

$$J_2(k+1) = \frac{G^{(1-\omega)}-1}{(1-\omega)^2} - \frac{G^{(1-\omega)}\ell nG}{1-\omega} - \omega\left[\frac{G^{(2-\omega)}-1}{(2-\omega)^2} - \frac{G^{(2-\omega)}\ell nG}{2-\omega}\right] + \frac{\omega(\omega-1)}{2!}\left[\frac{G^{(3-\omega)}-1}{(3-\omega)^2} + \frac{G^{(3-\omega)}\ell nG}{3-\omega}\right] + \cdots + (-1)^k\,\frac{\omega(\omega-1)\cdots(\omega-k+1)}{k!}\left[\frac{G^{(k+1-\omega)}-1}{(k+1-\omega)^2} - \frac{G^{(k+1-\omega)}\ell nG}{k+1-\omega}\right] \tag{A.11}$$

These sums of the first $k+1$ terms can be written in terms of the first k terms or

$$J_1(k+1) = J_1(k) + C(k)\,B_1(k) \tag{A.12}$$

and

$$J_2(k+1) = J_2(k) + C(k)\,B_2(k) \tag{A.13}$$

Here

$$C(k) = \frac{(-1)^k\omega(\omega-1)(\omega-2)\cdots(\omega-k+1)}{k!} = \frac{-\omega(1-\omega)(2-\omega)\cdots(k-1-\omega)}{k!} \tag{A.14}$$

$$B_1(k) = \frac{1-G^{(k+1-\omega)}}{k+1-\omega} \tag{A.15}$$

and

$$B_2(k) = \frac{G^{(k+1-\omega)}-1}{(k+1-\omega)^2} - \frac{G^{(k+1-\omega)}\ell nG}{k+1-\omega} \tag{A.16}$$

Let $$D(k) = k-\omega \tag{A.17}$$

and

$$E(k) = D(k) + 1 \tag{A.18}$$

Then Eq. A.14 becomes

$$C(k) = \frac{C(k-1)\ D(k-1)}{k} \text{ for } k \geq 1 \tag{A.19}$$

Also for $E(k) \neq 0$

$$B_1(k) = \frac{1-G^{E(k)}}{E(k)} \tag{A.20}$$

$$B_2(k) = -\frac{B_1(k)}{E(k)} - \frac{G^{E(k)}\ell nG}{E(k)} \tag{A.21}$$

and for $E(k) = 0$

$$B_1(k) = -\ell nG \tag{A.22}$$

$$B_2(k) = -\frac{1}{2}(\ell nG)^2 \tag{A.23}$$

The initial conditions are

$$J_1(0) = 0 \tag{A.24}$$

$$J_2(0) = 0 \tag{A.25}$$

$$C(0) = 1 \tag{A.26}$$

$$D(0) = -\omega \tag{A.27}$$

and

$$E(0) = 1 - \omega \tag{A.28}$$

From the above recursive relations, any order of approximation for J_1 and J_2 integrals can be obtained. A computer subroutine to carry out the above iteration procedure is given in Appendix C. (SUBROUTINE POWER). The efficiency of this new method and the criterion for convergence are presented below.

A.2.2. Comparison between power series expansion and Simpson's formula

As Simpson's formula is widely used and its accuracy has been considered acceptable (see Einstein, 1950), this formula was chosen to compare the applicability and efficiency with the new method.

Due to a wide range of values of J_1 and J_2 the comparison criterion for accuracy was based on the percentage deviation defined as

$$P_d = 100\left(\frac{\overline{X}-\overline{Y}}{\overline{Y}}\right) \tag{A.29}$$

in which P_d is the percentage deviation of the result by the new method from that by Simpson's formula, $\overline{X}$ is the value of J_1 or J_2 computed by the new method, and $\overline{Y}$ is the value of J_1 or J_2 computed by Simpson's formula.

As mentioned earlier, from the recursive relation for partial sum of the series (see Eqs. A.12 and A.13), any order of approximation may be obtained by the new method. The speed of convergence (or order of approximation required to satisfy certain convergence criterion) depends on values of ω and G and the chosen criterion for convergence. For example, if ω is an integer, the exact solution for any

value of G will be guaranteed when the order of approximation k is greater or equal to $\omega+1$.

Before deciding on the suitable criterion for convergence, it is useful to demonstrate some properties of a given order of approximation. The termination of computer subroutine is based on the chosen order of approximation.

(1) Variation of percentage deviation with changing ω

For a depth ratio, G = 0.5 and an order of approximation, k = 5, the variation of percentage deviation with changing ω from 0 to 5 is given in Fig. A.1. The maximum percentage deviation occurs around the middle of two consecutive integer values of ω. Therefore it is practical to determine the convergence criterion based on controlling the deviation for ω being the middle value of two consecutive integers.

(2) Relation between percentage deviation and order of approximation

From Eq. A.6 and Eq. A.8, one may imagine that for constant value of ω, the higher order terms are more likely to be negligible for smaller values of G. The accuracy of approximation is more dependent on the order of approximation for larger values of G than for smaller values of G.

The variation of percentage deviation for 1st and 10th order of approximation is given in Fig. A.2. The curves show that a negligible deviation is obtained by the 1st order approximation for $\omega \geq 1$ and $G \leq 10^{-2}$. Also the curves demonstrate that the 10th order approximation has nearly the equivalent accuracy as Simpson's formula for most values of ω and G. In Fig. A.3 the relation between percentage deviation and order of approximation for a depth ratio G = 0.9

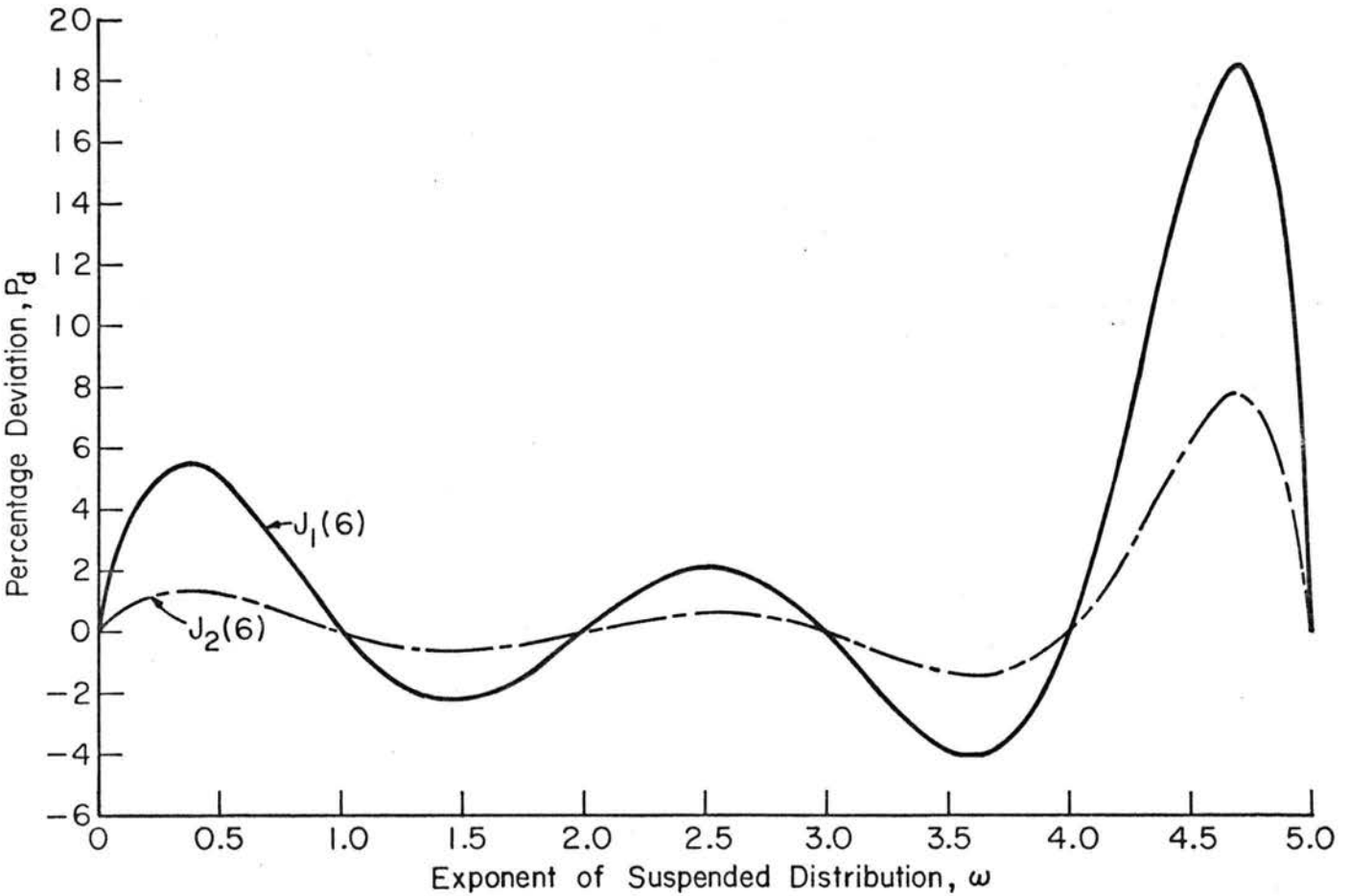

Fig. A.1 Variation of percentage deviation with exponent ω (G = 0.5)

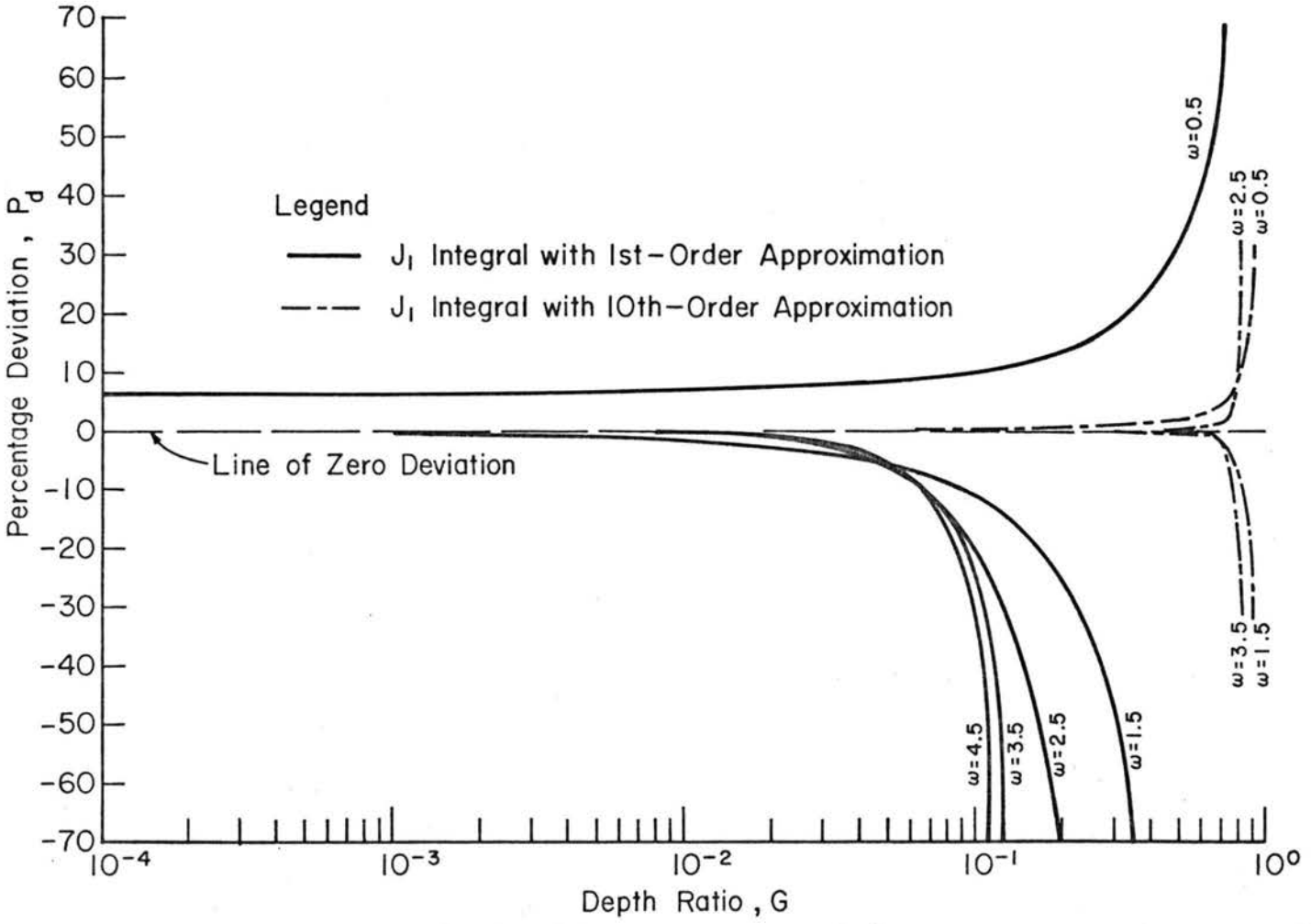

Fig. A.2 Variation of percentage deviation for 1st and 10th order approximation

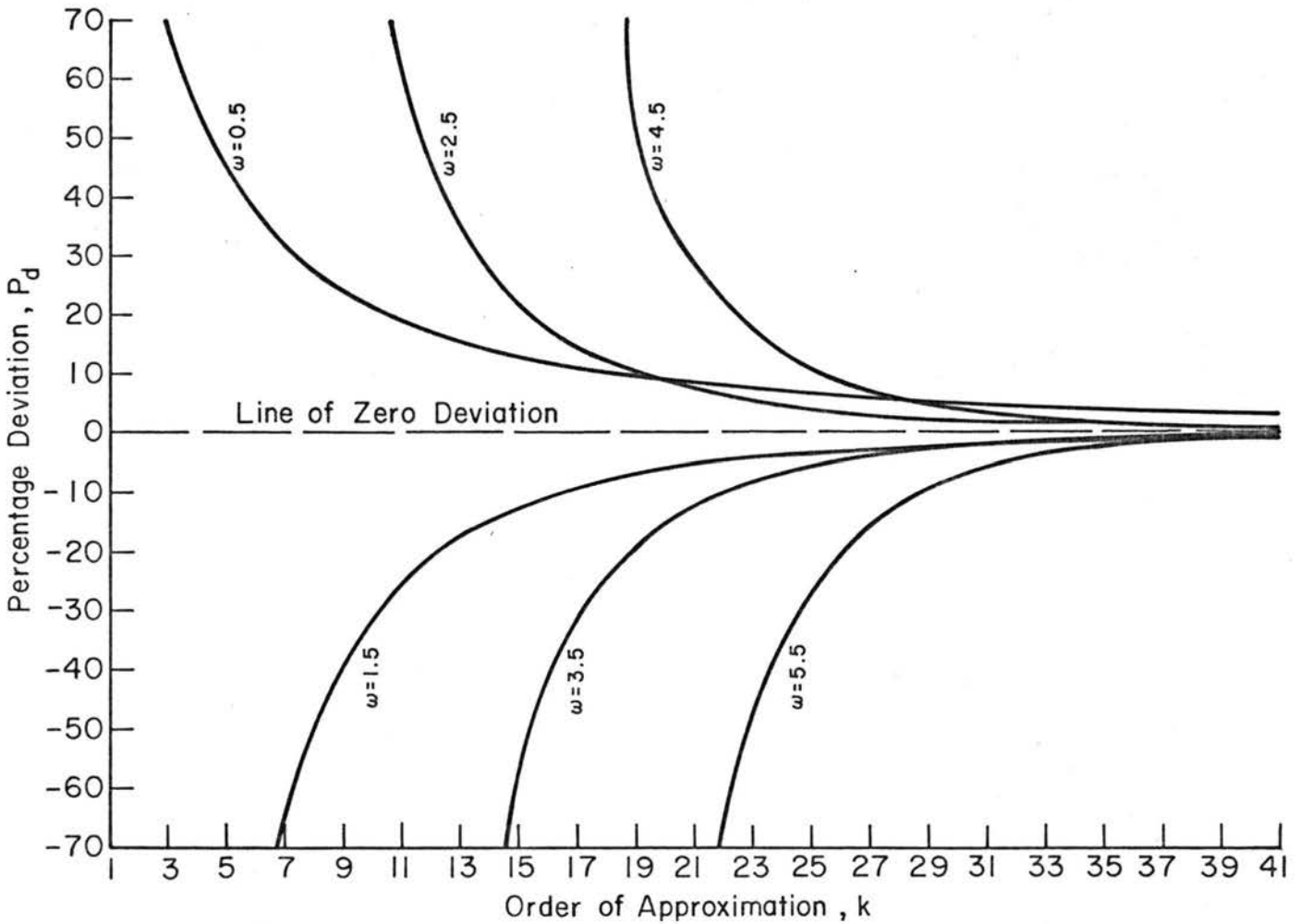

Fig. A.3 Relation between percentage deviation for J_1 and order of approximation (G = 0.9)

is given. This value of G is the largest value that would be encountered in most sediment transport problems. The curves in Fig. A.3 are the numerical proof of the convergence of the series solution.

(3) Comparison of computer time

The computer code for Simpson's formula developed by Rana (1971) was used to compare the efficiency with the new method. From 720 sample computations on a digital computer of CDC 6400 at Colorado State University, the average computer time (execution time only) for a sample computation (include J_1 and J_2) is given in Fig. A.4. This shows that 1st order approximation is nearly 14 times faster than the Simpson formula and 4 times faster is gained for 50th order approximation. These results indicate the potential of the new method.

A.2.3. Criterion for convergence of new method

As mentioned earlier, the k-order approximation necessary to yield a certain accuracy is dependent on the values of ω and G. A general and practical criterion for convergence to this accuracy is necessary. After a survey of possible criteria, the following convergence criterion was adopted.

The criterion is that the iteration procedure will be terminated if

$$\left.\begin{aligned} &\frac{J_1(k+1) - J_1(k)}{J_1(k+1)} \leq \varepsilon \\ &\text{and} \\ &\frac{J_2(k+1) - J_2(k)}{J_2(k+1)} \leq \varepsilon \end{aligned}\right\} \qquad (A.30)$$

in which ε is the limit of convergence.

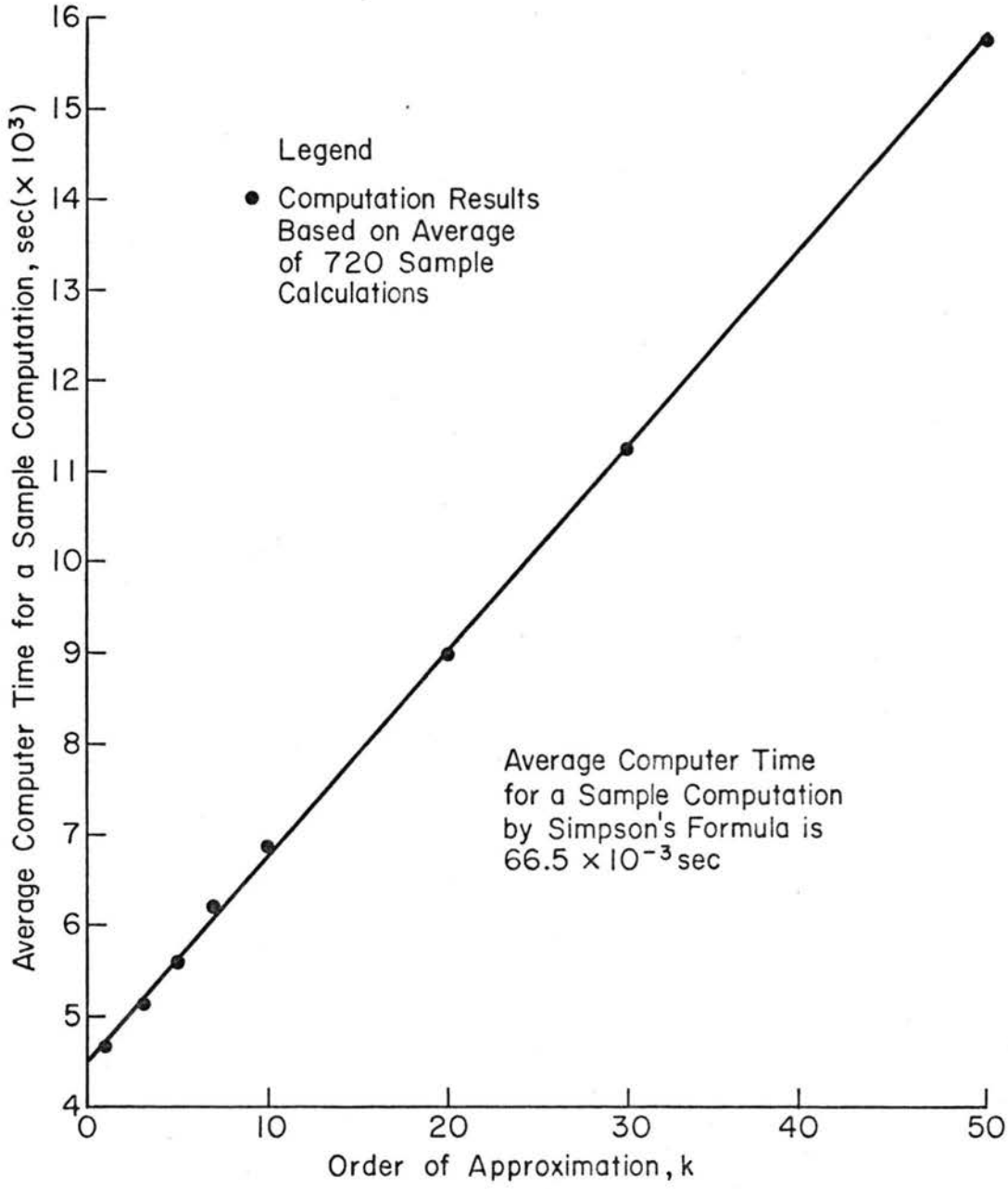

Fig. A.4 Relation between computer time and order of approximation

From tests for various values of ω and G (ω = 0.5, 1.5, 2.5, 3.5, 4.5 and 5.5 and $0.0001 \leq G \leq 0.9$), it was found that the equivalent accuracy as Simpson's formula could be obtained if the convergence limit ε was set to be 10^{-3}. The average order of approximation was about 7th order and the computer time required was only one-tenth of that for Simpson's formula. The examples of variation of order of approximation and percentage deviation with $\varepsilon = 10^{-3}$ and for ω = 2.5 and 3.5 are given in Fig. A.5. These testing results show the efficiency of the new method.

A.3. Summary

A new method based on power series expansion is developed to approximate J_1 and J_2 integrals for integration of suspended sediment load. This new method has advantages over other existing methods. (Einstein, 1950, Rana, 1971 and Chen, 1973). With nearly the same degree of accuracy, the new method requires only one-tenth of the computer time needed for the evaluation of the integrals by Simpson's formula. Different accuracies of approximation can be made in the new method. For obtaining the equivalent accuracy as Simpson's formula, it is recommended that the convergence limit be set at 10^{-3}.

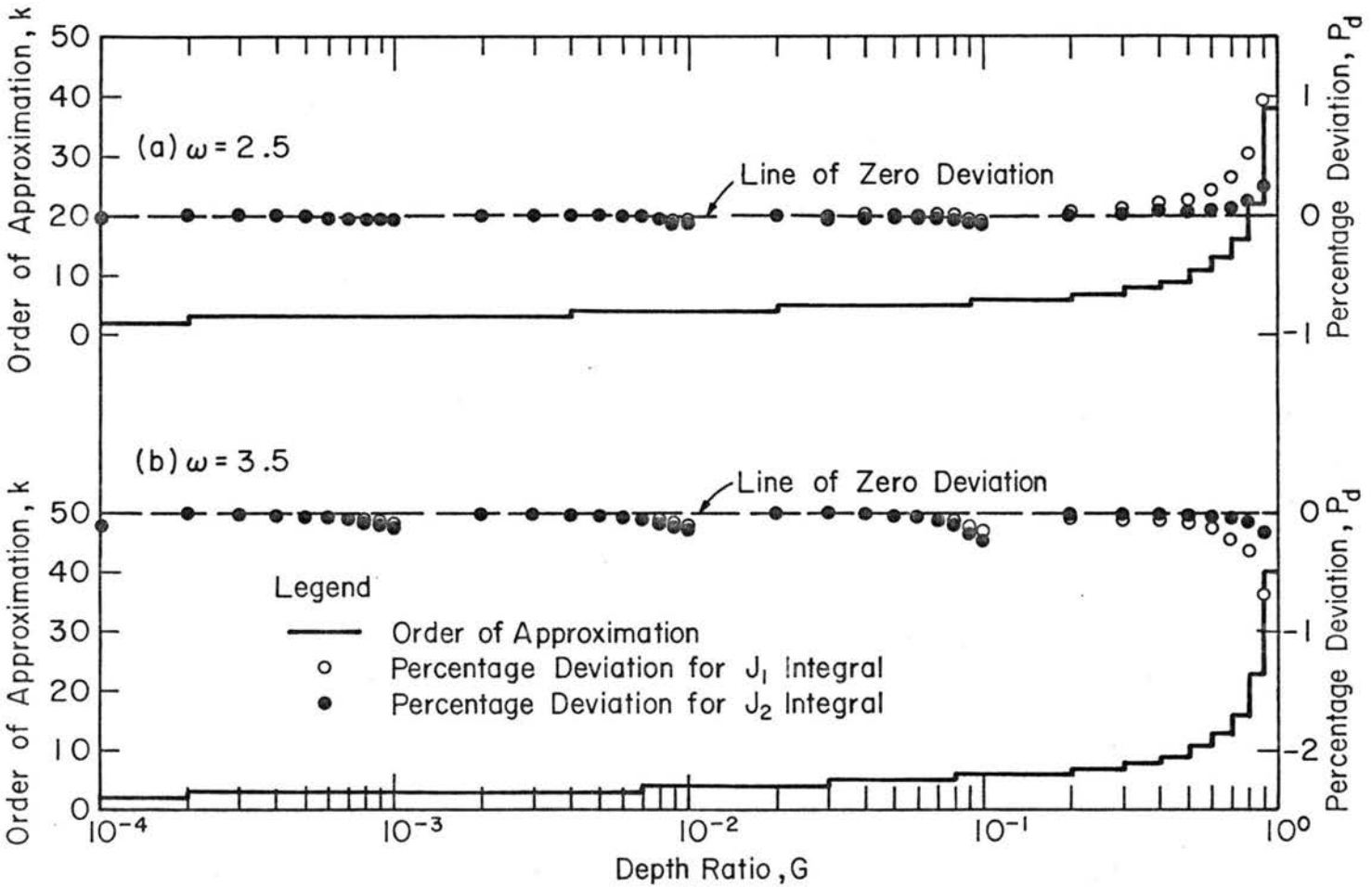

Fig. A.5 Variation of order of approximation and percentage deviation for convergence limit 10^{-3}

Appendix B

CALIBRATION TECHNIQUE FOR SYSTEM MODELING

B.1. Need for the Technique

In the mathematical modeling of system response, the identification of model parameters is often relied on an optimization scheme. The dependency on the optimization scheme may be reduced if the model is formulated according to the physical significance. For either a "black box" model or a physical simulation model, the calibration of a model is necessary when the model contains unknown parameters. The parameters of a "black box" model are not physically significant and hence, they are usually not predictable. While the ranges of parameters of a physical simulation model are well imposed by physical conditions or measured data, the exact values of the parameters which produce correct model response are usually not available. Hence, the model calibration is generally inevitable for most of the modeling problems.

The simplest calibration technique is the trial and error method. Except for some models which contain parameters with very narrow searching ranges, the trial and error procedure is inefficient for most of the problems. An efficient procedure is apparently needed for the model calibration.

In this study the Powell's unidimensional minimization technique (Powell, 1964) was used to calibrate the model with only one unknown parameter. However, certain modifications on this technique have been made to improve its efficiency. In addition, the Rosenbrock's (1960) optimization scheme was modified by coupling this modified Powell's

unidimensional search technique to calibrate the model having multiple unknown parameters. This modification shortened the computation time appreciably for the "Rosenbrock Function" (1960).

B.2. Minimization Problem

The identification of model parameters is a minimization problem. The problem is to find a set of parameters which produce the model response as close to the measured response as possible. In other words, this minimization problem is to select a set of parameters which minimize an objective function based on the desired error criterion within the constraints imposed by the physics of flow. The constraints in the parameter identification problem are usually the upper and the lower bounds of parameters. For example, the initial interception content must be between 0.0 and 1.0. In this study, the error criterion is based on either the sum of absolute deviations or the sum of squares of deviations between the simulated and the measured response. Consider the functional representation; the problem is

$$\underset{X_1,X_2,\ldots X_{N_p}}{\text{Minimize}} \quad F(X_1,X_2,\ldots X_{N_p}) \tag{B.1}$$

Subject to

$$X_i^{\ell} \leq X_i \leq X_i^{u} \quad \text{for } i = 1,2,\ldots N_p \tag{B.2}$$

in which N_p is the number of unknown parameters in a model, X_i's $(i = 1,2,\ldots N_p)$ are the unknown parameters, $F(X_1,X_2,\ldots X_{N_p})$ is the objective function which is a function of $X_1,X_2,\ldots X_{N_p}$ parameters, and X_i^{ℓ} and X_i^{u} are respectively the lower and the upper limits of the ith parameter.

The objective function in the parameter identification problem is generally not differentiable with respect to the parameters. This is due to the reason that the function is complicated in mathematical expressions and usually cannot be represented by a single equation. As the function is not differentiable, the optimization schemes using derivatives cannot be applied. An algorithm without using analytical derivatives is necessary for the calibration of a mathematical model.

B.3. One-Dimensional Calibration Technique

The one-dimensional search technique is a fundamental component of any multi-dimensional search technique. A good unidimensional search technique is necessary not only for solving one-dimensional problems but also for improving multi-dimensional search techniques.

There are various methods for unidimensional searches. For example, uniform search, dichotomous search, Fibonacci search, Golden Section search, DSC unidimensional search and Powell's unidimensional minimization (Himmelblau, 1972). After a survey of these available methods, the Powell's unidimensional minimization method was selected in this study.

For the one-dimensional problem, the functional representation is

$$\underset{X}{\text{Minimize}} \quad F(X) \tag{B.3}$$

Subject to

$$X_\ell \leq X \leq X_u \tag{B.4}$$

in which X is the unknown parameter, and X_ℓ and X_u are respectively the lower and the upper limits of this parameter.

The proposed method is carried out using the first three points obtained in the direction of search. The X corresponding to the minimum of the quadratic function is determined, and these quadratic approximations are continued until the minimum of F (X) is located to the required precision. The steps of search are as follows; examine Fig. B.1.

Step 1. From the base vector $X^{(1)}$ compute

$$X^{(2)} = X^{(1)} + \Delta X \tag{B.5}$$

Step 2. Compute F $(X^{(1)})$ and F $(X^{(2)})$

Step 3. Determine the third point required for quadratic approximation.

When F $(X^{(1)})$ is greater than F $(X^{(2)})$, let

$$X^{(3)} = X^{(1)} + 2\Delta X \quad \text{if } X^{(1)} + 2\Delta X \leq X_u \tag{B.6}$$

and

$$X^{(3)} = X_u \quad \text{if } X^{(1)} + 2\Delta X > X_u \tag{B.7}$$

When F $(X^{(1)})$ is less than or equal to F $(X^{(2)})$, let

$$X^{(3)} = X^{(1)} - \Delta X \quad \text{if } X^{(1)} - \Delta X \geq X_\ell \tag{B.8}$$

and

$$X^{(3)} = X_\ell \quad \text{if } X^{(1)} - \Delta X < X_\ell \tag{B.9}$$

Step 4. Compute F $(X^{(3)})$.

Step 5. Check the convexity of the quadratic equation, the optimal coefficient a* can be determined by

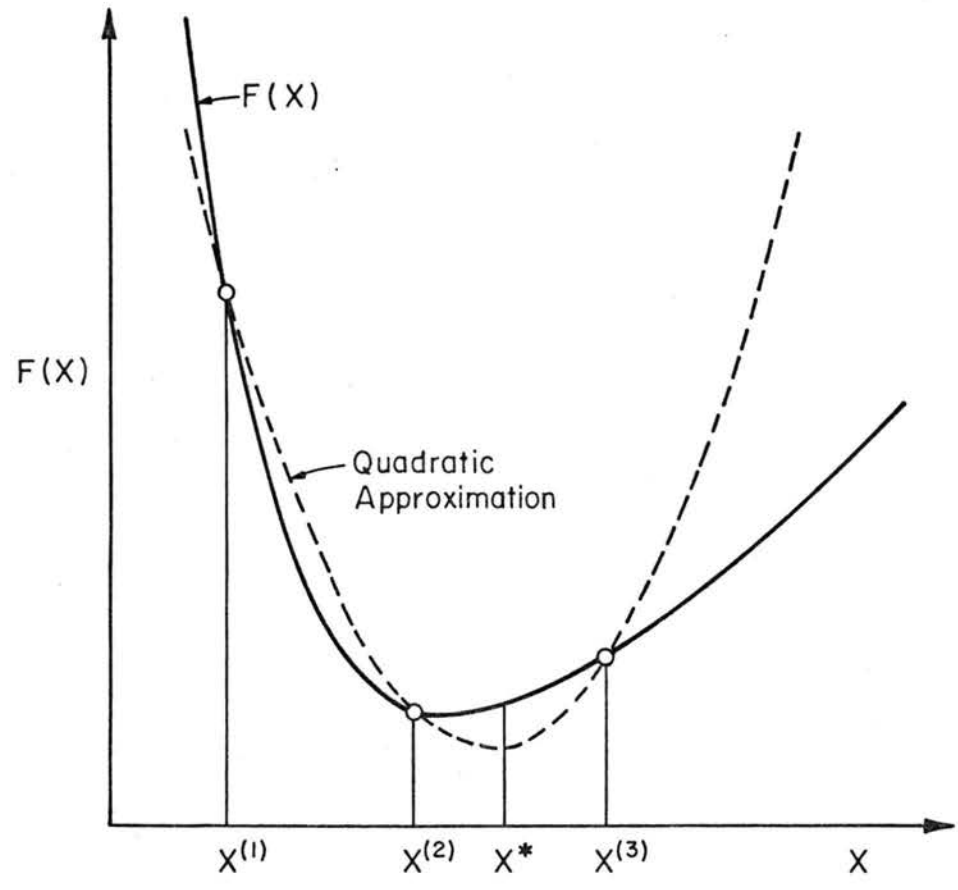

Fig. B.1 Quadratic approximation for unidimensional search

$$a^* = \frac{(X^{(2)}-X^{(3)})\ F\ (X^{(1)}) + (X^{(3)}-X^{(1)})\ F\ (X^{(2)}) + (X^{(1)}-X^{(2)})\ F\ (X^{(3)})}{(X^{(1)}-X^{(2)})\ (X^{(2)}-X^{(3)})\ (X^{(1)}-X^{(3)})} \tag{B.10}$$

If $a^* \geq 0$ the function is convex and the search is continued at step 6.

If $a^* < 0$ the function is concave, let

$$X_a = \text{Min. } \{X^{(1)}, X^{(2)}, X^{(3)}\} \tag{B.11}$$

$$X_b = \text{Max } \{X^{(1)}, X^{(2)}, X^{(3)}\} \tag{B.12}$$

then the search is returned to step 3 with the following information

$$\Delta X = X_b - X_a \tag{B.13}$$

$$X^{(1)} = X_a \tag{B.14}$$

$$F\ (X^{(1)}) = F\ (X_a) \tag{B.15}$$

$$X^{(2)} = X_b \tag{B.16}$$

$$F\ (X^{(2)}) = F\ (X_b) \tag{B.17}$$

Step 6. Estimate the value of X at the minimum of F (X). X*.

Compute the other optimal coefficient by

$$b^* = \frac{F\ (X^{(1)}) - F\ (X^{(2)})}{X^{(1)} - X^{(2)}} - a^*\ (X^{(1)} + X^{(2)}) \tag{B.18}$$

Then, estimate X* by

$$X^* = -\frac{b^*}{2a^*} \tag{B.19}$$

If $X_\ell \leq X^* \leq X_u$, the constraints are satisfied and then the search is continued at step 7.

If $X^* > X_u$ or $X^* < X_\ell$, the constraint is violated, boundary point is used as optimum value of X, i.e.,

$$X^* = X_u \quad \text{if} \quad F(X_a) > F(X_b) \tag{B.20}$$

and

$$X^* = X_\ell \quad \text{if} \quad F(X_a) \leq F(X_b) \tag{B.21}$$

Step 7. Compute $F(X^*)$.

Step 8. Termination of search

Let X° = whichever of $\{X^{(1)}, X^{(2)}, X^{(3)}\}$ corresponding to the smallest $F(X)$. The termination of search is made if

$$|F(X^*) - F(X^o)| \leq \varepsilon \tag{B.22}$$

in which ε is the convergence limit. If the convergence criterion is not satisfied, the search is repeated at step 3 with the following information.

Let

$$X_a = \text{Min. } \{X^o, X^*\} \tag{B.23}$$

$$X_b = \text{Max } \{X^o, X^*\} \tag{B.24}$$

Then, according to Eqs. B.13, B.14, B.15, B.16, and B.17

$$\Delta X = X_b - X_a$$

$$X^{(1)} = X_a$$

$$F\ (X^{(1)}) = F\ (X_a)$$

$$X^{(2)} = X_b$$

$$F\ (X^{(2)}) = F\ (X_b)$$

A computer program was developed to perform the above procedures. The listing of the computer program is given in Appendix C. (PROGRAM UNIMO).

In Fig. B.2, the path of the search for the minimization of a sample function by PROGRAM UNIMO is given. The function and the results are given below.

$$F\ (X) = (1 - X^2)^2 + (1 - X)^2 \qquad (B.25)$$

starting point: $X^{(1)} = 2.0$, convergence limit: $\varepsilon = 10^{-5}$ and initial step size: $\Delta X = 0.5$. The results are: $X^* = 1.0$, $F\ (X^*) = 1.71 \times 10^{-10}$ and the number of function evaluations, $N_F = 20$.

B.4. Multi-Dimensional Calibration Technique

In this study, Rosenbrock's optimization scheme (Rosenbrock, 1960) was modified by coupling the unidimensional search technique presented in the previous section.

Rosenbrock's method is an iterative procedure that small steps are taken during the search in orthogonal coordinates. Instead of continually searching the coordinates corresponding to the directions of the independent variables, an improvement is made after one cycle of coordinate search by lining the search directions up into an orthogonal system, with the overall step on the previous stage as the first building block for the new search coordinates. This method locates

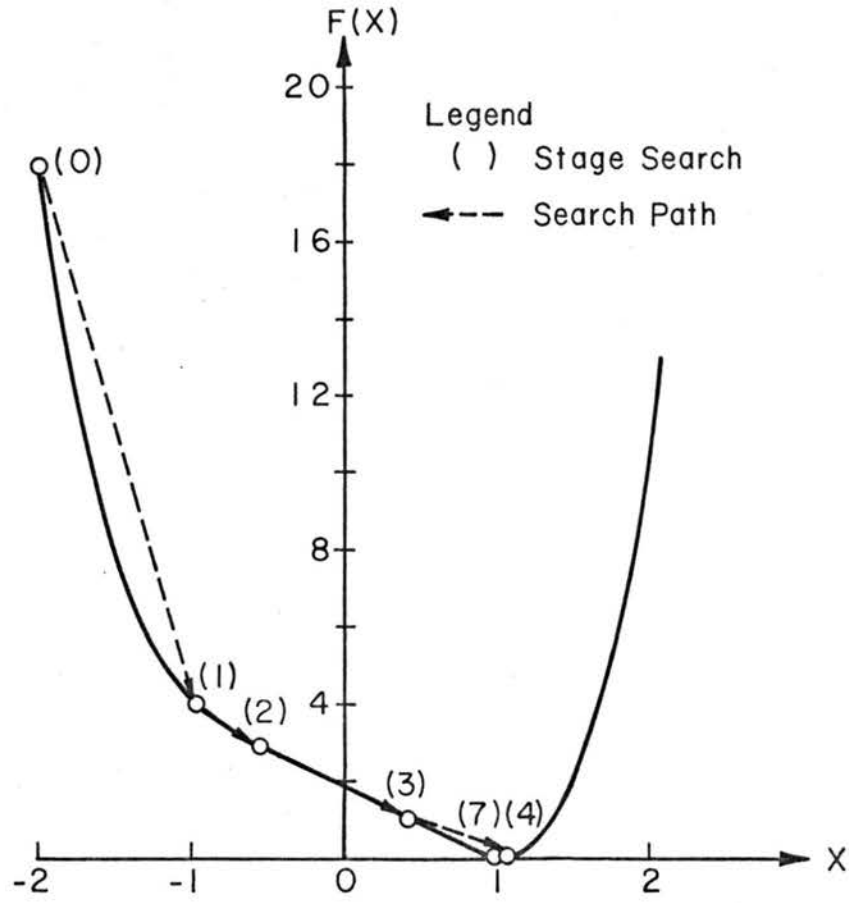

Fig. B.2 Search path for the sample problem

$X^{(k+1)}$ by successive unidimensional searches from an initial point $X^{(k)}$ along a set of othonormal directions $\hat{S}_1^{(k)}, \hat{S}_2^{(k)}, \ldots \hat{S}_{N_p}^{(k)}$. For the initial stage, k = 0, the directions $\hat{S}_1^{(0)}, \hat{S}_2^{(0)}, \ldots \hat{S}_{N_p}^{(0)}$ are usually taken to be parallel to the axes of $X_1, X_2, \ldots X_{N_p}$.

Let $X_i^{(k)}$ indicate the point at which $F(X_i^{(k)})$ is a minimum in the direction of $\hat{S}_i^{(k)}$, for each stage (k) there are N_p vectors $X_i^{(k)}$ and N_p optimal values of the objective function $F(X_i^{(k)})$; from $X_0^{(k)}$, determine optimal step length $\lambda_1^{*(k)}$ in the direction of $\hat{S}_1^{(k)}$ so that $F(X_0^{(k)} + \lambda_1^{*(k)} \hat{S}_1^{(k)})$ is a minimum and let $X_1^{(k)} = X_0^{(k)} + \lambda_1^{*(k)} \hat{S}_1^{(k)}$. Then from $X_1^{(k)}$, determine $\lambda_2^{*(k)}$ so that $F(X_1^{(k)} + \lambda_2^{*(k)} \hat{S}_2^{(k)})$ is a minimum and let $X_2^{(k)} = X_1^{(k)} + \lambda_2^{*(k)} \hat{S}_2^{(k)}$. The search pattern is generalized as follows; from $X_{i-1}^{(k)}$, determine $\lambda_i^{*(k)}$ in the direction of $\hat{S}_i^{(k)}$ so that $F(X_{i-1}^{(k)} + \lambda_1^{*(k)} \hat{S}_i^{(k)})$ is a minimum and let $X_i^{(k)} = X_{i-1}^{(k)} + \lambda_i^{*(k)} \hat{S}_i^{(k)}$. The search is repeated sequentially, always starting from the last immediate point in the sequence until all X_i, i=1, $\ldots N_p$ are determined. The unidimensional search technique described in the previous section (Section B.3.) was used to determine optimal step length $\lambda_i^{*(k)}$.

After the kth stage has been completed, the vectors for the new search directions are computed at the point $X_0^{(k+1)} = X_{N_p}^{(k)}$. Palmer's method (Palmer, 1969) for generating new set of direction is used in this study. His method is as follows.

$$A_i^{(k)} = \sum_{j=1}^{N_p} \lambda_j^{*(k)} \hat{S}_j^{(k)} \quad \text{for } 1 \leq i \leq N_p \tag{B.26}$$

$$\hat{S}_i^{(k+1)} = \frac{A_i^{(k)} \; || \, A_{i-1}^{(k)} \, ||^2 - A_{i-1}^{(k)} \; || \, A_i^{(k)} \, ||^2}{|| \, A_{i-1}^{(k)} \, || \; || \, A_i^{(k)} \, || \sqrt{|| \, A_{i-1}^{(k)} \, ||^2 - || \, A_i^{(k)} \, ||^2}} \tag{B.27}$$

for $2 \leq i \leq N_p$

in which $|| \; ||$ is the norm of the vector

and

$$S_1^{(k+1)} = \frac{A_1^{(k)}}{|| \, A_1^{(k)} \, ||} \tag{B.28}$$

If $\lambda_{i-1}^{*(k)} = 0$, $\hat{S}_i^{(k+1)} = \hat{S}_{i-1}^{(k)}$ unless $\Sigma \, \lambda_i^{*(k)} = 0$. The search is terminated when

$$F \, (X_{N_p}^{(k)}) - F \, (X_{N_p}^{(k+1)}) \leq \varepsilon \tag{B.29}$$

A computer program was developed to carry out the above procedure. In this program, the vector is normalized so that the ranges of the vector are within 0.0 and 1.0. The listing of the computer program is given in Appendix C. (PROGRAM BROSEN).

The number of function evaluations for the Rosenbrock's function (Rosenbrock, 1960) by the proposed algorithm is 30, which is much less than 206 function evaluations by the original Rosenbrock's method (Himmelblau, 1972). A sample problem with three variables is given herein for illustration.

The function is defined as

$$F \, (X) = (X_1 - X_2)^2 + (X_2 - 2X_3)^2 + (X_3 - 2)^2 \tag{B.30}$$

This problem is unconstrained and is highly interactive among variables. The initial vector is

$$X_0^{(0)} = [5.0,\ 2.0,\ 7.0]$$

The convergence limit, $\varepsilon = 10^{-5}$.

The search paths for each stage are given in Table B.1. This table shows the applicability of the proposed algorithm for the problem with highly interactive parameters.

Table B.1 Summary of Search Path for Each Stage

Stage	Current Vector			Current Objective Function	Cumulative No. Function Evaluation
	X_1	X_2	X_3		
0	5.000	2.000	7.000	0.178×10^{3}	0
1	2.000	8.000	3.600	0.392×10^{2}	16
2	7.005	8.220	3.386	0.549×10^{1}	31
3	8.142	7.709	3.435	0.295×10^{1}	46
4	7.871	7.366	3.336	0.252×10^{1}	61
5	5.950	5.847	2.751	0.694×10^{0}	76
6	4.213	4.278	2.112	0.198×10^{-1}	91
7	4.004	4.005	2.002	0.628×10^{-5}	106
8	4.000	4.000	2.000	0.101×10^{-7}	117

B.5. Summary

A one-dimensional calibration technique based on Powell's (1964) unidimensional minimization method is proposed to calibrate one-dimensional models. This unidimensional method is further applied to modify the Rosenbrock's (1960) method for the calibration of models

with multiple parameters. This modification shortened computer time appreciably for the "Rosenbrock Function".

Both one-dimensional and multi-dimensional calibration techniques are formulated to deal with bound constraints (i.e., the upper and lower bounds). These bound constraints are usually imposed in the mathematical models by physical conditions or measured data.

Appendix C

LISTINGS OF COMPUTER PROGRAMS

C.1. PROGRAM WATER: Rainfall-Runoff Model

```
                    PROGRAM WATER (INPUT,OUTPUT)

      PROGRAM WATER (INPUT,OUTPUT)                                          WAT   10
C                                                                           WAT   20
C     THIS IS A RAINFALL-RUNOFF MODEL                                       WAT   30
C     THIS PROGRAM IS DESIGNED TO SIMULATE WATER HYDROGRAPH FROM SMALL      WAT   40
C     WATERSHEDS                                                            WAT   50
C     NOTATIONS FOR THE MODEL INPUT AND OUTPUT                              WAT   60
C     TITLE = ALPHABETICAL OR NUMERICAL IDENTIFICATION OF THE PROBLEM       WAT   70
C     NOV = NUMBER OF OVERLAND FLOW SEGMENTS                                WAT   80
C     NCH = NUMBER OF CHANNEL FLOW SEGMENTS                                 WAT   90
C     NSEG = TOTAL NUMBER OF SEGMENTS                                       WAT  100
C     NDX = NUMBER OF SPACE INCREMENTS                                      WAT  110
C     NSTOM = NUMBER OF STORM FOR COMPUTATION                               WAT  120
C     NTO = OUTPUT INTERVALS                                                WAT  130
C     DT = TIME INCREMENT FOR NUMERICAL COMPUTATION                         WAT  140
C     SNU = KINEMATIC VISCOSITY OF WATER                                    WAT  150
C     AREA = TOTAL AREA OF THE WATERSHED                                    WAT  160
C     SEG = ALPHABETICAL OR NUMERICAL IDENTIFICATION OF SEGMENTS            WAT  170
C     SLEN = LENGTH OF AN OVERLAND FLOW PLOT OR A CHANNEL REACH             WAT  180
C     SLOPE = BED SLOPE                                                     WAT  190
C     AC,BC,A0,B0,AL = PARAMETERS DESCRIBING P-A RELATIONS                  WAT  200
C     ISEG = COMPUTATIONAL SEQUENCE                                         WAT  210
C     IUP = UPSTREAM INFLOW SEGMENT                                         WAT  220
C     ILAT = LATERAL INFLOW SEGMENT                                         WAT  230
C     PERM = COEFFICIENT OF PERMEABILITY OR HYDRAULIC CONDUCTIVITY          WAT  240
C     SM = MOISTURE CONTENT AT SATUATION                                    WAT  250
C     WP = MOISTURE CONTENT AT WILTING POINT                                WAT  260
C     CPW = CAPILLARY POTENTIAL HEAD AT WILTING POINT                       WAT  270
C     ETA = DEPTH OF THE ZONE OF AERATION                                   WAT  280
C     FK1,FK2,FK3 = CONSTANTS DESCRIBING DARCY-WEISBACH FRICTION FACTOR     WAT  290
C                   DUE TO GRAIN RESISTANCE ONLY                            WAT  300
C     XIC = BED FORM RESISTANCE DESCRIPTOR                                  WAT  310
C     XIO = GROUND COVER RESISTANCE DESCRIPTOR                              WAT  320
C     STORM = ALPHABETICAL OR NUMERICAL IDENTIFICATION OF STORMS            WAT  330
C     ITMAX = TOTAL NUMBER OF TIME INCREMENT AT THE END OF A STORM          WAT  340
C     ITCOM = TOTAL NUMBER OF TIME INCREMENT FOR COMPUTATION                WAT  350
C     EVP = MEAN EVAPORATION RATE                                           WAT  360
C     GRD = GROUND COVER RESISTANCE DESCRIPTOR, XIO                         WAT  370
C     VIN = INITIAL INTERCEPTION STORAGE CONTENT                            WAT  380
C     AMC = ANTECEDENT MOISTURE CONTENT                                     WAT  390
C     DR = RAINFALL INPUT                                                   WAT  400
C     SUMRF = AMOUNT OF DIRECT RUNOFF                                       WAT  410
C     QOUT = OUTFLOW HYDROGRAPH OF WATER                                    WAT  420
C                                                                           WAT  430
      DIMENSION ITCOM(10), QOUT(10,200), SEG(50), STORM(10), TITLE(10),     WAT  440
     1GRD(10)                                                               WAT  450
      COMMON /INO/ NSEG,NOV,NTO,NDX,DT,DTS,DTN,IT,EPS,IMAX,ITMAX(10)        WAT  460
      COMMON /FLO/ Q(50),A(50,10),DR(10,200),ER(200),EVP(10),VIN(10),AMCWAT  470
     1(10)                                                                  WAT  480
      COMMON /SEQ/ ISEG(50),IUP(50,3),ILAT(50,2)                            WAT  490
      COMMON /GEO/ SLEN(50),SLOPE(50),AC(50),BC(50),A0(50),B0(50),AL(50)WAT  500
      COMMON /REF/ PERM,SM,WP,CPW,ETA,CND,GCD,VOG,SRG,VOR,XIC,XIO           WAT  510
      COMMON /FRC/ QN,AN,SNU,SLP,FK1,FK2,FK3,XIR,ALP,BET,CPR,EPR,ARF        WAT  520
      IMAX=20                                                               WAT  530
      EPS=0.1                                                               WAT  540
C                                                                           WAT  550
```

```
      PROGRAM WATER (INPUT,OUTPUT)
C     INPUT AND OUTPUT TITLE                                                WAT  560
C                                                                           WAT  570
      READ 170, TITLE                                                       WAT  580
      PRINT 180, TITLE                                                      WAT  590
C                                                                           WAT  600
C     INPUT AND OUTPUT GENERAL INFORMATION                                  WAT  610
C                                                                           WAT  620
      READ 190, NOV,NCH,NDX,NSTOM,NTO,DT,SNU,AREA                           WAT  630
      NSEG=NOV+NCH                                                          WAT  640
      PRINT 200, NSEG,NDX,NSTOM,DT,SNU,AREA                                 WAT  650
C                                                                           WAT  660
C     INPUT AND OUTPUT BASIN CHARACTERISTICS DATA                           WAT  670
C     INPUT AND OUTPUT GEOMETRY DATA                                        WAT  680
C                                                                           WAT  690
      READ 210, (SEG(I),SLEN(I),SLOPE(I),AC(I),BC(I),AO(I),BO(I),AL(I),I   WAT  700
     1=1,NSEG)                                                              WAT  710
      PRINT 220, (SEG(I),SLEN(I),SLOPE(I),AC(I),BC(I),AO(I),BO(I),AL(I),   WAT  720
     1I=1,NSEG)                                                             WAT  730
C                                                                           WAT  740
C     INPUT AND OUTPUT COMPUTATION SEQUENCE                                 WAT  750
C                                                                           WAT  760
      READ 230, (ISEG(I),(IUP(I,J),J=1,3),(ILAT(I,J),J=1,2),I=1,NSEG)       WAT  770
      PRINT 240, (ISEG(I),(IUP(I,J),J=1,3),(ILAT(I,J),J=1,2),I=1,NSEG)      WAT  780
C                                                                           WAT  790
C     INPUT AND OUTPUT SOIL DATA                                            WAT  800
C                                                                           WAT  810
      READ 250, PERM,SM,WP,CPW,ETA                                          WAT  820
      PRINT 260, PERM,SM,WP,CPW,ETA                                         WAT  830
C                                                                           WAT  840
C     INPUT AND OUTPUT VEGETATION DATA                                      WAT  850
C                                                                           WAT  860
      READ 250, CND,GCD,VOG,SRG,VOR                                         WAT  870
      PRINT 270, CND,GCD,VOG,SRG,VOR                                        WAT  880
C                                                                           WAT  890
C     INPUT AND OUTPUT FLOW RESISTANCE PARAMETERS                           WAT  900
C                                                                           WAT  910
      READ 280, FK1,FK2,FK3,XIC                                             WAT  920
      PRINT 290, FK1,FK2,FK3,XIC                                            WAT  930
C                                                                           WAT  940
C     ESTABLISH SOME INVARIANT INFORMATION                                  WAT  950
C                                                                           WAT  960
      IOUT=ISEG(NSEG)                                                       WAT  970
      SNU=SNU/100000.                                                       WAT  980
      DT=DT/60.                                                             WAT  990
      DTS=DT*3600.                                                          WAT 1000
      DTN=DTS*FLOAT(NDX)                                                    WAT 1010
      FACT=12.*3600./(43560.*AREA)                                          WAT 1020
C                                                                           WAT 1030
C     INPUT AND OUTPUT STORM CHARACTERISTICS DATA                           WAT 1040
C                                                                           WAT 1050
      DO 110 L=1,NSTOM                                                      WAT 1060
         READ 300, STORM(L),ITMAX(L),ITCOM(L),EVP(L),GRD(L),VIN(L),AMC(L    WAT 1070
     1   )                                                                  WAT 1080
         PRINT 310, STORM(L),ITMAX(L),ITCOM(L),EVP(L),GRD(L),VIN(L),AMC(    WAT 1090
     1   L)                                                                 WAT 1100
```

```
                              PROGRAM WATER (INPUT,OUTPUT)

      PRINT 320                                                          WAT 1110
      IRAIN=ITMAX(L)                                                     WAT 1120
      READ 330, (DR(L,I),I=1,IRAIN)                                      WAT 1130
      PRINT 340, (I,DR(L,I),I=1,IRAIN)                                   WAT 1140
  110 CONTINUE                                                           WAT 1150
      DO 150 L=1,NSTOM                                                   WAT 1160
      NCOM=ITCOM(L)                                                      WAT 1170
      XIO=GRD(L)                                                         WAT 1180
C                                                                        WAT 1190
C     RAINFALL EXCESS DETERMINATION                                      WAT 1200
C                                                                        WAT 1210
      CALL RAINEX (L,NCOM)                                               WAT 1220
C                                                                        WAT 1230
C     INITIALIZE ENTIRE WATERSHED                                        WAT 1240
C                                                                        WAT 1250
      DO 130 I=1,NSEG                                                    WAT 1260
      Q(I)=0.                                                            WAT 1270
      DO 120 J=1,NDX                                                     WAT 1280
      A(I,J)=0.                                                          WAT 1290
  120 CONTINUE                                                           WAT 1300
  130 CONTINUE                                                           WAT 1310
C                                                                        WAT 1320
C     ROUTING FOR EACH TIME INCREMENT                                    WAT 1330
C                                                                        WAT 1340
      SUMRF=0.                                                           WAT 1350
      DO 140 IT=1,NCOM                                                   WAT 1360
      CALL ROUT (L)                                                      WAT 1370
      QOUT(L,IT)=Q(IOUT)                                                 WAT 1380
      SUMRF=SUMRF+Q(IOUT)                                                WAT 1390
  140 CONTINUE                                                           WAT 1400
C                                                                        WAT 1410
C     DETERMINE AMOUNT OF DIRECT RUNOFF                                  WAT 1420
C                                                                        WAT 1430
      SUMRF=SUMRF*DT*FACT                                                WAT 1440
      PRINT 350, SUMRF                                                   WAT 1450
  150 CONTINUE                                                           WAT 1460
      PRINT 360                                                          WAT 1470
      DO 160 I=1,NSTOM                                                   WAT 1480
      PRINT 370, STORM(I)                                                WAT 1490
      NCOM=ITCOM(I)                                                      WAT 1500
      PRINT 340, (J,QOUT(I,J),J=1,NCOM)                                  WAT 1510
  160 CONTINUE                                                           WAT 1520
      STOP                                                               WAT 1530
C                                                                        WAT 1540
  170 FORMAT (10A8)                                                      WAT 1550
  180 FORMAT (1H1/////40X,10A8)                                          WAT 1560
  190 FORMAT (5I5,3F10.3)                                                WAT 1570
  200 FORMAT (//48X,20HNUMBER OF SEGMENTS =,I5/44X,28HNUMBER OF SPACE INWAT 1580
     1TERVALS =,I3,/41X,34HNUMBER OF STORMS FOR COMPUTATION =,I4/45X,16HWAT 1590
     2TIME INCREMENT =,F7.3,8H MINUTES/45X,21HKINEMATIC VISCOSITY =,F10.WAT 1600
     35/46X,12HTOTAL AREA =,F10.5,6H ACRES)                              WAT 1610
  210 FORMAT (2X,A8,7F10.5)                                              WAT 1620
  220 FORMAT (//45X,31HGEOMETRY DATA FOR EACH SEGMENTS//(14X,A8,7F12.5))WAT 1630
  230 FORMAT (6I10)                                                      WAT 1640
  240 FORMAT (//50X,20HCOMPUTATION SEQUENCE//(30X,6I10))                 WAT 1650
```

```
                    PROGRAM WATER (INPUT,OUTPUT)

  250 FORMAT (5F10.4)                                                    WAT 1660
  260 FORMAT (55X,9HSOIL DATA//22X,5F15.5)                               WAT 1670
  270 FORMAT (52X,15HVEGETATION DATA//22X,5F15.5)                        WAT 1680
  280 FORMAT (4F10.5)                                                    WAT 1690
  290 FORMAT (//47X,26HFLOW RESISTANCE PARAMETERS//30X,4F15.5)           WAT 1700
  300 FORMAT (2X,A8,2I10,4F10.5)                                         WAT 1710
  310 FORMAT (//56X,A8/48X,19HRAINFALL DURATION =,I4/48X,20HCOMPUTATION WAT 1720
     1PERIOD =,I4/44X,23HMEAN EVAPORATION RATE =,F10.3/37X,36HGROUND COVWAT 1730
     2ER RESISTANCE DESCRIPTOR =,F10.3/36X,38HINITIAL INTERCEPTION STORAWAT 1740
     3GE CONTENT =,F10.5/40X,29HANTECEDENT MOISTURE CONTENT =,F10.5)     WAT 1750
  320 FORMAT (//53X,13HRAINFALL DATA)                                    WAT 1760
  330 FORMAT (16F5.2)                                                    WAT 1770
  340 FORMAT (48X,I10.4X,F10.5)                                          WAT 1780
  350 FORMAT (//42X,25HAMOUNT OF DIRECT RUNOFF =,F10.5)                  WAT 1790
  360 FORMAT (//45X,31H HYDROGRAPH AT WATERSHED OUTLET)                  WAT 1800
  370 FORMAT (//56X,A8)                                                  WAT 1810
C                                                                        WAT 1820
      END                                                                WAT 1830
```

SUBROUTINE ROUT(L)

```
      SUBROUTINE ROUT (L)                                                    ROU   10
C                                                                            ROU   20
C     THIS SUBROUTINE ROUTES THE FLOW OCCURRED IN OVERLAND LOOP AND          ROU   30
C     THROUGH CHANNEL SYSTEM                                                 ROU   40
C                                                                            ROU   50
      COMMON /INO/ NSEG,NOV,NTO,NDX,DT,DTS,DTN,IT,EPS,IMAX,ITMAX(10)         ROU   60
      COMMON /FLO/ Q(50),A(50,10),DR(10,200),ER(200),EVP(10),VIN(10),AMCROU   70
     1(10)                                                                   ROU   80
      COMMON /SEQ/ ISEG(50),IUP(50,3),ILAT(50,2)                             ROU   90
      COMMON /GEO/ SLEN(50),SLOPE(50),AC(50),BC(50),AQ(50),BQ(50),AL(50)ROU  100
      COMMON /REF/ PERM,SM,WP,CPW,ETA,CND,GCD,VOG,SRG,VOR,XIC,XIO            ROU  110
      COMMON /FRC/ ON,AN,SNU,SLP,FK1,FK2,FK3,XIR,ALP,BET,CPR,EPR,ARF         ROU  120
C                                                                            ROU  130
C     COMPUTE AT TIME IT (T+DT)                                              ROU  140
C     DETERMINATION OF RAINFALL INPUT                                        ROU  150
C                                                                            ROU  160
      IF (IT.GT.ITMAX(L)) GO TO 110                                          ROU  170
      DRF=DR(L,IT)                                                           ROU  180
      GO TO 120                                                              ROU  190
  110 DRF=0.                                                                 ROU  200
C                                                                            ROU  210
C     DETERMINE RAINFALL EXCESS                                              ROU  220
C                                                                            ROU  230
  120 EFRM=ER(IT)                                                            ROU  240
C                                                                            ROU  250
C     DETERMINE EFFECTIVE RAINFALL FOR RAINDROP IMPACT EFFECTS               ROU  260
C                                                                            ROU  270
      ARF=DRF*(1.-CND)*(1.-GCD)                                              ROU  280
C                                                                            ROU  290
C     WATER ROUTING FROM THE UPPER MOST SEGMENT TO THE WATERSHED OUTLET      ROU  300
C                                                                            ROU  310
      DO 290 I=1,NSEG                                                        ROU  320
         K=ISEG(I)                                                           ROU  330
         SLP=SLOPE(K)                                                        ROU  340
         DTX=DTN/SLEN(K)                                                     ROU  350
         QUP=0.                                                              ROU  360
         QLAT=0.                                                             ROU  370
C                                                                            ROU  380
C     DETERMINE THE UPSTREAM INFLOW RATE                                     ROU  390
C                                                                            ROU  400
         IF (IUP(K,1).EQ.0) GO TO 140                                        ROU  410
         DO 130 J=1,3                                                        ROU  420
            IF (IUP(K,J).EQ.0) GO TO 140                                     ROU  430
            JJ=IUP(K,J)                                                      ROU  440
            QUP=QUP+Q(JJ)                                                    ROU  450
  130    CONTINUE                                                            ROU  460
C                                                                            ROU  470
C     DETERMINE THE LATERAL INFLOW RATE                                      ROU  480
C                                                                            ROU  490
  140    IF (K.GT.NOV) GO TO 150                                             ROU  500
         QLAT=QLAT+EFRM/43200.                                               ROU  510
  150    IF (ILAT(K,1).EQ.0) GO TO 170                                       ROU  520
         DO 160 J=1,2                                                        ROU  530
            IF (ILAT(K,J).EQ.0) GO TO 170                                    ROU  540
            JJ=ILAT(K,J)                                                     ROU  550
```

SUBROUTINE ROUT(L)

```
            QLAT=QLAT+Q(JJ)                                          ROU  560
  160     CONTINUE                                                   ROU  570
C                                                                    ROU  580
C       NONLINEAR SCHEME FOR WATER ROUTING                           ROU  590
C                                                                    ROU  600
  170     ALAT=QLAT*DTS                                              ROU  610
          DO 280 J=1,NOX                                             ROU  620
            ASUM=ALAT+A(K,J)+DTX*QUP                                 ROU  630
            IF (ASUM.LE.1.0E-7) GO TO 270                            ROU  640
C                                                                    ROU  650
C       SET UP A-Q RELATIONSHIP                                      ROU  660
C                                                                    ROU  670
            QN=ASUM/DTX                                              ROU  680
            AN=0.5*ASUM                                              ROU  690
C                                                                    ROU  700
C       DETERMINE THE ADDED FRICTION FACTOR DUE TO FORM RESISTANCE   ROU  710
C                                                                    ROU  720
            IF (AN.GT.AL(K)) GO TO 180                               ROU  730
            CPR=AC(K)                                                ROU  740
            EPR=BC(K)                                                ROU  750
            XIR=XIC                                                  ROU  760
            GO TO 190                                                ROU  770
  180       CPR=AO(K)                                                ROU  780
            EPR=BO(K)                                                ROU  790
            PCH=CPR*AL(K)**EPR                                       ROU  800
            PTO=CPR*AN**EPR                                          ROU  810
            XIR=(XIC*PCH+(XIO*GCD+XIC)*(PTO-PCH))/PTO                ROU  820
C                                                                    ROU  830
C       DETERMINE THE COEFFICIENT AND THE EXPONENT IN A-Q RELATION   ROU  840
C                                                                    ROU  850
  190       CALL FRICT                                               ROU  860
            BEM=BET-1.                                               ROU  870
            BEN=BEM-1.                                               ROU  880
            ALBET=ALP*BET                                            ROU  890
            ALBEM=ALP*BET*BEM                                        ROU  900
            DTXA=DTX*ALP                                             ROU  910
            ERROR=EPS*ASUM                                           ROU  920
C                                                                    ROU  930
C       LINEAR SCHEME TO FIND THE FIRST APPROXIMATION                ROU  940
C                                                                    ROU  950
            ITER=0                                                   ROU  960
            QPRE=(A(K,J)/ALP)**(1./BET)                              ROU  970
            QAVE=0.5*(QUP+QPRE)                                      ROU  980
            IF (QAVE.LE.1.0E-7) GO TO 200                            ROU  990
            DAQ=ALBET*QAVE**BEM                                      ROU 1000
            QE=(ALAT+DTX*QUP+DAQ*QPRE)/(DTX+DAQ)                     ROU 1010
            GO TO 210                                                ROU 1020
  200       QE=ASUM/DTXA                                             ROU 1030
C                                                                    ROU 1040
C       NONLINEAR SCHEME TO REFINE THE SOLUTION                      ROU 1050
C                                                                    ROU 1060
  210       ITER=ITER+1                                              ROU 1070
            AEST=DTX*QE+ALP*QE**BET                                  ROU 1080
            ADEV=ASUM-AEST                                           ROU 1090
            IF (ABS(ADEV).LE.ERROR) GO TO 260                        ROU 1100
```

```
                        SUBROUTINE ROUT(L)
            IF (ITER.LT.IMAX) GO TO 220                                 ROU 1110
            PRINT 300, IT,K,J                                           ROU 1120
            STOP                                                        ROU 1130
  220       FDER=DTX+ALBET*QE**BEM                                      ROU 1140
            SDER=ALBEM*QE**BEN                                          ROU 1150
            BB=FDER/SDER                                                ROU 1160
            SC=2.*ADEV/SDER                                             ROU 1170
            STEM=BB*BB+SC                                               ROU 1180
            IF (STEM.GE.0.) GO TO 230                                   ROU 1190
            QE=QE+ADEV/FDER                                             ROU 1200
            GO TO 210                                                   ROU 1210
  230       STEM=SQRT(STEM)                                             ROU 1220
            IF (ADEV.GT.0.) GO TO 250                                   ROU 1230
            ETEM=BB+STEM                                                ROU 1240
            QE=QE-ETEM                                                  ROU 1250
            IF (QE.GT.0.) GO TO 210                                     ROU 1260
  240       ETEM=0.5*ETEM                                               ROU 1270
            QE=QE+ETEM                                                  ROU 1280
            IF (QE.GT.0.) GO TO 210                                     ROU 1290
            GO TO 240                                                   ROU 1300
  250       X1=QE-BB-STEM                                               ROU 1310
            X2=QE-BB+STEM                                               ROU 1320
            AD1=ABS(ASUM-DTX*X1-ALP*X1**BET)                            ROU 1330
            AD2=ABS(ASUM-DTX*X2-ALP*X2**BET)                            ROU 1340
            QE=X1                                                       ROU 1350
            IF (AD1.GT.AD2) QE=X2                                       ROU 1360
            GO TO 210                                                   ROU 1370
  260       A(K,J)=ALP*QE**BET                                          ROU 1380
            QUP=QE                                                      ROU 1390
            GO TO 280                                                   ROU 1400
  270       A(K,J)=0.                                                   ROU 1410
            QUP=0.                                                      ROU 1420
  280     CONTINUE                                                      ROU 1430
          Q(K)=QUP                                                      ROU 1440
  290 CONTINUE                                                          ROU 1450
      RETURN                                                            ROU 1460
C                                                                       ROU 1470
  300 FORMAT (30X,42HDO NOT CONVERGE FOR THE COMPUTATION POINT ,I5,2X,I5ROU 1480
     1,2X,I5)                                                           ROU 1490
C                                                                       ROU 1500
      END                                                               ROU 1510
```

SUBROUTINE RAINEX(L,NCOM)

```
      SUBROUTINE RAINEX (L,NCOM)                                        RAI   10
C                                                                       RAI   20
C     THIS SUBROUTINE DETERMINES THE OVERALL MEAN RAINFALL EXCESS RATE  RAI   30
C     THE RAINFALL EXCESS COMPUTATION IS CARRIED OUT FOR A POINT UNDER  RAI   40
C     CANOPY AND FOR ANOTHER POINT IN THE AREA WITHOUT TREES            RAI   50
C                                                                       RAI   60
      DIMENSION RCUM(2), SINT(2), CM(2), EFR(2)                         RAI   70
      COMMON /INO/ NSEG,NOV,NTO,NDX,DT,DTS,DTN,IT,EPS,IMAX,ITMAX(10)    RAI   80
      COMMON /FLO/ Q(50),A(50,10),DR(10,200),ER(200),EVP(10),VIN(10),AMCRAI   90
     1(10)                                                              RAI  100
      COMMON /REF/ PERM,SM,WP,CPW,ETA,CND,GCD,VOG,SRG,VOR,XIC,XIO       RAI  110
      IF (PERM.EQ.0.) GO TO 110                                         RAI  120
      CIF=4.*CPW/(PERM*(SM-WP)*DT)                                      RAI  130
      GO TO 120                                                         RAI  140
  110 CIF=0.                                                            RAI  150
C                                                                       RAI  160
C     DETERMINE THE INITIAL INTERCEPTION STORAGES                       RAI  170
C                                                                       RAI  180
  120 SINT(1)=GCD*VOG                                                   RAI  190
      SINT(2)=(VOR+GCD)*VOG                                             RAI  200
      RCUM(1)=VIN(L)*SINT(1)                                            RAI  210
      RCUM(2)=VIN(L)*SINT(2)                                            RAI  220
      CM(1)=AMC(L)                                                      RAI  230
      CM(2)=AMC(L)                                                      RAI  240
      ETEM=EVP(L)*DT                                                    RAI  250
      DO 200 IT=1,NCOM                                                  RAI  260
C                                                                       RAI  270
C     DETERMINE THE RATES OF RAINFALL INPUT                             RAI  280
C                                                                       RAI  290
         IF (IT.GT.ITMAX(L)) GO TO 130                                  RAI  300
         DRF=DR(L,IT)                                                   RAI  310
         GO TO 140                                                      RAI  320
  130    DRF=0.                                                         RAI  330
  140    DO 190 I=1,2                                                   RAI  340
C                                                                       RAI  350
C     DETERMINE THE AVERAGE NET RAINFALL RATE                           RAI  360
C                                                                       RAI  370
            S=GCD*SRG                                                   RAI  380
            IF (I.EQ.2) S=S+VOR*SRG                                     RAI  390
            RCUM(I)=RCUM(I)+DRF*DT-ETEM*S                               RAI  400
            IF (RCUM(I).LE.SINT(I)) GO TO 150                           RAI  410
            RNET=(RCUM(I)-SINT(I))/DT                                   RAI  420
            RCUM(I)=SINT(I)                                             RAI  430
            GO TO 160                                                   RAI  440
  150       IF (RCUM(I).LT.0.) RCUM(I)=0.                               RAI  450
            RNET=0.                                                     RAI  460
C                                                                       RAI  470
C     DETERMINE THE AVERAGE INFILTRATION RATE                           RAI  480
C                                                                       RAI  490
  160       RIF=0.5*PERM*(1.+SQRT(1.+CIF*(SM-CM(I))**2))                RAI  500
C                                                                       RAI  510
C     CHECK THE AVAILABILITY OF MOISTURE SUPPLY FOR INFILTRATION        RAI  520
C                                                                       RAI  530
            IF (RNET.GE.RIF) GO TO 170                                  RAI  540
            ERIF=RNET*(1.-0.5*RNET/RIF)                                 RAI  550
```

```
                    SUBROUTINE RAINEX(L,NCOM)
            GO TO 180                                                   RAI  560
  170       ERIF=0.5*RIF                                                RAI  570
C                                                                       RAI  580
C     DETERMINE THE AVERAGE RAINFALL EXCESS RATE                        RAI  590
C                                                                       RAI  600
  180       EFR(I)=RNET-ERIF                                            RAI  610
C                                                                       RAI  620
C     ADJUST MOISTURE CONTENT FOR NEXT TIME STEP                        RAI  630
C                                                                       RAI  640
            IF (ERIF.EQ.0.) GO TO 190                                   RAI  650
            CM(I)=(CM(I)*ETA+DT*ERIF)/ETA                               RAI  660
            IF (CM(I).GE.SM) CM(I)=SM                                   RAI  670
  190     CONTINUE                                                      RAI  680
C                                                                       RAI  690
C     COMPUTE THE OVERALL MEAN RAINFALL EXCESS RATE                     RAI  700
C                                                                       RAI  710
        ER(IT)=(1.-CND)*EFR(1)+CND*EFR(2)                               RAI  720
  200 CONTINUE                                                          RAI  730
      RETURN                                                            RAI  740
C                                                                       RAI  750
      END                                                               RAI  760
```

SUBROUTINE FRICT

```
      SUBROUTINE FRICT                                                      FRI   10
C                                                                           FRI   20
C     THIS SUBROUTINE DETERMINES THE COEFFICIENT AND THE EXPONENT IN A-QFRI   30
C     RELATION                                                              FRI   40
C                                                                           FRI   50
      COMMON /FRC/ QN,AN,SNU,SLOPE,FK1,FK2,FK3,XIR,ALP,BET,CPR,EPR,ARF      FRI   60
      SK1=(1.+XIR)*FK1*27.162*ARF**0.407                                    FRI   70
      SK2=(1.+XIR)*FK2                                                      FRI   80
      SK3=(1.+XIR)*FK3                                                      FRI   90
      RN=QN/(CPR*AN**EPR*SNU)                                               FRI  100
      IF (RN.GT.900.) GO TO 110                                             FRI  110
      ERF=1.                                                                FRI  120
      CRF=SK1                                                               FRI  130
      GO TO 150                                                             FRI  140
  110 IF (RN.GT.2000.) GO TO 120                                            FRI  150
      ERF=1.25234*ALOG(SK1/SK2)-6.13916                                     FRI  160
      TEM=900.**(ERF-1.)                                                    FRI  170
      CRF=SK1*TEM                                                           FRI  180
      GO TO 150                                                             FRI  190
  120 IF (RN.GT.25000.) GO TO 130                                           FRI  200
      ERF=0.25                                                              FRI  210
      CRF=SK2                                                               FRI  220
      GO TO 150                                                             FRI  230
  130 IF (RN.GT.100000.) GO TO 140                                          FRI  240
      ERF=0.72135*ALOG(SK2/SK3)-1.82621                                     FRI  250
      TEM=100000.**ERF                                                      FRI  260
      CRF=SK3*TEM                                                           FRI  270
      GO TO 150                                                             FRI  280
  140 ERF=0.                                                                FRI  290
      CRF=SK3                                                               FRI  300
  150 AEXP=1./(3.-EPR*(1.+ERF))                                             FRI  310
      ALP=(CPR**(1.+ERF)*CRF*SNU**ERF/(257.6*SLOPE))**AEXP                  FRI  320
      BET=(2.-ERF)*AEXP                                                     FRI  330
      RETURN                                                                FRI  340
C                                                                           FRI  350
      END                                                                   FRI  360
```

C.2. PROGRAM SEDIM: Rainfall Erosion Model

PROGRAM SEDIM (INPUT,OUTPUT)

```
      PROGRAM SEDIM (INPUT,OUTPUT)                                      SED   10
C                                                                       SED   20
C     THIS IS A RAINFALL-EROSION MODEL                                  SED   30
C     THIS PROGRAM ESTIMATES SOIL EROSION RATE FROM OVERLAND FLOW AREA   SED   40
C     NOTATIONS FOR MODEL INPUT AND OUTPUT                              SED   50
C     TITLE = ALPHABETICAL OR NUMERICAL IDENTIFICATION OF THE PROBLEM   SED   60
C     NX = NUMBER OF SPACE INCREMENTS                                   SED   70
C     NR = NUMBER OF RAINFALL EVENTS                                    SED   80
C     NTO = OUTPUT INTERVALS                                            SED   90
C     IPRINT = IDENTIFICATION FOR OUTPUT CONTROL                        SED  100
C     IPRINT = 0, --- ONLY OUTFLOW HYDROGRAPHS IS DESIRED               SED  110
C     IPRINT = 1, --- CURRENT ELEVATIONS ARE ALSO DESIRED               SED  120
C     IPRINT = 2, --- ROUTING INFORMATION AND CURRENT ELEVATION ARE     SED  130
C                     INCLUDED                                          SED  140
C     DT = TIME INCREMENT                                               SED  150
C     DX = SPACE INCREMENT                                              SED  160
C     DBM = MEDIAM DIAMETER OF THE SEDIMENT                             SED  170
C     PORB = POROSITY OF BED MATERIAL                                   SED  180
C     SKL = CONSTANT REPRESENTING DARCY-WEISBACH FRICTION FACTOR OF     SED  190
C           GRAIN RESISTANCE WITHOUT RAINFALL FOR FLOW REYNOLDS NUMBER  SED  200
C           LESS THAN OR EQUAL TO 900                                   SED  210
C     SKT = CONSTANT REPRESENTING DARCY-WEISBACH FRICTION FACTOR OF     SED  220
C           GRAIN RESISTANCE WITHOUT RAINFALL FOR FLOW REYNOLDS NUMBER  SED  230
C           BETWEEN 2000 AND 25000                                      SED  240
C     CTA = CONSTANT DESCRIBING THE CRITICAL TRACTIVE FORCE             SED  250
C     AGB = COEFFICIENT IN BED-LOAD SEDIMENT TRANSPORT EQUATION         SED  260
C     BEX = EXPONENT IN BED-LOAD SEDIMENT TRANSPORT EQUATION            SED  270
C     SQC = COEFFICIENT DESCRIBING THE SUSPENDED LOAD                   SED  280
C     RAIN = RAINFALL INTENSITY                                         SED  290
C     TEND = TIME AT THE END OF RAINSTORM                               SED  300
C     SKV = KINEMATIC VISCOSITY OF WATER                                SED  310
C     RIF = MEAN INFILTRATION RATE                                      SED  320
C     Z = BED ELEVATION                                                 SED  330
C     A = FLOW AREA OR FLOW DEPTH FOR OVERLAND FLOW                     SED  340
C     RB = SEDIMENT CONCENTRATION IN VOLUME                             SED  350
C     DZ = CHANG IN BED ELEVATION                                       SED  360
C     Q = FLOW DISCHARGE                                                SED  370
C     GB = SEDIMENT TRANSPORT RATE                                      SED  380
C     CB = SEDIMENT CONCENTRATION IN WEIGHT                             SED  390
C                                                                       SED  400
      COMMON /FRC/ ON,SNU,SLOPE,RSK,SKT,ALP,BET,CRF,ERF                 SED  410
      DIMENSION A(200), CB(200), T(200), Q(200), GB(200), RAIN(100), TENSED  420
     1D(100)                                                           SED  430
      DIMENSION TITLE(20), RB(200), Z(200), DZ(200), SKV(200), RIF(100) SED  440
      IMAX=20                                                           SED  450
      EPS=0.05                                                          SED  460
      READ 300, TITLE                                                   SED  470
      PRINT 310, TITLE                                                  SED  480
C                                                                       SED  490
C     INPUT AND OUTPUT GENERAL INFORMATION                              SED  500
C                                                                       SED  510
      READ 320, NX,NR,NTO,IPRINT                                        SED  520
      READ 330, DT,DX,DBM,PORB                                          SED  530
      PRINT 340, NX,NR,DT,DX,DBM,PORB                                   SED  540
C                                                                       SED  550
```

```
                      PROGRAM SEDIM (INPUT,OUTPUT)
C     INPUT AND OUTPUT MODEL PARAMETERS                                  SED  560
C                                                                        SED  570
      READ 350, SKL,SKT,CTA,AGB,BEX,SOC                                  SED  580
      PRINT 360, SKL,SKT,CTA,AGB,BEX,SOC                                 SED  590
C                                                                        SED  600
C     ESTABLISH SOME INVARIANT INFORMATION                               SED  610
C                                                                        SED  620
      DTS=DT*60.                                                         SED  630
      DTX=DTS/DX                                                         SED  640
      SLENG=FLOAT(NX)*DX                                                 SED  650
      FACTOR=43200./SLENG                                                SED  660
      DBM=DRM/304.8                                                      SED  670
      SMB=DBM                                                            SED  680
      CGB=CTA*DBM                                                        SED  690
      DO 290 M=1,NR                                                      SED  700
C                                                                        SED  710
C     INPUT RAINFALL AS STEP FUNCTIONS                                   SED  720
C                                                                        SED  730
         READ 370, RAIN(M),TEND(M),SKV(M),RIF(M)                         SED  740
         PRINT 380, M,RAIN(M),TEND(M),SKV(M),RIF(M)                      SED  750
C                                                                        SED  760
C     INPUT AND OUTPUT INITIAL ELEVATIONS                                SED  770
C                                                                        SED  780
         NXP=NX+1                                                        SED  790
         READ 390, (Z(I),I=1,NXP)                                        SED  800
         PRINT 400, (I,Z(I),I=1,NXP)                                     SED  810
C                                                                        SED  820
C     INITIALIZE THE BOUNDARY CONDITIONS                                 SED  830
C                                                                        SED  840
         DO 110 I=1,NX                                                   SED  850
            A(I)=0.                                                      SED  860
            RB(I)=0.                                                     SED  870
  110    CONTINUE                                                        SED  880
         TSUM=0.                                                         SED  890
         KOUT=1                                                          SED  900
         SNU=SKV(M)/100000.                                              SED  910
         FVR=(SQRT(35.42*DBM**3+36.*SNU**21-6.*SNU)/DBM                  SED  920
         EFRAIN=RAIN(M)-RIF(M)                                           SED  930
         RSK=SKL+27.162*EFRAIN**0.407                                    SED  940
         QLAT=EFRAIN/43200.                                              SED  950
         ALAT=QLAT*DTS                                                   SED  960
         LEND=TEND(M)/DT+0.1                                             SED  970
         DO 280 L=1,LEND                                                 SED  980
            TSUM=TSUM+DT                                                 SED  990
            QUP=0.                                                       SED 1000
            GBUP=0.                                                      SED 1010
            ZUP=0.                                                       SED 1020
            DO 260 J=1,NX                                                SED 1030
               ATEM=A(J)                                                 SED 1040
               BTEM=RB(J)                                                SED 1050
C                                                                        SED 1060
C     NONLINEAR SCHEME FOR WATER ROUTING                                 SED 1070
C                                                                        SED 1080
               ASUM=ALAT+A(J)+DTX*QUP                                    SED 1090
               IF (ASUM.LE.1.0E-10) GO TO 220                            SED 1100
```

```
                    PROGRAM SEDIM (INPUT,OUTPUT)
C                                                                       SED 1110
C     SET UP A-Q RELATIONSHIP                                           SED 1120
C                                                                       SED 1130
               QN=ASUM/DTX                                              SED 1140
               SLOPE=(Z(J)-Z(J+1))/DX                                   SED 1150
               IF (SLOPE.GT.0.) GO TO 120                               SED 1160
               PRINT 410                                                SED 1170
               GO TO 290                                                SED 1180
  120          CALL FRICT                                               SED 1190
               BEM=BET-1.                                               SED 1200
               BEN=BEM-1.                                               SED 1210
               ALBET=ALP*BET                                            SED 1220
               ALBEM=ALP*BET*BEM                                        SED 1230
               ERROR=EPS*ASUM                                           SED 1240
               ITER=0                                                   SED 1250
C                                                                       SED 1260
C     LINEAR SCHEME TO FIND THE FIRST APPROXIMATION                     SED 1270
C                                                                       SED 1280
               QPRE=(ATEM/ALP)**(1./BET)                                SED 1290
               QAVE=0.5*(QUP+QPRE)                                      SED 1300
               IF (QAVE.LE.1.0E-10) GO TO 130                           SED 1310
               DAQ=ALBET*QAVE**BEM                                      SED 1320
               QE=(ALAT+DTX*QUP+DAQ*QPRE)/(DTX+DAQ)                     SED 1330
               IF (QE.LE.0.) GO TO 130                                  SED 1340
               GO TO 140                                                SED 1350
  130          QE=ASUM/(DTX+ALP)                                        SED 1360
C                                                                       SED 1370
C     NONLINEAR SCHEME TO REFINE THE SOLUTION                           SED 1380
C                                                                       SED 1390
  140          ITER=ITER+1                                              SED 1400
               AEST=DTX*QE+ALP*QE**BET                                  SED 1410
               ADEV=ASUM-AEST                                           SED 1420
               IF (ABS(ADEV).LE.ERROR) GO TO 190                        SED 1430
               IF (ITER.LT.IMAX) GO TO 150                              SED 1440
               PRINT 420, L,J                                           SED 1450
               GO TO 290                                                SED 1460
  150          FDER=DTX+ALBET*QE**BEM                                   SED 1470
               SDER=ALBEM*QE**BEN                                       SED 1480
               BB=FDER/SDER                                             SED 1490
               SC=2.*ADEV/SDER                                          SED 1500
               STEM=BB*BB+SC                                            SED 1510
               IF (STEM.GE.0.) GO TO 160                                SED 1520
               QE=QE+ADEV/FDER                                          SED 1530
               GO TO 140                                                SED 1540
  160          STEM=SQRT(STEM)                                          SED 1550
               IF (ADEV.GT.0.) GO TO 180                                SED 1560
               ETEM=BB+STEM                                             SED 1570
               QE=QE-ETEM                                               SED 1580
               IF (QE.GT.0.) GO TO 140                                  SED 1590
  170          ETEM=0.5*ETEM                                            SED 1600
               QE=QE+ETEM                                               SED 1610
               IF (QE.GT.0.) GO TO 140                                  SED 1620
               GO TO 170                                                SED 1630
  180          X1=QE-BB-STEM                                            SED 1640
               X2=QE-BB+STEM                                            SED 1650
```

```
                        PROGRAM SEDIM (INPUT,OUTPUT)

                AD1=ABS(ASUM-DTX*X1-ALP*X1**BET)                        SED 1660
                AD2=ABS(ASUM-DTX*X2-ALP*X2**BET)                        SED 1670
                QE=X1                                                   SED 1680
                IF (AD1.GT.AD2) QE=X2                                   SED 1690
                GO TO 140                                               SED 1700
  190           DEPTH=ALP*QE**BET                                       SED 1710
                RN=QE/SNU                                               SED 1720
                BMV=2.5+SQRT(RN**ERF/CRF)                               SED 1730
                TAO=62.4*DEPTH*SLOPE                                    SED 1740
                SV=SQRT(TAO/1.9379)                                     SED 1750
C                                                                       SED 1760
C     BED MATERIAL LOAD ROUTING                                         SED 1770
C                                                                       SED 1780
                TTEM=TAO-CGB                                            SED 1790
                IF (TTEM.LE.0.) GO TO 230                               SED 1800
C                                                                       SED 1810
C     DETERMINATION OF RATIO OF SUSPENDED BED MATERIAL LOAD             SED 1820
C                                                                       SED 1830
                ZR=FVB/(0.4*SV)                                         SED 1840
                AR=SMB/DEPTH                                            SED 1850
                IF (ZR.GT.5.5.OR.AR.GT.0.9) GO TO 200                   SED 1860
                CALL POWER (ZR,AR,FJ,SJ,1.0E-3)                         SED 1870
                P=AR**(ZR-1.)/(SQC*(1.-AR)**ZR)                         SED 1880
                SUSP=P*(BMV*FJ+2.5*SJ)                                  SED 1890
                IF (SUSP.LT.0.) SUSP=0.                                 SED 1900
                GO TO 210                                               SED 1910
  200           SUSP=0.                                                 SED 1920
C                                                                       SED 1930
C     DETERMINATION OF FLOW TRANSPORTING CAPACITY OF BED MATERIAL LOAD  SED 1940
C                                                                       SED 1950
  210           GBC=(1.+SUSP)*AGB*TTEM**BEX                             SED 1960
C                                                                       SED 1970
C     DETERMINATION OF EROSION OF BED MATERIAL LOAD                     SED 1980
C                                                                       SED 1990
                RB(J)=GBC/QE                                            SED 2000
                EGB=(GBUP-RB(J)*QE)*DTX-RB(J)*DEPTH+BTEM*ATEM           SED 2010
                GO TO 240                                               SED 2020
  220           DEPTH=0.                                                SED 2030
                QE=0.                                                   SED 2040
  230           RB(J)=0.                                                SED 2050
                EGB=GBUP*DTX+BTEM*ATEM                                  SED 2060
  240           A(J)=DEPTH                                              SED 2070
                DZ(J)=EGB/(1.-PORB)                                     SED 2080
                IF (J.EQ.1) GO TO 250                                   SED 2090
                Z(J)=Z(J)+0.5*(ZUP+DZ(J))                               SED 2100
  250           QUP=QE                                                  SED 2110
                GBUP=RB(J)*QE                                           SED 2120
                ZUP=DZ(J)                                               SED 2130
  260         CONTINUE                                                  SED 2140
              T(L)=TSUM                                                 SED 2150
              Q(L)=QUP*FACTOR                                           SED 2160
              GB(L)=GBUP*102.96                                         SED 2170
              RATIO=1650./(QUP+1.65*GBUP)                               SED 2180
              CB(L)=GBUP*RATIO                                          SED 2190
              IF (IPRINT.EQ.0.OR.(L/NTO).NE.KOUT) GO TO 280             SED 2200
```

```
                        PROGRAM SEDIM (INPUT,OUTPUT)

            KOUT=KOUT+1                                                    SED 2210
            IF (IPRINT.EQ.1) GO TO 270                                     SED 2220
            PRINT 430, (L,K,A(K),RB(K),DZ(K),K=1,NX)                       SED 2230
  270       PRINT 440, (K,Z(K),K=1,NXP)                                    SED 2240
  280     CONTINUE                                                         SED 2250
C                                                                          SED 2260
C     OUTFLOW HYDROGRAPH                                                   SED 2270
C                                                                          SED 2280
          PRINT 450                                                        SED 2290
          PRINT 460, (T(I),Q(I),GB(I),CB(I),I=1,LEND)                      SED 2300
          IF (IPRINT.GT.0) GO TO 290                                       SED 2310
          PRINT 440, (I,Z(I),I=1,NXP)                                      SED 2320
  290 CONTINUE                                                             SED 2330
      STOP                                                                 SED 2340
C                                                                          SED 2350
  300 FORMAT (20A4)                                                        SED 2360
  310 FORMAT (1H1/////30X,20A4)                                            SED 2370
  320 FORMAT (4I10)                                                        SED 2380
  330 FORMAT (4F10.5)                                                      SED 2390
  340 FORMAT (50X, 19HGENERAL INFORMATION,//30X,2I10,4F10.5//)             SED 2400
  350 FORMAT (6F10.5)                                                      SED 2410
  360 FORMAT (52X, 16HMODEL PARAMETERS,//24X,6F12.5//)                     SED 2420
  370 FORMAT (4F10.5)                                                      SED 2430
  380 FORMAT (44X, 32HRAINFALL INPUT IN STEP FUNCTIONS,/(33X,I6,4F12.5))SED 2440
  390 FORMAT (8F10.5)                                                      SED 2450
  400 FORMAT (50X, 24HORIGINAL MEAN ELEVATIONS,//(5(4X,I10,F12.5)))      SED 2460
  410 FORMAT (/30X, 61HTHE TIME INCREMENT IS TOO LARGE TO DEVELOP A PROPSED 2470
     1ER LAND FORM)                                                        SED 2480
  420 FORMAT (33X, 42HDO NOT CONVERGE FOR THE COMPUTATION POINT ,I5,2X,ISED 2490
     15)                                                                   SED 2500
  430 FORMAT (/50X, 19HROUTING INFORMATION,//(32X,2I10,3F12.5))            SED 2510
  440 FORMAT (50X, 18HCURRENT ELEVATIONS,/(5(4X,I10,F12.5)))               SED 2520
  450 FORMAT (50X, 18HOUTFLOW HYDROGRAPH)                                  SED 2530
  460 FORMAT (25X,F10.3,3F20.5)                                            SED 2540
C                                                                          SED 2550
      END                                                                  SED 2560
```

SUBROUTINE POWER (Z,A,XJ1,XJ2,CONV)

```
      SUBROUTINE POWER (Z,A,XJ1,XJ2,CONV)                                POW   10
C                                                                        POW   20
C     THIS SUBROUTINE EVALUATE J1 AND J2 INTEGRALS                       POW   30
C     NOTATIONS                                                          POW   40
C     XJ1 = VALUE OF J1 INTEGRAL                                         POW   50
C     XJ2 = VALUE OF J2 INTEGRAL                                         POW   60
C     N = ORDER OF APPROXIMATION + 1                                     POW   70
C     CONV = CONVERGENCE CRITERION                                       POW   80
C                                                                        POW   90
      N=1                                                                POW  100
      XJ1=0.                                                             POW  110
      XJ2=0.                                                             POW  120
      ALG=ALOG(A)                                                        POW  130
      C=1.                                                               POW  140
      D=-Z                                                               POW  150
      E=D+1.                                                             POW  160
      FN=1.                                                              POW  170
      AEX=A**E                                                           POW  180
      GO TO 120                                                          POW  190
  110 N=N+1                                                              POW  200
      C=C*D/FN                                                           POW  210
      D=E                                                                POW  220
      E=D+1.                                                             POW  230
      FN=FLOAT(N)                                                        POW  240
      AEX=A**E                                                           POW  250
  120 IF (ABS(E).LE.0.001) GO TO 130                                     POW  260
      XJ1=XJ1+C*(1.-AEX)/E                                               POW  270
      XJ2=XJ2+C*((AEX-1.)/E**2-AEX*ALG/E)                                POW  280
      GO TO 140                                                          POW  290
  130 XJ1=XJ1-C*ALG                                                      POW  300
      XJ2=XJ2-0.5*C*ALG**2                                               POW  310
  140 IF (N.EQ.1) GO TO 150                                              POW  320
      CJ1=ABS(1.-FJ1/XJ1)                                                POW  330
      CJ2=ABS(1.-FJ2/XJ2)                                                POW  340
      IF (CJ1.LE.CONV.AND.CJ2.LE.CONV) RETURN                            POW  350
  150 FJ1=XJ1                                                            POW  360
      FJ2=XJ2                                                            POW  370
      GO TO 110                                                          POW  380
C                                                                        POW  390
      END                                                                POW  400
```

SUBROUTINE FRICT

```
      SUBROUTINE FRICT                                                  FRI   10
C                                                                       FRI   20
C     THIS SUBROUTINE DETERMINES A-Q RELATION                           FRI   30
C                                                                       FRI   40
      COMMON /FRC/ QN,SNU,SLOPE,RSK,SKT,ALP,BET,CRF,ERF                 FRI   50
      RN=QN/SNU                                                         FRI   60
      IF (RN.GT.1000.) GO TO 110                                        FRI   70
      ERF=1.                                                            FRI   80
      CRF=RSK                                                           FRI   90
      GO TO 130                                                         FRI  100
  110 IF (RN.GT.2000.) GO TO 120                                        FRI  110
      ERF=1.44270*ALOG(RSK/SKT)-7.22434                                 FRI  120
      CRF=RSK*1000.**(ERF-1.)                                           FRI  130
      GO TO 130                                                         FRI  140
  120 ERF=0.25                                                          FRI  150
      CRF=SKT                                                           FRI  160
  130 ALP=(CRF*SNU**ERF/(257.6*SLOPE))**(1./3.)                         FRI  170
      BET=2./3.-ERF/3.                                                  FRI  180
      RETURN                                                            FRI  190
C                                                                       FRI  200
      END                                                               FRI  210
```

C.3. PROGRAM UNIMO: One-Dimensional Calibration Technique

```
                PROGRAM UNIMO(INPUT,OUTPUT)

      PROGRAM UNIMO (INPUT,OUTPUT)                                      UNI   10
C                                                                       UNI   20
C     THIS PROGRAM SOLVES ONE-DIMENSIONAL CONSTRAINED MINIMIZATION      UNI   30
C     PROBLEM BY SUCCESSIVE QUADRATIC APPROXIMATION                     UNI   40
C     THE CONSTRAINTS ARE THE UPPER AND LOWER BOUNDS OF THE VECTOR      UNI   50
C     THE USER MUST SUPPLY A SUBROUTINE OBJECT FOR EVALUATION OF THE    UNI   60
C     OBJECTIVE FUNCTION                                                UNI   70
C     NOTATIONS FOR INPUT AND OUTPUT INFORMATION                        UNI   80
C     TITLE = ALPHABETICAL OR NUMERICAL IDENTIFICATION OF THE PROBLEM   UNI   90
C     MST = MAXIMUM LIMIT OF NUMBER OF STAGE SEARCH                     UNI  100
C     IPT = NUMERICAL IDENTIFICATION FOR OUTPUT CONTROL                 UNI  110
C     IPT = 0 --- ONLY THE FINAL ANSWER IS DESIRED                      UNI  120
C     IPT = 1 --- INTERMEDIATE VALUES OF EACH STAGE SEARCH IS DESIRED   UNI  130
C     XA = INITIAL GUESS OF THE VECTOR                                  UNI  140
C     DX = INITIAL STEP-SIZE                                            UNI  150
C     XUPL = UPPER BOUND                                                UNI  160
C     XLOL = LOWER BOUND                                                UNI  170
C     EPS = CONVERGENCE TOLERANCE BASED ON THE CHANGE OF STEP LENGTH    UNI  180
C                                                                       UNI  190
      DIMENSION E(3), Y(3), TITLE(20)                                   UNI  200
C                                                                       UNI  210
C     INPUT AND OUTPUT NECESSARY INFORMATION                            UNI  220
C                                                                       UNI  230
      READ 280, TITLE                                                   UNI  240
      PRINT 290, TITLE                                                  UNI  250
      READ 300, MST,IPT,XA,DX,XUPL,XLOL,EPS                             UNI  260
      PRINT 310, XA,XUPL,XLOL,EPS                                       UNI  270
C                                                                       UNI  280
C     STARTING OF STAGE SEARCH                                          UNI  290
C                                                                       UNI  300
      NEF=0                                                             UNI  310
      NS=0                                                              UNI  320
      CALL OBJECT (VALUE,NEF,XA)                                        UNI  330
      A=VALUE                                                           UNI  340
      XB=XA+DX                                                          UNI  350
      CALL OBJECT (VALUE,NEF,XB)                                        UNI  360
      B=VALUE                                                           UNI  370
C                                                                       UNI  380
C     DETERMINE THE THIRD POINT REQUIRED FOR APPROXIMATION              UNI  390
C                                                                       UNI  400
      IF (A.GT.B) GO TO 140                                             UNI  410
  110 XC=XA-DX                                                          UNI  420
      IF (XC.GE.XLOL) GO TO 120                                         UNI  430
      XC=XLOL                                                           UNI  440
  120 CALL OBJECT (VALUE,NEF,XC)                                        UNI  450
      C=VALUE                                                           UNI  460
      Y(1)=XC                                                           UNI  470
      Y(2)=XA                                                           UNI  480
      Y(3)=XB                                                           UNI  490
      E(1)=C                                                            UNI  500
      E(2)=A                                                            UNI  510
      E(3)=B                                                            UNI  520
      IF (C.LT.A) GO TO 130                                             UNI  530
      XINF=XA                                                           UNI  540
      FINF=A                                                            UNI  550
```

```
                    PROGRAM UNIMO(INPUT,OUTPUT)

      GO TO 170                                                          UNI  560
  130 XINF=XC                                                            UNI  570
      FINF=C                                                             UNI  580
      GO TO 170                                                          UNI  590
  140 XC=XA+2.*DX                                                        UNI  600
      IF (XC.LE.XUPL) GO TO 150                                          UNI  610
      XC=XUPL                                                            UNI  620
  150 CALL OBJECT (VALUE,NEF,XC)                                         UNI  630
      C=VALUE                                                            UNI  640
      Y(1)=XA                                                            UNI  650
      Y(2)=XB                                                            UNI  660
      Y(3)=XC                                                            UNI  670
      E(1)=A                                                             UNI  680
      E(2)=B                                                             UNI  690
      E(3)=C                                                             UNI  700
      IF (C.LT.B) GO TO 160                                              UNI  710
      XINF=XB                                                            UNI  720
      FINF=B                                                             UNI  730
      GO TO 170                                                          UNI  740
  160 XINF=XC                                                            UNI  750
      FINF=C                                                             UNI  760
C                                                                        UNI  770
C     ELIMINATE PREMATURE TERMINATION DUE TO EQUAL VALUES AT TWO END     UNI  780
C     POINTS IN THE FIRST SEARCH                                         UNI  790
C                                                                        UNI  800
  170 DEF=E(1)-E(3)                                                      UNI  810
      IF (NS.GT.0.OR.ABS(DEF).GT.EPS) GO TO 180                          UNI  820
      DX=0.5*DX                                                          UNI  830
      Y(2)=Y(1)+DX                                                       UNI  840
      CALL OBJECT (VALUE,NEF,Y(2))                                       UNI  850
      E(2)=VALUE                                                         UNI  860
      Y(3)=XINF                                                          UNI  870
      E(3)=FINF                                                          UNI  880
      DEF=E(1)-E(3)                                                      UNI  890
      IF (E(2).GT.FINF) GO TO 180                                        UNI  900
      XINF=Y(2)                                                          UNI  910
      FINF=E(2)                                                          UNI  920
C                                                                        UNI  930
C     CHECK THE CONVEXITY OF THE QUADRATIC FUNCTION                      UNI  940
C                                                                        UNI  950
  180 A1=(Y(1)-Y(2))*(Y(2)-Y(3))*(Y(1)-Y(3))                             UNI  960
      IF (ABS(A1).EQ.0.) GO TO 190                                       UNI  970
      A2=E(1)*(Y(2)-Y(3))+E(2)*(Y(3)-Y(1))+E(3)*(Y(1)-Y(2))              UNI  980
      SA=A2/A1                                                           UNI  990
      IF (SA.GE.0.) GO TO 200                                            UNI 1000
      DX=Y(3)-Y(1)                                                       UNI 1010
      XA=Y(1)                                                            UNI 1020
      A=E(1)                                                             UNI 1030
      XB=Y(3)                                                            UNI 1040
      B=E(3)                                                             UNI 1050
      IF (DEF.GT.0.) GO TO 140                                           UNI 1060
      GO TO 110                                                          UNI 1070
  190 XSTA=XINF                                                          UNI 1080
      FSTA=FINF                                                          UNI 1090
      GO TO 270                                                          UNI 1100
```

```
                      PROGRAM UNIMO(INPUT,OUTPUT)

C                                                                       UNI 1110
C     DETERMINE THE MINIMUM OF THE QUADRATIC FUNCTION                   UNI 1120
C                                                                       UNI 1130
  200 SB=(E(1)-E(2))/(Y(1)-Y(2))-SA*(Y(1)+Y(2))                         UNI 1140
      XSTA=-SB/(2.*SA)                                                  UNI 1150
      IF (XSTA.GE.XLOL.AND.XSTA.LE.XUPL) GO TO 220                      UNI 1160
      IF (DEF.GT.0.) GO TO 210                                          UNI 1170
      XSTA=XLOL                                                         UNI 1180
      GO TO 220                                                         UNI 1190
  210 XSTA=XUPL                                                         UNI 1200
  220 NS=NS+1                                                           UNI 1210
      CALL OBJECT (VALUE,NEF,XSTA)                                      UNI 1220
      FSTA=VALUE                                                        UNI 1230
      IF (FSTA.LE.FINF) GO TO 230                                       UNI 1240
      XTEM=XSTA                                                         UNI 1250
      XSTA=XINF                                                         UNI 1260
      XINF=XTEM                                                         UNI 1270
      FTEM=FSTA                                                         UNI 1280
      FSTA=FINF                                                         UNI 1290
      FINF=FTEM                                                         UNI 1300
  230 IF (IPT.EQ.0) GO TO 240                                           UNI 1310
      PRINT 320                                                         UNI 1320
      PRINT 330, NS                                                     UNI 1330
      PRINT 320                                                         UNI 1340
      PRINT 340, XSTA,FSTA                                              UNI 1350
C                                                                       UNI 1360
C     CHECK IF THE VALUE IS SATISFIED WITH CONVERGENCE TOLERANCE        UNI 1370
C                                                                       UNI 1380
  240 IF ((FINF-FSTA).LE.EPS) GO TO 270                                 UNI 1390
      DX=ABS(XINF-XSTA)                                                 UNI 1400
      IF (NS.LT.MST) GO TO 250                                          UNI 1410
      PRINT 320                                                         UNI 1420
      PRINT 350, MST                                                    UNI 1430
      PRINT 340, XSTA,FSTA                                              UNI 1440
      STOP                                                              UNI 1450
  250 IF (XSTA.GT.XINF) GO TO 260                                       UNI 1460
      XA=XSTA                                                           UNI 1470
      A=FSTA                                                            UNI 1480
      XB=XINF                                                           UNI 1490
      B=FINF                                                            UNI 1500
      GO TO 110                                                         UNI 1510
  260 XA=XINF                                                           UNI 1520
      A=FINF                                                            UNI 1530
      XB=XSTA                                                           UNI 1540
      B=FSTA                                                            UNI 1550
      GO TO 140                                                         UNI 1560
C                                                                       UNI 1570
C     A MINIMUM HAS BEEN FOUND                                          UNI 1580
C                                                                       UNI 1590
  270 PRINT 320                                                         UNI 1600
      PRINT 360, NS,NEF                                                 UNI 1610
      PRINT 370, FSTA,XSTA                                              UNI 1620
      STOP                                                              UNI 1630
C                                                                       UNI 1640
  280 FORMAT (20A4)                                                     UNI 1650
```

```
                PROGRAM UNIMO(INPUT,OUTPUT)
  290 FORMAT (1H1/////40X,20A4)                                          UNI 1660
  300 FORMAT (2I10,4F10.5,E10.3)                                         UNI 1670
  310 FORMAT (//35X,39HTHE INITIAL VECTOR CHOSEN BY THE USER =,F10.5//41UNI 1680
     1X,27HUPPER LIMIT OF THE VECTOR =,F10.5//41X,27HLOWER LIMIT OF THE UNI 1690
     2VECTOR =,F10.5//44X,23HCONVERGENCE TOLERANCE =,E10.3)              UNI 1700
  320 FORMAT (/40X,40H****************************************)         UNI 1710
  330 FORMAT (//48X,18HSTAGE SEARCH -----,I5)                            UNI 1720
  340 FORMAT (//45X,20HTHE CURRENT VECTOR =,F10.5//34X,32HTHE CURRENT OBUNI 1730
     1JECTIVE FUNCTION =,E20.8)                                          UNI 1740
  350 FORMAT (//40X,16HDO NOT CONVERGE IN,I5,5X,14HSTAGE SEARCHES)       UNI 1750
  360 FORMAT (//48X,24HA MINIMUM HAS BEEN FOUND//41X,30HTOTAL NUMBER OF UNI 1760
     1STAGE SEARCH =,I5//39X,37HTOTAL NUMBER OF FUNCTION EVALUATION =,I5UNI 1770
     2)                                                                  UNI 1780
  370 FORMAT (//38X,23HOPTIMIZATION FUNCTION =,E20.8//48X,14HFINAL VECTOUNI 1790
     1R =,F10.5)                                                         UNI 1800
C                                                                        UNI 1810
      END                                                                UNI 1820
```

SUBROUTINE OBJECT(VALUE,NEF,X)

```
      SUBROUTINE OBJECT (VALUE,NEF,X)                                   OBJ   10
C                                                                       OBJ   20
C     THIS FUNCTION EVALUATES THE VALUE OF THE OBJECTIVE FUNCTION       OBJ   30
C                                                                       OBJ   40
      NEF=NEF+1                                                         OBJ   50
      VALUE=(1.-X)**2+(1.-X*X)**2                                       OBJ   60
      RETURN                                                            OBJ   70
C                                                                       OBJ   80
      END                                                               OBJ   90
```

C.4. PROGRAM BROSEN: Multi-Dimensional Calibration Technique

PROGRAM BROSEN (INPUT,OUTPUT)

```
      PROGRAM BROSEN (INPUT,OUTPUT)                                          BRO   10
C                                                                            BRO   20
C     THIS PROGRAM SOLVES CONSTRAINED MINIMIZATION PROBLEM                   BRO   30
C     THE CONSTRAINTS ARE LIMITED TO BOUND CONSTRAINTS, OR UPPER AND         BRO   40
C     LOWER BOUND                                                            BRO   50
C     THE SOLUTION TECHNIQUE IS A MIX APPLICATION OF THE ORIGINAL            BRO   60
C     ROSENBROCK METHOD, POWELL MINIMIZATION, AND PALMER VERSION OF          BRO   70
C     GENERATING NEW SEARCH DIRECTIONS                                       BRO   80
C     THE USER MUST SUPPLY A SUBROUTINE OBJECT FOR EVALUATION OF THE         BRO   90
C     OBJECTIVE FUNCTION                                                     BRO  100
C     NOTATIONS FOR INPUT AND OUTPUT INFORMATION                             BRO  110
C     TITLE = ALPHABETICAL OR NUMERICAL IDENTIFICATION OF THE PROBLEM        BRO  120
C     N = NUMBER OF VARIABLES                                                BRO  130
C     MST = MAXIMUM LIMIT OF NUMBER OF STAGE SEARCH                          BRO  140
C     MCL = MAXIMUM LIMIT OF NUMBER OF CYCLE SEARCH                          BRO  150
C     IPT = NUMERICAL IDENTIFICATION FOR OUTPUT CONTROL                      BRO  160
C     IPT = 0 --- ONLY THE FINAL ANSWER IS DESIRED                           BRO  170
C     IPT = 1 --- INTERMEDIATE VALUES OF EACH STAGE SEARCH IS DESIRED        BRO  180
C     IPT = 2 --- INTERMEDIATE VALUES OF EACH CYCLE SEARCH IS DESIRED        BRO  190
C     EPS = CONVERGENCE TOLERANCE BASED ON THE CHANGE OF OBJECTIVE           BRO  200
C           FUNCTION                                                         BRO  210
C     EPX = CONVERGENCE TOLERANCE FOR CYCLE SEARCH                           BRO  220
C     V = INITIAL GUESS OF THE VECTOR                                        BRO  230
C     VUP = UPPER LIMIT OF THE VECTOR                                        BRO  240
C     VLO = LOWER LIMIT OF THE VECTOR                                        BRO  250
C     X = NORMALIZED INITIAL GUESS OF THE VECTOR                             BRO  260
C     PO = OPTIMUM VALUE OF THE OBJECTIVE FUNCTION                           BRO  270
C     NEF = NUMBER OF FUNCTION EVALUATION                                    BRO  280
C     NS = NUMBER OF STAGE SEARCH                                            BRO  290
C                                                                            BRO  300
      DIMENSION A(10), B(10), C(10), D(10), Z(10), TITLE(20)                 BRO  310
      COMMON DL,DX,PO,VALUE,N,NEF,S(10,10),X(10),V(10),VUP(10),VLO(10)       BRO  320
      COMMON /UNI/ MCL,EPX                                                   BRO  330
C                                                                            BRO  340
C     INPUT AND OUTPUT NECESSARY INFORMATION                                 BRO  350
C                                                                            BRO  360
      READ 290, TITLE                                                        BRO  370
      PRINT 300, TITLE                                                       BRO  380
      READ 310, N,MST,MCL,IPT,EPS                                            BRO  390
      EPX=10.*EPS                                                            BRO  400
      PRINT 320, N,EPS                                                       BRO  410
      READ 330, (V(I),VUP(I),VLO(I),I=1,N)                                   BRO  420
      PRINT 340                                                              BRO  430
      PRINT 350, (I,VUP(I),VLO(I),I=1,N)                                     BRO  440
      PRINT 360                                                              BRO  450
      PRINT 370, (I,V(I),I=1,N)                                              BRO  460
C                                                                            BRO  470
C     NORMALIZE THE VECTORS                                                  BRO  480
C                                                                            BRO  490
      DO 110 I=1,N                                                           BRO  500
         X(I)=(V(I)-VLO(I))/(VUP(I)-VLO(I))                                  BRO  510
         D(I)=0.5                                                            BRO  520
  110 CONTINUE                                                               BRO  530
C                                                                            BRO  540
C     SET THE INITIAL SEARCH DIRECTION                                       BRO  550
```

```
                    PROGRAM BROSEN (INPUT,OUTPUT)
C                                                                       BRO  560
      DO 130 I=1,N                                                      BRO  570
         DO 120 J=1,N                                                   BRO  580
            S(I,J)=0.                                                   BRO  590
            IF (J.EQ.I) S(I,J)=1.                                       BRO  600
  120    CONTINUE                                                       BRO  610
  130 CONTINUE                                                          BRO  620
C                                                                       BRO  630
C     STARTING OF STAGE SEARCH                                          BRO  640
C                                                                       BRO  650
      NS=0                                                              BRO  660
      NEF=0                                                             BRO  670
      CALL OBJECT (1,0.)                                                BRO  680
      PO=VALUE                                                          BRO  690
  140 NS=NS+1                                                           BRO  700
      OBJ=PO                                                            BRO  710
      IF (IPT.EQ.0) GO TO 150                                           BRO  720
      PRINT 380                                                         BRO  730
      PRINT 390, NS                                                     BRO  740
  150 DO 170 I=1,N                                                      BRO  750
         DX=D(I)                                                        BRO  760
         CALL UNIMO (I)                                                 BRO  770
         IF (IPT.NE.2) GO TO 160                                        BRO  780
         PRINT 400, I                                                   BRO  790
         PRINT 410, PO                                                  BRO  800
         PRINT 370, (J,V(J),J=1,N)                                      BRO  810
  160    Z(I)=DL                                                        BRO  820
         D(I)=ABS(DL)                                                   BRO  830
  170 CONTINUE                                                          BRO  840
C                                                                       BRO  850
C     CHECK IF THE RESULT IS SATISFIED WITH THE PREASSIGNED CONVERGENCE  BRO  860
C     TOLERANCE                                                         BRO  870
C                                                                       BRO  880
      IF ((OBJ-PO).LE.EPS) GO TO 280                                    BRO  890
C                                                                       BRO  900
C     CHECK IF THE NUMBER OF STAGE SEARCH GREATER THAN ASSIGNED LIMIT   BRO  910
C                                                                       BRO  920
      IF (NS.LT.MST) GO TO 180                                          BRO  930
      PRINT 380                                                         BRO  940
      PRINT 420, MST                                                    BRO  950
      PRINT 410, PO                                                     BRO  960
      PRINT 370, (I,V(I),I=1,N)                                         BRO  970
      STOP                                                              BRO  980
  180 PRINT 380                                                         BRO  990
      PRINT 430, NEF                                                    BRO 1000
      PRINT 410, PO                                                     BRO 1010
      PRINT 370, (I,V(I),I=1,N)                                         BRO 1020
C                                                                       BRO 1030
C     CALCULATE NEW SEARCH DIRECTION FOR NEXT STAGE SEARCH              BRO 1040
C     PALMERS VERSION IS USED TO COMPUTE THE NEW DIRECTION              BRO 1050
C                                                                       BRO 1060
      DO 270 I=1,N                                                      BRO 1070
         SUMA=0.                                                        BRO 1080
         DO 200 J=1,N                                                   BRO 1090
            A(J)=0.                                                     BRO 1100
```

```
                    PROGRAM BROSEN (INPUT,OUTPUT)

                DO 190 K=I,N                                                    BRO 1110
                   A(J)=A(J)+Z(K)*S(K,J)                                        BRO 1120
  190           CONTINUE                                                        BRO 1130
                SUMA=SUMA+A(J)**2                                               BRO 1140
  200       CONTINUE                                                          BRO 1150
            AA=SQRT(SUMA)                                                     BRO 1160
            IF (AA.EQ.0.) GO TO 140                                           BRO 1170
            IF (I.EQ.1) GO TO 220                                             BRO 1180
            IF (ABS(Z(I-1)).LE.EPS) GO TO 240                                 BRO 1190
            DA=1./SQRT(AB**2-AA**2)                                           BRO 1200
            RA=AB/AA                                                          BRO 1210
            CA=DA*RA                                                          BRO 1220
            CB=DA/RA                                                          BRO 1230
            DO 210 J=1,N                                                      BRO 1240
               C(J)=S(I,J)                                                    BRO 1250
               S(I,J)=A(J)*CA-B(J)*CB                                         BRO 1260
               B(J)=A(J)                                                      BRO 1270
  210       CONTINUE                                                          BRO 1280
            GO TO 260                                                         BRO 1290
  220       DO 230 J=1,N                                                      BRO 1300
               C(J)=S(I,J)                                                    BRO 1310
               S(I,J)=A(J)/AA                                                 BRO 1320
               B(J)=A(J)                                                      BRO 1330
  230       CONTINUE                                                          BRO 1340
            GO TO 260                                                         BRO 1350
  240       DO 250 J=1,N                                                      BRO 1360
               CTEM=S(I,J)                                                    BRO 1370
               S(I,J)=C(J)                                                    BRO 1380
               C(J)=CTEM                                                      BRO 1390
               B(J)=A(J)                                                      BRO 1400
  250       CONTINUE                                                          BRO 1410
  260       AB=AA                                                             BRO 1420
  270   CONTINUE                                                              BRO 1430
        GO TO 140                                                             BRO 1440
C                                                                             BRO 1450
C       A MINIMUM HAS BEEN FOUND                                              BRO 1460
C                                                                             BRO 1470
  280   PRINT 380                                                             BRO 1480
        PRINT 440, NS,NEF                                                     BRO 1490
        PRINT 450, PO                                                         BRO 1500
        PRINT 370, (I,V(I),I=1,N)                                             BRO 1510
        STOP                                                                  BRO 1520
C                                                                             BRO 1530
  290 FORMAT (20A4)                                                           BRO 1540
  300 FORMAT (1H1/////40X,20A4)                                               BRO 1550
  310 FORMAT (4I10,E10.3)                                                     BRO 1560
  320 FORMAT (//47X,21HNUMBER OF VARIABLES =,I5//44X,23HCONVERGENCE TOLERBRO 1570
     1RANCE =,E10.3)                                                          BRO 1580
  330 FORMAT (3F10.5)                                                         BRO 1590
  340 FORMAT (//44X,33HUPPER AND LOWER BOUNDS OF VECTORS)                     BRO 1600
  350 FORMAT (/10X,4(I6,2F12.5))                                              BRO 1610
  360 FORMAT (//40X,40HTHE INITIAL VECTOR CHOSEN BY THE USER IS)              BRO 1620
  370 FORMAT (/18X,5(I5,F12.5))                                               BRO 1630
  380 FORMAT (/40X,40H****************************************)              BRO 1640
  390 FORMAT (//48X,18HSTAGE SEARCH -----,I5)                                 BRO 1650
```

```
                    PROGRAM BROSEN (INPUT,OUTPUT)

  400 FORMAT (//40X,34HCYCLE SEARCH ALONG DIRECTION -----,I5)          BRO 1660
  410 FORMAT (//34X,32HTHE CURRENT OBJECTIVE FUNCTION =,E20.8//50X,21HTHBRO 1670
     1E CURRENT VECTOR IS)                                             BRO 1680
  420 FORMAT (//40X,18HDO NOT CONVERGE IN,I5,5X,14HSTAGE SEARCHES)     BRO 1690
  430 FORMAT (//36X,43HTHE CURRENT NUMBER OF FUNCTION EVALUATION =,I5) BRO 1700
  440 FORMAT (//48X,24HA MINIMUM HAS BEEN FOUND//41X,30HTOTAL NUMBER OF BRO 1710
     1STAGE SEARCH =,I5//39X,37HTOTAL NUMBER OF FUNCTION EVALUATION =,I5BRO 1720
     2)                                                                BRO 1730
  450 FORMAT (//38X,23HOPTIMIZATION FUNCTION =,E20.8//50X,15HFINAL VECTOBRO 1740
     1R IS)                                                            BRO 1750
C                                                                      BRO 1760
      END                                                              BRO 1770
```

SUBROUTINE UNIMO (IP)

```
      SUBROUTINE UNIMO (IP)                                                  UNI   10
C                                                                            UNI   20
C     THIS SUBROUTINE DETERMINES THE OPTIMAL STEP SIZE ALONG A DIRECTION     UNI   30
C                                                                            UNI   40
      DIMENSION E(3), Y(3)                                                   UNI   50
      COMMON DL,DX,PO,VALUE,N,NEF,S(10,10),X(10),V(10),VUP(10),VLO(10)       UNI   60
      COMMON /UNI/ MCL,EPX                                                   UNI   70
C                                                                            UNI   80
C     SET UP UPPER AND LOWER LIMITS                                          UNI   90
C                                                                            UNI  100
      XUPL=1.0E+10                                                           UNI  110
      XLOL=-1.0E+10                                                          UNI  120
      DO 120 I=1,N                                                           UNI  130
         IF (S(IP,I).EQ.0.) GO TO 120                                        UNI  140
         IF (S(IP,I).LT.0.) GO TO 110                                        UNI  150
         XTEM=(1.0-X(I))/S(IP,I)                                             UNI  160
         IF (XTEM.LT.XUPL) XUPL=XTEM                                         UNI  170
         XTEM=-X(I)/S(IP,I)                                                  UNI  180
         IF (XTEM.GT.XLOL) XLOL=XTEM                                         UNI  190
         GO TO 120                                                           UNI  200
  110    XTEM=(1.0-X(I))/S(IP,I)                                             UNI  210
         IF (XTEM.GT.XLOL) XLOL=XTEM                                         UNI  220
         XTEM=-X(I)/S(IP,I)                                                  UNI  230
         IF (XTEM.LT.XUPL) XUPL=XTEM                                         UNI  240
  120 CONTINUE                                                               UNI  250
      NC=0                                                                   UNI  260
      XA=0.                                                                  UNI  270
      A=PO                                                                   UNI  280
      XB=XA+DX                                                               UNI  290
      IF (XB.LE.XUPL) GO TO 130                                              UNI  300
      XB=XUPL                                                                UNI  310
      DX=XB                                                                  UNI  320
  130 CALL OBJECT (IP,XB)                                                    UNI  330
      B=VALUE                                                                UNI  340
C                                                                            UNI  350
C     DETERMINE THE THIRD POINT REQUIRED FOR APPROXIMATION                   UNI  360
C                                                                            UNI  370
      IF (A.GT.B) GO TO 170                                                  UNI  380
  140 XC=XA-DX                                                               UNI  390
      IF (XC.GE.XLOL) GO TO 150                                              UNI  400
      XC=XLOL                                                                UNI  410
  150 CALL OBJECT (IP,XC)                                                    UNI  420
      C=VALUE                                                                UNI  430
      Y(1)=XC                                                                UNI  440
      Y(2)=XA                                                                UNI  450
      Y(3)=XB                                                                UNI  460
      E(1)=C                                                                 UNI  470
      E(2)=A                                                                 UNI  480
      E(3)=B                                                                 UNI  490
      IF (C.LT.A) GO TO 160                                                  UNI  500
      XINF=XA                                                                UNI  510
      FINF=A                                                                 UNI  520
      GO TO 200                                                              UNI  530
  160 XINF=XC                                                                UNI  540
      FINF=C                                                                 UNI  550
```

```
                        SUBROUTINE UNIMO (IP)
      GO TO 200                                                          UNI  560
  170 XC=XA+2.*DX                                                        UNI  570
      IF (XC.LE.XUPL) GO TO 180                                          UNI  580
      XC=XUPL                                                            UNI  590
  180 CALL OBJECT (IP,XC)                                                UNI  600
      C=VALUE                                                            UNI  610
      Y(1)=XA                                                            UNI  620
      Y(2)=XB                                                            UNI  630
      Y(3)=XC                                                            UNI  640
      E(1)=A                                                             UNI  650
      E(2)=B                                                             UNI  660
      E(3)=C                                                             UNI  670
      IF (C.LT.B) GO TO 190                                              UNI  680
      XINF=XB                                                            UNI  690
      FINF=B                                                             UNI  700
      GO TO 200                                                          UNI  710
  190 XINF=XC                                                            UNI  720
      FINF=C                                                             UNI  730
C                                                                        UNI  740
C     ELIMINATE PREMATURE TERMINATION DUE TO EQUAL VALUES AT TWO END     UNI  750
C     POINTS IN THE FIRST SEARCH                                         UNI  760
C                                                                        UNI  770
  200 DEF=E(1)-E(3)                                                      UNI  780
      IF (NC.GT.0.OR.ABS(DEF).GT.EPX) GO TO 210                          UNI  790
      DX=0.5*DX                                                          UNI  800
      Y(2)=Y(1)+DX                                                       UNI  810
      CALL OBJECT (IP,Y(2))                                              UNI  820
      E(2)=VALUE                                                         UNI  830
      Y(3)=XINF                                                          UNI  840
      E(3)=FINF                                                          UNI  850
      DEF=E(1)-E(3)                                                      UNI  860
      IF (E(2).GT.FINF) GO TO 210                                        UNI  870
      XINF=Y(2)                                                          UNI  880
      FINF=E(2)                                                          UNI  890
C                                                                        UNI  900
C     CHECK THE CONVEXITY OF THE QUADRATIC FUNCTION                      UNI  910
C                                                                        UNI  920
  210 A1=(Y(1)-Y(2))*(Y(2)-Y(3))*(Y(1)-Y(3))                             UNI  930
      IF (ABS(A1).EQ.0.) GO TO 220                                       UNI  940
      A2=E(1)*(Y(2)-Y(3))+E(2)*(Y(3)-Y(1))+E(3)*(Y(1)-Y(2))              UNI  950
      SA=A2/A1                                                           UNI  960
      IF (SA.GE.0.) GO TO 230                                            UNI  970
      DX=Y(3)-Y(1)                                                       UNI  980
      XA=Y(1)                                                            UNI  990
      A=E(1)                                                             UNI 1000
      XB=Y(3)                                                            UNI 1010
      B=E(3)                                                             UNI 1020
      IF (DEF.GT.0.) GO TO 170                                           UNI 1030
      GO TO 140                                                          UNI 1040
  220 XSTA=XINF                                                          UNI 1050
      FSTA=FINF                                                          UNI 1060
      GO TO 290                                                          UNI 1070
C                                                                        UNI 1080
C     DETERMINE THE MINIMUM OF THE QUADRATIC FUNCTION                    UNI 1090
C                                                                        UNI 1100
```

```
                      SUBROUTINE UNIMO (IP)
  230 SB=(E(1)-E(2))/(Y(1)-Y(2))-SA*(Y(1)+Y(2))                    UNI 1110
      XSTA=-SB/(2.*SA)                                             UNI 1120
      IF (XSTA.GE.XLOL.AND.XSTA.LE.XUPL) GO TO 250                 UNI 1130
      IF (DEF.GT.0.) GO TO 240                                     UNI 1140
      XSTA=XLOL                                                    UNI 1150
      GO TO 250                                                    UNI 1160
  240 XSTA=XUPL                                                    UNI 1170
  250 NC=NC+1                                                      UNI 1180
      CALL OBJECT (IP,XSTA)                                        UNI 1190
      FSTA=VALUE                                                   UNI 1200
      IF (FSTA.LE.FINF) GO TO 260                                  UNI 1210
      XTEM=XSTA                                                    UNI 1220
      XSTA=XINF                                                    UNI 1230
      XINF=XTEM                                                    UNI 1240
      FTEM=FSTA                                                    UNI 1250
      FSTA=FINF                                                    UNI 1260
      FINF=FTEM                                                    UNI 1270
  260 IF ((FINF-FSTA).LE.EPX) GO TO 290                            UNI 1280
      DX=ABS(XINF-XSTA)                                            UNI 1290
      IF (NC.LT.MCL) GO TO 270                                     UNI 1300
      PRINT 310                                                    UNI 1310
      PRINT 320, MCL,IP                                            UNI 1320
      STOP                                                         UNI 1330
  270 IF (XSTA.GT.XINF) GO TO 280                                  UNI 1340
      XA=XSTA                                                      UNI 1350
      A=FSTA                                                       UNI 1360
      XB=XINF                                                      UNI 1370
      B=FINF                                                       UNI 1380
      GO TO 140                                                    UNI 1390
  280 XA=XINF                                                      UNI 1400
      A=FINF                                                       UNI 1410
      XB=XSTA                                                      UNI 1420
      B=FSTA                                                       UNI 1430
      GO TO 170                                                    UNI 1440
C                                                                  UNI 1450
C     A MINIMUM HAS BEEN FOUND                                     UNI 1460
C                                                                  UNI 1470
  290 DL=XSTA                                                      UNI 1480
      PO=FSTA                                                      UNI 1490
      DO 300 I=1,N                                                 UNI 1500
         X(I)=X(I)+XSTA*S(IP,I)                                    UNI 1510
         V(I)=VLO(I)+X(I)*(VUP(I)-VLO(I))                          UNI 1520
  300 CONTINUE                                                     UNI 1530
      RETURN                                                       UNI 1540
C                                                                  UNI 1550
  310 FORMAT (/40X,40H**********************************************) UNI 1560
  320 FORMAT (//28X,18HDO NOT CONVERGE IN,I5,5X,36HCYCLE SEARCHES ALONG UNI 1570
     1DIRECTION -----,I5)                                          UNI 1580
C                                                                  UNI 1590
      END                                                          UNI 1600
```

SUBROUTINE OBJECT(IP,Z)

```
      SUBROUTINE OBJECT (IP,Z)                                          OBJ   10
C                                                                       OBJ   20
C     THIS SUBROUTINE DETERMINES THE VALUE OF OBJECTIVE FUNCTION        OBJ   30
C                                                                       OBJ   40
      DIMENSION T(10), Y(10)                                            OBJ   50
      COMMON DL,DX,PO,VALUE,N,NEF,S(10,10),X(10),V(10),VUP(10),VLO(10)  OBJ   60
      NEF=NEF+1                                                         OBJ   70
      DO 110 I=1,N                                                      OBJ   80
         T(I)=X(I)+Z*S(IP,I)                                            OBJ   90
         Y(I)=VLO(I)+T(I)*(VUP(I)-VLO(I))                               OBJ  100
  110 CONTINUE                                                          OBJ  110
      VALUE=(Y(1)-Y(2))**2+(Y(2)-2.*Y(3))**2+(Y(3)-2.)**2               OBJ  120
      RETURN                                                            OBJ  130
C                                                                       OBJ  140
      END                                                               OBJ  150
```